Exocytosis-dependent p75NTR signaling in neurodevelopment and its regulation by RELL1

Mark Cumming
Integrated Program in Neuroscience
McGill University, Montreal

A thesis submitted to McGill University in partial fulfillment of the requirements of the degree of PhD Neuroscience

Table of Contents

Abstract

A member of the tumor necrosis factor receptor (TNFRSF) superfamily, the p75 neurotrophin receptor (p75NTR) is a major regulator of nervous system development and maintenance. Although p75NTR-dependent function across diverse neurological phenotypes—both physiological and pathophysiological—has been thoroughly studied, our knowledge of the underlying signaling mechanisms engaged by p75NTR remains severely limited. To address this problem, I begin by characterizing extracellular vesicles (EVs) as a novel p75NTR signaling platform. Using multiple assays, I demonstrate that p75NTR overexpression induces expansion in COS7 cells via a non-cell-autonomous signaling pathway. Non-cell-autonomous COS7 expansion requires p75NTR secretion via large EVs—highly enriched in p75NTR proteolytic cleavage products—and downstream engagement of NRAGE in the EV recipient cell. Moreover, COS7-derived p75NTR+ EVs induced expansion of growth cones in developing DRG sensory neurons in vitro. Next, I resolved the interactome of p75NTR—and its functional TNFRSF relatives DR6 and TROY—in a modified HEK293 cell line by proximity-dependent biotinylation (BioID). BioID revealed a set of 29 shared interactors between these 3 TNFRSFs, which included the extracellular domain (ECD)-truncated TNFRSF, RELT-Like 1 (RELL1). After validation of the RELL1-TNFRSF complexes by proximity ligation assay, functional assays revealed that RELL1 blocks non-cell-autonomous p75NTR-dependent COS7 expansion by inhibiting p75NTR exocytosis to large EVs. RELL1-dependent p75NTR inhibition requires formation of the RELL1-p75NTR complex as a novel non-p75NTR-binding mutant (RELL1ΔCR4-HA) failed to inhibit p75NTR-dependent cell expansion. Collectively, the data establish EVs as a novel p75NTR signaling platform and add to a growing body of evidence that ECD-truncated TNFRSFs are endogenous inhibitors of their full-length counterparts.

Résumé

Membre de la superfamille des récepteurs du facteur de nécrose tumorale (TNFRSF), le récepteur de neurotrophine p75 (p75NTR) est un régulateur majeur du développement et de l'entretien du système nerveux. Bien que la fonction dépendante du p75NTR dans divers phénotypes neurologiques, tant physiologiques que physiopathologiques, ait été étudiée à fond, nos connaissances des mécanismes de signalisation sous-jacents engagés par le p75NTR restent très limitées. Pour résoudre ce problème, je commence par caractériser les vésicules extracellulaires (VE) comme une nouvelle plateforme de signalisation p75NTR. À l'aide de tests multiples, je démontre que la surexpression du p75NTR induit une expansion dans les cellules COS7 via une voie de signalisation non autonome des ventes. L'expansion du COS7 non cellulaire autonome requiert la sécrétion du p75NTR par l'intermédiaire de VE de grande taille, hautement enrichis en produits de clivage protéolytique du p75NTR, et l'engagement en aval du NRAGE dans la cellule réceptrice du VE. De plus, les VE p75NTR+ dérivés du COS7 ont induit l'expansion de cônes de croissance développant des neurones sensoriels DRG in vitro. Ensuite, j'ai résolu l'interactome du p75NTR — et de ses TNFRSF relatifs fonctionnels DR6 et TROY — dans une lignée cellulaire HEK293 modifiée par biotinylation dépendante de la proximité (BioID). BioID a révélé un ensemble de 29 interacteurs partagés entre ces 3 TNFRSF, dont le domaine extracellulaire (ECD)-tronqué TNFRSF, RELT-Like 1 (RELL1). Après validation des complexes RELL1-TNFRSF par un essai de ligature de proximité, des essais fonctionnels ont révélé que le RELL1 bloque l'expansion du COS7 non dépendant du p75NTR en inhibant l'exocytose du p75NTR aux VE de grande taille. L'inhibition p75NTR dépendante du RELL1 nécessite la formation du complexe RELL1-p75NTR en tant que mutant nouveau non lié au RELL1 (RELL1ΔCR4-HA) n'a pas inhibé l'expansion cellulaire dépendante du p75NTR. Collectivement, les données établissent les VE comme une nouvelle plateforme de signalisation

p75NTR et ajoutent à un ensemble croissant de preuves que les TNFRSFs tronquées du ECD sont des inhibiteurs endogènes de leurs homologues de pleine longueur.

Contribution to original knowledge

This doctoral thesis: (i) describes a novel intercellular p75NTR signaling mechanism mediated by extracellular vesicles (EVs) that induces cell expansion events; (ii) resolves a protein interactome shared by p75NTR, DR6 and TROY; and (iii) characterizes RELL1 as an inhibitor of p75NTR exocytosis and EV-dependent signaling.

Acknowledgments

First and foremost, I want to thank my wife, Maddy, for her unwavering love and support in every ridiculous pursuit I take on in life (this doctorate certainly included.) To my parents, Rick & Adeline, thank you for never-ending support, especially in the tough moments. All of you mean the world to me. You have helped me see what's important in life at times when the rat race gets chaotic. I love you all very much.

To my advisor and mentor, Dr. Phil Barker, thank you for your time—and patience—to help sculpt me into the scientist I am today. His elite research caliber aside, Phil is an incredible leader. From lab meetings & personal discussions, I have observed & absorbed as much as I can to develop these skills within myself. By following his example, and learning to 'fail quickly,' I am confident in my ability to go out and conquer my professional ambitions. It is a privilege to have you as a mentor, Phil.

To my friends (you know who you are), thank you for the years of support, good times & laughter. The celebrations are great, but I appreciate you most during the stressful moments. You're my wolfpack for life. Ride or die, baby.

Thank you to my coworkers for creating such a great environment to come to each day. I want to thank Dr. Andres de Leon, a man of many talents, for the years of intellectual discussion & comradery. I hope we continue to work together; I bet we could create some incredible things. Thank you to Dr. Julien Gibon for years of scientific discussion. Not only have you benefitted this project, but I have grown as a scientist from our chats. Thanks to Tomas Filip for the daily chats; you are a great scientist & better friend.

"Don't try this at home" – Ryan Cohen

Author Contributions

Chapter 2: Extracellular vesicles mediate p75NTR signaling

Mark Cumming conceptualized and performed experiments; developed protocols to: identify and measure individual GFP^+ COS7 cells, identify and measure growth cones; and developed assays to measure non-cell-autonomous COS7 cell expansion events (co-culture and filter-based systems). Liubov Frolova contributed EV purification for Figures 2.4-2.6. Svetlana Simtchouk provided gRNA design and cell culturing for NRAGE knockout COS7 cell lines used in Figure 2.6.

Chapter 3: Resolution of the p75NTR-DR6-TROY interactome

Mark Cumming conceptualized and performed experiments; generated stably transfected Flp-In T-REx 293 cell lines with Tet-inducible expression of BioID baits; and ran gene ontology analyses. Dr. Etienne Coyaud and Dr. Brian Raught ran mass spectrometry and contributed to statistical analysis for Figures 3.2 and 3.3. Genevieve Dorval provided molecular cloning for BioID bait plasmids.

Chapter 4: RELL1 is an inhibitor of non-cell-autonomous p75NTR signaling

Mark Cumming conceptualized and performed experiments, and ran protein evolutionary analyses. Liubov Frolova contributed EV purification for Figure 4.6D. Svetlana Simtchouk provided molecular cloning for RELL1 deletion mutants used in Figures 4.1D and 4.3.

Chapter 1: Review of the relevant literature

1.1 Discovery of the TNF system

In the late 19th century, Dr. William B. Coley successfully induced stable remission of an inoperable sarcoma via injection of a bacterial immunogen directly into the primary tumour (1). In addition to sparking the field of immunology, this result founded the hypothesis of an anti-tumour immune response that went unexplored for the next 70 years [reviewed in (2)]. Coley's hypothesis was substantiated by Dr. W. Edward O'Malley and colleagues (1962) who discovered that serum derived from mice infected with *Serratia marcescens* polysaccharide could induce sarcoma regression *in vivo*, indicating that a "tumor necrotizing factor" must be present in sera (3). In 1975, this anti-tumoral serum factor was successfully isolated by Carswell and colleagues and became known simply as Tumour Necrosis Factor (TNF).

In parallel to the TNF discovery, two independent laboratories published the discovery of a cytotoxic factor secreted by lymphocytes—which was termed lymphotoxin (LT)—capable of inducing necrosis in the L-929 fibrosarcoma cell line (4,5). Nearly one decade after the TNF/LT discoveries, Dr. Bharat Aggarwal's group successfully purified human LT from conditioned medium of the RPMI 1788 lymphoblastoid cell line (6,7) and human TNF from conditioned medium of HL-60 promyelomonocytic cells (8) for structural characterization. Interestingly, TNF and LT showed very high sequence homology (~50%) (6–8), though both were immunologically distinct (9), and were subsequently re-named TNFα and TNFβ (or LT-α), respectively. Moreover, their expression profile differs in that TNFα is primarily macrophage-derived; whereas TNFβ is lymphocyte-derived (10). By the mid-1980s, the cDNAs encoding TNFα and TNFβ were successfully resolved (11,12). Beutler and colleagues (1985) revealed that a macrophage-derived factor, cachectin—known to drive cachexia—and TNFα were in fact the

same protein (13). Both TNFα and TNFβ were shown to engage the same cell surface receptor with similar affinity (9,14).

By the late 1980s, the focus of research shifted toward the potential for exploiting TNFα/β in the clinic. Dr. Anthony Cerami's group demonstrated that immunization against TNFα protects mice from lipopolysaccharide (LPS)-induced lethality (15) and septic shock (16). This demonstrated that, although TNFα can stimulate physiological inflammation, over-production of TNFα can be deleterious and may contribute to immunopathology. At present, TNFα has been broadly implicated in several autoimmune pathologies, including: multiple sclerosis, lupus erythematosus, uveitis, arthritis, psoriasis, and Crohn's disease [reviewed in (17,18)]. Thus, although TNF is an effective anti-tumoral factor, its utility is limited in the clinic due to its potent pro-inflammatory nature (19,20). However, in soft tissue carcinomas localized to the extremities, exogenous TNFα can be locally restricted by isolated limb perfusion (21–23). In these cases, TNFα has effective antitumoral activity with minimal safety concerns (21–23).

It is clear in hindsight that these pioneering studies in the TNF field merely scratched the surface of TNF biology. Currently, 19 TNF ligands and 29 TNF receptors (TNFRSFs) have been identified and functionally characterized in humans [reviewed in (18)]. Mice express orthologs of all 29 human receptors in addition to 3 murine-specific TNFRSFs (24). The field now recognizes that physiological and pathophysiological functions of the TNF system extend far beyond immunology and immuno-oncology. Aberrant TNF-TNFRSF signaling has been broadly implicated in: tumorigenesis (25–27), neuropsychiatric disorders (28–31), neurodegenerative disease (32–35), cardiovascular disease (36–41), diabetes (42), obesity (42–44), and pulmonary disease (45–49).

In recent decades, TNFRSFs have been firmly established as master regulators of nervous system development and maintenance. Three of the best characterized TNFRSFs in this regard include: the p75 neurotrophin receptor (p75NTR), death receptor 6 (DR6), and TROY (discussed further in Sections 1.4 to 1.6). These 3 TNFRSFs demonstrate functional overlap within the contexts of neurodegeneration—both physiological and pathophysiological—and neural plasticity (50–64). Despite the rapidly accumulating literature on the role of these 3 TNFRSFs in nervous system function, our knowledge of the core signaling mechanisms utilized by these receptors remains limited.

1.2 TNFRSF structure and function

TNF ligands are type II multi-pass transmembrane proteins structurally identifiable by a TNF homology domain (THD) (65,66). Although all TNFs exist in a transmembrane state, several TNF ligands can be proteolytically processed in a soluble extracellular form (67). TNFRSFs, on the other hand, are single-pass type I transmembrane proteins possessing one or more characteristic cysteine-rich domains (CRDs) within their extracellular domain (ECD). A CRD consists of six cysteine residues forming three independent disulfide linkages (65,66). Physical association of the THD and CRD mediates TNF-TNFRSF interactions (67). Several TNFRSFs—like their TNF counterparts—can be proteolytically cleaved to release the intracellular domain (ICD) into the cytosol and an ECD into the extracellular environment, both of which can be signaling-competent (67). Lastly, TNF ligands form functional homotrimers (67,68)—and TNFRSFs exist in pre-liganded homotrimers (69). Thus, TNF-TNFRSF signaling occurs in a conserved 3:3 stoichiometry (67). p75NTR is an exception, as p75NTR transduces signals from neurotrophin (NT) and proneurotrophin (proNT) ligands—or in a ligand-

independent manner—in active dimeric and monomeric states (70,71) [discussed further in Section 1.4.1].

TNFRSFs are structurally sub-categorized by the presence or absence of an ~80 amino acid (AA) pro-apoptotic domain in their ICD known as the death domain (DD) (72). The DD consists of 6 α-helices arranged in a globular conformation (73). TNFRSFs possessing an DD are referred to as death receptors (DRs). Canonically, DRs induce death signaling via the extrinsic apoptotic pathway, recruiting DD-containing effectors [Fas-associated protein with death domain (FADD), TNFRSF1-associated death domain protein (TRADD) or EDAR-associated adapter protein (EDARADD)] which in turn drive proteolytic activation of initiator caspase-8 and downstream activation of caspase-3 (74–76). p75NTR and DR6, however, are atypical DRs, in that they do not recruit FADD, TRADD or EDARADD and, in according, cannot activate the extrinsic apoptotic pathway (77,78). p75NTR induces apoptosis via the intrinsic, mitochondrial pathway culminating in activation of caspase-3 and the pro-apoptotic c-jun N-terminal kinase (JNK) (77). DR6, on the other hand, does not engage an apoptotic pathway, but rather signals cell death via the necroptotic pathway (78).

TNFRSFs are not enzymatic in nature, but rather initiate signaling events via the recruitment of adaptor proteins to the ICDs (65,66). A core group of these adaptors, known as TNFR-Associated Factors (TRAFs) associated with the ICD of TNFRSFs via their conserved TRAF domain (79). TRAFs function as E3 ubiquitin ligases to target substrates, and the TRAF itself, for proteosomal degradation via K48-linked ubiquitination (80–82). In parallel, TRAF E3 ligase activity can activate signaling cascades—such as the NFκB pathway—via K63-linked polyubiquitination; a function that requires physical association with the E2 ubiquitin ligase complex Ubc13/Uev1A (83). Although TRAFs represent a common family of TNFRSF

adaptors, each TNFRSF possesses its own unique complement of adaptors—and other interactors—to mediate TNFRSF-specific signaling events.

TNFRSFs are major regulators of survival and death signaling in wide-ranging cellular contexts, including in the nervous system. Survival signaling is mediated by downstream activation of nuclear factor κB (NFκB) and/or PI3K-Akt cascades (67). Apoptotic signaling, on the other hand, involves downstream activation of JNK, p38 MAPK and/or executioner caspases (67). These core pathways are common to TNFRSFs, but TNFRSF-specific regulation of survival, apoptosis, and a plethora of other cellular functions, relies on a diverse array of intracellular adaptors and their associated signaling cascades.

1.3 Evolutionary origins of the TNFRSF superfamily

Mammalian TNFRSFs have been successfully traced to single copy genes in arthropods [reviewed in (67). *Drosophila melanogaster* expresses a simple TNF system with structural and functional homology to the mammalian system (84,85). The *Drosophila* TNF system consists of 1 TNF ligand (Eiger) and 2 TNFRSFs [Wengen and Grindelwald] (84–86). Wengen is a structural and functional homolog of p75NTR—whereas Grnd appears to be *Drosophila*-specific, implicating p75NTR as the evolutionary ancestor of the TNFRSF superfamily (87,88).

Eiger-Wengen signaling activates a pro-apoptotic cascade via the JNK pathway (85). Eiger/Wengen-induced JNK activation requires a *Drosophila* homolog of TRAF6 (dTRAF2) (85,89), thus demonstrating signaling similarity to the mammalian system. Eiger/Wengen-dependent JNK activation regulates developmental apoptosis in photoreceptors (84)—a process dependent on Rac1-mediated endocytosis (88). Thus, p75NTR-dependent developmental neurodegeneration [reviewed in Section 1.4.6] represents an evolutionarily conserved TNFRSF function in arthropods. This is further exemplified by the simple neurotrophin system expressed

in *Daphnia pulex* consisting of a NT, a Trk, and a p75NTR ortholog (90), where the antagonistic Trk/p75NTR survival vs. death axis may regulate neurodevelopment on a large scale.

Recent evidence has shown the presence of TNFRSFs in pre-bilaterian Cnidarian species, including *Nematostella vectensis* (sea anemome) and *Hydra vulgaris* (hydra) (91). Cnidarians are the oldest animal phylum to develop a nervous system, possessing a primitive sensorimotor "nerve net" (92). Interestingly, back-tracing of mammalian TNFRSF CRD regions identifies a p75NTR ortholog expressed in both *N. vectensis* and *H. vulgaris* as the sole ancestor of the mammalian TNFRSF (Cumming et al., *under review*). Therefore, p75NTR may represent the evolutionary ancestor of all mammalian TNFRSFs. Moreover, p75NTR-dependent neurodevelopment may be the original TNFRSF-dependent function in the animal kingdom, existing prior to the chordate TNFRSF expansion event that drove development of the adaptive immune response (91).

1.4 The p75 neurotrophin receptor

The p75 neurotrophin receptor (p75NTR) is an atypical TNFRSF, insofar as it does not transduce signals from any known TNF ligand. Rather, p75NTR is a low-affinity receptor for all known mammalian neurotrophins (NTs) [nerve growth factor (NGF), brain-derived neurotrophic factor (BDNF), neurotrophin-3 (NT-3) and neurotrophin-4/5 (NT-4)] and immature, non-proteolytically processed proneurotrophins (proNTs) (proNGF, proBDNF, proNT-3 and proNT-4) abundantly expressed in diverse neuronal and glial cell lineages. In the CNS, p75NTR expression is generally most abundant during embryonic and early postnatal development, and gradually reduces—but remains biologically active—into adulthood (93). In developmental and post-developmental contexts, p75NTR can differentially augment or antagonize NT survival signaling via the high-affinity tropomyosin-related kinase (Trk) receptors. Functional antagonism

between NT/Trk survival signaling and proNT/p75NTR death signaling is a major regulatory mechanism shaping neurodevelopment and neural plasticity. The functionality of p75NTR as a master regulator of nervous system development and maintenance are reviewed in depth in the sub-sections to follow.

1.4.1 Structural biology of p75NTR

p75NTR is a 75 kDa, single-pass, type I transmembrane protein primarily localized to the plasma membrane. p75NTR possesses: (i) an N-terminal extracellular domain (ECD) of 250 amino acids (AA) which mediates ligand binding; (ii) a transmembrane domain (TMD) of 22 AA; and (iii) a C-terminal intracellular domain (ICD) of 155 AA which mediates signaling.

The p75NTR ECD (p75ECD) includes: 4 CRDs (designated CRD1-4; CRD1 is closest to the N-terminus), each CRD is separated by only 1-3 AAs, and a membrane-proximal stalk domain is located between CRD4 and the TMD. The 4 CRDs are required for ligand-binding (for NTs, proNTs and non-NT ligands) (65–69) though CRD3-4 primarily mediate NGF binding (94). p75NTR is a glycoprotein with an N-linked glycosylation site within CRD1, and multiple O-glycosylation sites within the stalk domain (95,96). p75NTR glycosylation states can be resolved by Western blotting, with non-glycosylated p75NTR observed at ~59 kDa, fully glycosylated p75NTR at 75 kDa, and partially glycosylated p75NTR polypeptides between 59 and 75 kDa (96).

The p75NTR ICD (p75ICD) includes: an ~80 AA death domain (DD)—separated from the TMD by a short, flexible juxtamembrane region known as the ‘chopper domain’—and a C-terminal PDZ-binding domain. The p75NTR DD consists of 6 α-helices arranged in a globular structure, as is the case for all death receptor DDs. However, unlike a canonical DD, the p75NTR DD shows weak homodimerization and cannot recruit DD-containing death effectors such as

TRADD, FADD or EDARADD. This deficiency in DD homodimerization and death effector recruitment is thought to result from the 1st α-helix of the p75NTR DD being positioned 90° off-axis relative to the 1st α-helix of the Fas DD (97,98), which can recruit FADD (99).

The stoichiometry of p75NTR is a complex issue. p75NTR can exist as a monomer or dimer in neural and non-neural cells (77,100). The existence of p75NTR trimers has been reported (101), but p75NTR trimerization has been heavily scrutinized in the field, and it is unclear if trimers are a physiologically relevant receptor conformation. The crystal structure of NT-3 in complex with glycosylated p75ECD revealed a 2:2 neurotrophin-to-p75NTR stoichiometry (102). Previous X-ray crystallography suggested a 2:1 stoichiometry (73), but this is argued to be a deglycosylation artifact (102). Thus a NT:p75NTR stoichiometry of 2:2 is confirmed, but 2:1 complexes may also exist. Unlike NT-binding, proNT-binding to p75NTR requires a co-receptor, specifically the Vps10p family member sortilin (103). ProNGF binding to the p75NTR-sortilin complex occurs in a 2:2 stoichiometry, as revealed by X-ray crystallography (104). Although oligomeric states of p75NTR are diverse, p75NTR monomers (71), dimers (77), and trimers (101) all show biological activity, and receptor oligomerization plays a major role in gating p75NTR signaling [discussed in Section 1.4.2].

The p75NTR activation mechanism has been studied in depth (70,105–109), but a comprehensive model of p75NTR conformation in liganded and unliganded states remains elusive. Dr. Carlos Ibanez's group established a 'scissor-tong' model whereby a pre-liganded p75NTR dimer will separate its intracellular DDs—via Cys257 in the TMD acting as a fulcrum—to allow access of a new complement of adaptors to the ICD (70,106). For instance, RIP2 and RhoGDI are p75NTR interactors that bind overlapping epitopes within the p75NTR DD (85). At baseline, RhoGDI can access the p75NTR DD to initiate signaling to RhoA (107).

Upon NT binding, DD separation allows RIP2 to access its DD epitope, and subsequently displace RhoGDI, to activate the nuclear factor κB (NFκB) pathway (107). Although this model rectified differential p75NTR signaling in liganded and unliganded states (105), its accuracy recently been called into question (109). The scissor-tong model requires conformational changes in the p75ECD and TMD (upon ligand binding) be coupled directly to conformational changes in the p75ICD. However, a recent report of p75NTR dynamics in lipid nanodiscs revealed that TMD motion is entirely uncoupled to ICD motion due to the highly flexible nature of the chopper domain (109), which nullifies an assumption of the scissor-tong model. Thus, although it is clear that interactions with adaptor proteins mediate p75NTR signaling outcomes (77,107,110), our understanding of the structural biology of p75NTR activation is incomplete.

1.4.2 p75NTR signaling mechanisms

p75NTR signaling is complex but falls into three major categories: (i) regulation of Trk survival signaling; and (ii) Trk-independent p75NTR survival signaling, and (iii) p75NTR death signaling [reviewed in (77)]. These three categories explain core tenets of p75NTR neurobiology but this is far from a comprehensive categorization. This section serves to provide the reader with a fundamental knowledge of p75NTR signaling. p75NTR signaling is far more complex than described here; and the diverse signaling mechanisms engaged by p75NTR in various neural contexts will be explored in detail in following sections.

1.4.2.1 p75NTR modulates Trk-dependent survival signaling

Tropomyosin related kinase (Trk) receptors are high-affinity neurotrophin (NT) receptors that signal neuronal survival upon NT binding (111). According to the neurotrophic factor hypothesis, developing axons compete for limited target-derived NT and axons receiving adequate trophic support survive; those that do not, degenerate and die off (111). This system

serves to ensure proper physical connectivity of the nervous system during development and maintenance of neural connectivity throughout the life span (77,111). Mammals express three Trk receptor isoforms (TrkA, TrkB, and TrkC) which demonstrate NT specificity (77,111). NGF binds TrkA; BDNF and NT-4/5 bind TrkB; and NT-3 binds TrkC (77,111).

Trk receptors are tyrosine receptor kinases (RTKs) and activate signaling cascades via autophosphorylation at intracellular tyrosine residues. NT-dependent Trk survival signaling requires phosphorylation at Y490 and Y785, which serve as docking sites for the major effectors Ras, PI3K and phospholipase C γ-isoform (PLCγ) (112–114). The Ras pathway signals survival via the MAPK/ERK pathway (115,116). The PI3K survival pathway requires downstream activation of Akt (77). In the PLCγ pathway, PLCγ hydrolyzes phosphatidyl inositides to produce inositol triphosphate (IP_3) and diacylglycerol (DAG), which in turn drives Ca^{2+} influx and PLCδ activity, respectively, to augment downstream ERK activation (117,118).

p75NTR physically binds Trk receptors to elicit a high-affinity NT binding site with ~100-fold lower K_d than Trk alone (119,120). In this NT-dependent context, the p75NTR augments Trk-dependent survival signaling via physical interaction with the Trk receptor (120–122). Proteolytic cleavage of p75NTR releases its soluble intracellular domain (p75ICD) into the cytosol (123,124) [reviewed in Section 1.4.3]. The soluble p75ICD can augment TrkA survival signaling in an NGF-dependent manner via a feedforward mechanism, whereby NGF/TrkA activation of MEK stimulates p75ICD production (123), which in turn augments NT-dependent Akt activation (124).

1.4.2.2 Trk-independent p75NTR survival signaling

p75NTR can signal neuronal survival independent of Trk receptors. p75NTR drives neuronal survival via downstream activation of nuclear factor κB (NFκB) and Akt pathways.

NFκB is a cytosolic transcription factor that, upon activation via phosphorylation, translocates to the nucleus to drive transcription of a diverse set of pro-survival genes (125). p75NTR-induced NFκB activation signals survive in diverse neuronal and non-neuronal populations (126–133). p75NTR induction of NFκB is mediated by the intracellular adaptors TRAF6 (134,135), RIP2 (132) and FAP-1 (136).

1.4.2.3 p75NTR death signaling

In direct contrast, unliganded p75NTR can induce apoptosis via activation of the mitochondrial apoptotic cascade—culminating in executioner caspase activation—and c-jun N-terminal kinase (JNK). Pro-apoptotic p75NTR adaptor proteins include Neurotrophin Receptor interacting MAGE Homolog (NRAGE) (137–139), p75NTR-associated cell death executor (NADE) (140), and neurotrophin receptor interacting factor (NRIF) (141). NRAGE is required for p75NTR activation of the mitochondrial apoptotic cascade—including mitochondrial outer membrane permeabilization (MOMP), cytochrome c release, and activation of executioner caspase-3—and the JNK cascade (137,138). Moreover, NRAGE can couple the soluble p75ICD to downstream Rac1 activation to regulate actin cytoskeletal dynamics (142). NADE is a DD-binding cytosolic adaptor required for ligand-dependent activation of caspase-3 (140). NRIF is a cytosolic zinc finger protein that, upon interaction with p75ICD, translocates to the nucleus to co-ordinate a pro-apoptotic transcriptional program (141,143,144). Lastly, p75NTR can form a complex with the Vps10 family member sortilin to bind proNTs and transduce a neuronal apoptotic signal (103).

1.4.3 Proteolytic cleavage of p75NTR influences signaling outcomes

In the late 1980s, it was discovered that multiple truncated p75NTR peptides could be purified from the conditioned medium of the A875 melanoma cell line, which included soluble

ECD and ICD fragments (145). Follow-up experiments from Dr. Phil Barker and colleagues (1991) determined that the solubilized truncated p75ECD fragment released by Schwann cells was not a splice variant, but rather arose from post-translational cleavage of full-length p75NTR (146). p75NTR cleavage was later confirmed to be mediated by metalloproteinase, and intrinsic functional properties of the soluble p75ICD were proposed (147). Dr. Barker's group later generated transgenic mice expressing p75ICD which showed enhanced developmental apoptosis of sympathetic, sensory, and cortical neurons *in vivo* and augmented motoneuron death post-axotomy (148). These foundational studies demonstrated that p75NTR is proteolytically cleaved, and showed that the soluble p75ICD released into the cytosol possesses intrinsic biological activity.

Today, we recognize that regulated intracellular proteolysis (RIP) of p75NTR is a two-step process. First, α-secretase cleavage of the membrane-proximal stalk region within the ECD by A Disintegrin And Metalloproteinase 17 (ADAM17) releases the p75ECD into the extracellular environment and leaves a C-terminal fragment (p75CTF) tethered to the plasma membrane by the TMD (124,149–151). Next, the p75CTF is cleaved within the TMD by the presenilin-containing γ-secretase complex to release the p75ICD into the cytosol (149,151) [the mechanism of p75NTR cleavage is discussed in greater detail in Section 1.4.4].

The cleaved p75ICD possesses unique signaling capabilities that differ from full-length p75NTR (77). First, p75NTR cleavage inhibits formation of the high-affinity NGF-binding complex between p75NTR and TrkA (152). Despite this, soluble p75ICD can still augment NT-dependent Trk survival signaling (123,124). NGF stimulates p75NTR cleavage in PC12 cells, where the p75ICD augmented Trk-dependent activation of Akt and ERK to drive survival signaling in PC12 cells (123,124) and cerebellar cerebellar granule neurons (CGNs) (124).

Elizabeth Coulson's group found this mechanism is required for NGF/TrkA-dependent neurite outgrowth in sympathetic neurons, and reported that the p75ICD was able to physically bind TrkA in this context to possibly form a high-affinity NGF complex, though this was unconfirmed (153). Soluble p75ICD can also augment survival signaling independent of Trk receptors via direct interaction with TRAF6 and subsequent induction of the NFkB axis (154), but this has not yet been investigated in a neuronal context.

In direct contrast to mediating NT-dependent survival signaling, soluble p75ICD can also act as a pro-apoptotic factor [reviewed in (155)]. In SCG sympathetic neurons, p75NTR RIP to produce the p75ICD was shown to be necessary for NRIF nuclear translocation and subsequent induction of developmental apoptosis *in vivo* (144). In DRG sensory neurons, local NGF deprivation to axons triggers p75NTR cleavage at the distal axon (156). This axonal p75ICD travels to the soma—dependent on $p150^{glued}$-mediated retrograde microtubule transport (157,158)—where it initiates an anterograde axonal degeneration program (156,159). It is unclear how p75ICD activates this cascade, but early evidence suggests that p75ICD may translocate to the nucleus (160,161) to regulate transcription (162).

RIP of p75NTR strongly influences signaling to the actin cytoskeleton. Zeinieh and colleagues (2015) found p75NTR overexpression in COS7 cells induced a cell expansion phenotype that was dependent on ADAM17- and γ-secretase-mediated cleavage of the receptor (142). In this context, p75ICD physically interacted with NRAGE to activate Rac1 via an intermediate adaptor protein, NEDD9 (142). Thus, the p75ICD is capable of activating Rac1 to drive actin polymerization (142). *In vivo*, p75ICD-dependent actin reorganization has been shown to drive invasion behaviour in several cancers (163–166). For instance, p75NTR drives tumour invasion and metastasis of multiple gliomas, including glioblastoma (163) and

medulloblastoma (164), which is dependent on γ-secretase-mediated cleavage (163,164). Furthermore, soluble p75ICD can drive proliferation and migration in multiple cancer cell lines—including glioblastoma—*in vitro* (108,109).

1.4.4 Mechanism of p75NTR proteolytic cleavage

Shortly after identification of ADAM17 and γ-secretase as executors of p75NTR cleavage (149,150,152), it was established that α-secretase (ADAM17-dependent) cleavage was the regulatory step, as γ-secretase cleavage constitutively follows (151). With respect to ligand requirement, p75NTR cleavage can proceed in a ligand-independent manner (144), but NGF stimulates p75NTR cleavage (160). Both neurotrophin-dependent (123,124,160,167,168) and neurotrophin-independent (144,154,156) p75NTR cleavage events have been described *in vitro* and *in vivo*.

Both ADAM17- and γ-secretase-mediated cleavage steps require co-endocytosis of p75NTR and the sheddases. Dr. Francesca Bronfman's group showed that p75CTF is almost exclusively localized to an endosomal compartment(s) in PC12 cells where γ-secretase-mediated cleavage—and release of the p75ICD—occurs (167). With respect to the ADAM17-dependent cleavage, published and unpublished laboratory work from Dr. Barker's group has clearly demonstrated a requirement for ADAM17 endocytosis for activation of its α-secretase function. Briefly, TrkA survival signaling activates MEK-dependent phosphorylation of ADAM17 at intracellular threonine 735 (124). T735-phosphorylated ADAM17 is subsequently endocytosed via a dynamin-dependent mechanism into a reactive oxygen species (ROS)-producing recycling endosome known as a 'redoxosome' (169). Endosomal ROS catalyze thiol-exchange reactions targeting the ADAM17 ectodomain that activate its sheddase activity (unpublished). Thus, the current model proposes that ADAM17- and p75NTR cleavage occurs in an endosomal

compartment—likely a redoxosome—and this process can be stimulated by, but does not require, NT activation of a Trk receptor.

1.4.5 p75NTR regulation of neurodevelopment

p75NTR plays a critical role in diverse aspects of neurodevelopment, including: neuronal survival (170–178), neurite outgrowth (78,96,124–138), axon guidance (194,195), myelination (132,134,182,196–200), neuronal migration (201,202), synaptogenesis (203,204), neurogenesis (205,206), and neurodegeneration (31,51,59,137–139,141,143,144,148,156,168,207–226) [the latter is reviewed in Section 1.4.6].

1.4.5.1 p75NTR regulation of neuronal survival

According to the neurotrophic hypothesis, axons receiving adequate neurotrophic support from their innervation targets will survive and form functional synapses (227). p75NTR is a major survival factor in this context and directly activates survival signaling cascades in response to NGF stimulation in the PNS (77,228). $TrkA^+$ DRG sensory axons are highly NGF-sensitive from E12 to E15 as their neurites reach their NGF-secreting targets (227). Acute p75NTR knockdown during E12-E15 strongly reduces survival of DRG axons *in vitro* (170). Moreover, application of an exogenous NGF mutant deficient in p75NTR—but not TrkA—shows lower survival rates in DRG explants relative to wild-type NGF (171). Dr. Chris Deppmann's group investigated the role of p75NTR as a survival factor within specific subpopulations of DRG sensory neurons (177). Utilizing p75NTR-/- mice, their investigation determined that p75NTR is required for survival of TrkA+ peptidergic nociceptors, TrkB+ mechanoreceptors and TrkC+ proprioceptors, but not Trk-negative nonpeptidergic nociceptors, *in vivo* (177).

Within the PNS, the p75NTR requirement for NGF-dependent survival is stronger for SCG sympathetic neurons than DRG sensory neurons (171). Nearly all (98%) trigeminal

sympathetic axons that successfully form a sympathetic plexus during development are TrkA+ and respond to NGF (172). In a p75NTR-/- background, these sympathosensory interactions are strongly reduced, and the sparse survivors form aberrant connections (172). Mechanistically, target-derived NGF binds a high-affinity TrkA-p75NTR complex at the distal axon, which in turn, drives internalization of the NGF-TrkA-p75NTR complex and Arf6-dependent retrograde transport to the soma to initiate the survival signal (176). This retrograde survival signaling occurs in parallel to local p75NTR translation and cell surface integration in the distal axon to drive axonal survival in a feedforward manner upon NGF engagement (176).

In the PNS, motoneurons have been less studied that sensory and sympathetic neuronal populations with respect to their requirement for p75NTR in developmental survival. The current evidence suggests that p75NTR is required for both NGF-dependent and NT-3-dependent motoneuron survival, as cultured p75NTR-/- motoneurons show a blunted NT-dependent survival response (173).

In the CNS, TrkA+ cholinergic neurons of the basal forebrain require p75NTR for survival (174,178). In a p75NTR-/- background, cholinergic innervation of the molecular and granular layers of the dentate gyrus is strongly reduced (174). This cholinergic hypoinnervation of hippocampal substructures mediates the enhanced anxiety-like behaviours observed in p75NTR-/- mice (175). A thorough analysis from Dr. Elizabeth Coulson's group extended upon this, demonstrating that survival rates of cortical pyramidal neurons, interneurons, cholinergic basal forebrain neurons, and striatal neuron are all reduced in p75NTR-/- mice *in vivo*, coinciding with volume reduction of the respective brain structures (178). Moreover, survival of neural progenitors in the CNS is strongly reduced in Nestin-Cre $p75NTR^{flox/flox}$ conditional knockout mice (178).

1.4.5.2 p75NTR regulation of neurite outgrowth

p75NTR regulates axonogenesis in numerous populations of developing peripheral and central neurons. p75NTR-mediated growth cone and axonal dynamics are strongly influenced by the presence, or absence, of a neurotrophic ligand. In general, NT stimulates growth cone expansion and neurite outgrowth via p75NTR; whereas trophic factor withdrawal generally induces growth cone collapse and axonal destruction.

In 1999, Dr. Yves Barde's group published a sentinel paper demonstrating that p75NTR regulated axonogenesis in retinal ganglion cells (RGCs) via co-ordination of Rho GTPase activity. In this study, it was determined that endogenous p75NTR in RGCs associates with RhoA. In the absence of neurotrophin, p75NTR activated RhoA to inhibit neurite outgrowth. Upon NT stimulation, p75NTR suppressed RhoA to promote neurite extension *in vitro* and *in vivo*. This study laid the foundational knowledge that p75NTR regulates axonogenesis via downstream co-ordination of Rho GTPases and subsequent remodelling of the actin cytoskeleton. Since this initial discovery, it has been established that p75NTR is required for: NGF-dependent neurite outgrowth in: DRG sensory neurons (182), sympathetic neurons (180,189), cerebellar Purkinje neurons (193), and PC12 cells (183,191,192).

NGF/p75NTR-dependent neurite extension requires coordinated downstream activation of Rac1 (179,183,184,187,189) and suppression of RhoA (181). The mechanism by which the NGF/p75NTR complex activates Rac1 in this context is unclear, but external evidence suggests a role for NRAGE (142); whereas p75NTR suppresses RhoA via activation of the transmembrane protein Kidins220, which sequesters RhoA via the RhoGEF adaptor Trio (187).

Although NTs and proNTs are generally antagonistic in nature, this may not be case within the context of neurite extension in SCGs (190). Dr. Alun Davies' group discovered that

proNGF, like mature NGF, signals neurite extension via p75NTR in cultured sympathetic axons (190). Perplexingly, proNGF had no effect on neurite dynamics within trigeminal sympathetic neurons, although promoted extension in all other sympathetic neuron subpopulations (190). More investigation into the role of proNTs in neurite dynamics is required to determine if NT/proNT functional antagonism applies within this context.

Lastly, growth cone dynamics largely determine neurite fate within developing axons: growth cone filopodial expansion or collapse precede neurite extension or destruction, respectively (229). Growth cone dynamics are regulated by Rho GTPases, with Rac1 and Cdc42 driving filopodial and lamellipodial extension, and RhoA driving collapse [reviewed in (179)]. p75NTR mediates growth cones dynamics in a ligand-dependent manner via downstream coordination of Rho GTPase activity (185,186,188,189). In developing RGCs and DRG sensory axons, unliganded p75NTR locally activates RhoA in growth cone to drive growth cone collapse (185). Similarly, proNGF binding to p75NTR drives growth cone collapse in central neurons via inhibition of Rac1 (188). Mechanistically, proNGF binds the p75NTR-SorCS2 complex, which triggers dissociation of Trio from the complex and localized suppression of Rac1 (188). Interestingly, both monomeric and dimeric p75NTR are capable of mediating proNGF-induced growth cone collapse (71), indicating that a SorCS2-independent mechanism must exist. In direct contrast to unliganded or proNT-bound p75NTR, NGF-bound p75NTR actively drives filopodial extension via downstream activation of Rac1 and subsequent actin nucleation by the Arp2/3 complex (183).

1.4.5.3 p75NTR regulation of axon guidance

p75NTR is most abundant in long-projection neurons (e.g. peripheral sensory, sympathetic and motor neurons; basal forebrain cholinergic neurons; cerebellar Purkinje

neurons; and RGCs) (230). It comes as little surprise, then, that p75NTR regulates axonal pathfinding during development of these far-reaching neuronal populations (194,195,231–234). Target-derived NTs not only drive neuronal survival, but also guide axons as chemoattractant factors as axons extend towards their target (231). DRG axons extend toward localized physiological doses of NGF *in vitro*, an effect which is abolished in a TrkA-/- or p75NTR-/- background, but engages a pathway distinct from survival signaling (231). In addition to NTs, p75NTR transduces chemorepellent signals from several major axon pathfinding ligands, including: A-class ephrins (195,233), B-class ephrins (232,234), and semaphorins (194,232).

The Ephrin-Eph axon pathfinding system utilizes forward (Ephrin ligand→Eph receptor) and reverse (Eph→Ephrin) signaling to guide axons in response to external ligand/receptor gradients (235). A-class ephrin ligands are GPI-linked to the plasma membrane and do not possess an intracellular domain (235). To transduce reverse Ephrin-A signaling, Ephrin-A ligands recruit p75NTR as a co-receptor to initiate axon repulsion in response to EphA binding (195). For instance, the developing retinocollicular neural pathway secretes a high-to-low gradient of EphA along the anterior-posterior axis (i.e. high [EphA] in the retina, low [EphA] in the superior colliculus (SC)] to drive RGC axon pathfinding towards the SC (236). p75NTR-/- RGC axons show no chemorepulsion to EphA *in vitro* or *in vivo*, resulting in an aberrant anterior shift in the retinocollicular topography (195). Interestingly, *in vitro* pharmacological evidence suggests that autocrine proBDNF release from RGC axons may be required for ephrinA/p75NTR-mediated EphA repulsion (233).

B-class ephrins possess a signaling-competent ICD, but require p75NTR for forward signaling (232,234). Ephrin-B2 induces growth cone collapse and axon repulsion in developing sympathetic neurons, which is abolished in a p75NTR-/- background (232). Ephrin-B2/p75NTR-

mediated axon repulsion requires downstream activation of RhoA within the growth cone (232). In the CNS, p75NTR-/- RGC axons fail to repel Ephrin-B3 (234). Ephrin-B3/p75NTR-mediated axon repulsion also requires localized downstream RhoA activation (234). Interestingly, although p75NTR is required for axonal chemorepulsion of B-class ephrins, no physical Ephrin-B/p75NTR complex has been successfully purified (232,234). Therefore, it remains unclear if p75NTR acts as a receptor/co-receptor to B-class ephrins or in parallel to an Ephrin-B/Eph complex.

Semaphorin3A (Sema3A) is an axonal chemorepellent that binds to a cell surface receptor complex of Neuropilin-1 and PlexinA4 to signal axon repulsion (237). Interestingly, p75NTR-/- DRG axons are hypersensitive to Sema3A-mediated repulsion cues (194). p75NTR physically interacts with—and sequesters—Neuropilin-1 and PlexinA4 in DRG growth cones, thereby restricting the availability of Neuropilin-1/PlexinA4 complex at the growth cone surface ready to respond to Sema3A (194). Conversely, sympathetic axons require p75NTR to mediate Sema3A- and Sema3F-dependent repulsion via downstream activation of RhoA within the growth cone (232). Thus, p75NTR mediates Sema3 axonal repulsion cues in a functionally distinct manner dependent on neuronal subtype.

1.4.5.4 p75NTR regulation of myelinating glia

Myelinating glia—oligodendrocytes (ODs) in the CNS and Schwann cells (SCs) in the PNS—require p75NTR for survival (132,134), migration (182,196,197), and myelination (198,199) in the developing nervous system. During embryogenesis, migrating SCs express p75NTR, but no Trk receptor. Anton and colleagues (1994) first explored SC responses to NGF and determined that exogenous and endogenous NGF stimulated SC migration along the sciatic nerve *in vivo* (196). Consistent with their NT receptor expression profile, NGF-induced SC

migration was found to be p75NTR-dependent (196). Dr. Eric Shooter's group later established that NT ligands stimulate SC migration via downstream co-activation of Rac1 and Cdc42 (197). BDNF is an exception, as it inhibits SC migration via downstream engagement of RhoA (197). More recent genetic evidence has demonstrated that p75NTR-/- SCs are deficient in migration to DRG axons at E12.5—a timepoint at which these axons are searching for target-derived NGF—which resulted in aberrant fasciculation of peripheral sensory nerves (182).

Target-derived NTs not only stimulate SC migration, but they provide trophic support to SCs themselves (132,134). Dr. Moses Chao's group firmly established that NGF promotes SC survival via activation of the NFκB axis downstream of the NGF/p75NTR complex (134). Mechanistically, the NGF/p75NTR complex recruits TRAF6 (134) and RIP2 (132) to the ICD to initiate survival signaling, as readout by nuclear accumulation of the p65 NFkB subunit (132,134).

Once SCs have successfully survived, migrated, and reached their axonal target, p75NTR is further required for myelination (198,199). At this stage, the polarity protein Par-3 binds and localizes p75NTR to the axon-glial interface (198). Knockdown of Par3 or p75NTR, or disruption of Par-3/p75NTR targeting to the axon-glial interface, severely inhibits myelination (198). Once localized to the axon-glial interface, p75NTR activates Rac1 in a NT-dependent manner to drive myelination in SCs (199).

1.4.5.5 p75NTR regulation of neuronal proliferation and migration

NT signaling through Trk receptors is crucial for correct migration of neurons and neural precursors in the developing CNS [reviewed in (238)]. Recent evidence has shown an antagonistic function of proNT/p75NTR signaling in the negative regulation of neuronal migration, specifically in the cerebellum (201,202). p75NTR is enriched in proliferating

cerebellar granule cell precursors (GCPs) as well as differentiated, migrating granule cells (GC) (77). During GCP proliferation, p75NTR promotes cell cycle exit via RhoA to restrain GCPs from excessive proliferation (202). In a p75NTR-/- background, the GCP cell cycle is accelerated, resulting in: delayed cell cycle exit, excessive proliferation, and excessive glutamatergic innervation of Purkinje neurons (202). p75NTR-dependent restriction of GCP proliferation is required for healthy cerebellar function, as excessive GCP proliferation in p75NTR-/- mice is associated with deficient cerebellar-dependent learning in a delayed eyeblink conditioning paradigm (202). With respect to ligand requirement, GCP proliferation is abolished by infusion of a proBDNF function-blocking antibody, an effect that is absent in p75NTR-/- mice (201). Thus, BDNF/TrkB signaling promotes GCP proliferation (239), while proBDNF/p75NTR signaling restricts this proliferation (201,202). In this manner, NT/proNT antagonism serves to ensure an optimal neurogenic rate and connectivity within the cerebellar granule layer.

1.4.5.6 p75NTR regulation of synaptogenesis

Recent evidence has shown a requirement for p75NTR in synaptogenesis within distinct neuronal subpopulations in the CNS (203) and the periphery (204). For example, parvalbumin^{+} (PV) inhibitory interneurons form extensive synaptic connections within the developing cortex in order refine the electrophysiological properties of mature cortical circuits [reviewed in (240)]. Basal p75NTR immunoreactivity is detected in PV interneurons during embryonic development, but drops drastically during the 2nd to 4th postnatal week—the adolescent timepoint at which PV synaptogenesis accelerates (203). Conditional p75NTR knockout in PV interneurons results in perisomatic hyperinnervation and aberrant formation of perineural nets (203). Therefore, it postulated that p75NTR coordinates the timing of the adolescent critical period via basal

inhibition of PV interneuron synaptogenesis in embryonic and early postnatal development (203).

In direct contrast to its role in PV interneurons, p75NTR promotes neuromuscular synaptogenesis in cholinergic motoneurons (204). p75NTR-/- neuromuscular junctions (NMJs) develop major structural and functional abnormalities, including: immature postsynaptic organization, reduced structural complexity, weakened nerve stimulation-induced muscle contraction, weakened force production, and impaired locomotion (204). NMJ maturation specifically requires presynaptic p75NTR (204). p75NTR-/- NMJ presynapses show a major depletion in the readily releasable pool of acetylcholine^{+} vesicles (204). Thus, p75NTR is required for neurotransmitter release in motoneurons—and potentially in other neuronal populations—though it is entirely unclear how this function is regulated by p75NTR at a mechanistic level.

1.4.6 p75NTR in developmental neurodegeneration

Despite the broad functionality of p75NTR in mammalian neurodevelopment [as outlined in Section 1.4.5], analyses of the arthropod p75NTR ortholog, Wengen (wgn), in *Drosophila melanogaster* established a conserved evolutionary function for p75NTR as a major executor of developmental neurodegeneration (84,85,87,88,241,242). Developmental neurodegeneration refers to the systematic removal of aberrant neuronal processes, or entire neurons, in a biologically regulated manner. p75NTR is required for developmental neurodegeneration in central and peripheral neuronal populations, including: SCG sympathetic neurons (51,137,139,143,144,156,168,176,208,213,217,222), cholinergic basal forebrain (cBF) neurons (31,207,214,216,218,220,221), hippocampal neurons (174,188,210,215,224), cortical neurons

(71,148,223,226), cerebellar granule cells (CGNs) (59,225), Purkinje neurons (193,212), retinal ganglion cells (RGCs) (141,209), and, possibly, DRG sensory neurons (170,177,219,243).

p75NTR is, at its core, a death receptor. As such, p75NTR-mediated neurodegeneration requires death signaling via the mitochondrial apoptotic pathway culminating with the activation of executioner caspases [reviewed in (71,200)]. The core p75NTR-mediated neurodegenerative mechanism involves downstream mitochondrial accumulation of Bax, which drives mitochondrial outer membrane permeabilization (MOMP) and subsequent release of mitochondrial apoptotic factors—including cytochrome c (cyt c)—into the cytosol (77). Cytochrome c release enables formation of the caspase-9/Apaf1/cytochrome c apoptosome, and subsequent procaspase-3 proteolytic cleavage to generate active cleaved caspase-3 (cCasp3) (77). cCasp3 cysteine protease activity physically cleaves neuronal substrates to initiate neurodegeneration (77,244). cCasp3 can be locally restricted by IAP family members, particularly XIAP in neurons, to confine neurodegeneration to a specific neuronal compartment (244,245). Unrestricted cCasp3 activation will initiate complete neuronal apoptosis (244). In parallel to caspase-3 activation, MOMP activates the pro-apoptotic kinase JNK, which serves as a retrograde neurodegenerative signal to drive expression of anterograde pro-apoptotic factors (138,159,211).

This core p75NTR-dependent neurodegenerative program shows minor mechanistic variability across neuronal populations, owing to the distinct subsets of p75NTR adaptors expressed by a given neuronal population (77). In the sub-sections that follow, the role of p75NTR in developmental neurodegeneration in distinct neuronal populations is reviewed, with an emphasis on the specific mechanisms engaged by p75NTR at the receptor level.

1.4.6.1 p75NTR-dependent developmental neurodegeneration in SCG sympathetic neurons

Developing SCG sympathetic compete for target-derived NGF in the periphery (208). Endocytosis of the NGF-TrkA complex and subsequent retrograde trafficking of the NGF-TrkA signaling endosome to the nucleus are required for SCG neuronal survival (217). In contrast, target-derived BDNF acts a pro-apoptotic factor that induces axonal degeneration and neuronal death (208). Genetic studies in BDNF-/- and p75NTR-/- mice demonstrated that BDNF-induced sympathetic neuron death is mediated exclusively by p75NTR, not TrkB, *in vitro* and *in vivo* (208). In distinct $p75NTR^{+}sortilin^{+}$ SCG subpopulations, proBDNF can replace BDNF as the target-derived apoptotic ligand (213). As such, local axonal BDNF stimulation, in addition to local NGF withdrawal, became complementary tools to investigate p75NTR-dependent neurodegenerative signaling in SCGs.

In both BDNF stimulation and NGF withdrawal models, NRAGE is required to initiate p75NTR-dependent death signaling via downstream activation of JNK and caspase-3 (113,161,167) and physical disruption of the TrkA-p75NTR high-affinity NGF complex (137). In addition, NRIF ubiquitination and nuclear translocation is required for p75NTR-induced SCG axon degeneration and apoptosis, as NRIF-/- sympathetic neurons are insensitive to NGF withdrawal (143) and BDNF stimulation (144). ADAM17- and γ-secretase-mediated p75NTR processing—to release the p75ICD—are required for the SCG death signal in NGF withdrawal and BDNF stimulation models (144,156,168). p75ICD-induced JNK activation drives further p75NTR proteolysis in a feedforward signaling loop in this context (168). Soluble p75ICD is required for the nuclear translocation of NRIF (144) and JNK activation (168), but may be required in other capacities at the soma (156). Retrograde endosomal trafficking of p75ICD to the nucleus—to transduce the apoptotic signal—involves an interaction with axonal histone

deacetylase 1 (HDAC1), which deacetylates the dynactin subunit $p150^{glued}$ to enable dynein-mediated transport (156).

1.4.6.2 p75NTR-dependent developmental neurodegeneration in cholinergic basal forebrain neurons

In the CNS, developmental neurodegeneration of cholinergic basal forebrain (cBF) neurons is dependent on p75NTR death signaling (31,207,214,216,218,220,221). Deficiencies in p75NTR-dependent cBF neurodegeneration results in diffuse cholinergic hyperinnervation in the cortex (220,221), hippocampus (207,216), and basolateral amygdala (31), which can lead to diverse cognitive (220) and affective (31) behavioural pathologies.

In 1997, Dr. William Mobley's group established that $TrkA^+$ cBF neurons—which require NGF for survival—heavily depend on p75NTR to execute developmental neurodegeneration *in vivo* (207). Conditional p75NTR KO in cholinergic neurons (ChAT-cre;$p75NTR^{fl/fl}$) results in increased cBF neuron count, cBF neuron size, and cortical cholinergic innervation (220); features that are absent in neighbouring cholinergic striatal neurons after full p75NTR KO (207). p75NTR-dependent apoptosis in cBF neurons is induced by NGF withdrawal or proNGF simulation (214,218). p75NTR-mediated cBF neuronal death relies on (i) downstream caspase-3 activation; and (ii) inhibition of Trk survival signaling via PI3K/Akt, MEK/ERK, and PTEN (phosphatase and tensin homolog deleted on chromosome 10) (214,218). PTEN, in particular, serves as a molecular switch between Trk-dependent survival and p75NTR-dependent apoptosis in cBF neurons (218). In parallel, the local presence of myelin can induce p75NTR-mediated axonal degeneration of cBF neurons *in vivo* dependent on RhoGDI sequestration to the p75NTR ICD and downstream activation of RhoA and caspase-6 (216).

1.4.6.3 p75NTR-dependent developmental neurodegeneration in the hippocampus

The developing hippocampus relies on p75NTR to eliminate excessive neurons and neuronal processes (188,210,215,224). Strikingly, all mature neurotrophins (NGF, BDNF, NT3 and NT4) are all capable of inducing p75NTR-dependent death in hippocampal neurons via the JNK pathway *in vitro* (210). *In vivo*, however, p75NTR-dependent developmental apoptosis of hippocampal neurons is induced by proNGF and mediated by the p75NTR-Sortilin co-receptor complex (224). Endocytosis of the intact proNGF-p75NTR-Sortilin complex is required to execute apoptosis (224). Following endocytosis of the ligand-receptor complex, p75NTR cleavage and interaction of the soluble p75ICD with NRIF—and subsequent nuclear translocation—mediates the apoptotic signal *in vitro* and *in vivo* (215). p75NTR-dependent hippocampal neuron death is mediated by the mitochondrial apoptotic pathway, and involves: MOMP, cytochrome c release from mitochondria, the caspase-9/Apaf-1 apoptosome, and activation of executioner caspases-3 and -6 (246).

1.4.6.4 p75NTR-dependent developmental neurodegeneration in the cortex

Dr. Phil Barker's group first demonstrated that the soluble p75ICD is a pro-apoptotic factor in the developing neocortex (148). Transgenic mice expressing p75ICD in a pan-neuronal marker exhibit massive cortical neuron loss, where endogenous p75NTR expression is minimal during development (148). p75ICD-induced cortical neuron death occurred independent of Trk survival signaling, thereby implicating a p75ICD-specific death pathway (148). With respect to ligand requirement, proNGF can induce growth cone collapse, axonal degeneration, and complete apoptosis in cultured cortical neurons; however, it is unclear if a proNGF-mediated mechanism is physiologically relevant *in vivo* (71).

Cajal-Retzius cells (CRCs)—a neuronal subpopulation localized to superficial cortical layers I/II—guide cortical circuit formation early in development, then die off within the first

postnatal week (P4-P8 in mice) (247). Programmed death of CRCs requires a unique excitotoxic mechanism dependent on p75NTR and the chloride transporter NKCC1 (*Slc12a2*) (223). Once integrated into a cortical circuit, CRCs are depolarized by GABA, rather than hyperpolarized—due to disproportional Cl- influx via NKCC1 with little Cl- efflux via the KCC2 transporter (an NKCC1 homolog) (223). This GABA-induced depolarization induces excitotoxic death in a p75NTR-dependent manner (223). Though it remains unclear how p75NTR mediates this death, an independent study from Riffault and colleagues (2018) showed that proBDNF-bound p75NTR inhibits Cl- efflux via KCC2 in GABA-responsive cortical neurons (226). Thus, it is possible p75NTR regulates developmental death of CRCs via regulation of NKCC1 or KCC2, but no physical interaction between p75NTR and NKCC1/KCC2 has been identified.

1.4.6.5 p75NTR-dependent developmental neurodegeneration in the cerebellum

In the embryonic and early postnatal cerebellar granule layer, p75NTR is abundant in CGNs, not only to coordinate their migration [as reviewed in Section 1.4.5.5], but to initiate developmental apoptosis (59,225). Mechanistically, p75NTR-dependent death relies on mutual exclusivity RIP2 and TRAF6 with respect to p75NTR binding (225). In RIP2-expressing CGNs, RIP2 binding to the p75NTR ICD excludes TRAF6 and vice versa (225). In RIP2-negative CGNs, however, the p75NTR-TRAF6 interaction is unimpeded, enabling p75NTR/TRAF6-mediated activation of the JNK pathway and neuronal death (225). Moreover, myelin-derived MAG from the cerebellar white matter is capable of inducing CGN death via the p75NTR-JNK axis, requiring MAG binding to the p75NTR/NgR1/LINGO-1 complex (59). MAG-induced CGN apoptosis in development is required for establishing the boundary between the cerebellar granule layer and white matter (59).

In the Purkinje layer of the cerebellum, p75NTR expression is relatively low throughout development, but persists into adulthood, unlike in CGNs (93). As in CGNs, p75NTR regulates developmental neuron death of Purkinje neurons (193,212). Curiously, p75NTR induces Purkinje neuronal death via activation of autophagy (212), in stark contrast to the JNK-mediated pathway in CGNs (225). In Purkinje neurons failing to acquire target-derived NGF, unliganded p75NTR induces autophagic vacuolation and subsequent neuronal death (212). Conditional p75NTR KO in murine Purkinje neurons (Pcp2-Cre:p75NTR$^{fl/fl}$) results in the development of autism-like phenotypes, such as: less allogrooming of conspecifics, less socialization, less play-fighting, less non-ambulatory environmental exploration, and stereotyped jumping behaviour (193). Thus, p75NTR-dependent developmental culling of Purkinje neurons is required for cerebellar function and social behaviour in adulthood. Insight into the mechanism underlying p75NTR-induced autophagy in this context is still needed.

1.4.7 p75NTR in pathological neurodegeneration

p75NTR drives developmental neurodegenerative programs in diverse neuronal populations within the CNS and PNS [reviewed in Section 1.4.6]. It is of little surprise, then, that aberrant p75NTR neurodegenerative signaling is implicated in the etiology of various neurodegenerative disease states, including: Alzheimer's Disease (248–259), status epilepticus (140,214,215,218,224,226,246,260), traumatic brain injury (261–269), spinal cord injury (62,270–272), retinopathy (273–278), Huntington's Disease (279–282), multiple sclerosis (283–285), and viral encephalopathy (286–288).

1.4.7.1 p75NTR in Alzheimer's Disease

Accumulation of amyloidogenic beta-amyloid (Aβ) is a hallmark of Alzheimer's Disease (AD) and drives pathological neurodegeneration of cholinergic basal forebrain (cBF) neurons of

the septohippocampal pathway that innervate the hippocampus [for recent review on the Aβ hypothesis, see (289–292)]. Progressive loss of cBF neurons results in cognitive impairment, particularly in hippocampal-dependent memory systems [reviewed in (293)]. Seminal studies in the late 1990s established p75NTR as an Aβ receptor capable of inducing neuronal apoptosis upon Aβ binding *in vitro* and *in vivo* (294–298). In 2008, Dr. Elizabeth Coulson's group firmly established a pathological Aβ-p75NTR pathway in the septohippocampal pathway, as intrahippocampal injection of exogenous Aβ induced massive death of cBF neurons in wild-type mice—a phenotype that was absent in p75NTR-/- mice (248). Aβ induces p75NTR cleavage *in vivo*, which initiates the p75NTR degenerative signal in cBF neurons (248). Aβ-p75NTR-induced neurodegeneration is an early feature of AD, driving local synaptic elimination between cBF and hippocampal neurons in early AD, eventually leading to complete neuronal destruction as the disease progresses (257). Upstream of Aβ production, p75NTR binds the amyloid precursor protein (APP) at the plasma membrane to inhibit APP internalization and promote amyloidogenic APP proteolytic cleavage in hippocampal neurons (299). Lastly, ProNT/p75NTR signaling has been shown to augment Aβ/p75NTR-induced cBF neuron death, as proBDNF drives Aβ accumulation (253) and proNGF drives tau hyperphosphorylation (255) (the other major hallmark of AD) and JNK activation (257,258) via p75NTR, resulting in a feedforward mechanism of catastrophic cBF neurodegeneration.

Consistent with these initial studies, p75ECD accumulation in the CSF and blood was initially identified as a reliable biomarker for AD diagnosis, particularly in combination with CSF Aβ and CSF phospho-tau181 (249). Targeting p75NTR has recently shown promising clinical potential in animal models of AD (54,250–252). In several mouse models, intrahippocampal (250) or intramuscular (252) injection of p75ECD-Fc—which binds Aβ

without inducing death—significantly attenuates AD-like phenotypes, including: Aβ accumulation, tau hyperphosphorylation, dendritic spine loss, neuronal death, neuroinflammation, and cognitive impairment (250,252). In parallel, immunological targeting of the Aβ-binding region on p75NTR [CRD2 and CRD4 (256)] has shown efficacy in reducing cBF neuronal death in olfactory bulbectomized mice (an infrequently used AD mouse model), representing another potential therapeutic avenue.

Thus, amyloidogenic Aβ drives cBF neuronal death via p75NTR in AD. Pharmacological candidates targeting the Aβ/p75NTR complex show potential for ameliorating AD-associated neurodegeneration in a field that has endured decades of clinical struggles.

1.4.7.2 p75NTR in status epilepticus-induced neurodegeneration

Temporal lobe epilepsy (TLE) involves periodic seizure activity originating from a localized focal point(s) within a subcortical limbic structure, particularly the hippocampus or entorhinal cortex [reviewed in (300)]. Repeated excitotoxic events (seizures) in TLE result in unilateral, progressive neurodegeneration in the dentate gyrus (DG) and cornu ammonis (CA) subregions of the hippocampus (301). These central features of TLE are recapitulated in status epilepticus (SE) murine models, including the current ‘gold standard’ pilocarpine model, which involves systemic injection of the cholinergic agonist pilocarpine [reviewed in (302)].

p75NTR mediates SE-induced hippocampal neuronal death *in vivo*. Pilocarpine-induced epileptiform activity results in hippocampal p75NTR upregulation (303) and p75NTR-induced neuronal apoptosis via the intrinsic mitochondrial pathway and downstream caspase-3 and -6 activation (246). Post-SE, p75NTR-/- hippocampi show no increase in cCasp3 immunoreactivity and a stark reduction in neuronal death (246). At the receptor level, p75NTR signaling via

NADE (140) and NRIF (214) is required for downstream caspase-3 activation; and PTEN acts to suppress TrkB survival signaling (218).

In the context of SE, proNT ligands activate the p75NTR death signal (214,215,218,224,226,260,304). Antibody-based sequestration of hippocampal proBDNF protected hippocampal neurons from pilocarpine treatment *in vitro* and *in vivo* (260,304). Moreover, proNGF—likely originating from astrocytes during SE (214)—binding to the p75NTR-sortilin complex contributes to pilocarpine-induced neuronal death *in vitro* and *in vivo* (214,224). Interestingly, lithium citrate—a commonly prescribed antipsychotic medication—effectively disrupts p75NTR-sortilin complex formation and internalization *in vivo*, and attenuates proNGF/p75NTR-mediated neuronal apoptosis post-SE (224). This represents a potential therapeutic approach to ameliorating p75NTR-dependent hippocampal neuronal loss in TLE patients.

1.4.7.3 p75NTR in traumatic brain injury

Early evidence for a role of p75NTR in traumatic brain injury (TBI)-induced neuronal death came from an *in vivo* study showing peri-infarct hippocampal neurons undergo p75NTR-dependent apoptosis via NADE and downstream caspase-3 activation (261). In TBI, specifically, proNGF is strongly upregulated in the injured cortical tissue, resulting in pathophysiological p75NTR death signaling an subsequent neuronal apoptosis (262). Transgenic mice lacking the proNGF-binding site, or wild-type mice injected with a p75NTR inhibitor (TAT-Pep5 or EVT901), show a stable reduction in lesion volume post-TBI and improved functional outcome (263,265,266). Moreover, p75NTR knockdown prior to irradiation-induced CNS injury prevents loss of hippocampal dendritic spines and promotes functional recovery of hippocampal-dependent cognition (267). Outside of injured neurons, mononuclear cell and astrocytic p75NTR

contribute to localized inflammation and astrocytosis post-TBI, however it remains unclear if this non-neuronal p75NTR directly contributes to neurodegeneration (264,266).

1.4.7.4 p75NTR in spinal cord injury

After a spinal cord injury (SCI), axonal regeneration in the spinal cord is inhibited due to plethora of axonal intrinsic and extrinsic factors [reviewed in (305)], and one such inhibitory factor is p75NTR (62,270–272). In severed spinal cord (SC) axons, the p75NTR/NgR1/LINGO-1 complex binds myelin-associated inhibitory factors—MAG, Nogo and OMgp—to inhibit neurite regeneration by downstream engagement of RhoA, which locally drives actin polymerization (62). Sustained activation of this p75NTR-RhoA axis may also drive neuronal apoptosis in injured SC neurons (271). Outside the injured axon, local proNGF binds oligodendrocyte-derived p75NTR to induce apoptotic clearance of oligodendrocytes (270). Pharmacological blockade of p75NTR-RhoA axis via p75ECD-Fc injection promotes axonal regeneration and functional recovery in a rat SCI model (272), indicating that p75NTR may be a targetable candidate on the path towards clinical restoration of spinal cord connectivity post-SCI.

1.4.7.5 p75NTR in retinopathy

Diabetic retinopathy is associated localized inflammation, glial activation, vascular dysfunction and pathological neurodegeneration of retinal ganglion cells (RGCs) in the retina [reviewed in (306)]. The proNGF-p75NTR signaling axis has been implicated in each aspect of this degenerative disease (275,278). In a mouse model of diabetic neuropathy—the streptozotocin model— proNGF (278) and p75NTR (275) are upregulated in the retina. In multiple diabetic neuropathy mouse models, the proNGF-p75NTR complex drives: inflammatory cytokine production, blood-retina barrier breakdown, disassembly of the neuro-glia-vascular unit, edema, and RGC neuronal death (275). Pharmacological blockade of p75NTR signaling,

with the small molecule compound LM11A-31, mitigated proNGF action and reduced retinal neuroinflammation and neurodegeneration (278).

Excitotoxic RGC neuronal death is also mediated by the proNGF-p75NTR axis, but involves a non-cell-autonomous mechanism (273,274). Local application of proNGF induces activation of the NFκB axis in Müller glia via the p75NTR-sortilin complex (274). This activated NFκB induces expression, and extracellular release, of TNFα, which acts on RGCs to trigger neuronal death (273,274). This non-cell-autonomous mechanism can be induced by exogenous NMDA (273), and thus represents a major excitotoxic RGC neuronal death pathway.

Lastly, aberrant proNGF-p75NTR signaling is implicated in retinitis pigmentosa (RP)—an inherited neurodegenerative disease characterized by progressive photoreceptor death (276). In a mouse model of RP, proNGF is upregulated immediately prior to photoreceptor death. proNGF induced p75NTR-dependent photoreceptor death and TNFα secretion; an effect which was ameliorated by pharmacological p75NTR antagonists (276). p75NTR-dependent neurodegeneration and neuroinflammation in RP not only resembles the excitotoxic RGC death mechanism (273,274), but closely mimics Egr/Wgn-induced photoreceptor death in *Drosophila melanogaster* (88). It is possible p75NTR regulation of neuronal apoptosis in the retina represents an evolutionarily conserved pathway.

1.4.7.6 p75NTR in Huntington's Disease

Huntington's Disease (HD) is an inherited neurodegenerative disorder caused by a trinucleotide repeat expansion within the Huntingtin (Htt) gene, resulting in Htt aggregates in the CNS and subsequent dysfunction in motor and cognitive processes (307). Widespread neurodegeneration in the striatum, hippocampus and cortex is observed in HD pathology (307). Recent evidence from Dr. Silvia Gines' group has established an imbalance in TrkB/p75NTR

neurotrophic vs. neurodegenerative signaling as a driver of pathological neurodegeneration in HD (308). In early HD, p75NTR drives synaptic elimination in the hippocampus and corticostriatal pathway via hyper-activation of the RhoA (309) and PTEN (310) signaling axes, respectively. Genetic deletion of p75NTR delays, but does not abolish, striatal neurodegeneration and motor dysfunction in a murine HD model (282). Intriguingly, pharmacological targeting of p75NTR directly with LM11A-31 (281), or indirectly with fingolimod (279), partially restored striatal and hippocampal spine density, and improved motor performance and cognition in the BACHD mouse model of HD. Thus, pharmacological p75NTR inhibition may represent a useful strategy for symptom management in HD but will likely be insufficient to fully prevent neurodegeneration.

1.4.7.7 p75NTR in multiple sclerosis

Multiple sclerosis (MS) is characterized by inflammatory demyelination and axonal degeneration in the PNS (311). Though a comprehensive model of MS etiology remains elusive, recent evidence from the experimental autoimmune encephalomyelitis (EAE) MS mouse model implicates p75NTR as a of driver peripheral demyelination and axonopathy in MS (283–285). p75NTR is locally upregulated in axons and oligodendrocytes at inflammatory lesion sites in the SC of EAE mice (284,285) and human MS patients (312). At this site, axonal p75NTR/NgR1/LINGO-1 complex acts to transduce inhibitory myelin signals via RhoA activation to inhibit axonal regeneration (313,314) and oligodendrocyte-derived p75NTR drives local oligodendrocyte death (270), a mechanism that has been postulated—but not definitively proven—to occur in EAE/MS (284). In support of this hypothesis, pharmacological stimulation of p75NTR cyclo-dPAKKR—a mimetic of BDNF-binding to the p75ECD—strongly attenuates inflammatory demyelination and axonal degeneration, co-incident to improved motor function,

in EAE mice (283). Thus, pharmacological approaches mimicking NT activation of p75NTR may be worth investigating in a clinical setting.

1.4.7.8 p75NTR mediates synapse elimination in HIV

The envelope protein (gp120) of human immunodeficiency virus-1 (HIV) triggers aberrant elimination of excitatory synapses in cortical and subcortical CNS regions [reviewed in (315)]. In gp120-expressing transgenic (gp120tg) mice, p75NTR haploinsufficiency rescued hippocampal synaptic density to wild-type levels, implicating p75NTR in gp120-induced synapse loss (286). This effect was recapitulated by Dr. Italo Mocchetti's group, who extended upon this finding by showing local proBDNF upregulation in the gp120tg hippocampus stimulated this p75NTR-dependent synapse elimination (288). At the behavioural level, p75NTR haploinsufficiency rescued cognitive deficits in gp120tg mice (288), revealing potential therapeutic merit in targeting p75NTR to stave off cognitive symptoms in HIV patients.

1.4.8 p75NTR regulation of synaptic plasticity in the CNS

In the mature CNS, low—but biologically active—levels of p75NTR persist in the hippocampus, cortex, and extrahippocampal subcortical structures (93). In this post-developmental context, p75NTR actively regulates synaptic plasticity to maintain nervous system function. Dysregulation of p75NTR-dependent synaptic plasticity is strongly associated with several neuropsychiatric disorders.

1.4.8.1 p75NTR regulation of hippocampal synaptic plasticity

Seminal papers from Dr. Yves Barde and Dr. Barbara Hempstead's laboratories demonstrated that p75NTR is required for induction of synaptic long-term depression (LTD), but not long-term potentiation (LTP), in the adult hippocampus (316,317). At Schaffer collaterals, proBDNF binds postsynaptic p75NTR to induce LTD via a mechanism that is NMDAR-

dependent (317) and drives internalization of AMPAR subunits GluR2 and GluR3, but not GluR1 or GluR4 (316). Postsynaptic proBDNF/p75NTR-dependent LTD antagonizes a postsynaptic BDNF/TrkB-dependent LTP (318,319), establishing NT/proNT functional antagonism as a major regulatory mechanism of hippocampal synaptic plasticity. Local co-ordination of Rho GTPases Rac1, RhoA and Cdc42 at dendritic spines is required for structural LTP (sLTP) in the BDNF-TrkB axis (319), and antagonistic Rho GTPase regulation by proBDNF/p75NTR is postulated to drive sLTD (320).

p75NTR regulates inhibitory tone in the hippocampus via maintenance of chloride homeostasis in innervating GABAergic neurons (226). Mechanistically, a proBDNF/p75NTR axis augments Cl- influx via KCC2 to maintain a high intracellular Cl- concentration (226). p75NTR-dependent Cl- regulation is required to maintain inhibitory GABAergic responses, and a failure to do so—such as after CNS injury (321)—can disinhibit glutamatergic hippocampal neurons to increase seizure susceptibility (226). BDNF-TrkB antagonizes proBDNF/p75NTR by suppressing GABAergic neurotransmission (322), extending NT/proNT functional antagonism as a major regulator of hippocampal plasticity in multiple neuronal subpopulations.

Hyperactivation of the hippocampal proBDNF/p75NTR LTD axis, and hypoactivation of the BDNF-TrkB LTP axis, is observed in age-related cognitive decline (320). Restoration of p75NTR/TrkB balance via intrahippocampal injection of TAT-Pep5 significantly improved cognitive performance and memory in wild-type mice in late adulthood (320). In addition, hyperactivation of p75NTR-dependent LTD is observed following sleep deprivation (323), highlighting the balance BDNF/proBDNF axes as a major regulatory checkpoint in hippocampal-dependent cognitive function.

1.4.8.2 p75NTR regulation of extrahippocampal synaptic plasticity

p75NTR mediates synaptic plasticity in extrahippocampal structures—particularly limbic structures—including the: medial entorhinal cortex (mEC) (324,325), medial prefrontal cortex (mPFC) (220), amygdala (220), striatum (326), and hypothalamus (327).

The mEC provides cholinergic innervation to the dentate gyrus (DG) and generates rapid bursts of electrical activity known as persistent firing (PF)—a phenomenon required for spatial working memory (328). Dr. Julien Gibon and colleagues (2016) established BDNF/proBDNF functional antagonism as a major regulatory mechanism of PF in layer V mEC neurons (325). At the presynapse, a BDNF-TrkB axis promotes glutamate release, in parallel to a proBDNF-p75NTR axis that inhibits glutamate release (324,325). Presynaptic proBDNF/p75NTR inhibits glutamate release—and subsequent PF—via local depletion of phosphatidylinositol-4,5-bisphosphate (PIP2) in a pathway involving Rac1 and PI4K (324). In p75NTR-/- mice, PF activity is augmented and coincides with improved working memory and increased seizure susceptibility (324).

cBF-derived p75NTR is required for physical and functional synaptic plasticity in the mPFC (220). cBF-specific p75NTR KO results in impaired consolidation of fear extinction relative to wild-type mice (220). Thus, cBF-derived p75NTR is required for homeostatic regulation of synaptic plasticity in the mPFC and mPFC-dependent cognitition.

p75NTR-/- mice display an anxiety-like phenotype, as revealed in multiple behavioural paradigms (31,175). Electrophysiological recording from the basolateral amygdala revealed deficient LTP—an effect independent of antagonistic TrkB (31). Though the mechanism of p75NTR-dependent LTP inhibition in the basolateral amygdala remains unresolved, these studies established that p75NTR-dependent LTP inhibition in the CNS is not specific to the BDNF/TrkB LTP axis.

The dorsolateral striatum (DLS) mediates cue-reward associations (329), including reward responses to alcohol consumption (330). A recent study from Darcq and colleagues (2016) established TrkB/p75NTR antagonism in the DLS as a regulatory mechanism underlying alcohol consumption behavior (326). Knockdown or pharmacological p75NTR inhibition in the DLS significantly attenuates binge drinking behaviour in rats (326). Thus DLS-derived p75NTR functionally antagonizes TrkB to promote alcohol seeking and may be represent a therapeutic target in the context of alcoholism.

AgRP hypothalamic neurons co-ordinate feeding behaviour to external environmental cues (331). AgRP-derived p75NTR negatively regulates food anticipatory behaviour, leading to weight loss in p75NTR-/- mice (327). In conjunction to the role of hepatocyte-derived p75NTR in regulation of lipid metabolism (332,333), this study firmly establishes p75NTR as a major regulator of hypothalamus-dependent food seeking behaviour.

1.4.9 p75NTR signaling in tumorigenesis and metastasis

Although p75NTR is generally a tumour suppressor—via p53 inhibition (334,335)—several cancers have successfully leveraged p75NTR signaling to drive tumour survival, invasion and metastasis, particularly melanoma (336–350) and glioma (163,164,166,351–356) tumours. The switch from tumour suppressive to oncogenic p75NTR appears to depend on receptor cleavage, as soluble p75ICD acts as a major driver of tumour invasion (154,165). Outside the context of melanoma and glioma, p75NTR mediates tumour survival and metastasis in other cancers, including: breast (357–360), gastric (361–364), prostate (365,366), renal (367), bladder (368), and pancreatic (369) cancers; however, our understanding of p75NTR function in these tumour settings is comparatively limited.

1.4.9.1 p75NTR drives melanoma invasion and metastasis

Early research demonstrated that p75NTR was enriched in malignant melanoma (276) and could drive melanoma metastasis in an NGF-dependent manner (336,340). p75NTR itself drives the oncogenic transition from melanocyte to melanoma (345,350). Over the years, it has been firmly established that $p75NTR^{+}$ melanoma subtypes—such as spindle cell and desmoplastic melanoma—are much more invasive and metastatic than $p75NTR^{-}$ melanomas (338,339,341,344,346–348). Moreover, xenografted p75NTR-/- melanoma tumour stem cells fail to develop into a melanoma tumour *in vivo* (345). p75NTR instills a neurotrophic survival mechanism in melanoma, actively engaging survival signaling in response to local NGF or proNGF in the tumour microenvironment (341,343) independent of TrkA (336). The mechanism of p75NTR-dependent melanoma tumour metastasis is incompletely resolved, but likely requires receptor cleavage (165) and downstream activation of Rac1 (370) and TRAF6-NFκB (154) signaling axes. Pharmacological p75NTR inhibition shows great therapeutic promise in melanoma, as small molecule targeting of the p75NTR TMD shifts p75NTR signaling to a constitutive JNK-activating pro-apoptotic state *in vivo* (349).

1.4.9.2 p75NTR drives glioma invasion

Similar to its tumorigenic role in melanoma, p75NTR is a master regulator of NGF-dependent (351,352) survival and invasion of multiple glioma subtypes, including glioblastoma (163,166,355) and medulloblastoma (164,353,354,356). p75NTR-mediated glioma invasion is dependent on receptor cleavage (163–165) and likely involves downstream Rac1 (371,372) and NFκB (154) activation. p75NTR expression is an accepted diagnostic marker of the SHH medulloblastoma subtype and inversely correlates with patient survival (356). Pharmacological inhibition of p75NTR proteolytic cleavage via targeting of the γ-secretase complex is effective in

preventing medulloblastoma metastasis to the spinal cord (164). This γ-secretase-targeting strategy shows therapeutic promise and recently entered Phase I/II clinical trials.

1.5 Death Receptor 6 (DR6)

Death Receptor 6 (DR6) is an orphan TNFRSF that is a major mediator of neurodegeneration—particularly axonal degeneration—in developmental (51,56,58,373) and pathological (57,374–380) contexts. Although DR6 does not bind a TNF ligand, accumulating evidence suggests DR6 is a receptor to the β-amyloid precursor protein (APP) (381,382)—as well as the amyloidogenic Aβ fragment (56,374)—to transduce death signaling in central and peripheral neuron populations.

1.5.1 Structural biology of DR6

Like p75NTR, DR6 is a single-pass type I transmembrane protein primarily localized to the plasma membrane (383) that is highly conserved in vertebrates (384). Mature, post-translationally modified DR6 is slightly larger than p75NTR (101 kDa vs. 75 kDa) and possesses: (i) an N-terminal ECD 349 AA in length that mediates ligand-binding, (ii) a TMD 20 AA in length, and (iii) a C-terminal ICD 285 AA in length that mediates signaling (383).

Like p75NTR, the DR6 ECD possesses 4 CRDs linked in tandem and a long stalk region—approximately 97 AA longer than p75NTR—linking the CRDs to the TMD (383). X-ray crystallography reveals that the DR6 CRDs arrange in a ‘rod-like’ conformation, which exposes DR6-specific motifs that mediate ligand-binding (381), including APP (382). APP-binding to cell surface DR6 via the extracellular ‘E2’ region—including all 4 CRDs—induces DR6 dimerization into an active conformation (382). The DR6 ECD is extensively glycosylated, with N-glycosylation at all 6 asparagine residues, and O-glycosylation at the Ser-Thr-Pro cluster immediately C-terminal to CRD4 (385).

DR6 is a death receptor and, accordingly, possesses a DD within its ICD (383). Like the p75NTR DD, the DR6 DD does not interact with death effectors FADD, TRADD or EDARADD, consistent with the inability of DR6 to activate the extrinsic apoptotic pathway (386). Conflicting reports suggest a DR6-TRADD may exist in specific non-neuronal biological contexts, but this complex has never been demonstrated under physiological conditions (383,387). Although DR6 does not engage the mitochondrial apoptotic pathway, a physical interaction between Bax and the DR6ICD has been reported (386), but the biological implication of this interaction remains elusive. Further, the DR6ICD physically interacts with the necroptosis mediators Receptor-Interacting Serine/Threonine-Protein Kinase 1 and 3 (RIPK1 and RIPK3) to mediate death signaling (78). Lastly, the DR6ICD is S-palmitoylated at a juxtamembrane cysteine residue (Cys368) (385). DR6 palmitoylation at this site does not regulate lipid raft localization and is postulated to mediate signaling (385).

1.5.2 DR6 signaling mechanisms

APP-binding to DR6 in *trans* signals cell death in the DR6-expressing cell via downstream activation of necroptosis (78). APP-bound DR6 recruits RIPK1/3 to its ICD, which in turn recruits caspase-8 to form the ‘necrosome’ that induces MLKL phosphorylation and downstream execution of the necroptosis (78,388). Parallel activation of caspase-8 cleavage—via independent pathways—inhibits APP/DR6-dependent necroptosis (78), indicating caspase-8 serves as the limiting factor in necrosome formation. *In vivo*, tumour-derived APP binds endothelial-derived DR6 in *trans* to induce necroptotic endothelial cell death, thereby promoting tumour metastasis and extravasation (78).

Unlike canonical death receptors, DR6 cannot initiate the extrinsic or intrinsic apoptotic pathway, showing no capacity to induce caspase-8 cleavage or MOMP, respectively (386).

However, DR6 overexpression can induce caspase-3 activation and apoptosis when overexpressed in multiple cell lines (383,386). This DR6 death pathway involves a physical interaction with Bax (386). Therefore, DR6 may be able to induce executioner caspase activation via an unknown Bax-dependent pathway (386). In light of recent evidence (78), it is possible this Bax interaction serves to positively regulate necroptotic signaling (389). Another possibility comes from immune cell lineages, where DR6 can engage a Bax-dependent, mitochondria-dependent apoptosis pathway via direct interaction with presenilin-associated protein (PSAP) (390). Interestingly, DR6-Bax exists exclusively at the cell surface, whereas PSAP-Bax localizes to mitochondria (390). DR6 may regulate mitochondrial permeabilization, and downstream executioner caspase activity, via competitive PSAP/Bax interactions within the DR6ICD.

DR6, like most TNFRSFs, appears to be able to activate NFκB (383,391,392). *In vitro*, ligand-dependent DR6 activation of an NFκB cascade is required for differentiation of THP-1 monocytes to differentiate into macrophages. *In vivo*, DR6-dependent NFκB activity promote tumour angiogenesis (392), consistent with the established role of DR6 as a pro-angiogenic factor in the developing CNS vasculature (393). Moreover, micro-RNA 210 (miR-210) was recently shown to inhibit NFκB by inhibiting translation of DR6 mRNA in immune cells; this miR-210-DR6-NFκB axis was shown to be dysregulated in osteoarthritis (394). Dysregulation of DR6 signaling in B cells was further shown to confer autoimmunity in a mouse model of systemic lupus erythematosus (395). Thus, the DR6-NFκB axis is important for immunoregulation, but its potential role in neural development or maintenance remains unexplored.

With respect to TRAF interactions, DR6 was recently shown to interact with TRAF4 in ovarian cancer cells *in vitro* and *in vivo* (396). Interestingly, the DR6-TRAF4 interaction

mediates ovarian cancer cell migration via a mechanism that requires the kinesin family member KIF11, possibly in a context of tripartite DR6-TRAF4-KIF11 complex (396). This initial study confirms that TRAFs—or at least TRAF4—mediate DR6 signaling in some unknown capacity.

1.5.3 DR6 in developmental neurodegeneration

DR6 is a major regulator of developmental axon degeneration in central and peripheral neurons (51,56,58). In 2009, a seminal paper from Dr. Marc Tessier-Lavigne's group showed that a soluble N-terminal fragment of APP—produced by β-secretase (BACE)-mediated cleavage—binds DR6 to induce axonal degeneration and apoptosis via distinct executioner caspases—caspase-6 and -3, respectively—following trophic factor deprivation in sympathetic neurons (56). After failed attempts to reproduce these results, a more recent publication revisited the model of APP-DR6 signaling in developmental axon degeneration. The current model, also proposed by Dr. Tessier-Lavigne's group, was resolved in the developing retinocollicular pathway, where RGCs extend past their superior colliculus (SC) destination, then prune back their axons to their final SC target. In this model, full-length APP binds DR6 in *cis*—thus, independent of BACE—to activate caspase-3, which drives developmental axon pruning in RGCs. The latter model is the currently accepted model of APP/DR6-induced axon degeneration.

Returning to SCG sympathetic neurons, Dr. Christopher Deppmann's group recently reveal that p75NTR and DR6 co-regulate developmental axon degeneration at distinct temporal stages. Following NT withdrawal, SCG axons remain intact for ~18 hours (latent phase) followed by period of catastrophic spheroid formation and axonal destruction (catastrophic phase; ~3 hours). DR6 is required for the transition from latent phase to catastrophic phase. p75NTR, on the other hand, drives spheroid formation and rupture during the catastrophic phase

via local RhoA activation. Thus, p75NTR and DR6 co-ordinate developmental axonal degeneration programs in parallel.

1.5.4 DR6 in pathological neurodegeneration

DR6 drives axonal degeneration and neuronal apoptosis in the context of multiple neurodegenerative diseases, including: AD (374,377), axotomy (57,380), prion disease (378), ALS (376), hypoxia-induced neurodegeneration (379) and, possibly, Down Syndrome (DS) (375).

DR6, like p75NTR, is a receptor for amyloidogenic Aβ capable of transducing the neurodegenerative signal (374,377,382). *In vitro,* DR6-/- cortical neurons are resistance to Aβ-induced apoptosis, an effect phenocopied in wild-type neurons exposed to a DR6 function blocking antibody (374,377). The Aβ/DR6 neurodegenerative signal requires the intracellular DD of DR6 and activates an apoptotic cascade culminating in caspase-3 activation (374). *In vivo,* DR6 upregulation is observed in the AD cortex, and its expression is enriched in subregions with elevated neuronal death (374). Thus, Aβ overproduction in AD kills cortical neurons, at least in part, via direct binding to DR6 and initiation of apoptotic cascade.

In the PNS, DR6 is a mediator of Wallerian degeneration of axons post-axotomy. *In vitro,* DR6 KO protects both sympathetic and sensory distal axons from Wallerian degeneration (57). *In vivo,* distal sensory axons are protected after a crush injury to the sciatic nerve (57). This axotomy-induced DR6 death pathway is axon-intrinsic and involves downstream activation of dual leucine zipper kinase (DLK) and JNK (57). The DLK/JNK axis is thought to act as a retrograde degenerative signal to the soma (380). In axotomized RGCs, the DR6-DLK-JNK degenerative signal is independent of the major Wallerian degeneration executor SARM1 (380).

These studies place DR6 as the only cell surface receptor known to mediate axotomy-induced neurodegeneration.

Aβ is not the only amyloidogenic peptide capable of binding DR6. Prion peptide PrP106-126 physically interacts with the DR6 ECD to transduce a pathological neuron death signal (378). In cultured rat spinal neurons, PrP106-126 binds DR6 to activate a pro-apoptotic cascade culminating in activation of executioner caspase-3 and -6, and subsequent neuronal death (378). Acute DR6 knockdown protects cultured spinal neurons from PrP106-126-induced neurodegeneration (378). Thus, DR6 can act as a receptor to induce neuronal death in prion disease.

After a bilateral common artery occlusion (2VO), hypoxic conditions trigger dendritic spine loss, followed by complete neuronal death, in the cortex and hippocampus. *In vivo*, downregulation of miR-195 in hypoxic neurons removes translational inhibition on DR6 mRNA, resulting in DR6 upregulation—in parallel to local Aβ production (379). Aβ/DR6-mediated activation of caspases-3 and -6 drives spine elimination and neuronal death post-2VO *in vivo* (379). Thus, DR6 neurodegenerative signaling is hyperactivated in hypoxia to drive pathological neuronal death in the CNS.

ALS neurodegeneration is characterized by motor axon degeneration, motoneuron death, and NMJ denervation (376). In cultured motoneurons derived from the SOD1(G93A) ALS model mice, DR6 functional blocking antibody is neuroprotective (376). DR6-dependent motoneuron neurodegeneration in the SOD1(G93A) model involves downstream caspase-3 activation, in parallel to Akt inhibition (376). Thus, in ALS, DR6 acts as a driver of motoneuron death by engaging pro-death, and suppressing pro-survival, pathways.

1.5.5 DR6 is required for post-developmental CNS maintenance

Paradoxically, DR6—an initiator of neurodegenerative signaling—is highly expressed in the adult CNS with a near-ubiquitous expression pattern (93). This implies that DR6 must play a central role in CNS maintenance independent from its death signaling. Consistent with this, DR6 was recently shown to drive physiological dendritic spine elimination an axonal pruning in the cortex and hippocampus (373) in an experience-dependent manner (397). DR6 mediates physiological spine elimination and axon pruning in both excitatory and inhibitory hippocampal population (397). Thus, DR6 may play a major role regulating neuronal remodeling in the mature CNS, particularly in localized degeneration of specific neuronal processes as required.

DR6 is a major regulator of myelinating glia function in the developing and mature CNS. In oligodendrocytes (ODs) and Schwann cells (SCs), DR6 acts as a negative regulator of OD/SC survival, maturation and myelination (398,399) via basal death signaling to caspase-3 (398). DR6-/- mice show deficient remyelination and demyelination in the CNS (398). A failure of constitutive DR6 apoptotic signaling in ODs is associated with an autoimmunity phenotype (398). Interestingly, EAE (MS model) mice are protected from autoimmunity (pathological CD4+ T cell expansion) in a DR6-/- background (400); an effect that has been reproduced independently (398). Thus, glial-derived DR6 maintains homeostatic myelination in the adult CNS and PNS.

1.6 TROY

TROY is a non-DD-containing TNFRSF binds myelin-associated inhibitory factors (MAIFs) in a co-receptor complex with the Nogo-66 receptor (NgR1) and LINGO-1 to regulate neurodevelopment, neural plasticity, and restrict neurite outgrowth after CNS injury (61,401–411). Independent of NgR1, TROY functions in parallel with DR6 to sculpt the CNS vasculature during development (393). NgR1-independent functions of TROY have been described in the

context of glioma, where TROY is leveraged as a survival- and invasion-promoting factor (412–418). TROY function in the context of glioma provides insight into how this orphan TNFRSF may regulate neural development and plasticity via NgR1-independent signaling mechanisms.

1.6.1 A TROY/NgR1/LINGO-1 complex restricts neurite outgrowth

TROY is capable of physically and functionally replacing p75NTR in the NgR1/LINGO-1 to transduce myelin inhibitory signals in p75NTR-negative neuronal populations (61,401). *In vitro*, the TROY/NgR1/LINGO-1 complex is capable of inhibiting neurite outgrowth in neuronal cultures treated with MAIFs, including MAG, OMgP, and Nogo-66 (61,401). Cultured TROY-/- neurons are resistant to the MAIF-mediated suppression of neurite outgrowth (61). Similar to the p75NTR/NgR1/LINGO-1 complex, the TROY/NgR1/LINGO-1 complex activates RhoA downstream of MAIF-binding to drive local actin depolymerization, thereby restricting neurite outgrowth (61). TROY-mediated RhoA activation in this context is mediated by a physical interaction with RhoGDI (419). Interestingly, TROY cannot functionally replace p75NTR in p75NTR-/- RGCs cultured in exogenous MAG (404), suggesting that cell-type specific preferences exist for utilizing p75NTR or TROY as a co-receptor in the NgR1 complex. Similar to p75NTR, TROY is locally upregulated at inflammatory lesions in EAE mice (model of MS), in both axons and inflammatory glia (403), suggesting that TROY/NgR1/LINGO-1-mediated inhibitory signaling directly contributes to MS neuropathology.

1.6.2 TROY is a major regulator of CNS development and maintenance

The TROY/NgR1/LINGO-1 complex is required to mediate CNS maintenance in a post-developmental context. In the adult hippocampus, the TROY/NgR1/LINGO-1 complex is required for structural fine-tuning of synapses to enable memory consolidation (406). In adult mice, acute TROY knockdown in the hippocampus *in vivo* results in poor performance at passive

avoidance and Morris water maze tasks (406). TROY/NgR1/LINGO-1-dependent synapse restriction in the hippocampus requires downstream signaling to RhoA (407). TROY-dependent synaptic remodeling in the hippocampus and cortex is mediated by interaction with Leucine-Rich Glioma-Inactivated Protein 1 (LGI1) (60). LGI1 binds TROY to physically—and functionally—disrupt the TROY/NgR1/LINGO-1 complex, thereby inhibiting downstream RhoA activation. LGI1-/- hippocampal and cortical neurons possesses fewer, smaller, and weaker synapses; an effect mediated by elevated basal RhoA activation (60).

Similar to DR6, TROY negatively regulates oligodendrocyte (OD) maturation and myelination (398,408). Acute TROY knockdown in OD precursor cells (OPCs) promotes OPC differentiation and myelination when grafted to an injured spinal cord. Mechanistically, TROY suppresses OPC differentiation via downstream activation of protein kinase C (PKC). Thus, DR6 and TROY are collaborative inhibitors of OD maturation and myelination (398,408) and serve to prevent excessive myelination in the developing nervous system.

TROY, like DR6, is required for co-ordinating vascularization of the developing CNS; a function that is conserved in mice and zebrafish (393). Although the signaling mechanism through which DR6/TROY co-ordinate vascularization is unknown, it is established that both receptors act as downstream transcriptional targets of Wnt signaling in this context (393). Dysregulation of TROY vascularization signaling may contribute to vascular dementia, as genetic variants of TROY have been identified as susceptibility risk factors (420).

1.6.3 TROY drives tumour invasion in glioma

Invasive gliomas upregulate TROY to mediate tumour survival and invasion (412,414), similar to p75NTR. TROY survival signaling in glioblastoma involves downstream activation of parallel Akt and NFκB cascades (414). TROY promotes perineural glioblastoma invasion via

downstream co-ordination of Rho GTPase activate. TROY activates Rac1 via direct association with the scaffolding protein Pyk2 (389). TROY concomitantly activates both Rac1 and RhoA via PDZ-RhoGEF; TROY-mediated dual activation of these antagonistic Rho GTPases promotes glioblastoma invasion *in vitro* and *in vivo* (416). TROY-mediated glioblastoma invasion signaling also requires the Raf Kinase Inhibitor Protein (RKIP), and pharmacological disruption of the TROY-RKIP interaction attenuates glioma development *in vivo* (418).

Recently, it was established that the chemotherapeutic agent propentofylline—commonly used in glioblastoma treatment—acts by targeted downregulation of TROY (413,415). Propentofylline successfully suppresses TROY survival signaling to Akt and NFκB (415); as well as TROY invasion signaling via Rac1 (413). These results indicating that TROY represents a promising therapeutic target in glioma treatment. Moreover, these studies dissecting TROY signaling in a neoplastic context indicate that TROY may regulate diverse aspects of neurodevelopment via regulation of canonical TNFRSF signaling axes, including Akt and NFκB.

1.7 Extracellular vesicles (EVs) mediate intercellular p75NTR trafficking

'Extracellular vesicles' (EVs) is a blanket term defining all membranous vesicles released from a cell into the extracellular milieu. EVs are highly heterogeneous—both between and within EV classes—and are secreted from many cell types. Though many subclasses have been described, EVs generally fall within two major classes: exosomes and microvesicles (MVs). Exosomes are small EVs (~30-100nm diameter) generated from membrane invaginations of early endosomes to generate intraluminal vesicles (ILVs) within the endosomal lumen to form multivesicular bodies (MVBs). If an MVB avoids the lysosomal route and fuses with the plasma membrane, ILVs are released from the cell and are then referred to as exosomes. MVs, on the

other hand, are large EVs (~100nm-1μm diameter) derived from outward budding of the plasma membrane (421).

EV cargo consists of diverse biomolecules, including protein, RNA and DNA. Though no 'EV targeting motif' has been discovered, EV cargo loading is a regulated process as EV content does not reflect the overall membrane/cytosol content of the cell (422). The cell secreting EVs is commonly referred as the 'donor cell' and the cell upon which EVs act is the 'recipient cell.' At the recipient cell, EVs can be internalized via receptor-mediated endocytosis, macropinocytosis, phagocytosis or lipid raft internalization (423); alternatively, EVs may fuse directly with the plasma membrane (PM) to 'spill' their contents into the cytosol (421). EVs have been shown to target recipient cells via autocrine, paracrine, or endocrine action (421). With respect to endocrine action, EVs are capable of bilateral crossing of both the blood-brain (BBB) and blood-CSF (BCB) barriers to mediate intercellular communication between the CNS and peripheral tissues [reviewed in depth by (424)]. Though early reports described the role for EVs in cargo trafficking and metabolic support, it has since become evident that EVs are important subcellular compartment mediating intercellular signaling events (421,425).

EVs regulate major neurodevelopmental processes, including: embryonic neurogenesis, gliogenesis, synaptic pruning, myelination, and adult neurogenesis [reviewed in (426)]. Neuron- and glia-derived exosomes are important for nervous system maintenance under physiological conditions, as has been emphasized by their role in coordinating synaptic plasticity [reviewed in (427)] In neuropathologies, locally-secreted EVs generally confer neuroprotection, as has been demonstrated within the contexts of stroke, traumatic brain injury, spinal cord injury, and peripheral nerve injury [reviewed in (428)]. It remains unclear whether EVs actively drive neurodegeneration in physiological or pathophysiological conditions.

1.7.1 Molecular mechanisms controlling EV biogenesis

Exosome biogenesis can occur via two canonical pathways: (i) the endosome sorting complexes require for transport (ESCRT)-dependent pathway, or (ii) the ceramide-dependent pathway (429). These pathways reflect independent mechanisms of MVB formation (i.e., early endosome membrane invagination to produce ILVs) but converge upon a common mechanism of MVB fusion to the plasma membrane (i.e., to release ILVs as exosomes).

ESCRT-dependent MVB biogenesis requires the formation of a large, multimeric structure on the inner membrane of an early endosome that consists of 4 ESCRT complexes (known as ESCRT-0, ESCRT-I, ESCRT-II, and ESCRT-III) and an accessory Vps4 complex (429). ESCRT and Vps4 complexes are comprised of multiple subunits with vacuolar protein sorting (VPS) family members primarily mediating intracomplex interactions; and clathrin (and other scaffolding proteins) mediating intercomplex interactions (429). In humans, the ESCRT-0 complex consists of STAM1/2 and HRS subunits. ESCRT-I consists of: VPS23/28/37A/37B/37C/37D, MVB12A/B, and UBAP1. ESCRT-II consists of VPS22/25/36. ESCRT-III consists of: VPS2A/B, VPS24, SNF7A/B/C, VPS20, DID2, VPS60, and CHMP7. The Vps4 complex is comprised of: VPS4A/B, LIP5, and the accessory protein ALIX (430–434). ESCRT machinery assembles via a defined temporal order: (i) ESCRT-0 associates with phosphatidylinositol-3-phosphate (PtdIns3P) at the endosomal membrane (435,436) via HRS (437) which subsequently recruits clathrin (438); (ii) PtdIns3P-bound ESCRT-0 recruits ESCRT-I via direct interaction of HRS with VPS23 (439–441); (iii) ESRCT-II recruitment via VPS20-VPS25 physical interaction (442,443); and (iv) ESCRT-III recruitment (444–446). ESCRT-II recruitment (step 3) initiates endosomal membrane invagination (447), while ESCRT-III recruitment (step 4) is required for ILV scission into the endosomal lumen (448–450).

Ceramide-dependent MVB biogenesis proceeds independent of ESCRT machinery. At the endosomal membrane, neutral sphingomyelinase (nSMase) synthesizes ceramide using sphingomyelin as a precursor (451). When enriched in a phospholipid membrane, ceramide spontaneously forms a negative membrane curvature—in this case driving ILV formation (451). The mechanism of ILV-to-MVB conversion in this pathway remains unclear but is thought to require ceramide-generated lipid rafts at the ILV surface (451).

After their biogenesis, MVBs are trafficked to the PM via microtubule transport (452,453) and direct interaction with the actin cytoskeleton (454) via the actin-binding protein cortactin (455). Multiple Rab GTPases mediate MVB transport to along the microtubule network, including: Rab27A/B, Rab7, Rab11, and Rab35 [reviewed in (429)]. Once at the inner surface of the PM, MVBs fuse to the PM via interactions of MVB docking proteins with a SNARE complex comprising of: SNAP23, Ykt6, VAMP7, and syntaxin 1A (456–465). Upon MVB fusion to the PM, its ILVs are secreted from the cell as exosomes.

MV biogenesis and release is not well-characterized but appears to proceed via separate ESCRT-dependent and -independent pathways [reviewed in (421)]. ESCRT-dependent MV biogenesis requires the subunits ALIX, VPS22, TSG101, CHMP1/3, and the VPS4 complex (466,467). Reminiscent of exosome biogenesis, a ceramide-dependent pathway mediated by the PM-localized acidic sphingomyelinase (aSMase) can drive MV formation and release (468,469). Lastly, a third MV biogenesis pathway has recently been described, involving the small GTPases ARF1/6 and RhoA (470–472). The ceramide- and GTPase-dependent MV biogenic pathways do not require ESCRT machinery (468–472).

1.7.2 Neuron- and glia-derived p75NTR is targeted to exosomes

Dr. Francisca Bronfman's group demonstrated that primary sympathetic neurons and PC12 cells secrete p75NTR$^+$ exosomes into the conditioned medium *in vitro* (473). p75NTR$^+$ MVBs are preferentially targeted for exosome release versus lysosomal degradation, and exosomal p75NTR release from SCGs is augmented by neuronal depolarization (473). Exosomal p75NTR release has also been detected from dedifferentiated Schwann cells (SCs) in response to axotomy in cultured DRG explants (474). Within the content of SCs, p75NTR was shown to influence exosomal RNA content (474), but the extent to which p75NTR regulates exosomal cargo loading is unclear. All detection of exosomal p75NTR to-date has come from EV purification methods that omit large structures. Thus, although it is clear p75NTR is secreted in exosomes, it is not known if p75NTR is released via MVs.

The only investigation into the biological function of exosomal p75NTR comes from the melanoma field (475). Garcia-Silva and colleagues found that metastatic melanoma cells secrete p75NTR$^+$ exosomes that target lymphatic endothelial cells, promote lymphangiogenesis, and establish a tumour microenvironment that facilitates the infiltration of melanoma metastases; effects that were blunted by exosome-specific p75NTR knockdown (475). Thus, exosomal p75NTR promotes tumour metastasis and metastatic niche formation, but the function of extracellular p75NTR in neurology—or any physiological context—remains unknown.

1.8 The RELT Family of TNF receptors

Of the 29 human TNFRSFs, Receptor Expressed in Lymphoid Tissues (RELT; TNFRSFSF19L) is among the poorest characterized in the literature. This is due, in part, to the recency of RELT discovery. In 2001, Dr. Lieping Chen's group first cloned RELT and reported its abundant expression in hematologic tissues including the lymph node, spleen, and blood-derived leukocytes (476). Structurally, RELT possesses 3 CRDs in tandem within its ECD and

no known functional domain within its ICD. Despite its canonical TNFRSF CRD cluster, neither human nor murine RELT binds any known TNF ligand (477). RELT remains classified as an orphan receptor as no ligand has been discovered to-date. With respect to TRAF engagement, contradictory reports suggest RELT binds TRAF1 (478) or no TRAF family member (479).

Physiological function of RELT *in vivo* is limited to a small number reports within the contexts of immunology (480) and odontogenesis (481–483). A recently developed RELT knockout mouse is deficient in tooth enamel development (481), a function ascribed to ADAM10-dependent proteolytic cleavage of the receptor (482). Consistent with this murine data, missense mutations in the TNFRSFSF19L (RELT gene) locus are associated amelogenesis imperfecta— enamel malformation—in humans (483). With respect to pathophysiology, RELT upregulation is associated with multiple cancers, including squamous cell (484), lung (485), gastric (486), and B-cell lymphoma (487).

Recently, two RELT homologs were identified: RELT-Like 1 (RELL1) and RELT-Like 2 (RELL2) (488). Compared to RELT, RELL1 and RELL2 are truncated in the ECD and lack the extracellular CRD cluster (488). RELL1 and RELL2 are encoded at independent genomic loci and do not represent alternative TNFRSFSF19L gene products (488). Not only are RELL1 and RELL2 sequences highly similar to each other but they share strong sequence identity to RELT (488). RELL1, RELL2 and RELT each possess a 35-residue 'RELT homology domain' (RHD) consisting of the TMD and N-terminal ICD amino acids that >90% sequence identity between the family members (488), though the function of this domain is unknown. All 3 RELT family members possess a 4-residue 'RFRV' motif capable of binding the sterile-20 kinases SPAK and OSR1 (488,489). The 3 RELT family members primarily localize to the plasma membrane and

have been shown to physically associate within one another in independent RELT-RELL1, RELT-RELL2, and RELL1-RELL2 complexes (488).

A central goal of this doctoral thesis is to identify p75NTR signaling mechanisms pertinent to nervous system development and maintenance. As part of this effort, an unbiased interactome screen identified RELL1, but not RELT or RELL2, as a p75NTR interactor (see Chapter 3). Considering this result, the remainder of this literature review section will focus exclusively on RELL1 biological function.

1.8.1 RELL1 expression profile in the nervous system

RELL1 expression in the nervous system is abundant, showing a progressive increase in CNS expression across development (490). At an overarching level, neural RELL1 expression is lowest during embryogenesis, increases sharply in early postnatal mice (P7), then progressively increases through adolescence (P15-30), eventually peaking in adulthood (P90) (490). Though developmental RELL1 expression profiles in the nervous system lack a comprehensive cell-type-specific profile, *in situ* expression within the adult CNS has been characterized (491,492). In adult C57BL/6 mice, RELL1 mRNA is highly enriched in layer 5 neocortex (absent in cortical layers 1-4, 6) and thalamus (491). RELL1 mRNA is detectable at lower levels in the hippocampus and spinal cord, but absent in the cerebellum and all other major brain regions not listed above (491). Consistent with the mRNA data, our in-house detection of RELL1 protein by immunoblot in the adult CNS showed highest expression in the cortex; low detection in the hippocampus and spinal cord; and no detectable expression in the cerebellum (Appendix 1). Single cell transcriptomics data in the adult brain shows RELL1 mRNA is highly expressed in oligodendrocytes and pyramidal neurons; low in other neuronal subtypes; and undetectable in non-myelinating glia (492).

1.8.2 Functional characterization of RELL1 *in vitro*

With respect to signaling capability, gain-of-function experiments in mammalian cell lines suggest RELL1 is capable of autonomous signaling. Cusick and colleagues found that overexpressed RELL1 induces apoptosis in HEK293 (488) and COS7 cell lines (479) via downstream activation of JNK and p38 (489). RELL1-induced cell death depends on its physical association with a sterile-20 kinase family member SPAK or osmotic stress-responsive 1 (OSR1) (479,488). SPAK/OSR1 phosphorylate RELL1 at an unknown residue (488), but it is unclear if this phosphorylation event pertains to this apoptotic cascade.

RELL1 may be a negative regulator of inflammation. In endothelial cells, an endogenous circular RNA (circ-RELL1)—which targets the RELL1 transcript for degradation—promotes downstream activation of MyD88/NFκB-dependent inflammatory cascade in response to oxidized low-density lipoprotein (493).

RELL1 may regulate viral entry into cells. In cultured MCR5 cells, and primary hematopoietic progenitor cells, RELL1 loss-of-function protects against cytomegalovirus (CMV) infection (494). Moreover, in macrophages, RELL1 knockdown reduces intracellular survival duration of the tuberculosis virion (*M. tuberculosis*) (495). Within a heterologous cell population, RELL1-high macrophages are particularly vulnerable to tuberculosis infection as they are deficient in autophagic clearance of the virion, suggesting RELL1 may be an endogenous inhibitor of autophagy (495).

The disparate and diverse nature of the *in vitro* literature reflect the reality that very little is known of the cellular function of this ECD-truncated TNFRSF.

1.8.3 Functional characterization of RELL1 *in vivo*

Recent reports have identified RELL1 as an oncogene in the context of tumour progression in glioma (496,497) gastric cancer (GC) (498). In glioma, high RELL1 expression is associated with poor prognostic outcomes (496) and an uncharacterized RELL1 mutant has been identified as the most common mutation within the cell surface proteome of glioblastoma (497). Though no mechanistic details of RELL1 function in glioma have been described, Sang and colleagues (2021) provide indirect evidence that RELL1-dependent regulation of autophagy contributes to GC tumour progression in gastric cancer (498). circRELL1 is downregulated in GC tumours, and this downregulation correlates with lymph node metastasis and poor prognosis (498). Interestingly, exogenous circRELL1—delivered via exosomes— inhibits tumour proliferation, invasion, and apoptotic resistance in human GC patients (498). Assuming circRELL1 confers protection *in vivo* by targeting RELL1 mRNA for degradation—and not another mechanism—then RELL1 may represent a viable therapeutic target in GC.

The International Mouse Phenotyping Consortium (IMPC) recently generated a RELL1 KO mouse and performed a phenotypic screen across developmental stages (499). Adult RELL1 KO mice exhibit neurobehavioural phenotypes, including auditory hypersensitivity (acoustic startle response at low-decibel sounds; and decreased pre-pulse inhibition in the auditory brainstem) and hyperactivity (499). Behavioural phenotypes were only tested in adults, thus neurodevelopmental data is still lacking. No non-behavioural phenotypes were observed in RELL1 KO mice by IMPC's test battery (499). These behavioural data—in conjunction with RELL1 CNS expression data—establish RELL1 as a mediator of nervous system development and/or function.

1.10 A critical review of interactomics approaches

The investigation into signaling mechanisms of any protein in any cellular context requires a thorough knowledge of the complement of proteins that act as interactors (the 'interactome') to the protein-of-interest. Despite our expanding knowledge of neurological and non-neurological functions associated with p75NTR, DR6 and TROY, our understanding of the core signaling mechanisms engaged by these TNFRSFs remains limited. To address this problem, I sought to reveal the complete interactome of p75NTR, DR6 and TROY (henceforth the 'p75NTR-DR6-TROY interactome') in live human cells (see Chapter 2). There are multiple interactomics tools available to accomplish this task, each with their own merits and caveats. This critical review of interactomics technologies – both biological and computational – identified proximity-dependent biotin identification (BioID) (500) as an optimal strategy to reveal the p75NTR-DR6-TROY interactome in an unbiased, high-throughput, high-confidence manner.

1.9.1 Traditional affinity purification-based techniques

The standard approach to resolve the interactome of a protein-of-interest ('bait') is to run an affinity purification of the bait – typically via antibody-based pulldown – followed by identification of all interacting partners ('prey') that co-purify with the bait by mass spectrometry (MS). This approach is referred to as affinity purification-mass spectrometry (AP-MS) [reviewed in (501,502)]. The core issue with the approach is that bait-prey interactions must be preserved during the affinity purification procedure. For this reason, AP-MS can only resolve stable protein complexes, and fails to detect transient protein-protein interactions (PPIs), or low-affinity PPIs, which are biologically relevant. Moreover, cell lysis buffers disrupt co-purified complexes, and even lysis buffer-resistant prey can be lost if they possess low solubility (503,504). Thus, AP-MS

is suited for detecting high-confidence, stable protein complexes, but fails to resolve a complete interactome dataset.

To address this core issue with AP-MS, chemical cross-linkers can be added to the cell culture or lysate to better preserve bait-prey interactions (505,506). However, this strategy increases the risk of false positive interactions, and only partially improves the ability of AP-MS to detect low-abundance PPIs (507).

In Chapter 2, I sought to resolve the p75NTR-DR6-TROY interactome in living human cells. To do so, it was necessary to utilize a more sensitive interactomics approach than traditional AP-MS strategies.

1.9.2 Novel proximity-dependent labeling techniques

In the past decade, novel techniques have been developed that allow permanent covalent labeling of prey proteins *in situ* [reviewed in (507)]. These techniques allow for detection of a prey protein after its interaction with the bait, thereby removing the necessity to preserve bait-prey interactions throughout the entire procedure. These novel techniques rely on labeling prey with a covalent modifier (typically biotin) when they enter the proximity of the bait – most commonly due to an interaction (507). This increased sensitivity comes at the cost of increased background, since a prey can be aberrantly labeled by entering into close vicinity of the bait without interaction (these prey are henceforth referred to as ‘contaminants’). However, this issue can be circumvented with computational tools, including: rigorous statistical analyses (508), cross-referencing to a contaminant repository (509), and the co-analysis of a diverse set of negative control baits. These novel proximity labeling approaches introduced drastic improvements in interactome sensitivity and, with application of stringent post-hoc analytical measures, can produce a high-confidence interactome largely free of false positive PPIs

(508,509). Currently, the most successful proximity-based interactomics technique—and the technique utilized in Chapter 2—is proximity-dependent biotin identification (BioID).

1.9.2.1 Proximity-Dependent Biotin Identification (BioID)

BioID was first described in 2012 (500) [reviewed in (507,510–513)] and exploits a naturally-occuring mutant of the *Escherichia coli* (*E. coli*) biotin ligase known as Bifunctional ligase/repressor (BirA). BioID has successfully resolved complete interactome datasets for multiple bait proteins, including: nucleoporins (514), E-cadherin (515), the ZEB1/NuRD complex (516), E3 ubiquitin ligases (517), and Hippo (518). BioID has also successfully revealed the proteome composition of several organelles, including: focal adhesions (519), cell junctions (515,520–522), stress granules (523), and the nuclear envelope (500). This robust tool has demonstrated the capability to generate interactome and proteome datasets with far greater scope than those generated by traditional AP-MS.

BirA, like all biotin ligases, enzymatically catalyzes substrate biotinylation in a 2-step process: (i) BirA uses a single ATP molecule to generate the reactive biotin intermediate biotinyl-5'-AMP; then (ii) biotinyl-5'-AMP reacts with the epsilon amine on the side chain of a lysine residue on the substrate (524,525). Substrate biotinylation can only occur at exposed lysine residues (524,525). In human cells, biotinylation is an extremely rare post-translational modification limited to several families of metabolic decarboxylase enzymes, including: PC, PCCA/PCCB, MCCC1/MCCC2, and ACACA/ACACB family members (526). Biotin cannot be synthesized in human cells, and requires dietary consumption and cellular uptake via the cell surface sodium multivitamin transporter (SMVT; gene *SLC5A6*) (527).

BirA is a type II biotin ligase (524) possessing: (i) a central catalytic domain for substrate biotinylation, (ii) a highly conserved C-terminal domain of unknown function (528), and (iii) an

N-terminal DNA-binding domain that acts as a biotin-dependent inhibitor of the biotin biosynthesis operon (529). When bound to biotin, the biotin-binding loop of BirA undergoes a structural rearrangement that enables ATP binding, which in turn rearranges the adenylate-binding loop, which stabilizes the bound ATP (524). Next, BirA lysine 183 (K183) undergoes a nucleophilic substitution reaction that catalyzes the fusion of biotin carboxylate to the α-phosphate of ATP, thereby producing the biotinyl-5'-AMP intermediate (524,530,531). Biotinyl-5'-AMP remains stably bound to R118 until the approach of a substrate lysine residue (524,530,531). Stabilization of biotinyl-5'-AMP binding to R118 is further mediated by a salt bridge that forms between R118 and D176 (530). Upon substrate interaction, biotinyl-5'-AMP undergoes a nucleophilic attack on the epsilon amine on the exposed lysine residue, resulting in covalent biotinylation of the substrate (532–534).

As mentioned above, BioID exploits a rare BirA mutant encoded by the BirA91 allele (535) that involves substitution of R118 for glutamate ($BirA^{R118G}$) (536). $BirA^{R118G}$ possesses ~100-fold increased affinity for biotin, and ~400-fold decreased affinity for biotinyl-5'-AMP compared to wild-type BirA (48-50). As a result, BirAR118G efficiently activates biotin, but dissociates from biotinyl-5'-AMP, thereby producing a reactive 'cloud' of biotinyl-5'-AMP around the enzyme (537–539). This free biotinyl-5'-AMP attacks amines on exposed lysines in proximal proteins (537–539). The 'cloud' of reactive biotinyl-5'-AMP generated by $BirA^{R118G}$ was determined to be ~100Å in radius, based on the fusion of $BirA^{R118G}$ with nucleoporin (Nup) subunits of the nuclear pore complex and detection of biotinylated subunits at a known distance from this Nup-$BirA^{R118G}$ bait (514).

In the BioID procedure, $BirA^{R118G}$ is fused to the bait protein (the 'BioID bait') to generate a 100Å-radius reactive cloud of biotinyl-5'AMP (500,514). This results in lysine-

mediated biotinylation of interacting partners and proximal proteins to the BioID bait *in situ* in the presence of exogenous biotin (500). Importantly, since lysine biotinylation is a covalent modification, all interacting partners are permanently labeled with biotin after interaction with the bait. After prey biotinylation, cells are lysed, and biotinylated prey are captured on streptavidin resin – leveraging the extremely strong avidin-biotin interaction (Kd ~ 10^{-14}M). The avidin-biotin interaction is resistant to harsh cell lysis conditions (ionizing detergents, high salt concentrations, denaturing compounds, etc.) enabling efficient purification of prey proteins from lysates that is not achievable using antibody-based pulldowns, as in AP-MS. Once purified, prey can be identified, and their abundance quantified, by mass spectrometry.

The BioID proximity-dependent labeling strategy is far more robust than AP-MS and can purify the complete interactome of a bait protein. Due to this increased sensitivity, however, BioID pulls out far more contaminants than AP-MS. If the experimenter applies rigorous statistical analysis to the preliminary BioID interactome, a final interactome dataset with a false discovery rate (FDR) ≤ 5% can be achieved, comparable to the low false-positive rates generated by AP-MS (508). Several freely available computational tools exist to accomplish this, including: (i) the Significance Analysis of Interactome (SAINT) algorithm capable of assigning probability scores to each interactor as a function of spectral count enrichment over negative controls and consistency of spectral count enrichment across replicates (508); and (ii) cross-referencing to the CRAPome (Contaminant Repository for Affinity Purification) database, which includes spectral count data for all common contaminants found in BioID experiments (and AP-MS) when run according to standardized protocols (509).

BioID can resolve the interactome of a bait protein *in situ* with far greater robustness than traditional AP-MS without sacrificing statistical confidence (500,507,508). Note, however, that

recent publications have attempted to improve upon the original BioID framework to generate an even more robust interactome dataset. These novel proximity-labeling techniques, however, do so at the expense of host cell health (i.e. BioID2, TurboID and miniTurbo) and/or are currently incompatible with the CRAPome database (discussed further in Section 1.7.2.2) (513,540,541). The latter poses a major barrier to achieving high statistical confidence in obtained interactome dataset, which is unacceptable, as such a dataset would initiate major research setbacks within the field. Therefore, BioID was selected as best available tool to resolve the p75NTR-DR6-TROY interactome (see Chapter 2).

1.9.2.2 Alternative approaches to BioID

Although BioID was established as the gold standard method for proximity-dependent biotinylation (PDB-MS), newer iterations of the technique have attempted to improve upon the existing framework. In 2015, Dr. Kyle Roux (who co-developed BioID) and colleagues discovered that a biotin ligase expressed by the gram-negative bacterium *Aquifex aeolicus*—referred to as BioID2—possessed higher affinity for biotin than $BirA^{R118G}$ and could generate a reactive biotinyl-5'-AMP cloud after an R40G mutation (542). Unlike $BirA^{R118G}$, BioID2 lacks an N-terminal DNA-binding domain resulting in less background labeling of chromatin-associated proteins (542,543). Although $BirA^{R118G}$ possesses an N-terminal DNA-binding domain that can lead to mislabeling of chromatin-associated proteins, this is only an issue if the BioID bait mislocalizes to the nucleus. Moreover, the advent of the CRAPome database of BioID contaminants allows for removal of these background proteins – thus this structural characteristic of BioID2 is not advantageous relative to $BirA^{R118G}$.

The enhanced biotin affinity enabled BioID2 to efficiently biotinylate interactors at lower concentrations of exogenous biotin resulting in an increased number of prey purified on

streptavidin resin compared to BirA^{R118G}-mediated proximity biotinylation. Although the enhanced biotin affinity of BioID2 relative to BirA^{R118G} appears advantageous, this property in fact deleterious in nature for two reasons. First, BioID2—unlike BirA^{R118G}—can scavenge endogenous biotin from media serum resulting in reduced decarboxylase function and a subsequent metabolic crisis within the cell (507,542). Thus, an interactome generated by BioID2 reflects the interactome of that bait protein in an unhealthy cell and calls into questions the reliability of the dataset (507,542). Second, any deviation in biotin ligase activity from the standard established by BirAR118G renders the dataset incompatible with the CRAPome database (508). Thus, the potential for accurate contaminant removal with BioID2 is reduced relative to the standard BioID procedure. Due to these concerns, BioID2 was not chosen for p75NTR-DR6-TROY interactome analysis in Chapter 2.

A similar approach was described by Branon and colleagues (540) who leveraged error-prone PCR, in tandem with a yeast display assay, to develop novel BirA mutants termed TurboID and miniTurbo. TurboID possesses 14 mutations to the BirA sequence; whereas miniTurbo possesses 12 mutations (identical to TurboID except for S263P and M241T) and an N-terminal truncation of the DNA-binding domain (540). PDB-MS analysis with TurboID and miniTurbo resulted in a 15- to 23-fold increase in prey labeling; however, it was not firmly established if these additional preys represent *bona fide* interactors or increased background (540). As is the case with BioID2, neither TurboID or miniTurbo are compatible with the CRAPome database, which reduces the rigour of statistical analysis (509). TurboID and miniTurbo both demonstrate increased biotin affinity relative to BirA^{R118G} and can syphon serum-derived biotin, resulting in decarboxylase dysfunction and metabolic crisis (507). For

these reasons, TurboID and miniTurbo were discarded as candidate techniques to reveal the p75NTR-DR6-TROY interactome (see Chapter 2).

PDB-MS techniques involving fusion of a biotin ligase to the Cas9 endonuclease have been described (544–546). These techniques are optimally suited to elucidating interactomes of DNA- and/or RNA-binding proteins (544–546). In Chapter 2, we sought to reveal the interactomes of transmembrane baits with no known affinity for nucleic acids; thus, these PDB-MS techniques were disregarded as candidates.

'Split BioID' protocols have been described using the concept of a protein fragment complementation to identify protein complexes (547,548). These approaches involve fusion of the bait to an N-terminal fragment of $BirA^{R118G}$ and the prey to the C-terminal fragment (547,548). Upon bait-prey interaction, $BirA^{R118G}$ reconstitutes into its biologically active conformation to biotinylate the bait, prey and other associated interactors (547,548). Split BioID is optimally suited for studying context-dependency of a known PPI and identifying any unknown interactors that may be involved in the process (547,548). Split BioID is not useful for resolution of a complete interactome and was discarded as a candidate method on this basis.

One caveat to standard BioID is the requirement of fusing the bait to a large enzyme ($BirA^{R118G}$ is ~35kDa in size). Chojnowski and colleagues (549) addressed this issue with the development of the 2C-BioID technique. The technique selectively recruits the biotin ligase to bait protein via inducible dimerization (549). The bait protein is fused to the small FK506-binding protein (FKBP) and the biotin ligase is fused to an FKBP-rapamycin binding (FRB) domain (549). Upon addition of an exogenous chemical dimerizer, the biotin ligase is recruited to the bait via the high-affinity FKBP-FRB interaction (549,550). This approach ensures the bait can traffic to these correct subcellular compartments and function appropriately without any

potential influence from the biotin ligase (549). There are, however, unique caveats to this approach. First, 2C-BioID can only investigate prey interactions when the bait is locked in an induced dimeric state. p75NTR, DR6 and TROY can exist in multiple oligomeric states—and only p75NTR is known to signal as a dimer—therefore this technique would not be able to resolve the complete interactome for these TNFRSFs. Moreover, 2C-BioID would not be compatible with the CRAPome database (509). Lastly, 2-component systems are generally more challenging to optimize and introduce issues of bait:biotin ligase stoichiometry that can introduce uncertainty into the statistical analysis of the interactome dataset (507,549). Though 2C-BioID shows promise to become a robust technique, it is not a suitable candidate in its current state to resolve the p75NTR-DR6-TROY interactome (see Chapter 2).

A novel approach to PDB-MS involves the use of peroxidases to label prey with redox-reactive biotin moieties (551–566). Peroxidases catalyze the reduction of hydrogen peroxide (H_2O_2) to produce water (H2O) and an active free radical (•AH) (567). Horseradish peroxidase C (HRP) can oxidize phenolic substrates (i.e. biotin-phenol) to produce a short-lived radical that will react with a nearby electron-dense amino acids (preferably tyrosine) (551). This property of HRP has been leveraged to generate HRP-fused baits that label prey in a proximity-dependent manner with redox-reactive biotin (552–554,556,557). Parallel development of two techniques have utilized HRP for interactome labeling: Enzyme-Mediated Activation of Radical Sources (EMARS), which uses arylazide-biotin as the HRP substrate (552,553); and Selective Proteomic Proximity Labeling using Tyramide (SPPLAT) uses biotinyl-tyramide as the substrate (554). The latter approach has been successfully coupled to MS to resolve the interactome of the DT40 B-cell receptor (554). As with BioID, HRP-catalyzed proximity labelling has also been exploited for proteomic profiling of cellular subdomains, including lipid rafts (556) and neuronal synaptic

clefts (557). The major limitation of HRP is its inactivation in reducing subcellular environments, such as the cytosol (558,568). This renders HRP incapable of labeling any TNFRSF interactome, since most interactors are cytosolic or possess a cytosolic domain. Thus, HRP-mediated proximity labeling was not selected as a suitable strategy to resolve the p75NTR-DR6-TROY interactome (see Chapter 2). Newer iterations of peroxidase-mediated proximity labeling have addressed this issue (541,560,561).

Ascorbate peroxidase (APX) regulates intracellular H_2O_2 concentrations in diverse plant species via oxidation of L-ascorbate (558,559,569,570). Martell and colleagues (2012) subjected APX to directed evolution to generate a mutant, named APEX, that could drive localized deposition of diaminobenzidine in mammalian cells for electron microscopy (558). APEX shows reduced dimerization (due to K14D and E112K mutations) and equal catalytic activity (due to a compensatory W41F mutation) relative to APX (559). Similar to HRP, APEX can oxidize phenol derivatives (560,561). Dr. Alice Ting's group successfully harnessed APEX for proximity labeling, using biotin-phenol as a substrate, to resolve the proteomic profile of whole mitochondria (560) and the mitochondrial intermembrane space (561) in live human cells. APEX-mediated proximity labeling has since been applied for proteomic profiling of: mitochondria (in *Drosophila melanogaster*) (562), a stress granule marker (563), and the lipid droplet (564). With respect to interactome labeling, APEX has successfully resolved the ligand-dependent interactomes of several G-protein coupled receptors (565,566). APEX can resolve interactomes with a similar signal-to-noise ratio as BioID within a shorter labeling timeframe (1 minute for APEX vs. 24 hours for BioID). A novel APEX mutant ($APEX^{A134P}$; termed APEX2) was recently described to demonstrate increased sensitivity for proteomics due to decreased H2O2-mediated inactivation and/or enhanced oxidation of biotin-phenol (541,571), although the

catalytic oxidation of phenolic substrates by APEX2 remains weaker than HRP (541). ‘Split APEX/APEX2’ techniques have been described but are better suited to investigating context dependencies of specific bait-prey interactions rather than full interactome resolution (572–574).

APEX2 and BioID were recently tested on the same baits within the ribosomal quality control pathway (575). This analysis revealed little overlap between the interactomes resolved by the two approaches (575). BioID demonstrated significantly better purification of known interactors from the literature than APEX2 (575). This study from Dr. Eric Bennett’s group cast major doubt onto the reliability of interactome data generated by APEX/APEX2 (575). Another caveat of peroxidase-based approaches (i.e. APEX/APEX2) is low-level catalytic cross-linking of tyrosine residues in the presence of H_2O_2 without biotin labeling (560,576–578). It is unclear at present if this side reaction interferes with proximity labeling to a significant degree – this issue must be resolved to restore confidence in APEX/APEX2-derived interactomes. Lastly, CRAPome data on APEX/APEX2-derived contaminants, and relative abundances, is lacking—this results in further reduced statistical confidence in APEX/APEX2-derived interactome data relative to BioID. Although peroxidase-based approaches show promise for efficient interactome resolution, the confidence in peroxidase-derived datasets is severely lacking at present for the reasons outlined above.

As a result of this critical review of available interactomics approaches, BioID was selected as the optimal tool to resolve the p75NTR-DR6-TROY interactome in live human cells (see Chapter 3) and this rich dataset revealed novel signaling insights (see Chapter 4).

1.10 Figures and Figure Legends

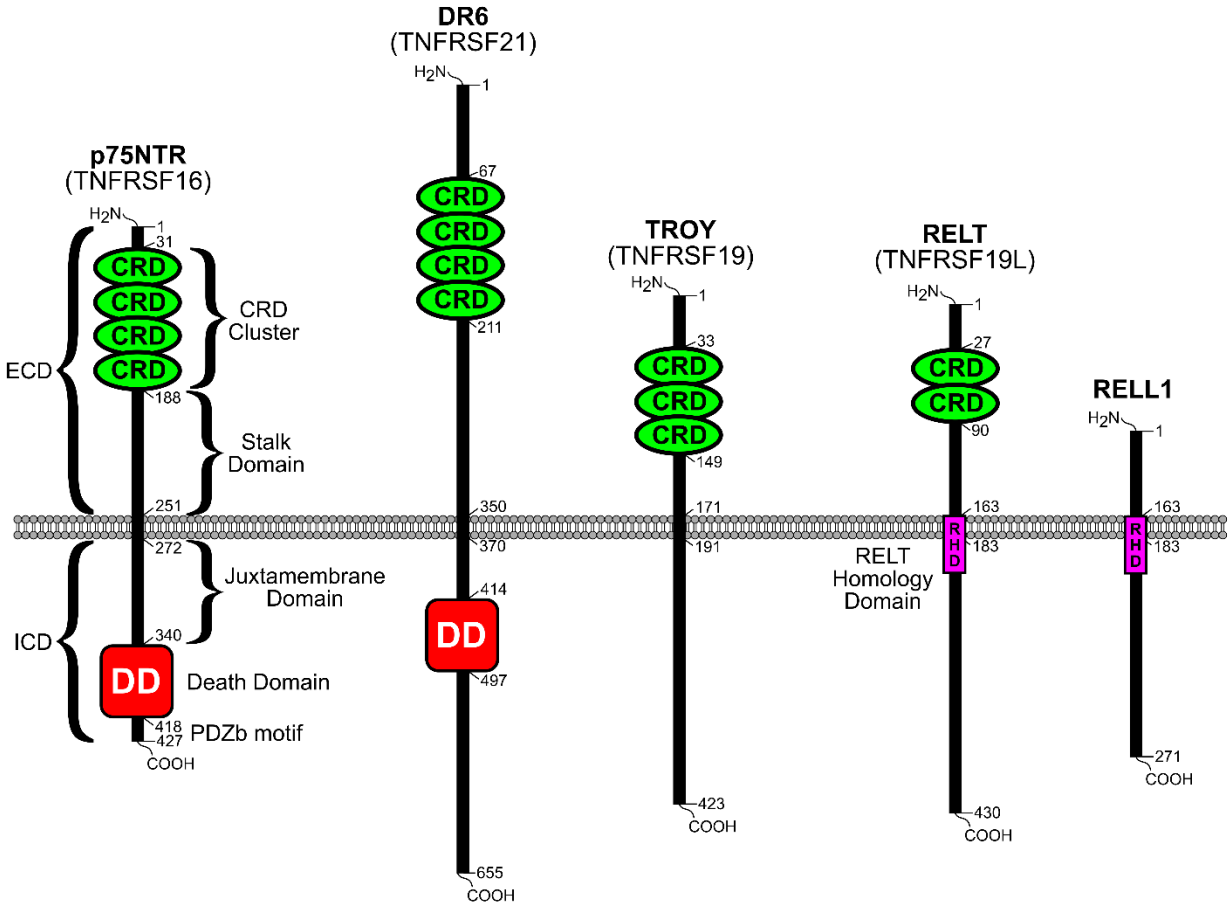

Figure 1. Protein structures of relevant TNFRSFs. Structures of human p75NTR, DR6, TROY, RELT and RELL1 (left-to-right). Primary sequence positions are denoted and all TNFRSFs are drawn to scale. Phospholipid bilayer (grey circles + lines) represents the plasma membrane to illustrate the positions of transmembrane domains.

Chapter 2: Extracellular vesicles mediate p75NTR signaling

2.1 Abstract

The p75 neurotrophin receptor (p75NTR) is trafficked in extracellular vesicles (EVs) *in vitro* and *in vivo* but the physiological relevance of p75NTRn in EVs remains unknown. To address this, we leveraged the p75NTR-dependent COS7 cell expansion phenotype assay. We observed that p75NTR+ COS7 cells seeded on a porous filter induce expansion of naïve COS7 cells on a coverslip below—revealing that p75NTR acts via a non-cell-autonomous mechanism. Size exclusion chromatography (SEC)-based fractionation of condition media (CM) components revealed that large, p75NTR+ EVs mediate the expansion phenotype. Strikingly, EV-derived p75NTR species are highly enriched in p75NTR proteolytic cleavage species (p75CTF and p75ICD). EV-derived p75ICD is sufficient to drive COS7 cell expansion and requires NRAGE in the recipient cell, as NRAGE KO COS7 cells fail to respond to p75NTR+ COS7 donor cells or purified p75NTR+ EVs. We extended this paradigm to a neuronal context, where we demonstrate that COS7-derived p75NTR+ EVs induce growth cone (GC) expansion in developing dorsal root ganglion (DRG) sensory neurons. These data establish EVs as a p75NTR signaling platform.

2.2 Introduction

p75NTR is a major regulator of nervous system development and maintenance. A member of the TNFRSF superfamily, p75NTR acts as a receptor to a diverse set of ligands, not limited to: neurotrophins (579), proneurotrophins (580,581), myelin-associated inhibitory factors (582), and neurotoxic Aβ (583). Structurally, p75NTR is a single-pass transmembrane protein: the p75 extracellular domain (p75ECD) possesses cysteine-rich domains (CRDs) in tandem that

mediate ligand binding, and the p75 intracellular domain (p75ICD) possesses a death domain (DD) and a C-terminal PDZ-binding motif that mediate receptor signaling and trafficking. p75NTR signals in ligand-dependent and -independent states to mediate distinct biological outcomes (579). p75NTR signaling is further regulated by proteolytic cleavage of the receptor via a 2-step mechanism. First, A Disintegrin And Metalloprotease (ADAM17) catalyzes α-secretase cleavage in the p75NTR stalk region to shed the p75ECD and produce the membrane-tethered p75 C-terminal fragment (p75CTF) (584–586). Second, the γ-secretase complex cleaves p75CTF within the transmembrane domain to release soluble p75ICD into the cytosol (585,586).

Despite an extensive literature on p75NTR neurobiology, our knowledge of p75NTR signaling is limited. Indeed, few assays exist to measure p75NTR signaling directly. To address this issue, Zeinieh and colleagues developed a robust p75NTR-dependent COS7 cell expansion assay (587). In this assay, overexpressed p75NTR in immortalized COS7 kidney-derived cell line induces a dramatic cell expansion phenotype. p75NTR-dependent COS7 cell expansion is ligand-independent and occurs via a signaling pathway involving: (i) ADAM17- and γ-secretase-dependent generation of p75ICD; (ii) physical interaction of p75ICD with NRAGE (neurotrophin receptor-associated MAGE homolog); and (iii) downstream activation of the small Rho GTPase Rac1, which drives F-actin polymerization and cell expansion (587). It remains unknown, however, if p75NTR-dependent COS7 expansion occurs via a cell autonomous or non-cell-autonomous mechanism.

Extracellular vesicles (EVs) consist of a highly heterogeneous group of cell-derived membranous structures possessing protein, RNA and DNA cargo (421). Though many subtypes of EVs have been described, most EVs fall into two main classes: exosomes and microvesicles (MVs). Exosomes are small EVs (30-100nm in diameter) generated via the endolysosomal

system. As an early endosome matures to a multivesicular body (MVB), the endosomal membrane invaginates and pinches off to form intraluminal vesicles (ILVs) within the MVB lumen (421,588). If an MVB subsequently avoids the lysosomal route and fuses with the plasma membrane, it releases its ILVs into the extracellular milieu, where they are then referred to as exosomes (421,588). MVs are large EVs (50-1000nm in diameter) derived from the outward budding of the plasma membrane (421,588). p75NTR has been shown to be present in exosomes from several neural cell types *in vitro* (473,589) and from melanoma xenografts *in vivo* (475) but functional characterization of EV-derived p75NTR is lacking. Whether EVs mediate p75NTR signaling events remains unknown.

In this chapter, we explored the nature of the p75NTR-dependent COS7 cell expansion signal. We discovered that p75NTR-dependent COS7 expansion occurs via a non-cell-autonomous mechanism. whereby p75NTR accumulates in an EV compartment. Within this compartment, p75NTR cleavage products are highly enriched. Downstream, p75NTR-containing EVs act on recipient cells in an NRAGE-dependent manner to induce cell expansion. In a neuronal setting, p75NTR-containing EVs induced GC expansion in developing DRG sensory neurons. These data establish EVs as a major p75NTR signaling platform and provide novel evidence that p75ICD can`` mediate non-cell autonomous signaling.

2.3 Materials and Methods

2.3.1 Plasmids, antibodies and reagents

Plasmids used encoded: pcDNA3 vector, GFP (pEGFP-N1 vector; Clontech; GenBank accession # U55762), full-length human p75NTR (subcloned into pCMX vector), and untagged human p75ICD (AA: 273-427; subcloned into pcDNA3 vector). Primary antibodies included:

anti-p75NTR (rabbit polyclonal targeting human p75ICD; produced in-house), anti-NRAGE (rabbit polyclonal targeting human NRAGE; produced in-house), anti-βIII-tubulin (mouse monoclonal; clone TUJ1; Covance), and anti-actin (mouse monoclonal; clone C4; ThermoFisher Scientific). Secondary antibodies included: horseradish peroxidase (HRP)-conjugated donkey anti-rabbit (Jackson ImmunoResearch Laboratories), HRP-conjugated donkey anti-mouse (Jackson ImmunoResearch Laboratories), and Alexa Fluor 647-conjugated goat anti-mouse (ThermoFisher Scientific). GM6001, compound XXI and epoxomicin were purchased from Calbiochem (San Diego, CA, USA). BB94 was purchased from Tocris Bioscience (Ellisville, MO, USA). Laminin was supplied by BD Biosciences (Mississauga, ON, Canada). Poly-D-lysine (PDL) was supplied by Sigma-Aldrich (Oakville, ON, Canada). Laminin-entactin complex was provided by Corning (Tewksbury, MA, USA). Bovine collagen was supplied by Advanced Biomatrix (Carlsbad, CA, USA). NGF was purchased from Alomone Laboratories (Jerusalem, Israel). B_{27} serum-free supplement (B_{27}), 5-fluoro-2'-deoxyuridine (FDU) were purchased from Invitrogen (Waltham, MA, USA). Dulbecco's Modified Eagle Medium (DMEM), penicillin-streptomycin (P/S), L-glutamine, and fetal bovine serum (FBS) were purchased from Wisent Bio Products (Burlington, ON, Canada). Exosome-deprived FBS and Pierce silver stain kits were supplied by ThermoFisher Scientific.

2.3.2 Cell culturing and transfection

COS7 cells were cultured in conditioned medium (CM) containing DMEM supplemented with 100mg/mL P/S, 2mM L-glutamine and 10% FBS. COS7 cell cultures were incubated at 37°C, 5% CO_2. COS7 transfection was performed using the JetPrime lipid nanoparticle-based system (PolyPlus, New York, NY, USA). Briefly, COS7 cells were seeded in a 6-well dish pre-coated with 50ng/mL PDL and a density of 100K cells per well. After 24h, CM was exchanged

for CM lacking P/S. To prepare the transfection mix: 0.5µg of plasmid (per construct) was added to 200µL JetPrime Buffer, vortexed, then 1µL of JetPrime Reagent (scaled up if multiple plasmids) was added, vortexed again, then left at room temperature (RT) for 10 minutes undisturbed. After the 10-minute period, 200µL of transfection mix was applied to COS7 cells for 24h. After the 24h transfection, the transfection medium was washed off 2x in fresh CM, then the transfected COS7 cells were incubated a further 24h in CM.

IMS32 cells were grown in CM consisting of Prigrow III medium (ABM, Richmond, BC, Canada) supplemented with 100mg/mL P/S and 10% FBS. Plastic cell culture dishes were precoated 24h in a proprietary extracellular matrix solution (G422, ABM, Richmond, BC, Canada) and airdried for at least 2h prior to seeding IMS32 cells.

DRG explants were collected from E13.5 mouse embryos using a previously described method (590). Glass-bottom cell culture dishes were precoated in three 24h steps: 1mg/mL PDL, 10µg/mL laminin-entactin complex, and 0.1mg/mL bovine collagen. DRGs were cultured in neurobasal medium supplemented with 2% B_{27} and 10µM FDU.

2.3.3 EV purification

Cells were seeded on precoated 150mm plates at a density of $1.5x10^7$ (COS7) or $5x10^7$ (IMS32) cells per plate. After transfection (if applicable), cells were incubated in 12 mL CM containing exosome-free FBS (exosome-free CM). After a 24h incubation, 10 mL CM was collected and precleared via 3 sequential centrifugation steps at 4°C (collecting supernatant after each): (i) 10 minutes at 300g, (ii) 20 minutes, and (iii) 30 minutes at 10,000g. Precleared CM was then loaded onto an Amicon Ultra-15 centrifugal filter unit and concentrated to 150µL by centrifugation (25 minutes at 4000g, 4°C). 150µL concentrated, clarified CM overlayed onto a

70nm qEV column (Izon). An initial void volume of 1mL was discarded, followed by collection of 12 x 200 µL eluate fractions.

2.3.4 Generation of NRAGE KO COS7 cell lines

Pre-designed gRNA were selected to exons 2 and 3 of the *Maged1* (NRAGE) genomic locus in *Chlorocebus sabaeus* **(**NW_023666086.1) (IDT, USA). Independent preformed crRNA:tracrRNA duplexes bound to Cas9 (IDT, USA) were used to bind gRNAs targeting exons 2 and 3 (CD.Cas9.LBJJ3096.AC and CD.Cas9.LBJJ3096.AB, respectively). $4x10^4$ COS7 cells were seeded per well of a 96-well dish and transfected with 10nM of purified ribonucleoprotein (RNP) complex in antibiotic-free media for 48h using Lipofectamine RNAiMAX (Invitrogen, USA). Single-cell NRAGE KO clones were grown to confluency and NRAGE gene knockout was validated by immunoblot.

2.3.5 COS7 cell expansion assay

The COS7 cell expansion assay is a modification of the protocol described by Zeinieh and colleagues (587). In all iterations of the assay, ‘donor’ COS7 cells secrete factor(s) that act on ‘recipient’ COS7 cells.

Donor and recipient COS7 cells are seeded in independent wells of a 6-well plate at a density of 100K cells/well. Recipient COS7 cells are transfected 24 h with GFP plasmid; donor cells are transfected 24 h with plasmid constructs unique to each experiment. Post-transfection, recipient GFP+ cells are seeded on PDL-coated coverslips at a density of 4K cells/coverslip. For each experimental condition, 3 coverslips of GFP+ recipient cells are seeded and imaged.

In the ‘filter assay’, donor cells are seeded onto PDL-coated 8µm porous 24-well filters (8K cells/filter), and GFP+ recipient cells onto PDL-coated coverslips (4K cells/well) in a 24-well dish. After a 24h incubation, filters containing donor cells are suspended above the

coverslips containing recipient cells within the same well of a 24-well dish for 24h. After this period, donor cells are discarded and recipient cells are fixed in 4% paraformaldehyde (PFA) for 15 minutes at RT. Fixed recipient cells are then washed 3x in PBS and mounted on glass slides with Fluoroshield mounting medium (ThermoFisher). Whole coverslips of GFP+ recipient cells are then imaged by widefield microscopy at 10x magnification. Images are then subjected to pixel intensity-based thresholding in ImageJ, converted to a binary image, and exported to a machine learning algorithm we developed in ilastik (Figure 2.1) (591). In this algorithm, objects are sorted into: (i) individual cells, (ii) cell clusters (which can include mitotic cells), and (iii) cell debris (Figure 2.1). The ilastik output file separates these 3 objects by thresholding in ImageJ (e.g., upper bound = 1, lower bound = 1 will only show individual cells identified by the ilastik algorithm) (Figure 2.1). Only individual GFP+ recipient cells were measured – this was achieved by particle analysis in ImageJ. For each condition, all cells across all 3 coverslips of GFP+ recipient cells were imaged

In the 'co-culture' assay (Figure 2.3A-B), donor cells are co-seeded with recipient cells on the same coverslip (4K donor + 4K recipient cells per coverslip). Cells are then fixed, mounted, imaged and analyzed for GFP+ recipient cell size using the workflow described for the filter assay above.

2.3.6 DRG growth cone assay

DRG explants dissected from E13.5 CD1 mice were seeded on 35mm glass-bottom dishes at a density of 4 DRGs/dish. DRGs were grown 24 h in the presence of NGF. 200 µL of purified COS7-derived EVs (pooled CM fractions #1-3) were co-applied during this 24 h period. After the 24 h growth period, DRGs were fixed in 4% PFA and stained for βIII-tubulin (Alexa Fluor 546-conjugated anti-mouse secondary) and F-actin (Alexa Fluor 488-conjugated

phalloidin). DRG growth cone (GC) fields were imaged by confocal microscopy and 63x magnification. To avoid experimenter sampling bias, 4 exact regions-of-interest (ROIs) within DRG GC fields were pre-selected ahead of imaging. Per each experimental condition, 16 ROIs across 4 DRGs were imaged, and all GCs within those ROIs were measured.

To measure GC area, we developed a machine-learning algorithm in ilastik (Figure 2.2). Prior to machine learning, βIII-tubulin+ axon signal was masked out in ImageJ and the remaining phalloidin+ structures were sent to the ilastik protocol. The ilastik-based algorithm was trained to identify GCs from the masked phalloidin+ signal, and remove non-GC phalloidin+ structures (e.g., small actin filaments along the axon) and debris (Figure 2.2). GCs identified by the ilastik protocol were then measured by particle analysis in ImageJ.

2.3.7 Immunocytochemistry (ICC)

Cells were fixed in 4% PFA (15 minutes at RT), permeabilized (2.5% BSA + 0.2% Triton-X in PBS; 20 minutes at RT) and blocked (2.5% BSA + 0.02% Triton-X; 60 minutes at RT) prior to overnight 4°C incubation in blocking solution containing primary antibody. The following day, the primary antibody was washed off 3x with PBS, then secondary antibody solution (2.5% BSA + 1% serum + secondary antibody) was applied for 1h at RT. The secondary antibody was then washed off with PBS. If phalloidin-488 was required, it was applied for 1h at RT at this time, then washed off 3x with PBS.

2.3.8 Immunoblot (IB)

Harvested cells were lysed in RIPA buffer containing protease inhibitor cocktail and 1μM epoxomicin. 2x Laemmli Sample Buffer (2x SB) was added 1:1 to protein samples, boiled for 5 minutes, then loaded into polyacrylamide gel for subsequent electrophoresis by SDS-PAGE. After SDS-PAGE, proteins were transferred to a nitrocellulose membrane and blocked

for 1 hour, at room temperature, in 5% (w/v) skim milk powder in TBS-T (10mM Tris pH 8.0, 150mM NaCl, 2% Tween-20). Primary antibody incubation was performed in blocking solution at 4°C overnight. Membranes were then washed in TBS-T (6x 10-minute washes) and incubated in HRP-conjugated secondary antibody (diluted in blocking solution) for 1 hour at room temperature. Membranes were then washed in TBS-T (6x 10-minute washes) and immunoreactive bands were detected by chemiluminescence (Clarity Western ECL substrate, BioRad) using the ChemiDoc MP imaging system (BioRad).

2.3.9 Statistics

Gaussian distribution of all datasets was assessed by the Shapiro-Wilk test prior to statistical hypothesis testing. Statistical tests were selected based on the design of each experiment—and distribution of data points—and are described in figure legends. Conservative *posthoc* tests were selected for one- and two-ANOVA analyses. All statistical tests are two-tailed. Statistical significance is defined as $p \leq \alpha \leq .05$. Lastly, *N* is defined as a single technical replicate in all experiments.

2.4 Results

2.4.1 p75NTR induces COS7 cell expansion via a non-cell-autonomous mechanism

p75NTR regulates neurodevelopment, in part, via non-cell-autonomous signaling events *in vivo* (579,580,592). To investigate if the p75NTR-dependent COS7 cell expansion phenotype depends on cell-autonomous or non-cell-autonomous signaling, we performed a COS7 co-culture assay. In this experimental paradigm, naïve GFP^+ COS7 cells were co-cultured with GFP^- cells expressing p75NTR, p75ICD or empty vector and GFP^+ cell size was measured 24h after co-culture (Figure 2.3A). Interestingly, GFP^+ COS7 cell size was significantly larger when co-cultured with COS7 cells expressing p75NTR or p75ICD (~50%; $p < .001$) compared to empty

vector (Figure 2.3B-C). Thus, p75NTR induces COS7 expansion can occur a non-cell-autonomous mechanism.

COS7 cells readily form cell-cell contacts. These structures remain intact in the co-culture assay (Figure 2.3B) so to investigate if p75NTR cell expansion phenotype depends on cell contacts, we developed a 'filter assay' to spatially segregate naïve GFP^+ COS7 cells from p75NTR-expressing cells. Cells expressing p75NTR, p75ICD or empty vector were seeded on a porous filter ('donor' cells) and then suspended above GFP^+ cells that had been pre-plated on a coverslip ('recipient' cells) (Figure 2.3D). After 24h co-culture, GFP^+ recipient cells cultured below $p75NTR^+$ or $p75ICD^+$ donor cells were ~50% larger in size than those cultured with $vector^+$ donor cells ($p < .01$; Figure 2.3E-F), demonstrating that cell contacts are not required for p75NTR-dependent expansion. These data demonstrate that p75NTR-dependent COS7 cell expansion occurs via non-cell-autonomous signaling mechanism that does not require cell-cell contacts.

2.4.2 EVs mediate p75NTR-dependent COS7 cell expansion

We next sought to investigate the nature of the non-cell-autonomous expansion signal induced by p75NTR. Specifically, we investigated if p75NTR-dependent cell expansion relied on the secretion of a large, membranous structure (e.g., EVs) or a small soluble factor (e.g., cytokines, growth factors, etc.).

To ensure that membranous structures purified from conditioned medium (CM) are cell-derived—as opposed to serum-derived—we repeated the filter assay in CM lacking serum-derived exosomes ('exosome-free CM'). Figure 2.4A shows that p75NTR-dependent non-cell-autonomous COS7 expansion occurred in exosome-free CM ($p < .0001$; Figure 2.4A). Next, we applied size exclusion chromatography (SEC) to CM collected from $vector^+$ or $p75NTR^+$ COS7

cells. 12 CM fractions were collected after elution from 70nm qEV columns and total protein content was measured by silver stain to assess EV purification quality. As expected, protein content was lowest in early fractions eluting large EVs (#1-3), slightly higher for small EV fractions (#4-5), then very high for soluble factor fractions (#6-12) (Figure 2.4B). These protein content data are consistent with the literature on EV purification by 70nm qEV-based SEC.

We applied all CM fractions (#1-12) derived from p75NTR+ or vector + COS7 cells directly to GFP+ COS7 cells for 24h and measured cell size. Strikingly, CM fractions #1-5 derived from p75NTR^{+} COS7 cells induced expansion in GFP+_COS7 cells ($p < .0001$; Figure 2.4C) whereas fraction 6-12 did not. Thus, p75NTR-dependent COS7 cell expansion via the non-cell-autonomous pathway is mediated by EVs.

2.4.3 p75NTR is targeted to EVs

Several reports have demonstrated that p75NTR is readily secreted in small EVs—such as exosomes—*in vivo* (473,475,589). This prompted us to ask if p75NTR itself is targeted to the EV compartment(s). To address this, CM was collected from vector^{+} and p75NTR^{+} COS7 cells, fractionated, and analyzed by immunoblot. We found that COS7-derived p75NTR is abundant in large EV fractions (#1-3), but undetectable in small EV fractions (#4-5) and soluble protein fractions (#6-12) (Figure 2.5A). Therefore, p75NTR is targeted to the EV compartment(s) that mediate COS7 cell expansion, suggesting that p75NTR is the non-cell-autonomous factor that mediates this expansion. When analyzed in COS7 cells, p75NTR is preferentially targeted to large EVs.

Given that the COS7 model relies on p75NTR overexpression, we next investigated if cell types that normally express p75NTR generate EVs that are p75NTR positive. To do this, we used an immortalized Schwann cell-like cell line, IMS32, which expresses high levels of

p75NTR. CM was collected from IMS32 cells after 24h incubation. Immunoblot revealed that p75NTR is present in IMS32 CM fractions #1-5, demonstrating that endogenous p75NTR is readily secreted in EVs. Consistent with the p75NTR overexpression data, endogenous p75NTR from IMS32 cells is preferentially targeted to large EVs (fractions #1-3) rather than small EVs (fractions #4-5).

2.4.4 p75NTR cleavage products are enriched in EVs

In Figure 2.5, immunoblots of purified EVs show low MW bands at 22kDa and 18kDa at a greater signal intensity than FL p75NTR (75kDa). Given that the p75NTR antibody used targets the ICD, it is possible these bands reflect p75NTR cleavage products. To test this, $p75NTR^{+}$ COS7 cells were incubated 48h in the presence or absence of GM6001 + BB94 (α-secretase inhibitors) or compound XXI (γ-secretase inhibitor), which are known to inhibit the generation of p75CTF and soluble p75ICD, respectively (585–587). Purified large EVs fractions #1-3 were pooled together for subsequent p75NTR immunoblot. GM6001 + BB94 reduced the 22kDa band in EVs and whole cell lysate, indicating that p75CTF is present in EVs (Figure 2.6). Unexpectedly, an unknown 55kDa p75NTR species unique to EVs was strongly downregulated in the presence of GM6001 + BB94, suggesting that an alternative α-secretase-dependent p75NTR cleavage may be present in EVs (Figure 2.6). Compound XXI strongly reduced the 18kDa band in EVs and whole cell lysate—together with an increase in p75CTF—indicating that this species is soluble p75ICD (Figure 2.6). In conclusion, p75NTR cleavage products are highly enriched in EVs. In a complete reversal compared to cell lysates, p75NTR α- and γ-secretase cleavage products are more abundant than FL p75NTR in the EV compartment.

2.4.5 NRAGE acts downstream of p75NTR+ EVs to mediate COS7 cell expansion

Zeinieh and colleagues (2015) demonstrated that p75ICD is the functional p75 species mediating the COS7 cell expansion phenotype and that it requires NRAGE as a downstream binding partner. To investigate if NRAGE mediates p75NTR-dependent COS7 expansion via the non-cell-autonomous pathway, we applied CRISPR gene editing to the NRAGE genomic locus *MAGED1* to generate two independent NRAGE knockout COS7 cell lines (NRAGE KO #1 and #2; Figure 2.7A).

To assess if NRAGE is required in donor and/or recipient COS7 cells to mediate p75NTR-dependent expansion, we used the filter assay approach. We observed that NRAGE KO in donor cells had no effect on p75NTR-dependent expansion of GFP^+ recipient cells (Figure 2.7B-C). In contrast, $p75NTR^+$ donor cells failed to induce expansion in NRAGE KO recipient cells (Figure 2.7D-E). To test if NRAGE acted downstream of $p75NTR^+$ EVs, we directly applied EVs derived from $vector^+$ or $p75NTR^+$ donor cells onto WT and NRAGE KO recipient cells. WT recipient cells expanded in response to $p75NTR^+$ EVs, whereas NRAGE KO recipient cells did not (Figure 2.7F). These data establish recipient cell-derived NRAGE as a necessary mediator of p75NTR-dependent, non-cell-autonomous COS7 cell expansion.

2.4.6 p75NTR+ EVs induce growth cone expansion in developing DRG sensory neurons

We next asked whether p75NTR+ EVs induce expansion events in a neuronal setting. Given that p75NTR is a major regulator of growth cone (GC) dynamics in the developing nervous system (593–597), we investigated if COS7-derived p75NTR EVs exert an effect on growth cone size in DRG sensory neurons. Briefly, E13.5 murine DRG explants were cultured for 24 h *in vitro* in media containing NGF and EVs derived from either $vector^+$ or $p75NTR^+$ COS7 cells. After 24h, DRGs were fixed and co-stained with the axonal marker βIII-tubulin and phalloidin to label GCs. Figure 2.8 shows that p75NTR+ EVs induced a ~20% increase in GC

area relative to vector$^+$ EVs ($p < .0001$; Figure 2.8). Thus, p75NTR$^+$ EVs can induce cytoskeletal expansion in a neuronal context.

2.5 Discussion

These data collectively establish EVs as a p75NTR signaling platform. We demonstrate that p75NTR-dependent COS7 cell expansion occurs via a non-cell-autonomous mechanism as p75NTR+ donor cells induce expansion in spatially segregated GFP+ recipient cells. Using CM fractionation, we identified large, p75NTR+ EVs as the structural entity mediating the non-cell-autonomous expansion events. Strikingly, p75NTR α- and γ-secretase cleavage products (p75CTF and p75ICD, respectively) were found to be highly enriched in EVs. Downstream of p75NTR+ EVs, recipient cell-derived NRAGE is required to execute the expansion signal. Lastly, p75NTR+ EVs induce expansion in a neuronal setting. Specifically, we demonstrate that p75NTR+ EVs induce expansion of GCs in developing DRG sensory neurons *in vitro*.

Although p75NTR has been previously detected in exosomes (473,475,589), we provide novel evidence that p75NTR is targeted to large EVs with an elution profile most akin to plasma membrane-derived MVs. The endogenous p75NTR exocytosis assay in IMS32 Schwann-like cells (Figure 2.6) indicated that a small amount of p75NTR is targeted to small EVs (such as exosomes), but most is found in large EVs. We provide the first evidence that EV-derived p75NTR is biologically active—specifically, we demonstrate that p75NTR+ EVs can mediate cell expansion through an NRAGE-dependent signaling pathway. Previous literature has shown that melanoma-derived p75NTR+ exosomes can facilitate metastatic niche formation in lymph nodes (475), but the nature of p75NTR signaling in this setting was not explored. Given our

findings, it would be interesting to know if melanoma-derived EVs require p75NTR to drive metastasis and niche formation—and, if so—is this reliant on recipient cell-derived NRAGE.

The subcellular compartment(s) mediating p75NTR proteolytic cleavage is unknown. An interesting discovery in this project was the abundance of p75NTR cleavage products (p75CTF and p75ICD) in EVs. We also observed a novel 55kDa p75NTR species unique to EVs that we suspect to be an alternative α-secretase cleavage product, as its abundance is reduced by pharmacological alpha-secretase inhibition (Figure 2.6). These data establish that EVs traffic p75NTR cleavage products and may be a site for p75NTR cleavage events. However, we cannot rule out the possibility of intracellular generation of p75NTR cleavage products that are then targeted to EVs via an unknown mechanism. Given that p75ICD undergoes rapid turnover in the cytosol (585,586), it is possible that EVs serve to protect p75ICD from the proteasome, thus allowing large quantities to accumulate and act locally in the recipient cell prior to turnover.

An outstanding question that emerges from this project is how exocytosis of p75NTR+ vesicles occurs. Exosomes and MVs can be generated via local accumulation of ceramide in a membranous compartment (451,468). Although multiple ceramide biosynthesis pathways exist, exosome and MV biogenesis relies largely on sphingomyelinase (SMase)-dependent ceramide synthesis. Interestingly, p75NTR has been to induce SMase-dependent ceramide production in central neurons and some cell lines (598,599). This raises the intriguing possibility that p75NTR-dependent ceramide generation may promote the generation of p75NTR-containing EVs.

The discovery of EVs as a p75NTR signaling platform has implications for the field of p75NTR biology. EVs can act in an autocrine, paracrine, or endocrine manner to coordinate intercellular communication. Thus, p75NTR expression patterns alone may not necessarily reflect sites of p75NTR action *in vivo* since EVs can act locally or distally. Our data raise the

possibility that p75NTR can act systemically to exert biological effects on distal tissues. Further work will be required to test this possibility in the context of nervous system development and maintenance.

2.6 Figures and Figure Legends

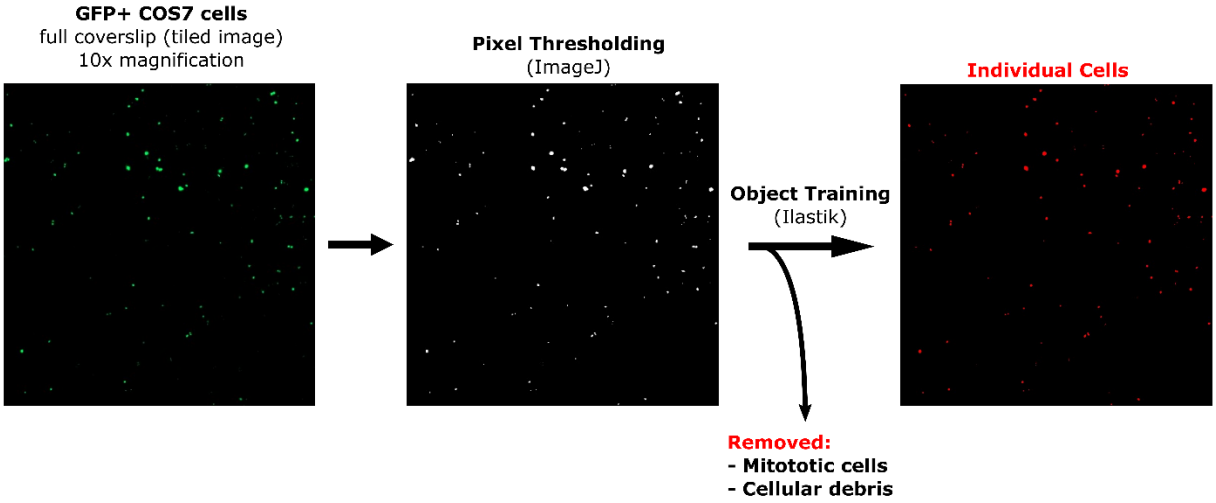

Figure 2.1. Isolation of individual GFP+ COS7 cells for cell size analysis. Whole coverslips of GFP+ COS7 cells were imaged by widefield microscopy (10x magnification; tiled image). Pixel thresholding was performed in ImageJ to isolate the GFP signal. Object training was performed in Ilastik using machine learning algorithms to identify individual GFP^+ cells for analysis.

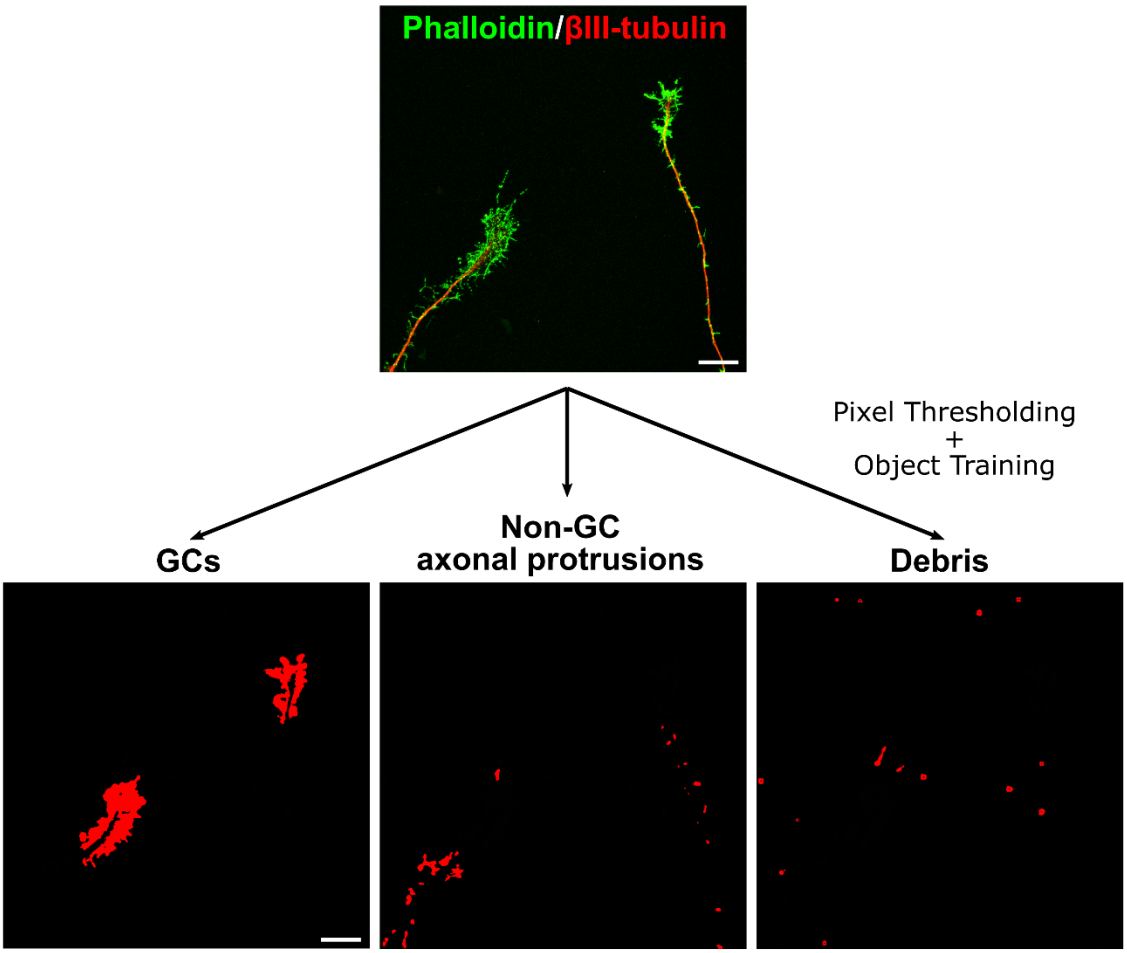

Figure 2.2. Isolation of DRG growth cones for size analysis. E13.5 DRG explants were cultured in the presence of NGF for 24h, fixed and stained for βIII-tubulin and F-actin (phalloidin). βIII-tubulin^{+} axon signal was masked out to isolate phalloidin^{+} filamentous structures. Machine learning algorithms were applied to isolate GCs and remove non-GC phalloidin^{+} structures and nonspecific signal.

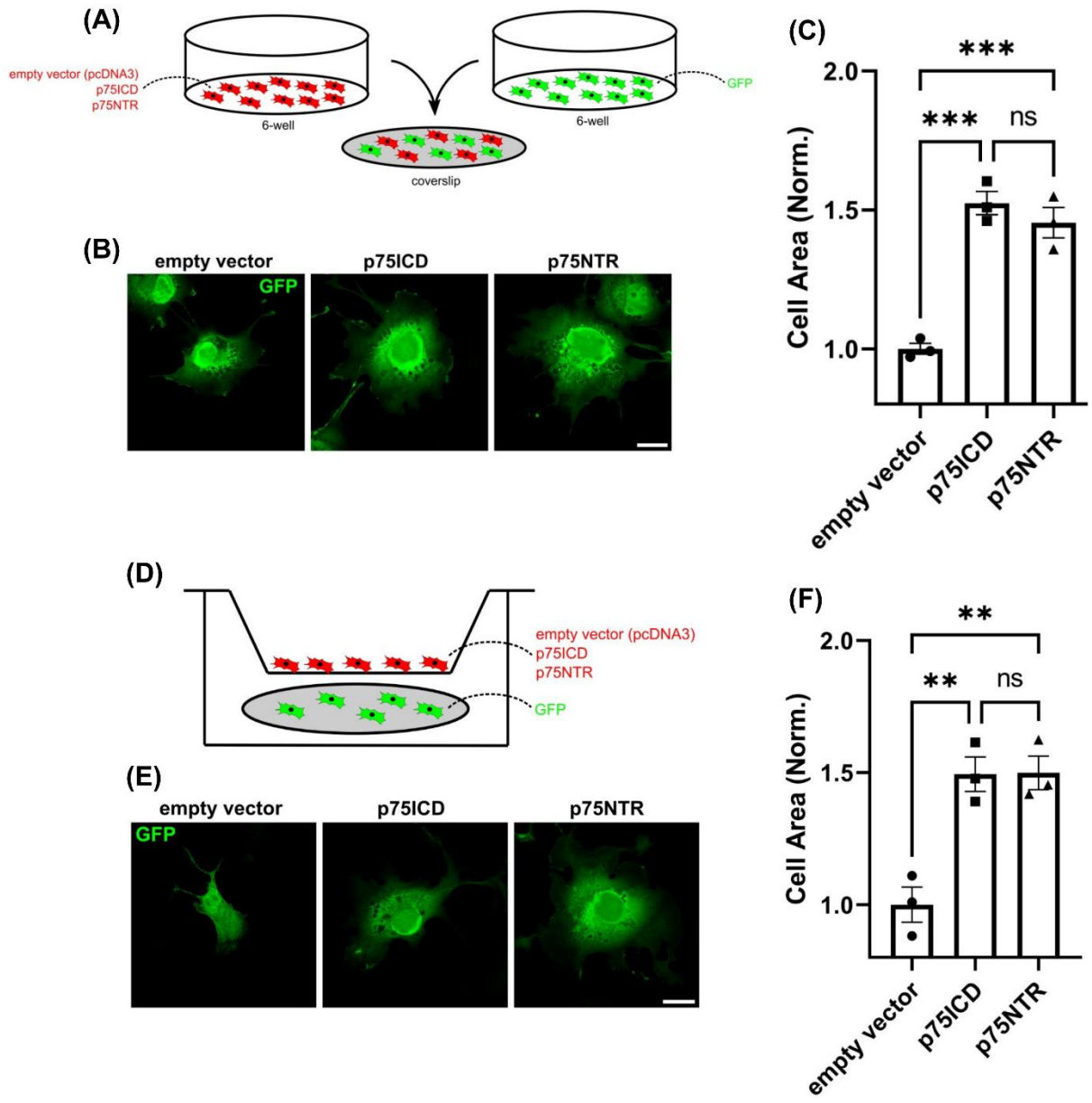

Figure 2.3. p75NTR induces COS7 cell expansion via a non-cell-autonomous mechanism.

(A) Co-culture assay to measure non-cell-autonomous effects on COS7 cell size. (B) Representative confocal images of naïve GFP+ COS7 co-cultured with COS7 cells overexpressing the indicated constructs. (C) Quantification of GFP+ COS7 cell area from the co-culture assay. (D) Filter-based assay to spatially segregate donor COS7 cells from naïve GFP+ recipient COS7 cells. (E) Representative confocal images of GFP+ recipient cells cultured below donor cells overexpressing: vector, p75ICD or p75NTR. (F) Quantification of GFP+ recipient

cell area from the filter assay. N=3 independent experiments. ≥ 200 cells measured per condition per technical repeat. One-way ANOVA with Tukey post-hoc test. $**p < 0.01$; $***p < 0.001$; ns – not significant. Error bars represent +/- SEM. Scale bar = 20µm.

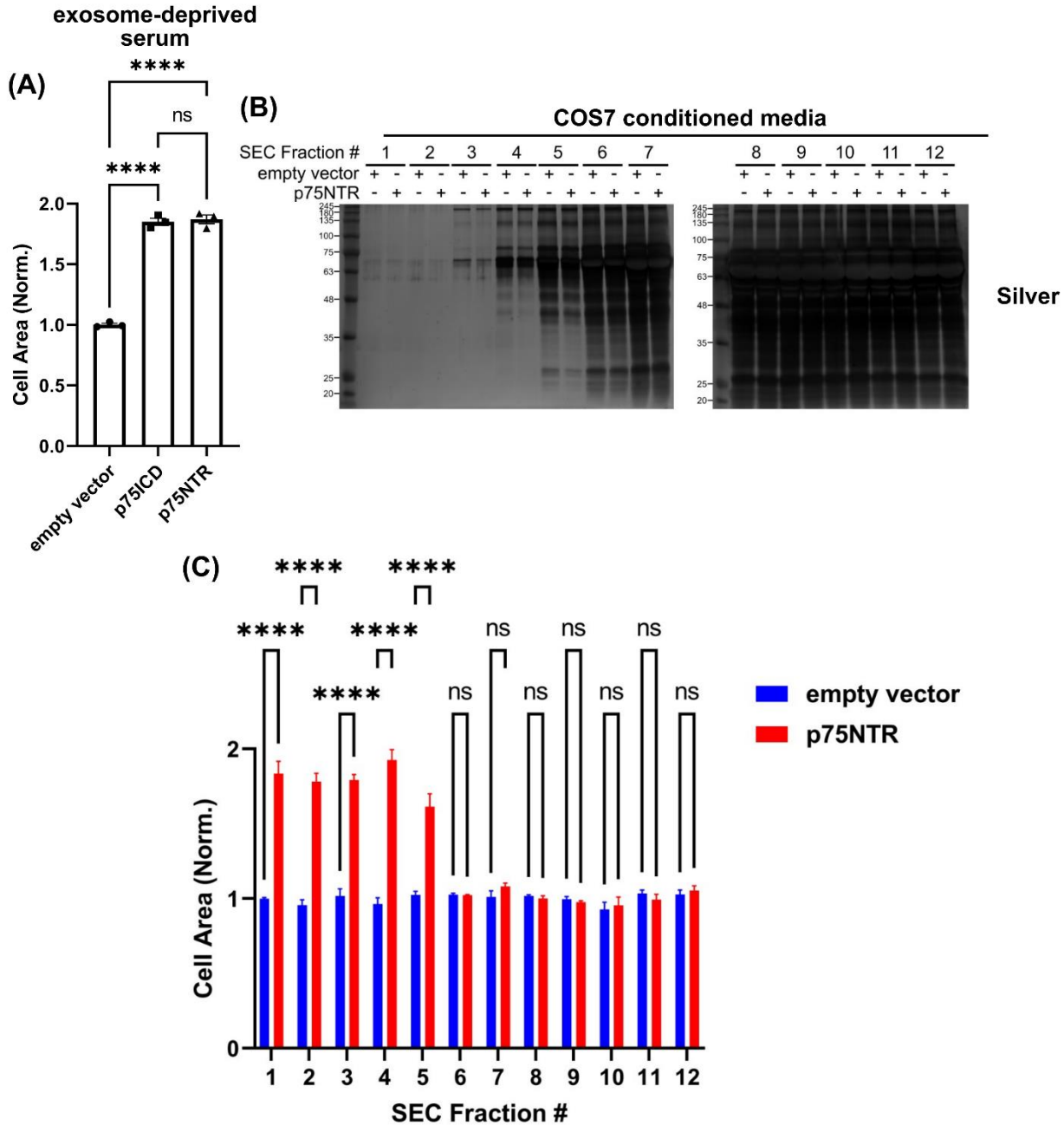

Figure 2.4. Extracellular vesicles mediate p75NTR-dependent COS7 cell expansion. (A) Filter-based COS7 expansion assay in exosome-free CM. Donor cell transfection conditions are shown on the x-axis. GFP+ recipient cell area is quantified. N = 3 independent experiments. ≥ 200 cells measured per condition per technical repeat. One-way ANOVA with Tukey post-hoc test. ****$p < 0.0001$; ns – not significant. (B) Silver protein stain for SEC fractions collected

from COS7 conditioned medium. (C) Cell area of GFP+ COS7 cells after 24h exposure to purified EVs (pooled SEC fractions #1-3) derived from donor COS7 cells. N = 3 independent experiments. ≥ 200 cells measured per condition per technical repeat. Two-way ANOVA with Sidak post-hoc test. ****$p < 0.0001$; ns – not significant. Error bars represent +/- SEM.

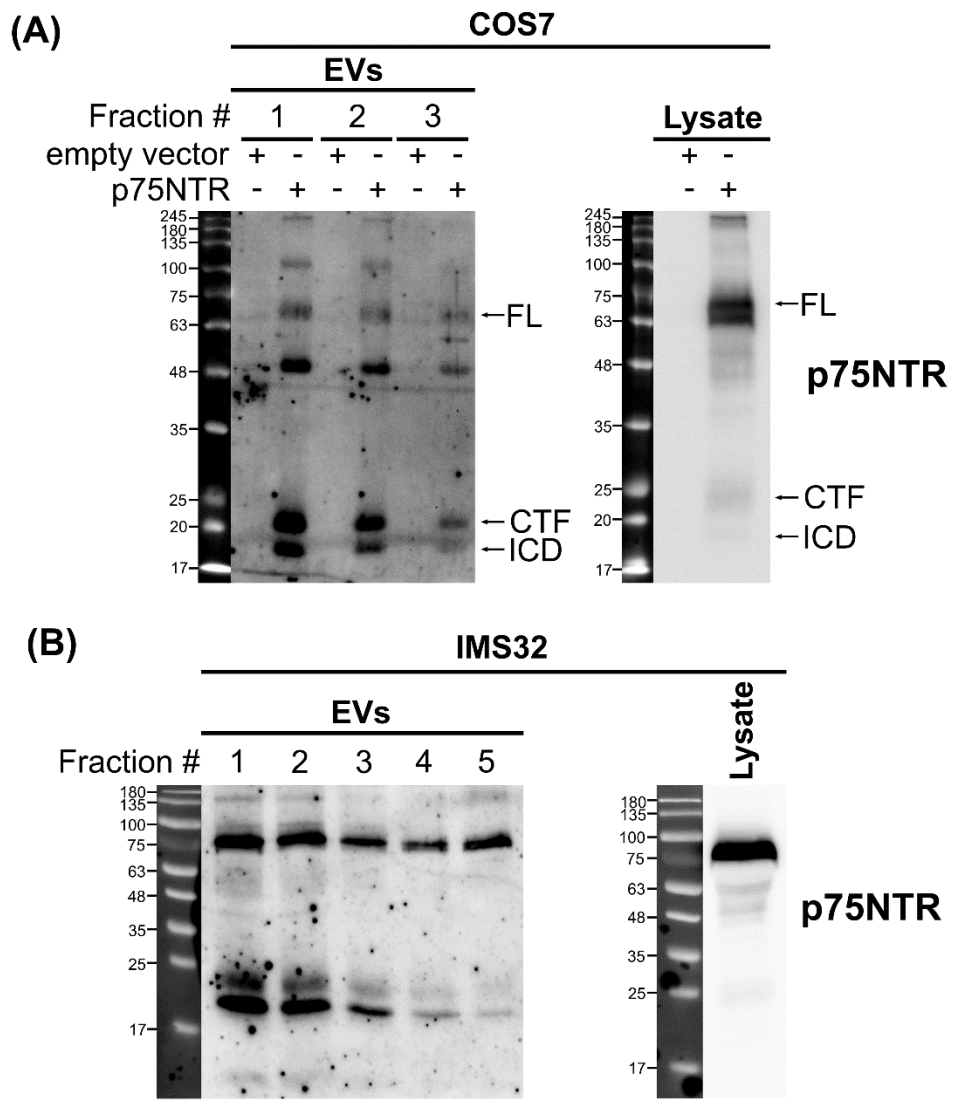

Figure 2.5. p75NTR is secreted in extracellular vesicles. (A) p75NTR immunoblot of purified EVs derived from the conditioned medium of COS7 cells overexpressing vector or p75NTR. (B) Detection of endogenous p75NTR in purified EVs derived from the conditioned medium of IMS32 cells by immunoblot.

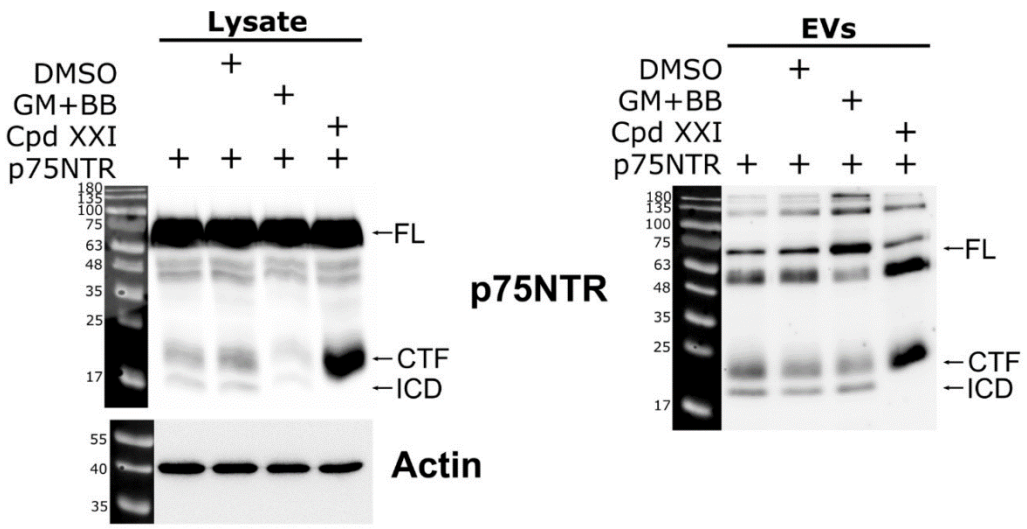

Figure 2.6. p75NTR cleavage products are enriched in extracellular vesicles. p75NTR immunoblot of purified EVs and lysates derived COS7 cells overexpressing p75NTR. Cells were treated 48h with: (i) nothing, (ii) DMSO, (iii) GM6001+BB94, or (iv) compound XXI. Bands corresponding to full-length (FL) p75NTR and proteolytic cleavage products (CTF, ICD) are labeled. N = 3 independent experiments.

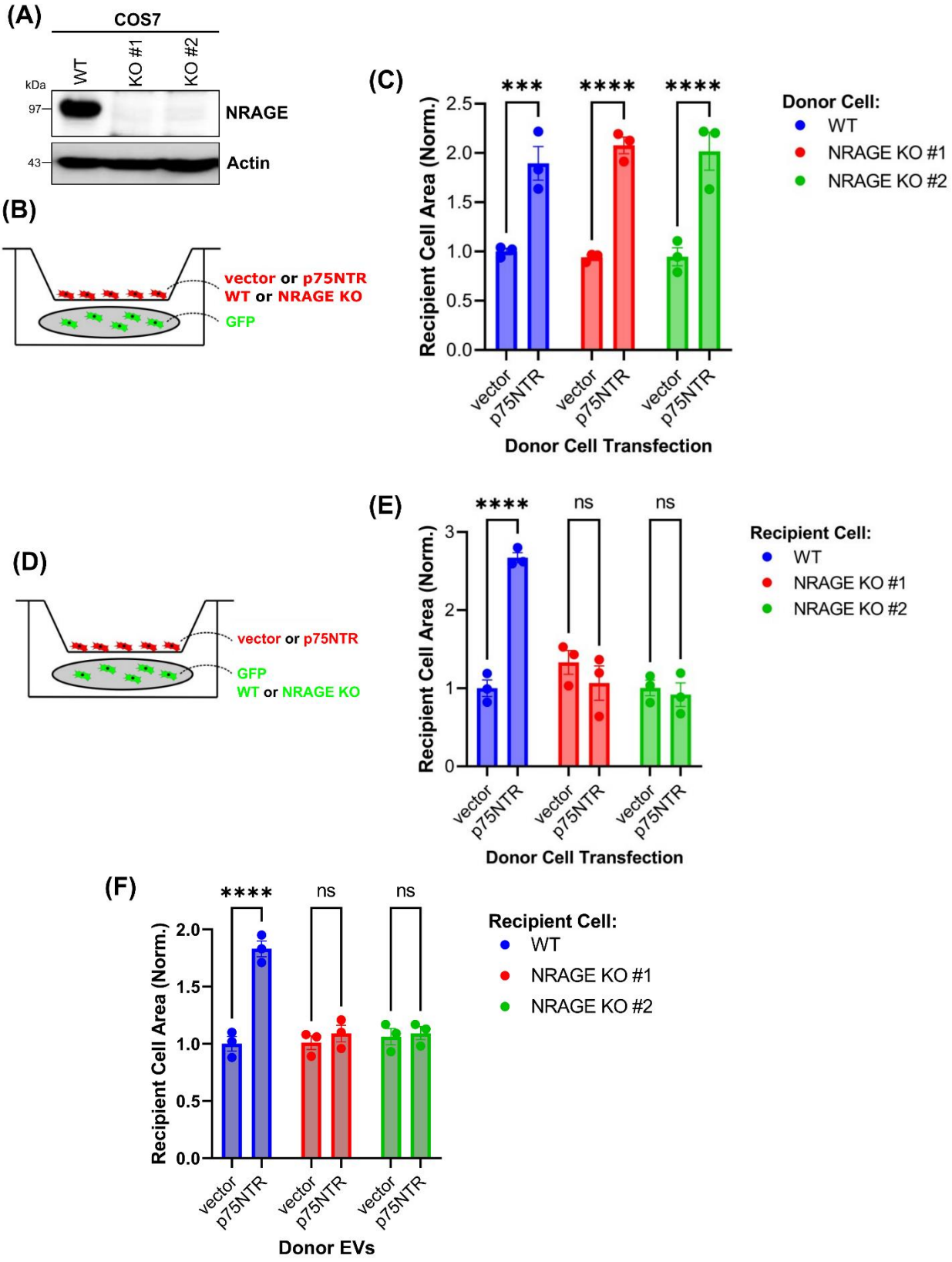
(A)
COS7
WT
KO #1
KO #2
kDa
97
NRAGE
43
Actin
(B)
vector or p75NTR
WT or NRAGE KO
GFP
(C)
***
****
****
Recipient Cell Area (Norm.)
2.5
2.0
1.5
1.0
0.5
0.0
vector
p75NTR
Donor Cell Transfection
Donor Cell:
WT
NRAGE KO #1
NRAGE KO #2
(D)
vector or p75NTR
GFP
WT or NRAGE KO
(E)
****
ns
ns
Recipient Cell Area (Norm.)
3
2
1
0
Donor Cell Transfection
Recipient Cell:
WT
NRAGE KO #1
NRAGE KO #2
(F)
****
ns
ns
Recipient Cell Area (Norm.)
2.0
1.5
1.0
0.5
0.0
Donor EVs
Recipient Cell:
WT
NRAGE KO #1
NRAGE KO #2

Figure 2.7. Recipient cell-derived NRAGE is required for p75NTR EV-induced COS7 expansion. (A) Generation of two independent NRAGE KO COS7 cell lines by CRISPR. NRAGE immunoblot is shown. (B-C) Filter assay design (B) and recipient cell areas (C). WT vs. NRAGE KO donor cells were transfected with vector or p75NTR. GFP^+ recipient cell area is quantified. (D-E) Filter assay design (D) and recipient cell areas (E). WT donor cells were transfected with vector or p75NTR. Recipient cells are WT or NRAGE KO. GFP+ recipient cells area is quantified. (F) Purified EVs—derived from vector- or p75NTR-expressing donor COS7 cells—were applied to GFP+ recipient COS7 cells from WT and NRAGE KO backgrounds. GFP+ cell area is quantified. N = 3 independent experiments. ≥ 200 cells measured per condition per technical repeat. Two-way ANOVA with Sidak post-hoc test. ****$p < 0.0001$; ns – not significant. Error bars represent +/- SEM.

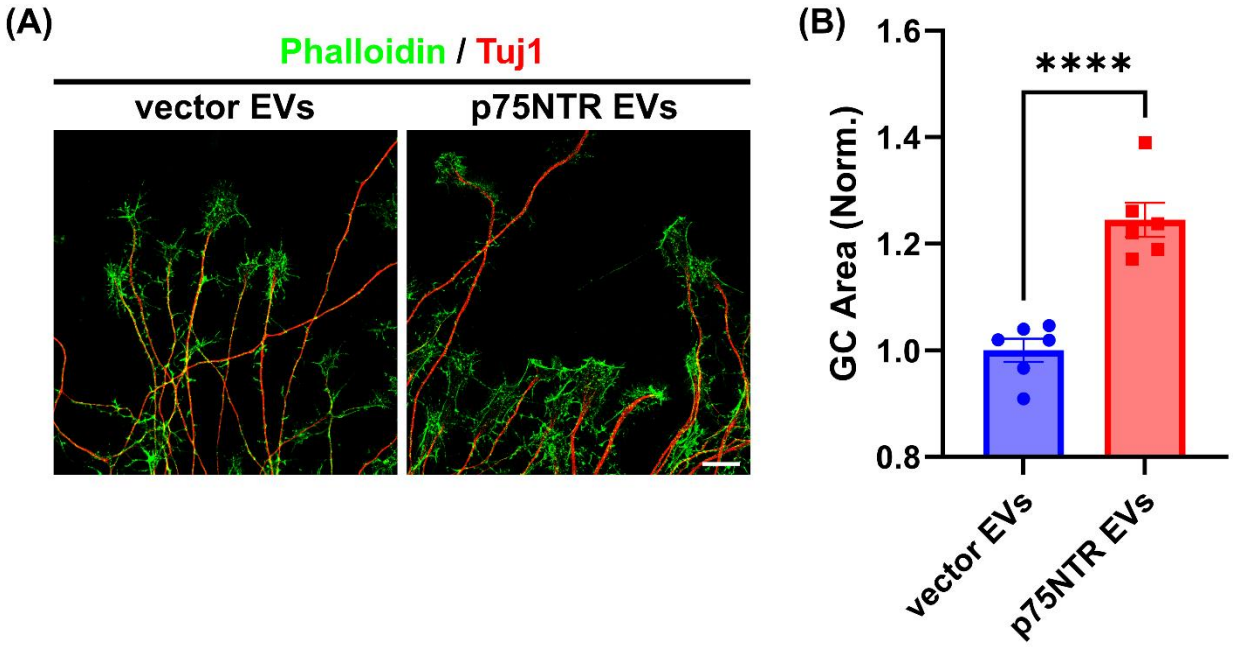

Figure 2.8. Exogenous p75NTR+ EVs induce DRG growth cone expansion *in vitro*. (A) E13.5 DRG explants were grown for 24h in the presence of NGF. COS7-derived EVs (vector vs. p75NTR) were co-applied for the full 24h incubation. DRGs were co-stained with anti-βIII-tubulin and phalloidin. Phalloidin+ GCs were identified by machine learning and GC area was quantified in (B). N = 6 independent experiments. 16 GC fields were measured across 4 DRGs per technical repeat (4 ROIs per DRG x 4 DRGs; ~100 GCs total). Independent samples t-test. ****$p < 0.0001$. Scale bar = 20µm. Error bars represent +/- SEM.

Chapter 3: Resolution of the p75NTR-DR6-TROY interactome

3.1 Abstract

The p75 neurotrophin receptor (p75NTR), death receptor 6 (DR6) and TROY are tumour necrosis factor receptors (TNFRSFs) with functionally redundant roles nervous system development and maintenance, including: axonal degeneration, pathological neurodegeneration, synaptic plasticity, and neuronal remodeling (80-88). Despite this extensive phenotypic characterization, our understanding of the core signaling mechanisms engaged by these receptors remains elusive. To address this problem, we leverage a novel proximity labeling interactomics approach (BioID) (500) to resolve the interactome of p75NTR, DR6 and TROY in live human cells. BioID revealed that full-length (FL) p75NTR, DR6 and TROY show substantial overlap in the interactors they engage with and identified a core network of 29 proteins that interact with all 3 receptors. The core network that was identified implicated several major signaling pathways, including: ephrin-mediated axon guidance (EFNB1 and EFNB2), PI4K signaling (EFR3A and EFR3B), and cellular ion homeostasis [e.g. multiple members of the solute carrier (SLC) family]. BioID also revealed a conserved TNFRSF, RELL1, that interacts with each of the bait TNFRSFs. Lastly, proteolytic cleavage of these receptors to release their intracellular domain (ICD) into the cytosol initiates divergent signaling outcomes (399). Strikingly, the ICD-specific interactome of these 3 TNFRSFs showed nearly no overlap, in direct contrast to their full-length counterparts. In conclusion, we successfully resolved the p75NTR-DR6-TROY interactome in living human cells, which will serve as a critical foundation to explore the signaling mechanisms underlying TNFRSF-dependent nervous system function, and may identify novel therapeutic strategies for targeting neurodegenerative and neuropsychiatric disorders.

3.2 Introduction

The p75 neurotrophin receptor (p75NTR), death receptor 6 (DR6) and TROY are TNF receptors (TNFRSFs) with redundant functionality in nervous system development (51,52,56,57,61,77,373,375,600), nervous system maintenance (193,202,316,317,374,380,399,411,601), and tumorigenesis (78,360,412,414,416,417,602–604). p75NTR and DR6 initiate axonal degeneration in developmental (51,52,64,156,176,216,605) and pathological contexts. p75NTR and TROY can each serve as a co-receptor in complex with the Nogo receptor (NgR1) and LINGO-1 to bind myelin-associated inhibitory factors (MAIFs) and restrict neurite outgrowth in the CNS (59,61,411,600,606). DR6 and TROY are critical regulators of axonal remodeling (51,56–58,61,380,398) and angiogenesis (393) within the CNS.

With respect to signaling properties, p75NTR, DR6 and TROY are atypical TNFRSFs insofar as none of these receptors bind a known TNF ligand (607). Rather, p75NTR acts as a receptor to all mammalian neurotrophins (NGF, BDNF, NT3 and NT4) and immature, non-proteolytically processed proneurotrophins (proNGF, proBDNF, proNT3 and proNT4) [reviewed in (608)]. DR6 is a receptor for the β-amyloid precursor protein (APP) (58,78,373,381) and pathogenic β-amyloid-mediated neurodegeneration is initiated via both p75NTR and DR6 (250,256,374,382,609,610). The TROY ligand remains to be identified—if it exists at all—but both p75NTR and TROY can bind MAIFs in complex with NgR1 and LINGO-1 as described above (59,61,411,600,606). p75NTR possesses ligand-dependent and ligand-independent signaling properties [reviewed in (77)], though it remains unclear if the same is true of DR6 and TROY. To add to this complexity, p75NTR (90, 125-128), DR6 (399), and TROY (unpublished) can be proteolytically cleaved to release their soluble intracellular domain (ICD) into the cytosol. In the case of p75NTR and DR6, and likely TROY, the soluble ICD mediates signaling outcomes distinct from the full-length (FL) receptor (90, 125-128).

Despite the extensive phenotypic characterization of p75NTR, DR6 and TROY in the nervous system—and the emerging trend of functional redundancy amongst these TNFRSFs—our knowledge of the core signaling mechanisms engaged by these receptors is limited. To address this issue, we sought to resolve the p75NTR-DR6-TROY interactome in a live, human cell line. To accomplish this daunting task, we employed the next-generation interactomics tool BioID (1) (see Section 1.11.1).

BioID successfully resolved the p75NTR-DR6-TROY interactome and revealed extensive interactor overlap between these TNFRSFs, consistent with their overlapping functionality in nervous system development and maintenance. BioID revealed a core group of 29 prey finding all 3 receptors, which may be of particular interest to explore in the context of the nervous system. GO analysis identified multiple signaling pathways enriched within the p75NTR-DR6-TROY interactome, not limited to: ephrin signaling, ion transport, immune regulation, and receptor trafficking. Interestingly, all 3 TNFRSFs interacted with the TNFRSF superfamily member Receptor Expressed in Lymphoid Tissues-Like 1 (RELL1)—suggesting an entire novel heterotypic TNFRSF complex, which may provide insight into a major new regulatory mechanism of TNF signaling (see Chapter 3). Successful resolution of the p75NTR-DR6-TROY interactome will accelerate research into TNFRSF regulation of the nervous system and may identify novel therapeutic targets for pathological neurodegeneration and neuropsychiatric disorders.

3.3 Materials and Methods

3.3.1 Cell maintenance and transfection

Flp-In T-TREx 293 cells were maintained in Dulbecco's Modified Eagle Medium (DMEM) supplemented with 5% bovine calf serum, 5% fetal bovine serum, 2mM L-glutamine,

and 100mg/mL penicillin/streptomycin at 37°C in 5% CO_2. Lipid-based transfection of Flp-In T-REx 293 cells was performed with JetPrime (PolyPlus) according to a modified protocol from manufacturer instructions. Briefly, $1x10^6$ Flp-In T-REx 293 cells were seeded onto a single well of an uncoated 6-well plate. The Flp-In T-REx 293 were transfected in antibody-free complete medium with 200uL of a mastermix containing 0.5µg of plasmid and 1µL of JetPrime reagent. If co-transfection was necessary, the JetPrime reagent volume was held equal across conditions (using the quantity required by the condition with most co-transfected plasmids) to prevent inequalities in transfection efficiency between conditions. Flp-In T-REx 293 cells were transfected for 24 hours, followed by 24-hour incubation in fresh complete medium, prior to experimentation.

3.3.2 Plasmids and reagents

Full-length (FL) TNFRSF BioID constructs p75NTR-BirA^{R118G}-FLAG, DR6-BirA^{R118G}-FLAG and TROY-BirA^{R118G}-FLAG were subcloned into pcDNA5 FRT/TO vector. To generate cleavage-resistant (CR) BioID constructs, the TMD of p75NTR, DR6 and TROY was exchanged with Fas TMD prior to subcloning in pcDNA5 FRT/TO vector. All FL and CR TNFRSF-BirA^{R118G}-FLAG plasmids were generated in-house. Stable integration of BioID constructs into the Flp-In T-REx 293 cell line (ThermoFisher, USA) was mediate by co-transfection of pOG44 Flp recombinase expression vector (ThermoFisher, USA). During the BioID procedute, 1µM tetracycline (Tet) (ThermoFisher, USA, catalog # A39246) was applied for 24h to induce expression of TNFRSF-BirAR118G-FLAG expression in Flp-In T-REx 293 cells.

3.3.3 BioID: Protocol

Flp-In T-REx 293 cells were co-transfected with pcDNA5 FRT/TO (TNFRSF-BirAR118G-FLAG bait expression vector) and pOG44 (Flp recombinase expression vector)

plasmids. Successful genomic integration of the TNFRSF-BirA*-FLAG construct (p75NTR, DR6 or TROY; full-length (FL) or cleavage-resistant (CR) conferred hygromycin-resistance and individual TNFRSF-BirA-FLAG$^+$ cell colonies were selected in complete media containing 200 µg/mL hygromycin B. TNFRSF-BirA*-FLAG$^+$ Flp-In T-REx 293 cells were passaged to 5x 150mm plastic dishes and grown to 70% confluency. Expression of the TNFRSF-BirA*-FLAG bait and stimulation of proximity-dependent biotinylation in TNFRSF-BirA*-FLAG$^+$ Flp-In T-REx 293 cells was induced by incubation in 10mL of conditioned media containing 1 µg/mL tetracycline and 50µM biotin for 24 hours (at 37°C, 5% CO_2). After the 24-hour period, a pooled cell pellet was collected from all 5x 150mm plates of TNFRSF-BirA*-FLAG$^+$ Flp-In T-REx cells and centrifuged at 1500rpm (5 min, RT). Cell pellets were washed 3x in ice-cold PBS, dried, and stored at -80°C. Cell pellets were subsequently lysed and biotinylated prey were captured on streptavidin-coated resin. Streptavidin-purified prey were then trypin digested and subjected to mass spectrometric analysis for peptide identification and abundance quantification.

3.3.4 BioID: Statistical Analysis and Contaminant Removal

All BioID runs (for each TNFRSF) were performed in biological and technical duplicate. Pooled mean spectral counts for each prey were calculated and subject to a battery of controls. First, after application of standardized BioID protocols, all prey spectral counts were cross-referenced to the associated mean spectral count for that specific prey in the CRAPome contaminant repository (611). All prey with ≤ 2-fold spectral count enrichment relative to CRAPome abundances were categorized as background and removed from subsequent analyses. Next, all remaining prey spectral counts were input into the Significance Analysis of Interactome (SAINT) algorithm (612) to assign probabilistic scores to each prey with 1% false-discovery rate (FDR) parameters input into the Bayesian matrix. Prey with a SAINT score ≤ 0.74 (analogous to

$p \leq 0.05$) were labelled as contaminants and removed. Lastly, mean prey spectral counts were compared to their spectral counts from 22 internal control BioID baits (8 unrelated transmembrane protein BirA^{R118G}-FLAG fusion baits, 6 E-cadherin-BirA^{R118G}-FLAG cell junction control baits, 4 'BirA^{R118G}-FLAG-only' controls, and 4 'no transfection' controls). All prey with ≥ 2-fold spectral count enrichment relative to all control baits were identified as *bona fide* high-confidence interactors.

3.3.5 Gene Ontology (GO) Analysis

GO functional analysis was performed using the Database for Annotation, Visualization and Integrated Discovery (DAVID) platform (613,614). All gene IDs from the p75NTR-DR6-TROY interactome were input into the DAVID platform, and enriched functional GO terms were identified via cross-referencing to the Reactome cell pathway database (615). Raw *p*-values associated with specific GO terms were corrected *post hoc* according to the Benjamini-Hochberg procedure (616) to maintain an overall false discovery rate (FDR) at 5%. An obtained Benjamini-Hochberg-corrected p-value (BH*p*) < 0.05 was deemed a significantly enriched GO term.

3.3.6 Cell Surface Biotinylation

Cells were washed 3x in cold PBS, then incubated in 0.1mg/mL EZ-Link™ NHS-LC-Biotin (ThermoFisher) dissolved in PBS on ice for 45 minutes. Free NHS-LC-Biotin was quenched by 3x washes in TBS/Glycine buffer (20mM Tris, 150mM NaCl, 10mM glycine, pH 7.5) on ice. Cells lysates were collected in 1mL RIPA lysis buffer (supplemented with protease inhibitor cocktail) and centrifuged at 12,000 rpm for 10 minutes at 4°C. For input control, 50µL lysate supernatant was mixed with 50µL 2x SB, boiled for 5 minutes, and stored at -20°C. For

purification of cell surface biotinylated proteins, 850µL lysate was incubated with 50µL streptavidin-agarose on a rotator for 2 hours at 4°C. Streptavidin pulldowns were subsequently centrifuged at 4000rpm for 1 minute at 4°C, then washed 3x in RIPA buffer (centrifugation at: 4,000 rpm, 1 minute, 4°C between each wash). After careful removal of excess RIPA buffer via aspiration, 50µL 2x SB was added to the streptavidin pulldown, and samples were subsequently boiled for 5 minutes and stored at -20°C until immunoblot analysis.

3.4 Results

3.4.1 Inducible expression of BioID constructs in Flp-In T-REx 293 cells

To enable inducible expression of BioID baits we utilized the Flp-In T-REx 293 cell line which constitutively expresses the Tet repressor (TetR) and possesses a Flp-recognition target (FRT) at a distinct locus to enable Flp-mediated recombination for stable genomic integration of the BioID baits. BioID baits consisted of FL or cleavage-resistant (CR) TNFRSF (i.e. p75NTR, DR6 or TROY) fused to BirA* and a FLAG epitope tag at the C-terminus (the 'TNFRSF-BirA*-FLAG' bait). CR baits were generated via exchange of the transmembrane domain (TMD) for the TMD of the non-proteolytically cleaved TNFRSF, Fas. Flp-In T-REx 293 cells were co-transfected with Flp and TNFRSF-BirA*-FLAG expression vectors to enable Flp-mediated recombination and stable integration of the TNFRSF-BirA*-FLAG bait into the genome. 2x $TetO_2$ sequences were inserted immediately upstream of the TNFRSF-BirA*-FLAG locus to bind constitutively-expressed TetR and suppress transcription of the TNFRSF-BirA*-FLAG bait in unstimulated cells. In the presence of exogenous tetracycline (Tet), Tet complexes to TetR to facilitate its dissociation from the 2x $TetO_2$ sequence to activate transcription of the TNFRSF-BirA*-FLAG bait (Figure 3.1).

3.4.2 BioID resolved the p75NTR-DR6-TROY interactome

To resolve the p75NTR-DR6-TROY interactome, full-length (FL) TNFRSF-BirA*-FLAG+ Flp-In T-REx 293 cells were co-stimulated for 24 hours with 1µg/mL Tet + 50mM biotin to induce expression of the FL TNFRSF-BirA*-FLAG bait and activate proximity-dependent biotinylation. Biotinylated prey were then captured from cell lysates on streptavidin resin, trypsin digested, and subjected to mass spectrometry for identification and abundance quantification.

BioID analysis revealed the p75NTR-DR6-TROY interactome in Flp-In T-REx 293 cells consisting of 446 high-confidence prey (SAINT > 0.74) in total (Figure 3.3A). $TROY^{FL}$ was the most promiscuous TNFRSF finding 340 interactors, followed by $p75NTR^{FL}$ (136 interactors) and $DR6^{FL}$ (112 interactors) (Figure 3.3A). The p75NTR-DR6-TROY interactome revealed substantial overlap between the 3 TNFRSFs with 89.3% of $DR6^{FL}$ interactors finding at least one other FL TNFRSF bait compared to 42.65% of $p75NTR^{FL}$ interactors and 28.5% of $TROY^{FL}$ interactors (Figure 3.3A). The p75NTR-DR6-TROY interactome breaks down as follows: 29 interactors were common to $p75NTR^{FL}$, $DR6^{FL}$ and $TROY^{FL}$ baits; 16 interactors were specific to $p75NTR^{FL}$ and $DR6^{FL}$; 55 interactors were specific to $DR6^{FL}$ and $TROY^{FL}$; 13 interactors were specific to $p75NTR^{FL}$ and $TROY^{FL}$; 78 interactors are $p75NTR^{FL}$-specific; 12 interactors are $DR6^{FL}$-specific; and 243 interactors are $TROY^{FL}$-specific (Figure 3.3A).

3.4.3 BioID revealed a core network of interactors shared by p75NTR, DR6 and TROY

BioID identified a core network of 29 interactors common to p75NTR, DR6 and TROY (Figure 3.3A-B). This core network included: B-class ephrin ligands (EFNB1 and EFNB2), EFR3 homologs of the PI4K complex (EFR3A and EFR3B), a palmitoyl-acyltransferase (DHHC5) and, unexpectedly, a TNFRSF superfamily member (RELL1). Strikingly, the core network also included multiple plasma membrane-localized ion transporters of the Solute Carrier

(SLC) gene family, including: SLC12A2 (Na+/K+ co-transporter) , SLC30A1 (Zn2+ transporter), SLC38A1 (amino acid transporter), SLC38A2 (amino acid transporter), SLC3A2 (amino acid transporter heavy chain), SLC4A7 (Na+/HCO3- co-transporter), SLC6A15 (neurotransmitter transporter), and SLC6A8 (neurotransmitter transporter) (Figure 3B). Thus, BioID successfully identified a core signaling network common to p75NTR, DR6 and TROY that consists almost entirely of novel interactors, with the exception of the known complexes between p75NTR and ephrin ligands (195,232–234,324,617).

3.4.4 BioID identified ICD-specific interactomes unique to p75NTR, DR6 and TROY

p75NTR, DR6 and TROY can be proteolytically cleaved to release their soluble ICD into cytosol to mediate distinct signaling outcomes (123,124,142,165,399). To resolve the unique interactomes of the cleaved ICDs of p75NTR, DR6 and TROY (the 'p75NTR-DR6-TROY ICD interactome') we performed BioID using cleavage-resistant (CR) baits (Figure 3.2). CR baits were generated by exchanging the receptor's transmembrane domain (TMD) for the TMD of the Fas receptor – a TNFRSF that does not undergo proteolytic cleavage (618). Prey that found a FL receptor, but not the corresponding CR receptor (i.e. interacted with $p75NTR^{FL}$ but not $p75NTR^{CR}$), were designated as ICD-specific interactors. BioID revealed a robust interactome for CR baits of a similar scale to FL baits (Figure 3.4A). This approach resolved a p75NTR-DR6-TROY ICD interactome, consisting of 43 p75ICD interactors, 53 DR6ICD interactors, and 69 TROYICD interactors (Figure 3.4B). Strikingly, ICD-specific prey exhibited very little overlap between the TNFRSFs (163 of 165 ICD-specific prey showed no overlap), which was not the case for the FL p75NTR-DR6-TROY interactome (Figure 3.4B). Thus, BioID successfully resolved the ICD-specific interactomes of p75NTR, DR6 and TROY; and

established that ICD-specific signaling properties of each receptor are highly dissimilar, unlike their full-length counterparts.

3.4.5 GO analysis identified core cellular functions common to p75NTR, DR6 and TROY

To identify biological functions implicated within the FL p75NTR-DR6-TROY interactome —that may underlie their redundant function in the nervous system—we performed Gene Ontology (GO) analysis using the DAVID (613,614) platform with cross-refencing to the Reactome (615) cell pathway database (Figure 3.5A). GO analysis revealed several significantly enriched signaling pathways within the FL p75NTR-DR6-TROY interactome, including: "Eph-ephrin mediated repulsion of cells" (9 prey; BH*p* = $1.4x10^{-3}$), "synthesis of PIPs at the plasma membrane" (6 prey; BH*p* = $4.2x10^{-2}$) and "EGFR downregulation" (5 prey; BH*p* = $4.6x10^{-2}$) (Figure 3.5B; Appendix 2). Multiple protein trafficking-associated GO terms were significantly enriched within the p75NTR-DR6-TROY interactome, including: "COPII-mediated vesicle transport" (24 prey; BH*p* = $7.9x10^{-18}$), "COPI-mediated anterograde transport" (15 prey; BH*p* = $9.9x10^{-6}$) "Golgi-associated vesicle biogenesis" (17 prey; BH*p* = $3.2x10^{-11}$), "lysosome vesicle biogenesis" (11 prey; BH*p* = $1.2x10^{-6}$), "cargo concentration in the ER" (7 prey; BH*p* = $5.8x10^{-3}$), and "transferrin endocytosis and recycling" (6 prey; BH*p* = $2.0x10^{-2}$). Consistent with the established role of TNFRSF signaling in immune system function, several immunity-associated GO terms were significantly enriched, including: "antigen presentation: folding, assembly and peptide loading of class I MHC" (8 prey; BHp = $1.4x10^{-3}$), "MHC class II antigen presentation" (14 prey; BHp = $5.9x10^{-4}$), "Nef mediated CD8 down-regulation" (4 prey; BHp = $1.6x10^{-2}$), and "Nef mediated CD4 down-regulation" (4 prey; BHp = $3.1x10^{-2}$).

The core network of p75NTR/DR6/TROY shared interactors included multiple members of the SLC family of ion transporters (Figure 3.3A,C). Consistent with this, the GO terms

"amino acid transport across the plasma membrane" (10 prey; $4.40x10^{-6}$) and "cation-coupled chloride cotransporters" (4 prey; $1.60x10^{-2}$) were significantly enriched. This further suggests that p75NTR, DR6 and TROY may act as major co-regulators of intracellular ion homeostasis.

3.5 Discussion

BioID successfully resolved the p75NTR-DR6-TROY interactome in a live, human cell line. This interactome reveals robust overlap in interactors between the FL receptors providing robust insight into the signaling and trafficking mechanisms common to these receptors. Interactors finding some combination of TNFRSF baits should be prioritized as candidates for research into the core signaling pathways engaged by p75NTR, DR6 and/or TROY during neural development and maintenance. Interestingly, although the FL receptors showed substantial prey overlap, the ICD-specific prey showed almost no overlap. This suggests that cleavage-dependent signaling pathways initiated by p75NTR, DR6 and TROY fundamentally differ.

The FL p75NTR-DR6-TROY interactome revealed a small core network of interactors common to all three receptors. Unexpectedly, this core network included the TNFRSF superfamily member RELL1. RELL1 is a homolog of the TNFRSF Receptor Expressed in Lymphoid Tissues (RELT) and possesses high sequence similarity to RELT, but lacks most of the extracellular domain (ECD) including the ligand-binding cysteine-rich domains (CRDs). This heterotypic TNFRSF complexes between RELL1 and p75NTR/DR6/TROY represent a significant new insight into TNFRSF structural biology, as TNFRSFs almost exclusively homo-oligomerize to initiate signaling cascades [reviewed in (619)]. Because of this, it is difficult to interpret the biological significance of a heterotypic complex with RELL1 – does RELL1 act as an adaptor protein to p75NTR/DR6/TROY? Does it act as an inhibitor? Or does it have some other modulatory role? The heterotypic TNFRSF complex will be explored in depth in Chapter

3, where we establish that RELL1 acts as a negative regulator of p75NTR signaling to the actin cytoskeleton by directly antagonizing binding to the p75NTR adaptor Neurotrophin Receptor-Interacting MAGE Homolog (NRAGE) (137–139,142).

The core network of p75NTR-DR6-TROY interactors also included the palmitoyl-acyltransferase (PAT) DHHC5. PAT enzymes catalyze S-palmitoylation of a substate cysteine residue via formation of a thioester linkage. DHHC5, specifically, is highly expressed in the adult nervous system—primarily in neurons—and shows near ubiquitous expression throughout the CNS. p75NTR (620) and DR6 (385) are known substrates for S-palmitoylation, with their palmitoylated cysteine located in the juxtamembrane region within their ICD (Cys279 in rat p75NTR sequence; C368 in human DR6 sequence). TROY palmitoylation status is unconfirmed, but mathematical modelling (621) predicts a juxtamembrane cysteine (Cys600) is a palmitoylation substrate. Although it is known that two of these TNFRSFs— p75NTR and TROY—are palmitoylation substrates, the enzyme(s) catalyzing these palmitoylation events has remained elusive.

The p75NTR-DR6-TROY interactome identified two B-class ephrin ligands, ephrin-B1 (EFNB1) and ephrin-B2 (EFNB2), as interactors common to these three receptors. Multiple reports have suggested that p75NTR can collaborate with ephrin receptors to mediate axonal guidance during development (195,233,234,617). These reports, in combinations with our novel finding that EFNB1 and EFNB2 are shared p75NTR/DR6/TROY interacting partners, suggest that these TNFRSFs may play a central role in the transduction of ephrin-dependent axonal guidance cues.

Lastly, 8 of the 29 prey that make up the core network of shared p75NTR-DR6-TROY interactors are cell surface ion transporters of the SLC gene family. The SLC transporters

regulate cellular ion homeostasis, and dysregulation of SLC genes has been implicated in a range of neuropsychiatric and neurodegenerative disorders [reviewed in (622)]. Interestingly, SLC6 subfamily members identified in the BioID screen—SLC6A8 and SLC6A15—are neurotransmitter transporters [reviewed in (623,624)] and p75NTR knockout mice were recently shown to exhibit severe deficits in presynaptic acetylcholine quantal content and cholinergic neurotransmission at the neuromuscular junction (NMJ) (204,625). It will be interesting to explore if DR6 and TROY are also required for synaptic neurotransmission and, if so, if this is dependent on an interaction with SLC6A8 and SLC6A15. Beyond neurotransmission, however, the abundance of SLC family members within the p75NTR-DR6-TROY interactome—and their re-appearance in GO analysis—suggests these receptors may play a significant role in cellular ion homeostasis.

In agreement with the literature, the p75NTR-DR6-TROY interactome revealed a physical interaction with NKCC1. Previous research has demonstrated that p75NTR functionally interacts with NKCC1—and the neuron-specific homolog KCC2—to regulate intracellular chloride homeostasis and subsequently establish depolarizing or hyperpolarizing postsynaptic responses to GABA (223,226). This finding demonstrates that p75NTR likely regulates GABAergic responses by directly influencing NKCC1/KCC2 Cl- transporter activity in response to neuron intrinsic and extrinsic signals.

This BioID analysis successfully resolved the p75NTR-DR6-TROY interactome in a non-neuronal cell line. Future research should focus on introducing perturbations to this interactome (e.g. ligands) and investigate how it changes over time, preferably within a neuronal context. Such an endeavour would best be achieved using an interactomics strategy with minimal time required for proximity labeling, such as APEX2 (541).

3.6 Figures and Figure Legends

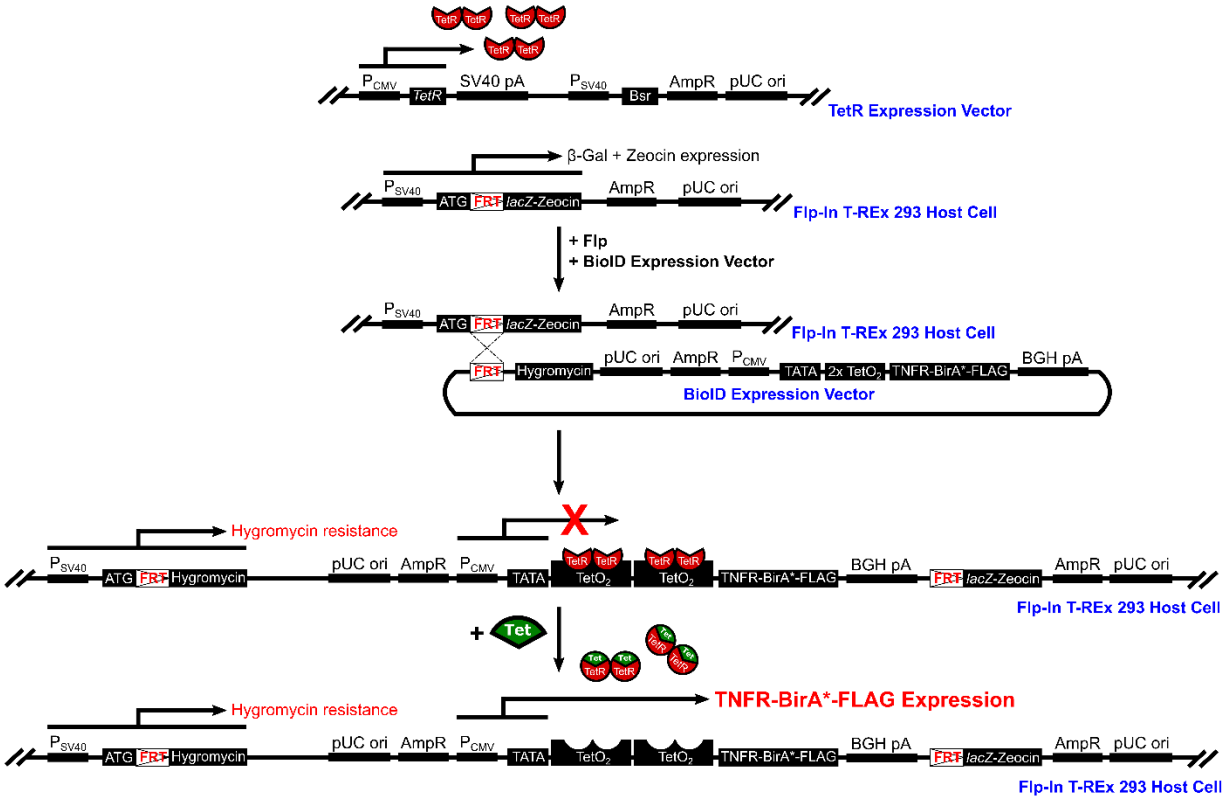

Figure 3.1. Generation of Flp-In T-REx 293 cell lines with stable genomic integration, and inducible expression, of BioID constructs. Schematic illustrating the generation Flp-In T-REx 293 cell lines with inducible expression of TNFRSF-BirA*-FLAG (BioID) constructs. TNFRSF-BirA*-FLAG is stably integrated into the host cell genome by Flp-mediated recombination at FRT sites on the host cell genome and BioID expression vector. Upon Flp-mediated recombination, hygromycin resistance is conferred to enable selection of TNFRSF-BirA*-FLAG+ clones. TNFRSF-BirA*-FLAG expression is controlled at 2 upstream $TetO_2$ elements. At baseline, Flp-In T-REx 293 cells stably express TetR, which occupies TetO2 elements to inhibit transcription of TNFRSF-BirA*-FLAG. Exogenous Tet binds TetR, abolishing its affinity for TetO2, thereby disinhibiting transcription of TNFRSF-BirA*-FLAG.

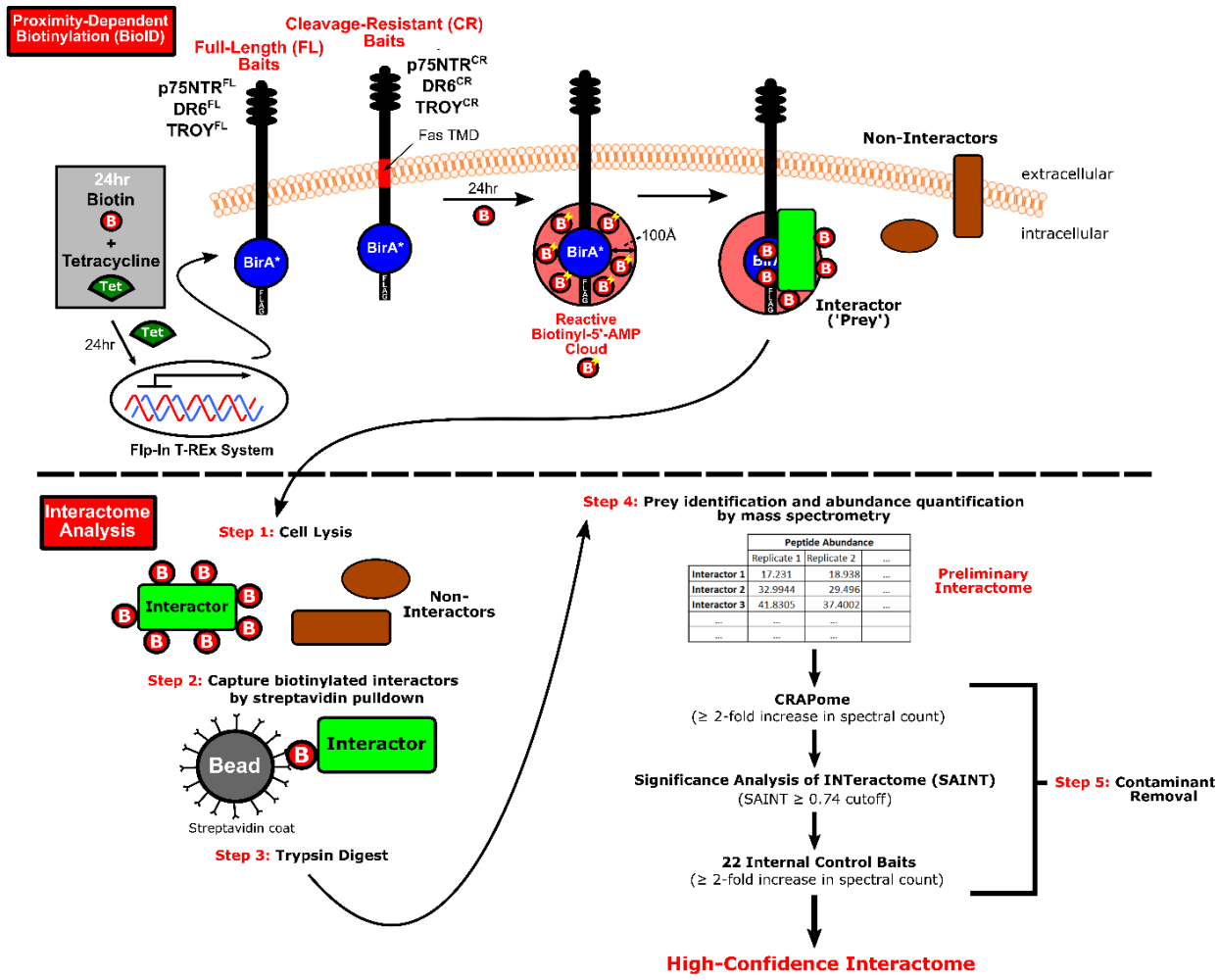

Figure 3.2. Schematic of the BioID pipeline. BioID was performed FL and CR constructs for p75NTR, DR6 and TROY with C-terminal BirA*-FLAG fusion. Flp-In T-REx 293 BioID clones were co-stimulated with Tet and biotin for 24 hours to induce TNFRSF-BirA*-FLAG expression and enable BirA* to produce a ~100Å radius cloud of reactive biotinyl-5'-AMP. Activated biotinyl-5'-AMP biotinylates interactors (prey) and proximal proteins to at exposed lysine residues while leaving distal non-interactors unmodified. After 24 hours, the cells were lysed and biotinylated prey were captured on streptavidin agarose. Samples were then trypsin digested then analyzed by mass spectrometry to identify, and quantify the abundance of, biotinylated prey. This preliminary interactome was subject to rigorous statistical analysis to remove contaminants

(i.e. background prey and proximal non-interactors). Prey with a mean spectral count < a 2-fold increase over their background spectral count listed in the CRAPome repository were eliminated. Next, probabilistic scoring of individual prey was carried out by SAINT analysis, and prey with a SAINT score less than 0.74 were eliminated. Lastly, prey spectral counts were compared to a list of 22 internal control baits, including the following: no bait (x4), BirA* only baits (x4), unrelated transmembrane BirA* fusion baits (x4) and E-cadherin-BirA* baits (x12) (to remove contaminants that were biotinylated as a result of co-localization at a cell junction). Any prey that did not display > 2-fold increase in spectral count over these internal controls was eliminated. Prey that met the requirements of these stringent statistical analyses were concluded as *bona fide* interactors to the bait protein. All BioID analyses were run in biological and technical duplicate.

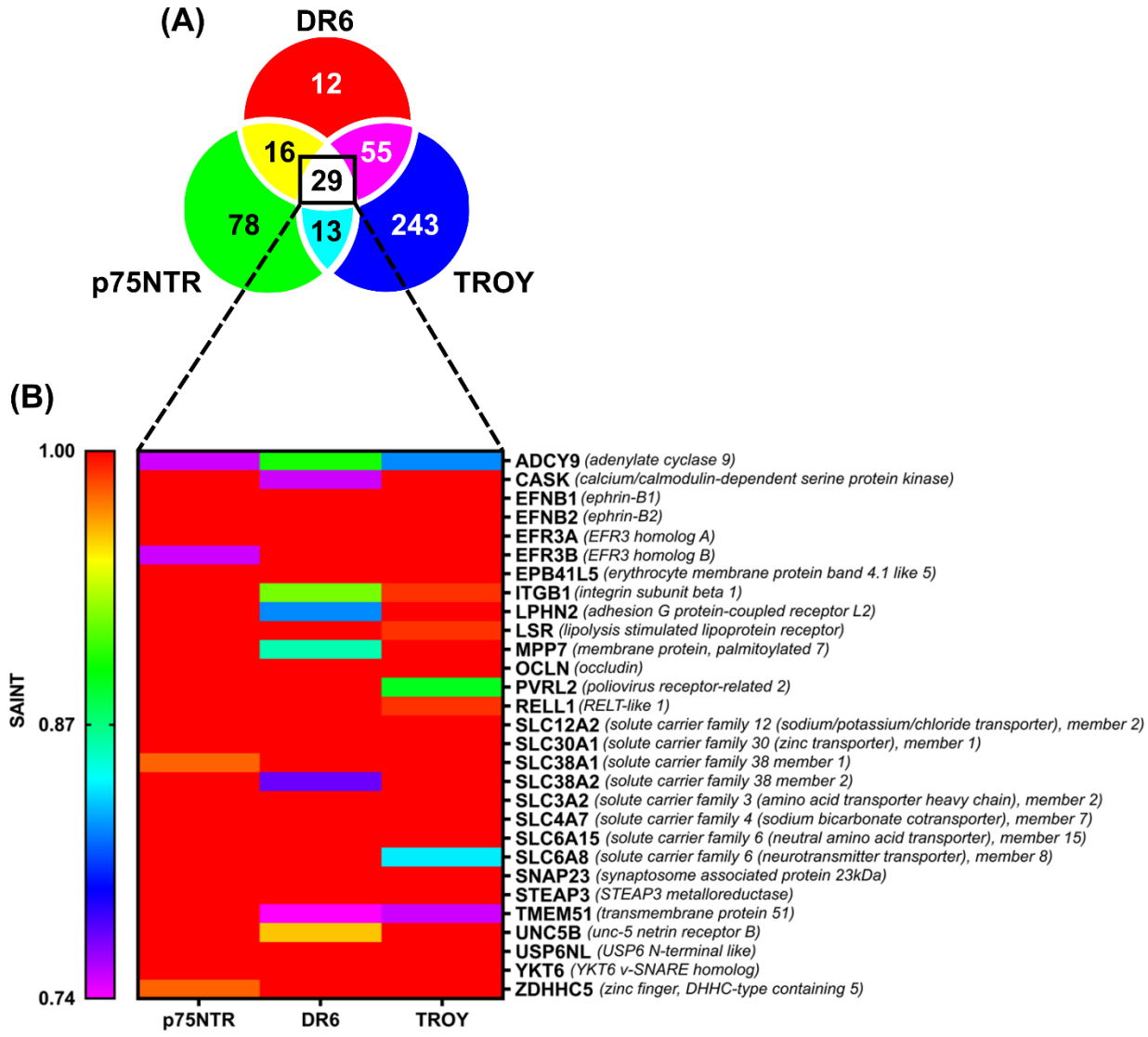

Figure 3.3. BioID revealed the interactome of p75NTR, DR6 and TROY and identified a core network of 29 signaling partners shared by these TNFRSFs. (A) Venn diagram depicting the number of *bona fide* interactors for full-length p75NTR, DR6 and TROY—or combination thereof—in the Flp-In T-Rex 293 cell line. (B) A core group of 29 interactors common to p75NTR, DR6 and TROY and their associated SAINT scores for each full-length TNFRSF bait.

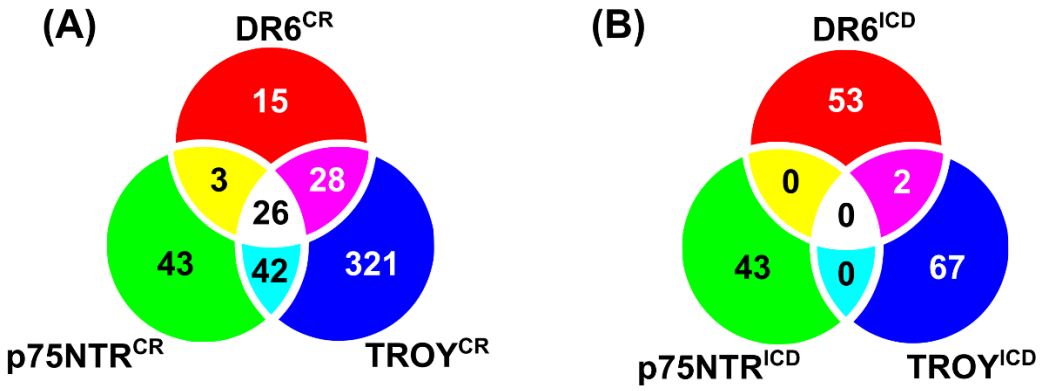

Figure 3.4. Cleavage-resistant BioID baits elucidated the ICD-specific interactome of p75NTR, DR6 and TROY. (A) Venn diagram depicting the number of *bona fide* interactors for each CR TNFRSF bait or combination of CR TNFRSF baits. (B) Venn diagram breakdown of ICD-specific prey for each TNFRSF, or combination thereof, which found the FL bait but not the CR bait of the same receptor.

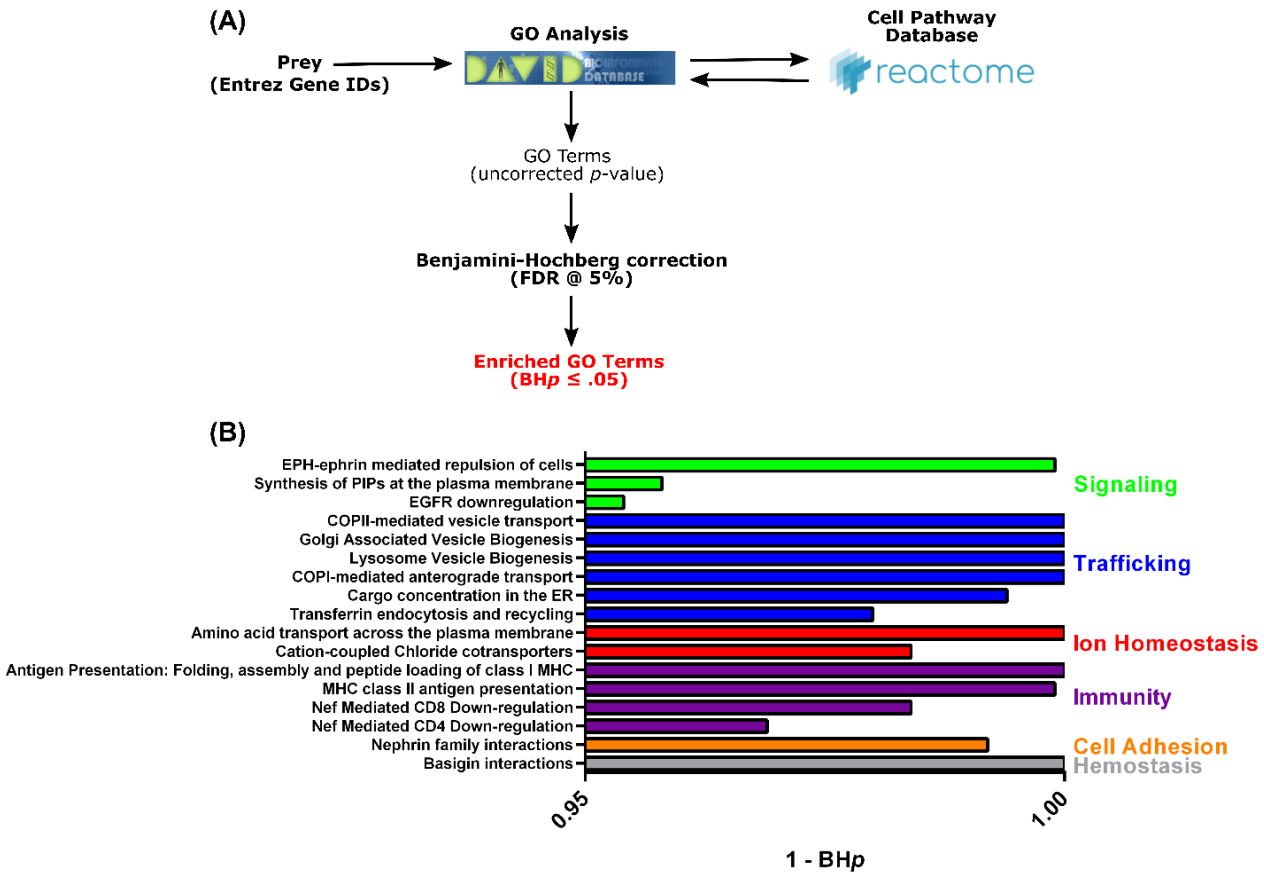

Figure 3.5. GO analysis of the p75NTR-DR6-TROY interactome revealed enriched cell signaling and trafficking pathways. (A) Schematic of the GO analysis pipeline. Gene identifiers for the complete FL interactome of p75NTR, DR6 and TROY were input into the DAVID database. DAVID cross-referenced the Reactome database of cell signaling pathways to identify enriched GO terms. The Bonferroni-Hochberg correction was applied to raw p-values for each GO term to maintain an overall false discovery rate (FDR) at 5%. Bonferroni-Hochberg-corrected p-values (BHp) ≤ 0.05 were deemed statistically significant. (B) Visualization of significantly enriched GO terms for the p75NTR-DR6-TROY interactome. 1-BHp value is plotted on the x-axis (bar length is proportional to statistical confidence for the corresponding GO term).

Chapter 4: RELL1 is an inhibitor on non-cell-autonomous p75NTR signaling

4.1 Abstract

Proteomic evidence has revealed the existence of a heterotypic TNF receptor (TNFRSF) complex between Receptor Expressed in Lymphoid Tissues-Like 1 (RELL1) and the p75 neurotrophin receptor (p75NTR). RELL1 is a truncated RELT homolog lacking the extracellular cysteine-rich domains (CRDs) that mediate ligand-binding in TNFRSFs. Given that TNFRSF-TNFRSF interactions are almost exclusively homotypic, we sought to functionally characterize this unexpected RELL1-p75NTR complex. Leveraging the COS7 cell expansion assay, we demonstrate that RELL1 is an inhibitor of non-cell-autonomous p75NTR-dependent cell expansion. Mechanistically, RELL1 inhibits p75NTR exocytosis into large extracellular vesicles (EVs) known to mediate p75NTR-dependent COS7 expansion. Consistent with this, RELL1 attenuates the interaction of p75NTR with the requisite signaling partner NRAGE in recipient COS7 cells, effectively inhibiting p75NTR-dependent expansion. Proximity ligation assay (PLA) revealed that the RELL1-p75NTR complex formation is dependent on C-terminal interactions and is localized exclusively to an intracellular compartment. These findings add to a growing body of evidence that CRD-lacking TNFRSF homologs act as endogenous inhibitors of TNFRSF signaling.

4.2 Introduction

The Receptor Expressed in Lymphoid Tissues (RELT) family of TNFRSFs consists of three members: RELT, RELL1 and RELL2. Structurally, RELT is a canonical TNFRSF possessing 3 extracellular CRDs yet no RELT ligand has been discovered to date. RELL1 and RELL2 are truncated RELT homologs lacking most of the extracellular domain (ECD)—

including the CRD cluster—and possessing very high sequence homology to RELT in their respective transmembrane (TMD) and intracellular domain (ICD) (488). RELL1 possesses no known functional motifs aside from an RSRV motif within the ICD that mediates binding to sterile-20 (Ste20) kinases (488). RELL1 is expressed in central and peripheral neurons with the highest expression levels observed in adulthood (490,491). No neuronal function has been ascribed to RELL1; however, a recently generated RELL1 knockout mouse shows behavioural phenotypes including hyperactivity and acoustic hypersensitivity (499) suggesting neural functionality.

It remains unclear if RELL1 possesses intrinsic signaling properties and/or acts as a signaling modulator—whether as an adaptor, effector, or inhibitor. Evidence from overexpression models suggests RELL1 is capable of autonomous signaling *in vitro* (488,489,626). RELL1 has been shown to physically interact with multiple TNFRSFs, including RELT (626), p75NTR, DR6 and TROY (see Chapter 3), suggesting that RELL1 may act as an adaptor or inhibitor to TNF-TNFRSF signaling.

To address this question, we investigated RELL1 modulation of p75NTR signaling, leveraging the p75NTR-dependent COS7 cell expansion model as a functional readout. We demonstrate that RELL1 acts as an inhibitor of p75NTR-dependent cell expansion. Mechanistically, RELL1 inhibits p75NTR targeting to large EVs known to mediate cell expansion (Chapter 3). Moreover, RELL1-dependent p75NTR inhibition requires the formation of the RELL1-p75NTR complex via C-terminal interactions. Our data collectively establish RELL1 as an inhibitor of exocytosis-dependent p75NTR signaling and add to a growing body of evidence that ECD-truncated TNFRSFs function as endogenous inhibitors of their full-length counterparts.

4.3 Materials and Methods

4.3.1 Plasmids, antibodies and reagents

Plasmids used encoded: pcDNA3 vector, GFP (pEGFP-N1 vector; Clontech; GenBank accession # U55762), untagged human p75NTR (subcloned into pCMX vector), p75NTR-FLAG (subcloned into pcDNA3), untagged human p75ICD (AA: 273-427; subcloned into pcDNA3 vector), RELL1-HA (courtesy of Dr. John Cusick), RELL1$^{\Delta CR4}$-HA, and RELL1$^{\Delta CR3,4}$-HA. Primary antibodies included: anti-p75NTR (rabbit monoclonal targeting human p75ICD; produced in-house; also known as 'Buster'), anti-NRAGE (rabbit monoclonal targeting human NRAGE; produced in-house), anti-HA (mouse monoclonal; ThermoFisher) and anti-actin (mouse monoclonal; clone C4; ThermoFisher Scientific). Secondary antibodies included: horseradish peroxidase (HRP)-conjugated donkey anti-rabbit (Jackson ImmunoResearch Laboratories), HRP-conjugated donkey anti-mouse (Jackson ImmunoResearch Laboratories), and Alexa Fluor 647-conjugated goat anti-mouse (ThermoFisher Scientific). PDL was supplied by Sigma-Aldrich (Oakville, ON, Canada). Dulbecco's Modified Eagle Medium (DMEM), penicillin-streptomycin (P/S), L-glutamine, and fetal bovine serum (FBS) were purchased from Wisent Bio Products (Burlington, ON, Canada). Exosome-deprived FBS was supplied by ThermoFisher Scientific.

4.3.2 Cell culturing and transfection

COS7 cells were cultured in conditioned medium (CM) containing DMEM supplemented with 100mg/mL P/S, 2mM L-glutamine and 10% FBS. COS7 cell cultures were incubated at 37°C, 5% CO_2. COS7 transfection was performed using the JetPrime lipid nanoparticle-based system (PolyPlus, New York, NY, USA). Briefly, COS7 cells were seeded in a 6-well dish pre-

coated with 50ng/mL PDL and a density of 100K cells per well. After 24h, CM was exchanged for CM lacking P/S. To prepare the transfection mix: 0.5µg of plasmid (per construct) was added to 200µL JetPrime Buffer, vortexed, then 1µL of JetPrime Reagent (scaled up if multiple plasmids) was added, vortexed again, then left at room temperature (RT) for 10 minutes undisturbed. After the 10-minute period, 200µL of transfection mix was applied to COS7 cells for 24h. After the 24h transfection, the transfection medium was washed off 2x in fresh CM, then the transfected COS7 cells were incubated a further 24h in CM. Re-seeding of transfected COS7 cells onto coverslips or 8µm porous filters was preceded by 24h precoating in 50ng/mL PDL.

4.3.3 EV purification

Cells were seeded on precoated 150mm plates at a density of $1.5x10^7$ (COS7) or $5x10^7$ (IMS32) cells per plate. After transfection (if applicable), cells were incubated in 12mL CM containing exosome-free FBS (exosome-free CM). After 24h incubation, 10mL CM was collected and precleared via a 3 sequential centrifugation steps at 4°C (collecting supernatant after each): (i) 10 minutes at 300g, (ii) 20 minutes, and (iii) 30 minutes at 10,000g. Precleared CM was then loaded onto an Amicon Ultra-15 centrifugal filter unit and concentrated to 150µL by centrifugation (25 minutes at 4000g, 4°C). 150µL concentrated, clarified CM overlayed onto a 70nm qEV column (Izon). An initial void volume of 1mL was discarded, followed by collection of 12 200µL eluate fractions.

4.3.4 COS7 cell expansion assay

The COS7 cell expansion assay is a modification of the protocol described by Zeinieh and colleagues (587), and was designed to test non-cell-autonomous mechanism(s) mediating p75NTR-dependent COS7 cell expansion. In all iterations of the assay, ‘donor’ COS7 cells secrete factor(s) that act on ‘recipient’ COS7 cells.

Donor and recipient COS7 cells are seeded in independent wells of a 6-well plate at a density of 100K cells/well. Recipient COS7 cells are transfected 24h with GFP plasmid; donor cells are transfected 24h with plasmid constructs unique to each experiment. Post-transfection, recipient GFP+ cells are seeded on PDL-coated coverslips at a density of 4K cells/coverslip. For each experimental condition, 3 coverslips of GFP+ recipient cells are seeded and imaged.

In the 'filter assay', donor cells are seeded onto PDL-coated 8µm porous 24-well filters (8K cells/filter), and GFP+ recipient cells onto PDL-coated coverslips (4K cells/well) in a 24-well dish. After a 24h incubation, filters containing donor cells are suspended above the coverslips containing recipient cells within the same well of a 24-well dish for 24h. After this period, donor cells are discarded and recipient cells are fixed in 4% paraformaldehyde (PFA) for 15 minutes at RT. Fixed recipient cells are then washed 3x in PBS and mounted on glass slides with Fluoroshield mounting medium (ThermoFisher). Whole coverslips of GFP+ recipient cells are then imaged by widefield microscopy at 10x magnification. Images are then subjected to pixel intensity-based thresholding in ImageJ, converted to a binary image, and exported to a machine learning algorithm we developed in ilastik (Figure 2.1) (591). In this algorithm, objects are sorted into: (i) individual cells, (ii) cell clusters (which can include mitotic cells), and (iii) cell debris (Figure 2.1). The ilastik output file separates these 3 objects by thresholding in ImageJ (e.g., upper bound = 1, lower bound = 1 will only show individual cells identified by the ilastik algorithm) (Figure 2.1). Only individual GFP+ recipient cells were measured – this was achieved by particle analysis in ImageJ. For each condition, all cells across all 3 coverslips of GFP+ recipient cells were imaged

In the 'co-culture' assay (Figure 2.3A-B), donor cells are co-seeded with recipient cells on the same coverslip (4K donor + 4K recipient cells per coverslip). Cells are then fixed,

mounted, imaged and analyzed for GFP+ recipient cell size using the workflow described for the filter assay above.

4.3.5 Immunocytochemistry (ICC)

Cells were fixed in 4% PFA (15 minutes at RT), permeabilized (2.5% BSA + 0.2% Triton-X in PBS; 20 minutes at RT) and blocked (2.5% BSA + 0.02% Triton-X; 60 minutes at RT) prior to overnight 4°C incubation in blocking solution containing primary antibody. The following day, primary antibody was washed off 3x with PBS, then secondary antibody solution (2.5% BSA + 1% serum + secondary antibody) was applied for 1h at RT. Secondary antibody was then washed off with PBS. If phalloidin-488 was required, it was applied for 1h at RT at this time, then washed off 3x with PBS.

4.3.6 Immunoblot (IB)

Harvested cells were lysed in RIPA buffer containing protease inhibitor cocktail (and 1µM epoxomicin. 2x Laemmli Sample Buffer (2x SB) was added 1:1 to protein samples, boiled for 5 minutes, then loaded into polyacrylamide gel for subsequent electrophoresis by SDS-PAGE. After SDS-PAGE, proteins were transferred to a nitrocellulose membrane and blocked for 1 hour, at room temperature, in 5% (w/v) skim milk powder in TBS-T (10mM Tris pH 8.0, 150mM NaCl, 2% Tween-20). Primary antibody incubation was performed in blocking solution at 4°C overnight. Membranes were then washed in TBS-T (6x 10-minute washes) and incubated in HRP-conjugated secondary antibody (diluted in blocking solution) for 1 hour at room temperature. Membranes were then washed in TBS-T (6x 10-minute washes) and immunoreactive bands were detected by chemiluminescence (Clarity Western ECL substrate, BioRad) using the ChemiDoc MP imaging system (BioRad).

4.3.7 Statistics

Gaussian distribution of all datasets was assessed by Shapiro-Wilk test prior to statistical hypothesis testing. Statistical tests were selected based on the design of each experiment—and distribution of data points—and are described in figure legends. Conservative *post-hoc* tests were selected for one- and two-ANOVA analyses. All statistical tests are two-tailed. Statistical significance is defined as $p \leq \alpha \leq .05$. Lastly, *N* is defined as a single technical replicate in all experiments.

4.4 Results

4.4.1 RELL1 possesses evolutionarily conserved motifs within its intracellular domain

To gain functional insight into the RELL1-p75NTR complex, we investigated the evolutionary conservation of the RELL1 primary sequence to identify conserved motifs. To accomplish this, we queried the complete human RELL1 sequence within Class Vertebrata using ConSurf (627) and ran a sequence alignment of the top 150 hits. Sequence identity of individual residues across all 150 homologs revealed 4 regions of strong evolutionary conservation (80-100% identity) within the RELL1 intracellular domain (ICD) that we designated conserved region 1-4 (CR1-4) (Figure 4.1B). CR1 is located at the most N-terminal position within the ICD and CR4 most C-terminal (Figure 4.1B). Moreover, we observed that the transmembrane domain (TMD) is highly conserved in vertebrates, whereas the ECD is poorly conserved. Based on CR1-4 positions, we generated hemagglutinin (HA)-tagged C-terminal RELL1 mutants lacking CR4 (RELL1$^{\Delta CR4}$-HA) and CR3+4 (RELL1$^{\Delta CR3,4}$-HA) plus all amino acids C-terminal to these motifs (Figure 4.1C). We confirmed the expression of the RELL1$^{\Delta CR4}$-HA and RELL1$^{\Delta CR3,4}$-HA in COS7 cells by immunoblot (Figure 4.1D) and verified that these RELL1-HA deletion mutants show a similar subcellular distribution as WT RELL1-HA by immunocytochemistry (Figure

4.3). These data constitute the first evolutionary analysis of the RELL1 sequence and identify 4 highly conserved regions (CR1-4) within the RELL1 ICD of unknown structure and function.

4.4.2 RELL1 complexes with p75NTR, DR6 and TROY in an intracellular compartment

BioID interactome analysis identified RELL1 as a common interacting partner to p75NTR, DR6 and TROY (Figure 3.3). To validate and explore RELL1-TNFRSF complexes *in situ*, we performed proximity ligation assays (PLA) in COS7 cells. First, immunocytochemistry revealed that RELL1-HA strongly colocalizes with p75NTR at the cell surface and intracellular compartments (Figure 4.2A). Strikingly, despite RELL1-p75NTR colocalization throughout the cell, RELL1-HA:p75NTR PLA signal is exclusively intracellular (Figure 4.2B). Importantly, RELL1-HA:p75NTR PLA signal is lost when p75NTR or RELL1-HA is absent, confirming the signal originates from a RELL1-HA:p75NTR protein complex (Figure 4.2B). GFP co-transfection confirmed the RELL1-HA:p75NTR PLA signal is unique to successfully transfected COS7 cells (Figure 4.2B). Next, we investigated RELL1 binding to DR6 and TROY. Like the RELL1-p75NTR complex, we observed that RELL1-HA strongly colocalizes with DR6-FLAG and TROY-FLAG at the cell surface and intracellular compartments (Figures 4.2C and E, respectively). *In situ*, RELL1-HA:DR6-FLAG (Figure 4.2D) and RELL1-HA:TROY-FLAG (Figure 4.2F) PLA signals are exclusively observed in an intracellular context. RELL1-HA:DR6-FLAG and RELL1-HA:TROY-FLAG PLA signals were exclusive to transfected GFP+ COS7 cells and are absent in cells lacking overexpression of RELL1-HA, DR6-FLAG (Figure 4.2D) or TROY-FLAG (Figure 4.2F) constructs.

Based on these data, we conclude that RELL1 interacts with p75NTR, DR6, TROY in an intracellular compartment but not at the plasma membrane.

4.4.3 C-terminal interactions mediate the RELL1-p75NTR complex

To decipher the structural basis of the RELL1-p75NTR complex, we transfected COS7 cells with p75NTR and WT or C-terminal truncated RELL1-HA (ΔCR4; ΔCR3,4). The RELL1-p75NTR PLA signal is nearly abolished in cells expressing RELL1$^{\Delta CR4}$-HA or RELL1$^{\Delta CR3,4}$-HA (Figure 4.3A), demonstrating that the RELL1 C-terminus is required for p75NTR binding. ICC revealed that RELL1$^{\Delta CR4}$-HA and RELL1$^{\Delta CR3,4}$-HA show similar subcellular distribution as WT RELL1-HA thereby ruling out RELL1 mislocalization as a possible explanation for the loss of p75NTR PLA signal (Figure 4.3A).

Given that the RELL1 ICD mediates p75NTR binding, we next asked if RELL1 can physically associate with soluble p75ICD. Figure 4.3B shows that WT RELL1-HA—but not RELL1$^{\Delta CR4}$-HA or RELL1$^{\Delta CR3,4}$-HA—elicits a PLA signal when co-transfected with p75ICD (Figure 4.3B). Thus, RELL1 physically associates with full-length p75NTR and soluble p75ICD and these interactions require the RELL1 C-terminus.

4.4.4 RELL1 inhibits p75NTR-dependent COS7 cell expansion via its physical association with p75NTR

We next sought to functionally characterize the RELL1-p75NTR complex. We began by exploring the morphological effects associated with siRNA-mediated knockdown of endogenous RELL1 in COS7 cells (Figure 4.4A). Unexpectedly, we observed that RELL1 siRNA induced a COS7 cell expansion phenotype (Figure 4.4B-C). In contrast, RELL1-HA overexpression had no effect on cell size (Figure 4.4B-C). Given that endogenous RELL1 regulates COS7 cell size, we next asked if RELL1 is a modulator of p75NTR-dependent cell expansion. Strikingly, when co-expressed, RELL1-HA completely blocked p75NTR-dependent COS7 expansion (Figure 4.4D-E). Given that RELL1 physically interacts with the p75ICD, we next asked if RELL1 inhibits p75ICD-dependent cell expansion, as well. Indeed, RELL1-HA co-transfection abolished the

p75ICD-dependent COS7 expansion phenotype (Figure 4.4F-G).

Lastly, we sought to determine if RELL1-dependent p75NTR inhibition relied on its physical association with p75NTR. To answer this, we utilized the non-p75NTR-binding RELL1 mutant (RELL1$^{\Delta CR4}$-HA) characterized above (Figure 4.3). Interestingly, RELL1$^{\Delta CR4}$-HA failed to inhibit p75NTR-dependent COS7 expansion (Figure 4.4H-I), suggesting that RELL1 inhibits p75NTR cell expansion signaling via a physical association with p75NTR. These combined data establish RELL1 as inhibitor of p75NTR-dependent cell expansion.

4.4.5 RELL1 acts upstream of NRAGE to inhibit p75NTR-dependent cell expansion

p75NTR-dependent COS7 cell expansion requires p75NTR proteolytic cleavage and downstream formation of a p75ICD-NRAGE complex to initiate the signaling cascade (587). Given that RELL1-mediated inhibition of p75NTR-dependent cell expansion requires its physical interaction with p75NTR, we tested the hypothesis that RELL1 inhibits p75NTR-induced expansion via a mechanism upstream of NRAGE. NRAGE is a cytosolic protein enriched near the nucleus in COS7 cells (Figure 4.5A). Consistent with this subcellular distribution, PLA analysis revealed that exogenous p75NTR-FLAG interacts with endogenous NRAGE in an intracellular context with high PLA signal density near the nucleus (Figure 4.5B). To test if RELL1 affects formation of the p75NTR-NRAGE complex, we measured p75NTR-FLAG:NRAGE PLA puncta in COS7 cells co-transfected with RELL1-HA or empty vector (Figure 4.5C). Strikingly, RELL1-HA attenuated the p75NTR-FLAG:NRAGE signal (Figure 4.5C) indicating that RELL1 acts upstream of NRAGE to inhibit the signaling cascade. Thus, the mechanism of RELL1-dependent p75NTR inhibition may occur at the level of the RELL1-p75NTR complex itself.

4.4.6 RELL1 inhibits p75NTR targeting to extracellular vesicles

p75NTR exocytosis in large extracellular vesicles (EVs) is a requisite event in the p75NTR-dependent cell expansion cascade (Figures 2.3-2.7). Given that RELL1 acts upstream of NRAGE to inhibit this signaling event (Figure 4.5) we tested the hypothesis that RELL1 affects p75NTR exocytosis. First, we investigated if RELL1 influences p75NTR-dependent expansion via the non-cell-autonomous pathway by leveraging the filter assay (described in Chapter 2). Vector+ and p75NTR+ donor COS7 cells were co-transfected with or without RELL1-HA (Figure 4.6A). RELL1-HA expression in the donor cell blocked p75NTR-dependent COS7 expansion (Figure 4.6B-C) consistent with a possible role in p75NTR exocytosis. Next, we purified large EVs from vector+ and p75NTR+ COS7 cells co-transfected +/- RELL1-HA. Strikingly, RELL1-HA abolished p75NTR targeting to large EVs (Figure 4.6D). These data establish RELL1 as an inhibitor of p75NTR exocytosis and exocytosis-dependent signaling.

4.5 Discussion

Our study establishes RELL1 as an inhibitor of exocytosis-dependent p75NTR signaling. Mechanistically, RELL1 disrupts p75NTR targeting to large EVs, thereby preventing downstream formation of the p75ICD-NRAGE complex. Consistent with this, the p75NTR-NRAGE physical association is strongly attenuated by RELL1 overexpression, as demonstrated by proximity ligation assay. RELL1-dependent p75NTR inhibition requires physical association of RELL1 with p75NTR, an interaction mediated by the RELL1 C-terminus. We identified 4 highly conserved motifs within the RELL1 ICD—with no homology to known motifs/domains—which we designate conserved regions (CRs) 1-4, adding to the structural knowledge of this ECD-truncated TNFRSF.

Exocytosis via large EVs mediates p75NTR signaling (Chapters 2 and 4). Within EVs, p75NTR cleavage products—both CTF and ICD—are highly enriched (Chapter 2). Thus,

exocytosis may act as a subcellular switch for p75NTR functions, specifically gating ICD-dependent and full-length p75NTR-dependent events. As we demonstrated in this study, RELL1 acts as an inhibitor of p75NTR exocytosis, thereby describing the first regulatory mechanism controlling exocytosis-dependent p75NTR signaling. Although this effect is clear in a 'whole cell' context like the COS7 cell expansion assay, it will be critical to characterize RELL1-dependent inhibition of p75NTR exocytosis on the subcellular level. Is there an overarching paradigm at play, whereby RELL1 exerts spatiotemporal control of p75NTR exocytosis, thereby restricting where and when $p75NTR^{+}$ EVs act on a cell? Further investigation into the biogenesis, trafficking and function of p75NTR+ EVs *in vivo* will be required to better understand the contextual relevance of RELL1-dependent inhibition of non-cell-autonomous p75NTR signaling.

Our study characterizes RELL1 as an upstream regulator of p75NTR signaling but does not explore the possibility of an inverse relationship whereby p75NTR acts upstream of RELL1. Given that RELL1 has been reported to autonomously engage apoptotic signaling via the Ste20 kinases OSR1 and SPAK (488), it is possible that p75NTR binding may affect the signaling properties of RELL1. Although more research is needed to characterize RELL1 signaling across cell types, it will be important to investigate if p75NTR—and/or DR6, TROY, RELT, other TNFRSFs—modulate the biological function of RELL1.

Most current knowledge of ECD-truncated TNFRSF function comes from studies on the p75NTR homolog neurotrophin receptor homolog-2 (NRH2). Interestingly, like RELL1, NRH2 can act as a p75NTR inhibitor (628). Formation of a heterotypic NRH2-p75NTR complex inhibits p75NTR-dependent neurite collapse via reduced downstream activation of RhoA in response to myelin-associated inhibitory factors (628). In addition to its p75NTR inhibitory role,

NRH2 possesses intrinsic signaling capability as shown in diverse neurodevelopmental contexts (629–633). Thus, NRH2 function appears analogous to RELL1. Both act as p75NTR inhibitors and both possess intrinsic signaling properties independent of their p75NTR association. Given that RELL1 binds multiple TNFRSFs (Chapter 3), future research could expand upon existing NRH2/RELL1/RELL2 relationships to determine if ECD-truncated TNFRSFs are endogenous inhibitors of TNFRSF signaling *in vivo*. If true, targeting ECD-truncated TNFRSFs may represent a novel therapeutic strategy in disease states associated with aberrant TNFRSF function.

4.6 Figures and Figure Legends

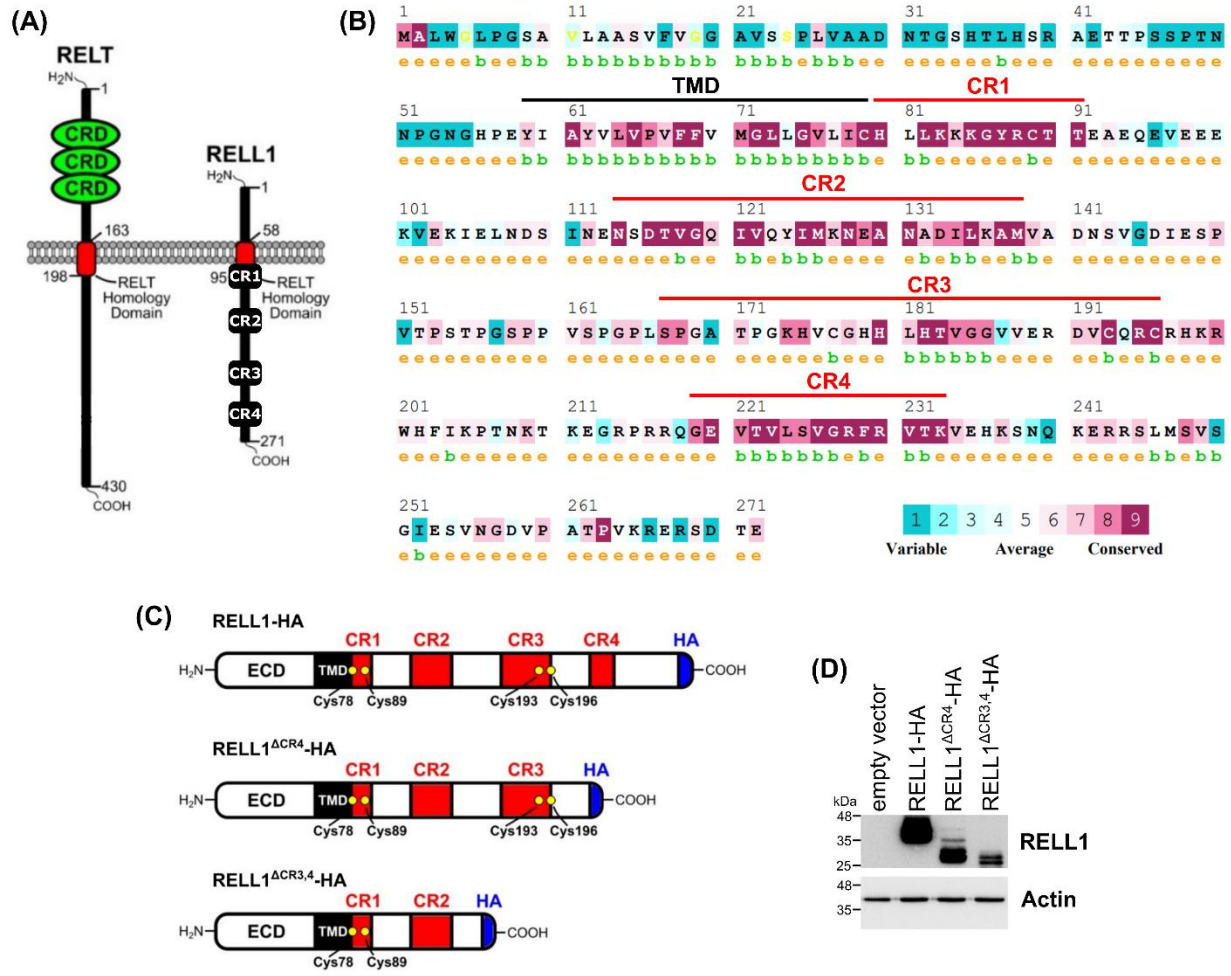

Figure 4.1. Identification of evolutionarily conserved regions in the RELL1 intracellular domain. (A) Structural schematic of human RELT and RELL1. (B) Conservation of human RELL1 primary sequence across 150 vertebrate species. Conservation of each residue is represented along a blue-red gradient scale (blue ≤ 10% identity; red ≥ 90% identity). 4 conserved regions (CR1-4) within the ICD and the transmembrane domain (TMD) are labeled. (C) Schematic representation of HA-tagged RELL1 C-terminal deletion mutants. (D) Immunoblot detection of RELL1-HA C-terminal deletion mutants overexpressed in COS7 cells.

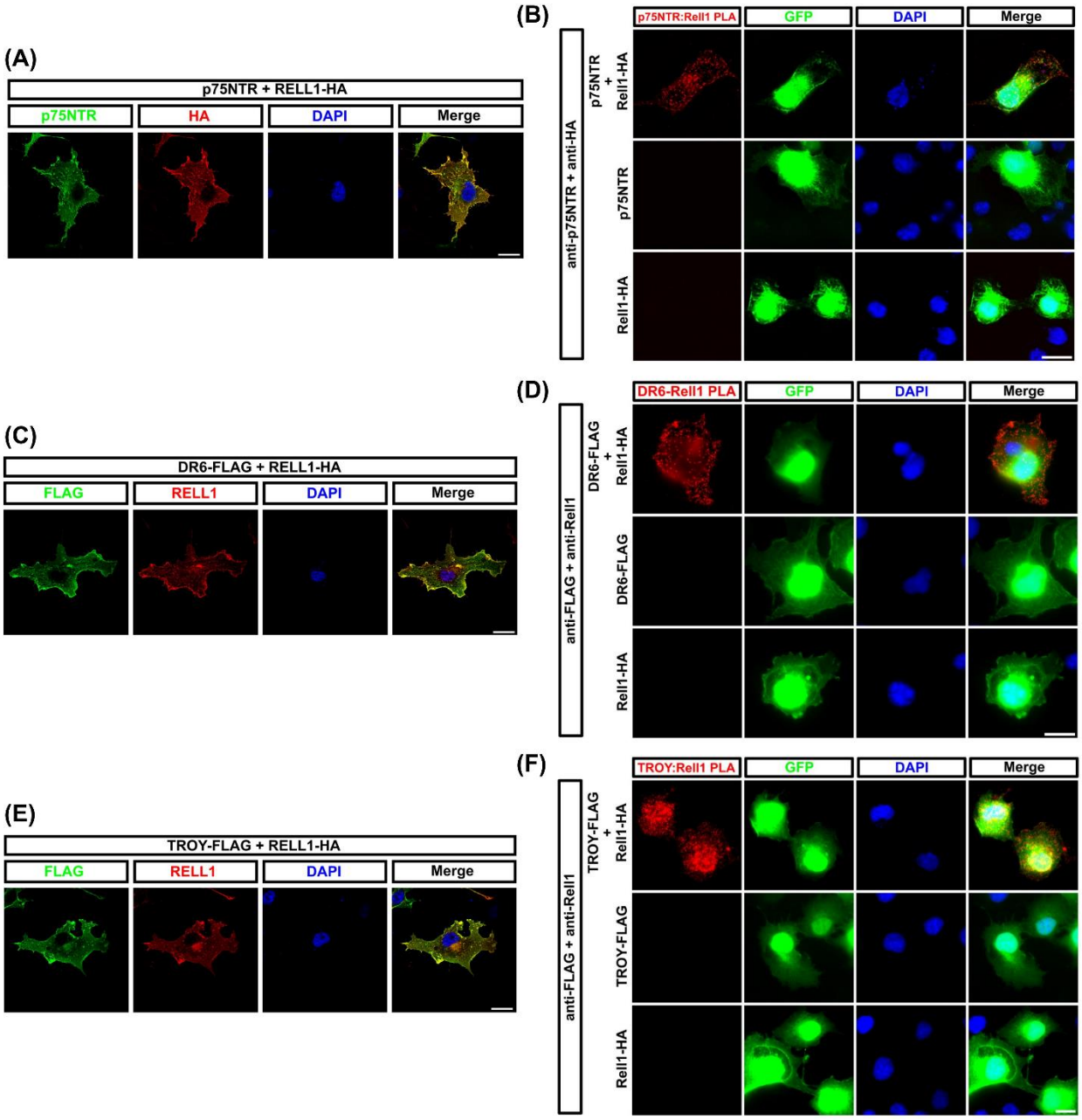

Figure 4.2. RELL1 interacts with p75NTR, DR6 and TROY in an intracellular compartment. (A-B) ICC (A) and PLA (B) of RELL1-HA and p75NTR in COS7 cells. (C-D) ICC (C) and PLA (D) of RELL1-HA and DR6-FLAG in COS7 cells. (E-F) ICC (E) and PLA (F) of RELL1-HA with TROY-FLAG. Transfected constructs and primary antibodies used in ICC (A,C,E) and PLA (B,D,F) analyses are indicated. For PLA analyses, GFP was co-transfected to

visualize transfected COS7 cells. ICC images were acquired by confocal microscopy at 63x magnification; and PLA images were acquired by widefield microscopy at 40x magnification. Scale bar = 20μm. N = 3 independent experiments for all panels with representative images shown.

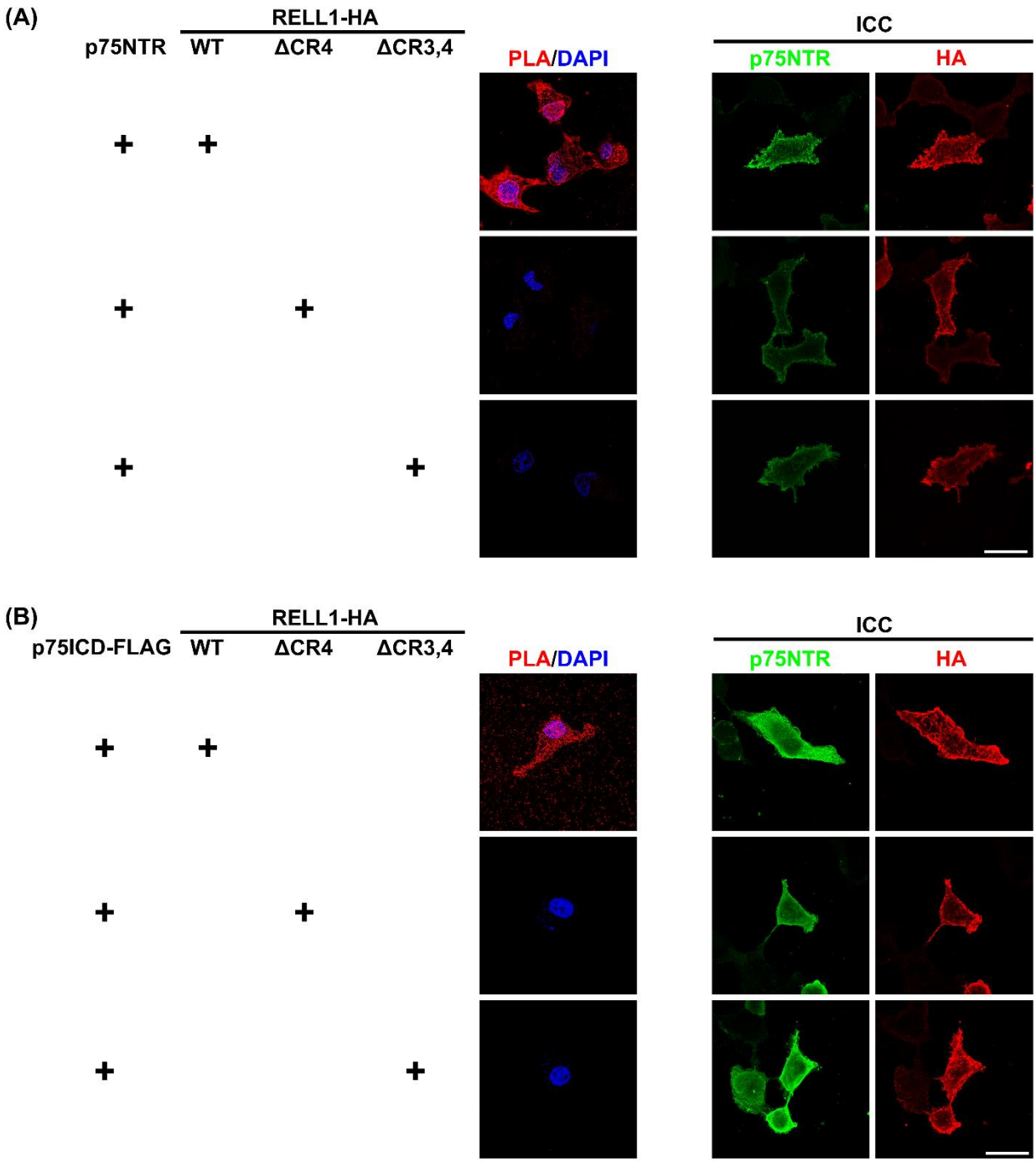

Figure 4.3. RELL1 C-terminus is required for its interaction with p75NTR. (A) Representative PLA and ICC of COS7 cells overexpressing p75NTR and WT RELL1-HA or a RELL1-HA C-terminal deletion mutant (ΔCR4; ΔCR3,4). (B) Representative PLA and ICC of COS7 cells overexpressing p75ICD and WT RELL1-HA or a RELL1-HA C-terminal deletion

mutant (ΔCR4; ΔCR3,4). In all panels (A-B), rabbit anti-p75ICD and mouse anti-HA monoclonal primary antibodies were used for both PLA and ICC. N = 3 independent experiments for all panels. Scale bar = 20μm.

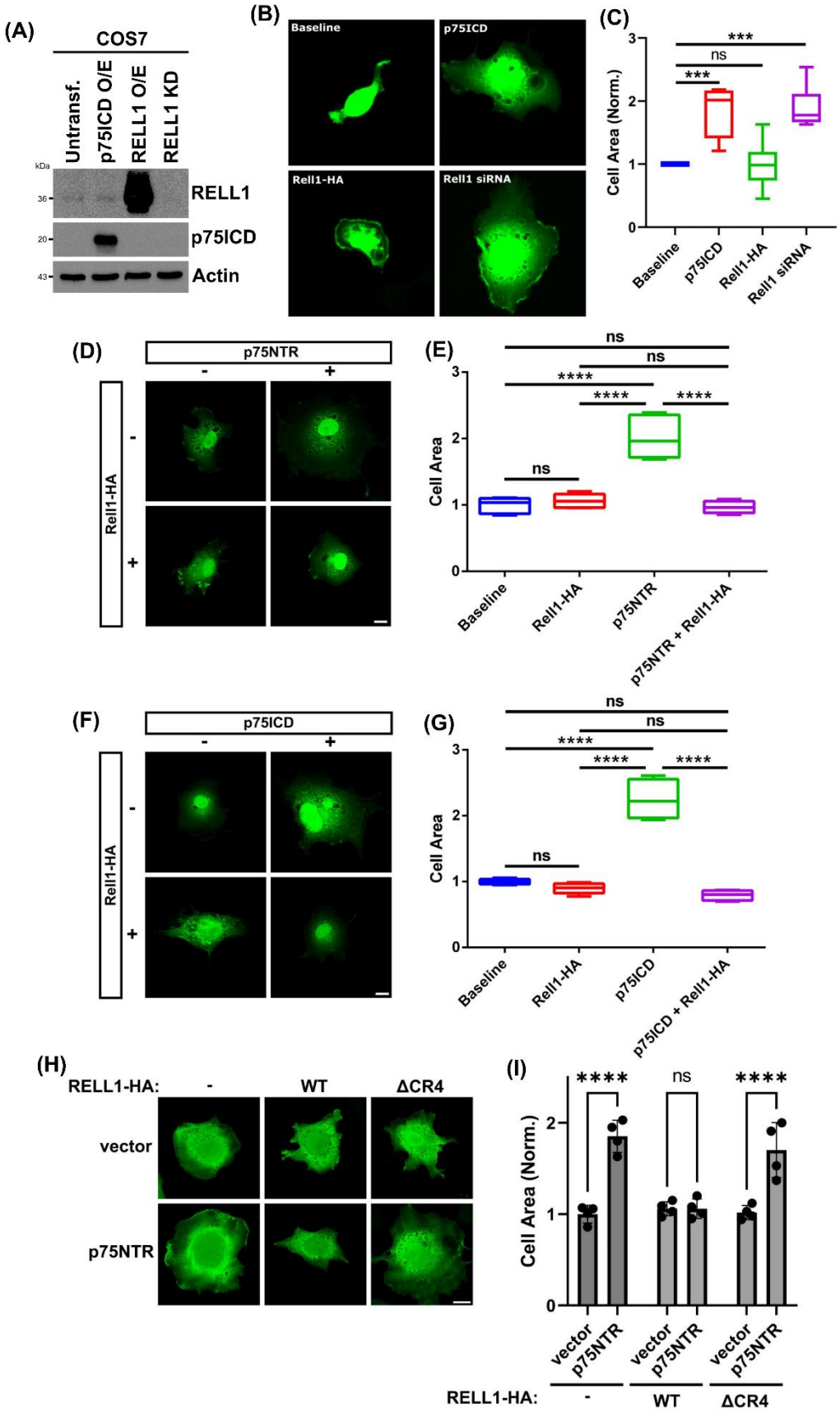
(A)
COS7
Untransf.
p75ICD O/E
RELL1 O/E
RELL1 KD
kDa
36
20
43
RELL1
p75ICD
Actin
(B)
Baseline
p75ICD
Rell1-HA
Rell1 siRNA
(C)
Cell Area (Norm.)
***
ns
***
Baseline
p75ICD
Rell1-HA
Rell1 siRNA
(D)
p75NTR
-
+
Rell1-HA
(E)
Cell Area
ns
ns
****
****
****
ns
Baseline
Rell1-HA
p75NTR
p75NTR + Rell1-HA
(F)
p75ICD
Rell1-HA
(G)
Cell Area
p75ICD + Rell1-HA
(H)
RELL1-HA:
WT
ΔCR4
vector
p75NTR
(I)
Cell Area (Norm.)
****
ns
****
RELL1-HA:

Figure 4.4. RELL1 inhibits p75NTR-dependent COS7 cell expansion via its physical interaction with p75NTR. (A) Validation of siRNA-mediated knockdown of endogenous RELL1 in COS7 cells. (B-C) Representative images (B) and cell area quantification (C) of GFP^+ COS7 cells transfected with: empty vector (negative control), p75ICD (positive control), RELL1-HA, or RELL1 siRNA. N = 6 independent experiments. One-way ANOVA with Dunnett *post hoc* test. Scale bar = 10µm. (D-E) Representative images (D) and cell area quantification (E) of GFP^+ COS7 cells overexpressing: empty vector, p75NTR, RELL1-HA, or p75NTR + RELL1-HA. N = 6 independent experiments. Two-way ANOVA with Tukey *post hoc* test. Scale bar = 10µm. (F-G) Representative images (F) and cell area quantification (G) of GFP^+ COS7 cells overexpressing: empty vector, p75ICD, RELL1-HA, or p75ICD + RELL1-HA. N = 6 independent experiments. Two-way ANOVA with Tukey *post hoc* test. Scale bar = 20µm. (H-I) Representative images (H) and cell area quantification (I) of GFP^+ COS7 cells co-transfected with empty vector or p75NTR and a RELL1-HA construct (WT, ΔCR4 or no RELL1-HA). N = 4 independent experiments. Two-way ANOVA with Sidak *post hoc* test. Scale bar = 20µm. All representative images (B,D,F,H) were acquired by confocal microscopy at 63x magnification. For all quantifications (C,E,G,I), *ns* denotes not significant; *** denotes $p \leq .001$; **** denotes $p \leq .0001$.

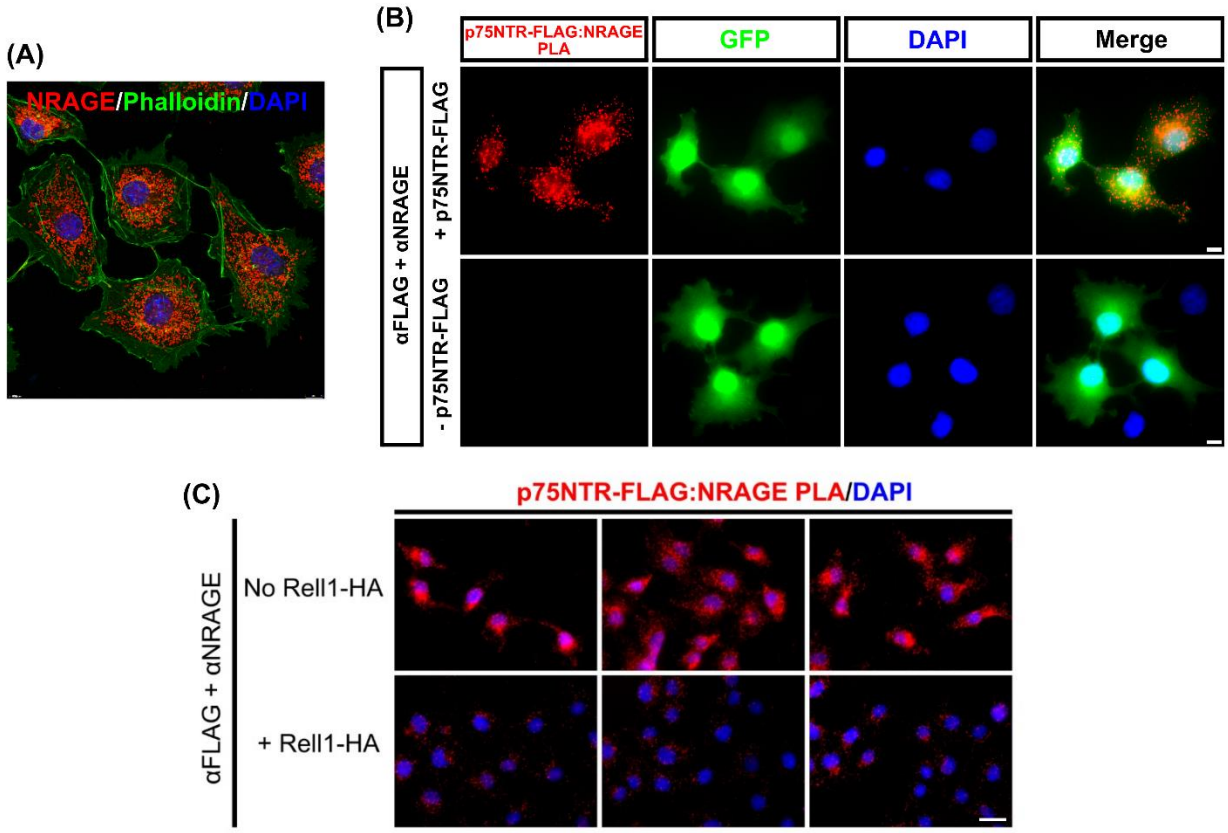

Figure 4.5. RELL1 disrupts formation of the p75NTR-NRAGE complex. (A) Endogenous NRAGE ICC in COS7 cells. (B) PLA of overexpressed p75NTR-FLAG with endogenous NRAGE in COS7 cells. GFP was co-expressed to identify transfected cells. Monoclonal mouse anti-FLAG and polyclonal rabbit anti-NRAGE primary antibodies were used. Widefield microscopy images were acquired at 40x magnification. Scale bar = 10µm. (C) p75NTR-FLAG:NRAGE PLA in COS7 cells co-expressing p75NTR-FLAG and empty vector ('no RELL1-HA') or RELL1-HA. Widefield microscopy images were acquired at 10x magnification. Scale bar = 50µm.

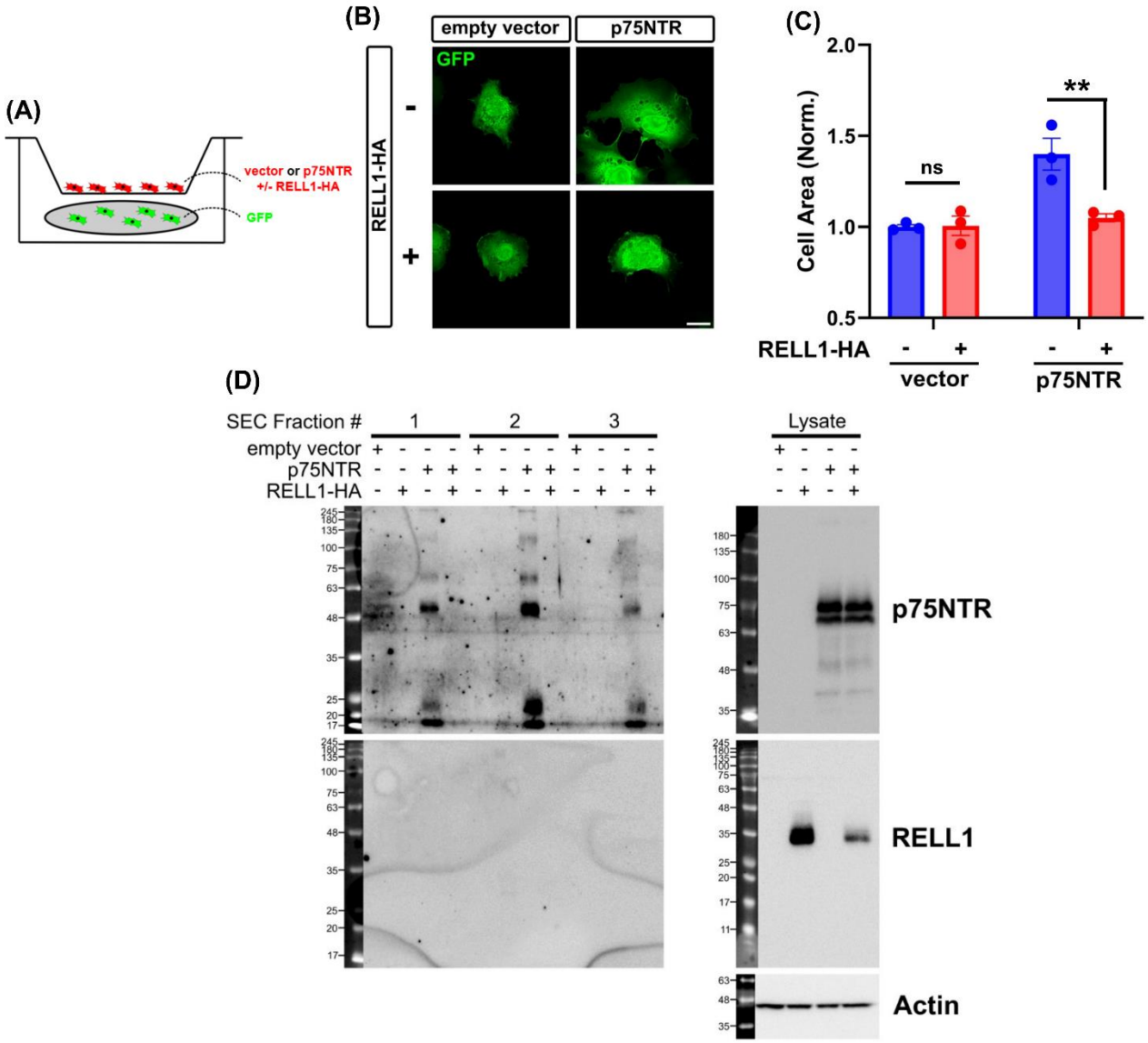

Figure 4.6. RELL1 is an inhibitor of p75NTR exocytosis. (A) Schematic representation of the filter-based non-cell-autonomous COS7 expansion assay with indicated transfection conditions. (B-C) Representative confocal images (B) and cell area quantification (C) of GFP^+ recipient COS7 cells seeded below donor COS7 cells expressing vector or p75NTR +/- RELL1-HA. N = 3 independent experiments. Two-way ANOVA with Sidak *post hoc* test. *ns* – not significant; ** denotes $p \leq .01$. Scale bar = 20µm. (D) p75NTR immunoblot analysis of EVs isolated from the conditioned medium of COS7 cells overexpressing: empty vector, RELL1-HA, p75NTR, or

p75NTR + RELL1-HA. For each condition, media SEC fractions #1-3 and whole cell lysates were subjected to immunoblot. Representative immunoblots are shown from N = 3 technical replicates.

Chapter 5: Overarching Discussion

In this doctoral thesis, I sought to characterize novel signaling mechanisms engaged by p75NTR to better understand the functional properties of this enigmatic receptor with diverse roles in nervous system development and maintenance. To this end, I demonstrated that p75NTR-dependent COS7 cell expansion (587) occurs via a non-cell-autonomous pathway—as $p75NTR^{+}$ cells induce expansion of spatially-segregated GFP^{+} cells across a porous filter (Chapter 2). Subsequent media fractionation experiments revealed that a large, membranous extracellular structure mediates this non-cell-autonomous signaling event. Immunoblot analysis revealed that p75NTR is targeted to large extracellular vesicles (EVs) which induce expansion in naïve GFP^{+} COS7 cells. Strikingly, p75NTR proteolytic cleavage products (p75CTF and p75ICD) are highly enriched in this EV compartment. $p75NTR^{+}$ EVs induce expansion events in both COS7 cells and developing DRG sensory neurons. $p75NTR^{+}$ EV-dependent expansion requires downstream engagement of recipient cell-derived NRAGE as the expansion phenotype is abolished by CRISPR-mediated NRAGE knockout in distinct COS7 lines.

To study p75NTR signaling from a broader perspective, we leveraged proximity-dependent biotinylation (BioID) to resolve the common interactome of p75NTR and two functionally-related TNFRSFs, DR6 and TROY—in a modified HEK293 cell line (Flp-In 293 TREx) (Chapter 3). This strategy identified 29 interactors that are shared by p75NTR, DR6 and TROY, including a truncated TNFRSF, RELT-Like 1 (RELL1).

In Chapter 4, I validated the RELL1-p75NTR complex by proximity ligation assay (PLA) and sought to functionally characterize this novel heterotypic TNFRSF complex. Interestingly, exogenous RELL1 completely blocked p75NTR-dependent COS7 cell expansion via the exocytosis-dependent pathway. A physical association of RELL1with p75NTR via C-terminal

interactions mediates RELL1-dependent p75NTR inhibition as a non-p75NTR-binding RELL1 mutant (RELL1$^{\Delta CRD4}$-HA) fails to block p75NTR-dependent cell expansion. RELL1 inhibits p75NTR targeting to EVs, thereby blocking any downstream p75NTR action in recipient cells. Thus, we establish RELL1 as a negative regulator of exocytosis-dependent p75NTR signaling and provide new evidence that ECD-truncated TNFRSFs can act as endogenous TNFRSF inhibitors.

5.1 Extracellular vesicles are a novel p75NTR signaling platform

p75NTR exocytosis via exosomes has been described in cultured SCG neurons (473) and de-differentiated Schwann cells (589). The biological function of extracellular p75NTR, however, has not been investigated in the nervous system. One report on melanoma suggests that exosome-derived p75NTR promotes tumour metastasis (475)— this provides some evidence consistent with our finding that extracellular p75NTR can influence cell morphology, but the mechanism of EV-dependent p75NTR signaling has not been explored. Partly to blame is the lack of adequate tools to investigate p75NTR-specific function in an EV context. EVs are highly complex and heterogenous structures that exert effects locally on recipient cells, making phenotypes difficult to detect. To this end, we described a non-cell-autonomous COS7 cell expansion assay as a robust assay system for investigating EV-specific p75NTR functions. Our future research will leverage the COS7 cell expansion platform as a reliable *in vitro* assay to investigate this novel intercellular p75NTR signaling mechanism.

All studies of p75NTR exocytosis performed to date have applied ultracentrifugation-based EV purification protocols which remove large membranous structures such as microvesicles (MVs) (473,475). The size exclusion chromatography approach we applied to conditioned medium (Figure 2.5) shows that most extracellular p75NTR elutes in large EVs

(fractions 1-3), though small EV-derived p75NTR (fractions 4-5) is detected at low levels. COS7 and IMS32 cell lines target overexpressed (COS7) and endogenous (IMS32) p75NTR to large EVs. These data suggest that p75NTR may be primarily exocytosed via MVs rather than exosomes. In-depth structural and biochemical characterization of the large $p75NTR^+$ EV compartment (SEC fractions 1-3) will be required to definitively identify this structure. Our studies suggest that SEC-based EV purification captures the full range of $p75NTR^+$ EVs and prevents inadvertent discard of the large $p75NTR^+$ structures.

Exocytosis of exogenous p75NTR in COS7 (Figure 2.5A) and endogenous p75NTR in IMS32 cells (Figure 2.5B) occurs constitutively in the absence of an applied ligand. However, even in the absence of applied ligand, one cannot rule the possibility of an unknown endogenous ligand driving p75NTR EV targeting in COS7 and IMS32 lines. As reviewed in Chapter 1, p75NTR is known to signal in ligand-bound and -unbound states; and associates with a diverse set of ligands, including NTs, proNTs, myelin-associated inhibitory factors and Aβ. Future work is needed into the influence of ligands on p75NTR exocytosis to assess the possibility of ligand modulation of EV targeting. Understanding ligand dependency, or lack thereof, will inform new hypotheses into exocytosis-dependent p75NTR signaling *in vivo*.

Immunoblot detection of EV-derived p75NTR using a p75ICD-targeting antibody revealed that most p75 species in EVs are cleavage products (p75CTF and p75ICD), as verified by pharmacological inhibition of α- and γ-secretases (Figure 2.6). This was an unexpected finding, as lysate-derived p75NTR:p75CTF or p75NTR:p75ICD ratios are typically 99:1 or greater in neural and non-neural cell types. The magnitude of p75CTF/ICD enrichment in EVs is particularly striking, as p75 cleavage products are more abundant than FL p75 in this compartment—representing an inversion of the p75NTR:p75ICD ratio observed in whole cell

lysates. A next logical step is to investigate if p75NTR cleavage occurs within the EV context. Interestingly, ADAM17—the metalloprotease that mediates the α-secretase p75NTR cleavage step—has been shown to be catalytically active in EVs (634). The subcellular compartment mediating p75NTR cleavage is unknown to-date. Given the massive abundance of p75CTF and ICD in EVs, it is possible that cleavage event(s) occur within an EV context. Lastly, it is known that p75ICD is rapidly turned over in the cytosol, providing tight spatiotemporal control of p75ICD-dependent signaling events. EVs are protected from proteasomal turnover by trafficking outside cell boundaries. EVs, therefore, may confer protection for soluble p75ICD to accumulate to act in large quantities at target recipient cells and thereby prolong ICD-dependent signaling events. Such a model could reconcile the seemingly contradictory observations that p75ICD targets intracellular compartments distal to the plasma membrane—such as the nucleus (635)—despite its rapid turnover kinetics. Future investigation into the turnover rate of EV-derived p75ICD *in vitro* and *in vivo* would further our understanding of intercellular p75NTR signaling.

5.2 ECD-truncated TNFRSFs are a distinct TNFRSF family that may function as TNFRSF inhibitors

In Chapter 4, we discovered that RELL1 is an inhibitor of intercellular p75NTR signaling that blocks p75NTR targeting to EVs. This novel discovery shows functional parallels to the NRH2-p75NTR interaction. NRH2 (ECD-truncated p75NTR paralog) binds p75NTR to inhibit complex formation with NgR and downstream RhoA activation and inhibition of neurite outgrowth (628). Though the experimental contexts of the RELL1-p75NTR (Chapter 4) and NRH2-p75NTR (628) differ, the concept that ECD-truncated TNFRSFs disrupt downstream signaling events of their FL counterparts is consistent. The hypothesis that ECD-truncated TNFRSFs as endogenous TNFRSF inhibitors is not new and warrants further investigation.

Given that ECD-truncated TNFRSFs may not be constrained to homotypic interactions with their homologous CRD-possessing TNFRSF—as is the case for TNFRSF-TNFRSF interactions—their potential inhibitory influence on TNFRSF signaling could be far-reaching *in vivo*. Future characterization of ECD-truncated TNFRSF as TNFRSF inhibitors could yield novel therapeutic strategies to combat aberrant TNF/TNFRSF function associated with neurological and immunological disease states.

In humans and mice, the only known ECD-truncated TNFRSF genes are RELL1, RELL2 and NRH2. However, it is possible other ECD-truncated TNFRSFs are expressed via alternative gene transcription sites or mRNA splice variation, for example. To address this possibility, I screened the NCBI Protein database for human CRD-lacking proteins with strong sequence homology ($E \leq 10^{-15}$) to a TNFRSF by BLAST queries of full-length TNFRSF sequences (Appendix 3). As expected, this screen found RELL1/2 and NRH2 as ECD-truncated RELT and p75NTR homologs, respectively. Interestingly, this BLAST screen identified two novel ECD-truncated TNFRSFs lacking the CRD cluster within human proteome investigations (*NP_* prefix in NCBI Protein; Appendix 3). These included an ECD-truncated homolog of CD27 (NP_001036029.1) (636–645) and Fn14 (NP_001155218.1) (646–655) (Appendix 3). Therefore, humans may express a diverse set of ECD-truncated TNFRSFs that consists of a minimum of 5 curated proteins (NP_ prefix) with other computationally predicted (XP_ prefix) family members possible (Appendix 3). Given that ECD-truncated TNFRSFs do not necessarily form homotypic complexes with their full-length TNFRSF homolog—as demonstrated by RELL1 interaction with p75NTR, DR6 and TROY (Chapter 3) in addition to RELT (488)—we propose that ECD-truncated TNFRSFs represent a distinct TNFRSF family that may possess broad TNFRSF

inhibitor function. We highly encourage the field to explore the physical and functional relationships between TNFRSFs and the ECD-truncated TNFRSF family.

5.3 Analysis of the 29-protein interactome common to p75NTR, DR6 and TROY

Given the functional redundancy of p75NTR, DR6 and TROY in nervous system development and maintenance, and tumour metastasis (reviewed in sections 1.4-1.6), it was not surprising to discover that these TNFRSF brethren share a common set of interactors (Chapter 3). Irreversible labeling of interactors with biotin (BioID)—coupled to stringent contaminant removal controls and statistical analyses—identified a set of 29 interactors shared by p75NTR, DR6 and TROY (the 'p75NTR-DR6-TROY' interactome). Though this doctoral thesis focused on the RELL1-p75NTR complex, other interactors included: solute carriers (SLCs), soluble N-ethylmaleimide-sensitive fusion protein attachment protein receptors (SNAREs), B-class ephrin ligands, EFR3 homologs (EFR3A/B), and the pan-neuronal palmitoyl-acyltransferase ZDHHC5. The BioID was performed in Flp-In 293 T-REx cell line yet nearly all of the p75NTR-DR6-TROY interactome members are expressed in the nervous system. The proof-of-concept provided by the RELL1-p75NTR data in Chapter 4 indicates that this interactome will stimulate new research avenues into TNFRSF-mediated control of nervous system development/maintenance.

SLCs are diverse family of transmembrane ion transporters that regulate cellular ion homeostasis across development (656). Within the p75NTR-DR6-TROY interactome, SLCs identified include: SLC12A2 (sodium/potassium/chloride transporter), SLC30A1 (zinc transporter), SLC38A1/2 (glutamine transporters), SLC3A2 (amino acid transporter), SLC4A7 (sodium bicarbonate cotransporter), SLC6A15 (neutral amino acid transporter), and SLC6A8 (neurotransmitter transporter). These SLCs are all expressed in neural tissues with known

functions in neuronal settings. Several of these SLCs have are directly involved in neurotransmitter release. Interestingly, p75NTR-/- are deficient in ACh release at neuromuscular junctions where the readily releasable pool of presynaptic ACh+ vesicles is strongly reduced (657). The coupling of p75NTR to neurotransmitter release via these SLCs—particularly within cholinergic neurons—warrants further investigation.

The chloride channel SLC12A2 regulates the developmental switch of postsynaptic GABAergic gradient potentials from depolarizing to hyperpolarizing (658). Postsynaptic GABA-induced chloride currents are gated by intracellular chloride (Cl^-) concentrations, which are regulated by SLC12A2 and SLC12A1 functional antagonism (658). SLC12A1 is a Cl- importer, whereas SLC12A2 is a Cl^- exporter. In the neonate and early postnatal CNS, SLC12A1 expression is elevated to drive high intracellular [Cl^-] causing Cl^- efflux (depolarization) when GABA receptors are activated (658,659). Later in development, high neuronal SLC12A2 expression—and SLC12A1 downregulation—lowers intracellular [Cl^-] to cause GABA-induced Cl- influx (hyperpolarization) (660). Interestingly, proBDNF-bound p75NTR has been shown to maintain high intracellular [Cl-] in juvenile neurons via a downstream functional association with SLC12A2 (661). Given our finding that SLC12A2 is part of the p75NTR-DR6-TROY interactome, we suspect this physical interaction may be relevant within the context of developmental chloride homeostasis in central neurons.

SNARE complexes catalyze the fusion of endosomes to the PM and are critical mediators of exosome and neurotransmitter release. Several SNARE complex subunits in the p75NTR-DR6-TROY are known mediators of MVB-PM fusion including Ykt6 (464) and SNAP23 (457,465). Given that p75NTR is secreted in exosomes, these interactors may regulate p75NTR-DR6-TROY exocytosis, which could influence receptor signaling behaviours as is the case for

p75NTR (Chapter 2). In parallel, when considered alongside the SLC interactors, there may be a larger story in which p75NTR-DR6-TROY regulates neurotransmitter release at a broad level that includes SNARE interactions. The Ykt6 and SNAP23 common interactions warrant further investigation in the contexts of neurodevelopment and neuronal function.

Ephrins mediate axon guidance via their cognate Eph receptors. Ephrins are classified as A- or B-class on a structural basis. Ephrin-A ligands are anchored to the PM via a glycosylphosphatidylinositol (GPI) linkage and lack transmembrane or intracellular domains (662). Ephrin-Bs are single-pass transmembrane ligands possessing an intracellular domain (662). Ephrin-A and ephrin-B ligands bind EphA and EphB receptors, respectively (662). p75NTR has been shown to mediate ephrin-A-dependent axon repulsion via a tripartite complex ephrinA-p75NTR-NogoR complex that transduces the repulsion signal (663–665). Moreover, p75NTR is required for ephrin-B2-dependent growth cone collapse in sympathetic neurons (595) and ephrin-B3-dependent axon growth inhibition in cortical neurons (666). Thus, p75NTR is already a known mediator of ephrin signaling in axonogenesis and axon pathfinding. Given that two B-class ephrins (ephrin-B1 and B2) were found in the p75NTR-DR6-TROY interactome, we suspect that death receptors may play a major role in ephrin signaling in neurodevelopment and encourage the field to explore this hypothesis.

Work of Gibon and colleagues established p75NTR as a negative regulator of excitability and persistent firing (PF) in cortical neurons of the entorhinal cortex (581,667)—a neuronal electrophysiological property with critical roles in learning and memory (668). Mechanistically, proBDNF-bound p75NTR activates PI4K to produce PIP2 downstream which ultimately acts on PIP2-sensitive TRPC channels to inhibit excitability and PF (581). However, the mechanism of p75NTR-induced PI4K activation remains unknown. Insight into this process may come from

the discovery of EFR3 homologs (EFR3A and EFR3B) in the p75NTR-DR6-TROY interactome. Palmitoylated EFR3 associates with the PM and recruits the subunits PI4KIIIα and TTC7 to assemble the active PI4K complex (669). Given this literature, we propose a hypothesis for future investigation that p75NTR may activate PI4K via EFR3A/B recruitment and this activity may extend to DR6 and TROY.

ZDHHC5—a ubiquitous, PM-localized palmitoyl-acyltransferase (PAT) in the nervous system—tightly coordinates postsynaptic structure and electrophysiology (670,671). p75NTR and DR6 are palmitoylation substrates (672–674) but the PAT(s) catalyzing their palmitoylation remains to be identified. Asking if ZDHHC5 mediates p75NTR/DR6 (TROY?) palmitoylation will be an interesting topic for future studies.

Conclusions

This doctoral thesis investigated signaling mechanisms of the p75 neurotrophin receptor (p75NTR): a TNFRSF that functions a major regulator of nervous system development and maintenance. In chapter 2, we discovered and characterized extracellular vesicles (EVs) as a p75NTR signaling platform. p75NTR+ EVs are highly enriched in p75NTR proteolytic cleavage products (p75CTF and p75ICD) and induce expansion events in COS7 cells and DRG growth cones; the former requiring downstream engagement of NRAGE in the recipient cell. In chapter 3, we provide evidence for a shared set of interactors between p75NTR, DR6 and TROY—TNFRSFs with overlapping function in the nervous system. In chapter 4, we characterized one of these shared interactors—the ECD-truncated TNFRSF RELL1—and demonstrated physical RELL1 binding to p75NTR inhibits p75NTR targeting to EVs and downstream intercellular signaling events. Collectively, these data represent an advancement of our knowledge of

p75NTR signaling mechanisms and facilitate new research into how this enigmatic receptor regulates neural function in physiological and pathophysiological contexts.

Appendices

All appendices are accessible online at:

https://drive.google.com/open?id=1Dxp9AdRHNttKCJNHQCREdyryU5fPFKwZ

Appendix 1. RELL1 expression in the P0 mouse brain. Immunoblot detection of RELL1 protein from P0 CNS lysates, including the: neocortex, hippocampus, cerebellum, whole brain, and spinal cord.

Appendix 2. Excel file of enriched GO terms (cell pathways). Prey list & statistics associated with each significant GO term for the p75NTR-DR6-TROY FL interactome.

Appendix 3. Identification of novel ECD-truncated TNFRSF gene products. Full-length human TNFRSF primary sequences were queried against the human proteome using Basic Local Alignment Search Tool (BLAST). TNFRSF homologs were identified using a strict E-value cutoff of $\leq 10^{-10}$. Using the NCBI Protein database, each homolog was characterized according to: number of CRDs; ECD length; ICD length; genomic locus; exon count; splice variation relative to homologous FL receptor (if applicable); and sequence identity relative to homologous FL receptor. ECD-truncated TNFRSFs with successful curation in the literature (*NP_* prefix) are highlight in green. Computationally predicted proteins lacking experimental validation (*XP_* prefix) are not highlighted.

References

1. Coley WB. The treatment of malignant tumors by repeated innoculations of erysipelas: with a report of ten original cases. Am J Med Sci. 1893;10:487–511.

2. Decker WK, Safdar A. Bioimmunoadjuvants for the treatment of neoplastic and infectious disease: Coley's legacy revisited. Cytokine Growth Factor Rev. 2009 Aug;20(4):271–81.

3. O'malley WE, Achinstein B, Shear MJ. ACTION OF BACTERIAL POLYSACCHARIDE ON TUMORS. III. REPEATED RESPONSE OF SARCOMA 37, IN TOLERANT MICE, TO SERRATIA MARCESCENS ENDOTOXIN. Cancer Res. 1963 Jul;23:890–5.

4. Kolb WP, Granger GA. Lymphocyte in vitro cytotoxicity: characterization of human lymphotoxin. Proc Natl Acad Sci U S A. 1968 Dec;61(4):1250–5.

5. Ruddle NH, Waksman BH. Cytotoxicity mediated by soluble antigen and lymphocytes in delayed hypersensitivity. 3. Analysis of mechanism. J Exp Med. 1968 Dec 1;128(6):1267–79.

6. Aggarwal BB, Moffat B, Harkins RN. Human lymphotoxin. Production by a lymphoblastoid cell line, purification, and initial characterization. J Biol Chem. 1984 Jan 10;259(1):686–91.

7. Aggarwal BB, Henzel WJ, Moffat B, Kohr WJ, Harkins RN. Primary structure of human lymphotoxin derived from 1788 lymphoblastoid cell line. J Biol Chem. 1985 Feb 25;260(4):2334–44.

8. Aggarwal BB, Kohr WJ, Hass PE, Moffat B, Spencer SA, Henzel WJ, et al. Human tumor necrosis factor. Production, purification, and characterization. J Biol Chem. 1985 Feb 25;260(4):2345–54.

9. Bringman TS, Aggarwal BB. Monoclonal antibodies to human tumor necrosis factors alpha and beta: application for affinity purification, immunoassays, and as structural probes. Hybridoma. 1987 Oct;6(5):489–507.

10. Kelker HC, Oppenheim JD, Stone-Wolff D, Henriksen-DeStefano D, Aggarwal BB, Stevenson HC, et al. Characterization of human tumor necrosis factor produced by peripheral blood monocytes and its separation from lymphotoxin. Int J Cancer. 1985 Jul 15;36(1):69–73.

11. Pennica D, Nedwin GE, Hayflick JS, Seeburg PH, Derynck R, Palladino MA, et al. Human tumour necrosis factor: precursor structure, expression and homology to lymphotoxin. Nature. 1984 Jan 20;312(5996):724–9.

12. Gray PW, Aggarwal BB, Benton CV, Bringman TS, Henzel WJ, Jarrett JA, et al. Cloning and expression of cDNA for human lymphotoxin, a lymphokine with tumour necrosis activity. Nature. 1984 Jan 20;312(5996):721–4.

13. Beutler B, Greenwald D, Hulmes JD, Chang M, Pan YC, Mathison J, et al. Identity of tumour necrosis factor and the macrophage-secreted factor cachectin. Nature. 1985 Aug 8;316(6028):552–4.

14. Aggarwal BB, Eessalu TE, Hass PE. Characterization of receptors for human tumour necrosis factor and their regulation by gamma-interferon. Nature. 1985 Jan 19;318(6047):665–7.

15. Beutler B, Milsark IW, Cerami AC. Passive immunization against cachectin/tumor necrosis factor protects mice from lethal effect of endotoxin. Science, 1985, 229(4716):869-871. Classical article. J Immunol Baltim Md 1950. 2008 Jul 1;181(1):7–9.

16. Tracey KJ, Fong Y, Hesse DG, Manogue KR, Lee AT, Kuo GC, et al. Anti-cachectin/TNF monoclonal antibodies prevent septic shock during lethal bacteraemia. Nature. 1987 Dec 17;330(6149):662–4.

17. Vinay DS, Kwon BS. The tumour necrosis factor/TNF receptor superfamily: therapeutic targets in autoimmune diseases. Clin Exp Immunol. 2011 May;164(2):145–57.

18. Aggarwal BB, Gupta SC, Kim JH. Historical perspectives on tumor necrosis factor and its superfamily: 25 years later, a golden journey. Blood. 2012 Jan 19;119(3):651–65.

19. Moore RJ, Owens DM, Stamp G, Arnott C, Burke F, East N, et al. Mice deficient in tumor necrosis factor-alpha are resistant to skin carcinogenesis. Nat Med. 1999 Jul;5(7):828–31.

20. Balkwill F. TNF-alpha in promotion and progression of cancer. Cancer Metastasis Rev. 2006 Sep;25(3):409–16.

21. Deroose JP, Eggermont AMM, van Geel AN, Burger JWA, den Bakker MA, de Wilt JHW, et al. Long-term results of tumor necrosis factor alpha- and melphalan-based isolated limb perfusion in locally advanced extremity soft tissue sarcomas. J Clin Oncol Off J Am Soc Clin Oncol. 2011 Oct 20;29(30):4036–44.

22. Deroose JP, Eggermont AMM, van Geel AN, de Wilt JHW, Burger JWA, Verhoef C. 20 years experience of TNF-based isolated limb perfusion for in-transit melanoma metastases: TNF dose matters. Ann Surg Oncol. 2012 Feb;19(2):627–35.

23. Grünhagen DJG, de Wilt JHW, van Geel AN, Verhoef C, Eggermont AMM. Isolated limb perfusion with TNF-alpha and melphalan in locally advanced soft tissue sarcomas of the extremities. Recent Results Cancer Res Fortschritte Krebsforsch Progres Dans Rech Sur Cancer. 2009;179:257–70.

24. Schneider P, Olson D, Tardivel A, Browning B, Lugovskoy A, Gong D, et al. Identification of a new murine tumor necrosis factor receptor locus that contains two novel murine receptors for tumor necrosis factor-related apoptosis-inducing ligand (TRAIL). J Biol Chem. 2003 Feb 14;278(7):5444–54.

25. Balkwill F. Tumour necrosis factor and cancer. Nat Rev Cancer. 2009 May;9(5):361–71.

26. Aggarwal BB, Shishodia S, Sandur SK, Pandey MK, Sethi G. Inflammation and cancer: how hot is the link? Biochem Pharmacol. 2006 Nov 30;72(11):1605–21.

27. Wiley SR, Schooley K, Smolak PJ, Din WS, Huang CP, Nicholl JK, et al. Identification and characterization of a new member of the TNF family that induces apoptosis. Immunity. 1995 Dec;3(6):673–82.

28. Dowlati Y, Herrmann N, Swardfager W, Liu H, Sham L, Reim EK, et al. A meta-analysis of cytokines in major depression. Biol Psychiatry. 2010 Mar 1;67(5):446–57.

29. Brietzke E, Kapczinski F. TNF-alpha as a molecular target in bipolar disorder. Prog Neuropsychopharmacol Biol Psychiatry. 2008 Aug 1;32(6):1355–61.

30. Murashima YL, Suzuki J, Yoshii M. Role of cytokines during epileptogenesis and in the transition from the interictal to the ictal state in the epileptic mutant EL mouse. Gene Regul Syst Biol. 2008 Aug 27;2:267–74.

31. Busch R, Baldus M, Vogt MA, Berger SM, Bartsch D, Gass P, et al. Effects of p75NTR deficiency on cholinergic innervation of the amygdala and anxiety-like behavior. J Neurochem. 2017;141(3):461–71.

32. Zeng F, Lu JJ, Zhou XF, Wang YJ. Roles of p75NTR in the pathogenesis of Alzheimer's disease: a novel therapeutic target. Biochem Pharmacol. 2011 Nov 15;82(10):1500–9.

33. Swardfager W, Lanctôt K, Rothenburg L, Wong A, Cappell J, Herrmann N. A meta-analysis of cytokines in Alzheimer's disease. Biol Psychiatry. 2010 Nov 15;68(10):930–41.

34. Nagatsu T, Sawada M. Inflammatory process in Parkinson's disease: role for cytokines. Curr Pharm Des. 2005;11(8):999–1016.

35. Sayed BA, Christy AL, Walker ME, Brown MA. Meningeal mast cells affect early T cell central nervous system infiltration and blood-brain barrier integrity through TNF: a role for neutrophil recruitment? J Immunol Baltim Md 1950. 2010 Jun 15;184(12):6891–900.

36. Kapadia S, Lee J, Torre-Amione G, Birdsall HH, Ma TS, Mann DL. Tumor necrosis factor-alpha gene and protein expression in adult feline myocardium after endotoxin administration. J Clin Invest. 1995 Aug;96(2):1042–52.

37. Levine B, Kalman J, Mayer L, Fillit HM, Packer M. Elevated circulating levels of tumor necrosis factor in severe chronic heart failure. N Engl J Med. 1990 Jul 26;323(4):236–41.

38. Feldman AM, Combes A, Wagner D, Kadakomi T, Kubota T, Li YY, et al. The role of tumor necrosis factor in the pathophysiology of heart failure. J Am Coll Cardiol. 2000 Mar 1;35(3):537–44.

39. Diwan A, Tran T, Misra A, Mann DL. Inflammatory mediators and the failing heart: a translational approach. Curr Mol Med. 2003 Mar;3(2):161–82.

40. McKellar GE, McCarey DW, Sattar N, McInnes IB. Role for TNF in atherosclerosis? Lessons from autoimmune disease. Nat Rev Cardiol. 2009 Jun;6(6):410–7.

41. Aviña-Zubieta JA, Choi HK, Sadatsafavi M, Etminan M, Esdaile JM, Lacaille D. Risk of cardiovascular mortality in patients with rheumatoid arthritis: a meta-analysis of observational studies. Arthritis Rheum. 2008 Dec 15;59(12):1690–7.

42. Dandona P, Aljada A, Bandyopadhyay A. Inflammation: the link between insulin resistance, obesity and diabetes. Trends Immunol. 2004 Jan;25(1):4–7.

43. Hotamisligil GS, Shargill NS, Spiegelman BM. Adipose expression of tumor necrosis factor-alpha: direct role in obesity-linked insulin resistance. Science. 1993 Jan 1;259(5091):87–91.

44. Tzanavari T, Giannogonas P, Karalis KP. TNF-alpha and obesity. Curr Dir Autoimmun. 2010;11:145–56.

45. Matera MG, Calzetta L, Cazzola M. TNF-alpha inhibitors in asthma and COPD: we must not throw the baby out with the bath water. Pulm Pharmacol Ther. 2010 Apr;23(2):121–8.

46. Kips JC, Tavernier JH, Joos GF, Peleman RA, Pauwels RA. The potential role of tumour necrosis factor alpha in asthma. Clin Exp Allergy J Br Soc Allergy Clin Immunol. 1993 Apr;23(4):247–50.

47. Lundblad LKA, Thompson-Figueroa J, Leclair T, Sullivan MJ, Poynter ME, Irvin CG, et al. Tumor necrosis factor-alpha overexpression in lung disease: a single cause behind a complex phenotype. Am J Respir Crit Care Med. 2005 Jun 15;171(12):1363–70.

48. Collison A, Foster PS, Mattes J. Emerging role of tumour necrosis factor-related apoptosis-inducing ligand (TRAIL) as a key regulator of inflammatory responses. Clin Exp Pharmacol Physiol. 2009 Nov;36(11):1049–53.

49. Schreiber TH, Wolf D, Tsai MS, Chirinos J, Deyev VV, Gonzalez L, et al. Therapeutic Treg expansion in mice by TNFRSF25 prevents allergic lung inflammation. J Clin Invest. 2010 Oct;120(10):3629–40.

50. Mi S, Lee X, Shao Z, Thill G, Ji B, Relton J, et al. LINGO-1 is a component of the Nogo-66 receptor/p75 signaling complex. Nat Neurosci. 2004 Mar;7(3):221–8.

51. Yong Y, Gamage K, Cheng I, Barford K, Spano A, Winckler B, et al. p75NTR and DR6 Regulate Distinct Phases of Axon Degeneration Demarcated by Spheroid Rupture. J Neurosci Off J Soc Neurosci. 2019 Nov 27;39(48):9503–20.

52. Singh KK, Park KJ, Hong EJ, Kramer BM, Greenberg ME, Kaplan DR, et al. Developmental axon pruning mediated by BDNF-p75NTR-dependent axon degeneration. Nat Neurosci. 2008 Jun;11(6):649–58.

53. Knowles JK, Simmons DA, Nguyen TVV, Vander Griend L, Xie Y, Zhang H, et al. Small molecule p75NTR ligand prevents cognitive deficits and neurite degeneration in an Alzheimer's mouse model. Neurobiol Aging. 2013 Aug;34(8):2052–63.

54. Simmons DA, Knowles JK, Belichenko NP, Banerjee G, Finkle C, Massa SM, et al. A small molecule p75NTR ligand, LM11A-31, reverses cholinergic neurite dystrophy in Alzheimer's disease mouse models with mid- to late-stage disease progression. PloS One. 2014;9(8):e102136.

55. Lorentz CU, Parrish DC, Alston EN, Pellegrino MJ, Woodward WR, Hempstead BL, et al. Sympathetic denervation of peri-infarct myocardium requires the p75 neurotrophin receptor. Exp Neurol. 2013 Nov;249:111–9.

56. Nikolaev A, McLaughlin T, O'Leary DDM, Tessier-Lavigne M. APP binds DR6 to trigger axon pruning and neuron death via distinct caspases. Nature. 2009 Feb 19;457(7232):981–9.

57. Gamage KK, Cheng I, Park RE, Karim MS, Edamura K, Hughes C, et al. Death Receptor 6 Promotes Wallerian Degeneration in Peripheral Axons. Curr Biol CB. 2017 Mar 20;27(6):890–6.

58. Olsen O, Kallop DY, McLaughlin T, Huntwork-Rodriguez S, Wu Z, Duggan CD, et al. Genetic analysis reveals that amyloid precursor protein and death receptor 6 function in the same pathway to control axonal pruning independent of β-secretase. J Neurosci Off J Soc Neurosci. 2014 May 7;34(19):6438–47.

59. Fernández-Suárez D, Krapacher FA, Andersson A, Ibáñez CF, Kisiswa L. MAG induces apoptosis in cerebellar granule neurons through p75NTR demarcating granule layer/white matter boundary. Cell Death Dis. 2019 30;10(10):732.

60. Thomas RA, Gibon J, Chen CXQ, Chierzi S, Soubannier VG, Baulac S, et al. The Nogo Receptor Ligand LGI1 Regulates Synapse Number and Synaptic Activity in Hippocampal and Cortical Neurons. eNeuro. 2018 Aug;5(4).

61. Shao Z, Browning JL, Lee X, Scott ML, Shulga-Morskaya S, Allaire N, et al. TAJ/TROY, an orphan TNF receptor family member, binds Nogo-66 receptor 1 and regulates axonal regeneration. Neuron. 2005 Feb 3;45(3):353–9.

62. Wang KC, Kim JA, Sivasankaran R, Segal R, He Z. P75 interacts with the Nogo receptor as a co-receptor for Nogo, MAG and OMgp. Nature. 2002 Nov 7;420(6911):74–8.

63. Wong ST, Henley JR, Kanning KC, Huang K hua, Bothwell M, Poo M ming. A p75(NTR) and Nogo receptor complex mediates repulsive signaling by myelin-associated glycoprotein. Nat Neurosci. 2002 Dec;5(12):1302–8.

64. Ibáñez CF, Simi A. p75 neurotrophin receptor signaling in nervous system injury and degeneration: paradox and opportunity. Trends Neurosci. 2012 Jul;35(7):431–40.

65. Locksley RM, Killeen N, Lenardo MJ. The TNF and TNF receptor superfamilies: integrating mammalian biology. Cell. 2001 Feb 23;104(4):487–501.

66. Bodmer JL, Schneider P, Tschopp J. The molecular architecture of the TNF superfamily. Trends Biochem Sci. 2002 Jan;27(1):19–26.

67. Dostert C, Grusdat M, Letellier E, Brenner D. The TNF Family of Ligands and Receptors: Communication Modules in the Immune System and Beyond. Physiol Rev. 2019 01;99(1):115–60.

68. Tang P, Hung M-C null, Klostergaard J. Human pro-tumor necrosis factor is a homotrimer. Biochemistry. 1996 Jun 25;35(25):8216–25.

69. Chan FK, Chun HJ, Zheng L, Siegel RM, Bui KL, Lenardo MJ. A domain in TNF receptors that mediates ligand-independent receptor assembly and signaling. Science. 2000 Jun 30;288(5475):2351–4.

70. Vilar M, Charalampopoulos I, Kenchappa RS, Simi A, Karaca E, Reversi A, et al. Activation of the p75 neurotrophin receptor through conformational rearrangement of disulphide-linked receptor dimers. Neuron. 2009 Apr 16;62(1):72–83.

71. Marchetti L, Bonsignore F, Gobbo F, Amodeo R, Calvello M, Jacob A, et al. Fast-diffusing p75NTR monomers support apoptosis and growth cone collapse by neurotrophin ligands. Proc Natl Acad Sci U S A. 2019 22;116(43):21563–72.

72. Weber CH, Vincenz C. A docking model of key components of the DISC complex: death domain superfamily interactions redefined. FEBS Lett. 2001 Mar 16;492(3):171–6.

73. He XL, Garcia KC. Structure of nerve growth factor complexed with the shared neurotrophin receptor p75. Science. 2004 May 7;304(5672):870–5.

74. Hsu H, Xiong J, Goeddel DV. The TNF receptor 1-associated protein TRADD signals cell death and NF-kappa B activation. Cell. 1995 May 19;81(4):495–504.

75. Chinnaiyan AM, O'Rourke K, Tewari M, Dixit VM. FADD, a novel death domain-containing protein, interacts with the death domain of Fas and initiates apoptosis. Cell. 1995 May 19;81(4):505–12.

76. Headon DJ, Emmal SA, Ferguson BM, Tucker AS, Justice MJ, Sharpe PT, et al. Gene defect in ectodermal dysplasia implicates a death domain adapter in development. Nature. 2001 Dec 20;414(6866):913–6.

77. Roux PP, Barker PA. Neurotrophin signaling through the p75 neurotrophin receptor. Prog Neurobiol. 2002 Jun;67(3):203–33.

78. Strilic B, Yang L, Albarrán-Juárez J, Wachsmuth L, Han K, Müller UC, et al. Tumour-cell-induced endothelial cell necroptosis via death receptor 6 promotes metastasis. Nature. 2016 11;536(7615):215–8.

79. Chung JY, Park YC, Ye H, Wu H. All TRAFs are not created equal: common and distinct molecular mechanisms of TRAF-mediated signal transduction. J Cell Sci. 2002 Feb 15;115(Pt 4):679–88.

80. Brown KD, Hostager BS, Bishop GA. Regulation of TRAF2 signaling by self-induced degradation. J Biol Chem. 2002 May 31;277(22):19433–8.

81. Hostager BS, Haxhinasto SA, Rowland SL, Bishop GA. Tumor necrosis factor receptor-associated factor 2 (TRAF2)-deficient B lymphocytes reveal novel roles for TRAF2 in CD40 signaling. J Biol Chem. 2003 Nov 14;278(46):45382–90.

82. Liao G, Zhang M, Harhaj EW, Sun SC. Regulation of the NF-kappaB-inducing kinase by tumor necrosis factor receptor-associated factor 3-induced degradation. J Biol Chem. 2004 Jun 18;279(25):26243–50.

83. Chen ZJ. Ubiquitin signalling in the NF-kappaB pathway. Nat Cell Biol. 2005 Aug;7(8):758–65.

84. Kanda H, Igaki T, Kanuka H, Yagi T, Miura M. Wengen, a member of the Drosophila tumor necrosis factor receptor superfamily, is required for Eiger signaling. J Biol Chem. 2002 Aug 9;277(32):28372–5.

85. Kauppila S, Maaty WSA, Chen P, Tomar RS, Eby MT, Chapo J, et al. Eiger and its receptor, Wengen, comprise a TNF-like system in Drosophila. Oncogene. 2003 Jul 31;22(31):4860–7.

86. Andersen DS, Colombani J, Palmerini V, Chakrabandhu K, Boone E, Röthlisberger M, et al. The Drosophila TNF receptor Grindelwald couples loss of cell polarity and neoplastic growth. Nature. 2015 Jun 25;522(7557):482–6.

87. Ruan W, Unsain N, Desbarats J, Fon EA, Barker PA. Wengen, the sole tumour necrosis factor receptor in Drosophila, collaborates with moesin to control photoreceptor axon targeting during development. PloS One. 2013;8(3):e60091.

88. Ruan W, Srinivasan A, Lin S, Kara k I, Barker PA. Eiger-induced cell death relies on Rac1-dependent endocytosis. Cell Death Dis. 2016 Apr 7;7:e2181.

89. Grech A, Quinn R, Srinivasan D, Badoux X, Brink R. Complete structural characterisation of the mammalian and Drosophila TRAF genes: implications for TRAF evolution and the role of RING finger splice variants. Mol Immunol. 2000 Sep;37(12–13):721–34.

90. Wilson KHS. The genome sequence of the protostome Daphnia pulex encodes respective orthologues of a neurotrophin, a Trk and a p75NTR: evolution of neurotrophin signaling components and related proteins in the bilateria. BMC Evol Biol. 2009 Oct 6;9:243.

91. Quistad SD, Traylor-Knowles N. Precambrian origins of the TNFR superfamily. Cell Death Discov. 2016 Jul 18;2:16058.

92. Passano KN, Passano LM. The endodermal nerve net of scyphozoa. J Morphol. 1971 Jan;133(1):105–23.

93. Thompson CL, Ng L, Menon V, Martinez S, Lee CK, Glattfelder K, et al. A high-resolution spatiotemporal atlas of gene expression of the developing mouse brain. Neuron. 2014 Jul 16;83(2):309–23.

94. Yan H, Chao MV. Disruption of cysteine-rich repeats of the p75 nerve growth factor receptor leads to loss of ligand binding. J Biol Chem. 1991 Jun 25;266(18):12099–104.

95. Large TH, Weskamp G, Helder JC, Radeke MJ, Misko TP, Shooter EM, et al. Structure and developmental expression of the nerve growth factor receptor in the chicken central nervous system. Neuron. 1989 Feb;2(2):1123–34.

96. Grob PM, Ross AH, Koprowski H, Bothwell M. Characterization of the human melanoma nerve growth factor receptor. J Biol Chem. 1985 Jul 5;260(13):8044–9.

97. Huang B, Eberstadt M, Olejniczak ET, Meadows RP, Fesik SW. NMR structure and mutagenesis of the Fas (APO-1/CD95) death domain. Nature. 1996 Dec 19;384(6610):638–41.

98. Liepinsh E, Ilag LL, Otting G, Ibáñez CF. NMR structure of the death domain of the p75 neurotrophin receptor. EMBO J. 1997 Aug 15;16(16):4999–5005.

99. Scott FL, Stec B, Pop C, Dobaczewska MK, Lee JJ, Monosov E, et al. The Fas-FADD death domain complex structure unravels signalling by receptor clustering. Nature. 2009 Feb 19;457(7232):1019–22.

100. Charalampopoulos I, Vicario A, Pediaditakis I, Gravanis A, Simi A, Ibáñez CF. Genetic dissection of neurotrophin signaling through the p75 neurotrophin receptor. Cell Rep. 2012 Dec 27;2(6):1563–70.

101. Anastasia A, Barker PA, Chao MV, Hempstead BL. Detection of p75NTR Trimers: Implications for Receptor Stoichiometry and Activation. J Neurosci Off J Soc Neurosci. 2015 Aug 26;35(34):11911–20.

102. Gong Y, Cao P, Yu H jun, Jiang T. Crystal structure of the neurotrophin-3 and p75NTR symmetrical complex. Nature. 2008 Aug 7;454(7205):789–93.

103. Nykjaer A, Lee R, Teng KK, Jansen P, Madsen P, Nielsen MS, et al. Sortilin is essential for proNGF-induced neuronal cell death. Nature. 2004 Feb 26;427(6977):843–8.

104. Feng D, Kim T, Ozkan E, Light M, Torkin R, Teng KK, et al. Molecular and structural insight into proNGF engagement of p75NTR and sortilin. J Mol Biol. 2010 Mar 5;396(4):967–84.

105. Vilar M, Charalampopoulos I, Kenchappa RS, Reversi A, Klos-Applequist JM, Karaca E, et al. Ligand-independent signaling by disulfide-crosslinked dimers of the p75 neurotrophin receptor. J Cell Sci. 2009 Sep 15;122(Pt 18):3351–7.

106. Tanaka K, Kelly CE, Goh KY, Lim KB, Ibáñez CF. Death Domain Signaling by Disulfide-Linked Dimers of the p75 Neurotrophin Receptor Mediates Neuronal Death in the CNS. J Neurosci Off J Soc Neurosci. 2016 18;36(20):5587–95.

107. Lin Z, Tann JY, Goh ETH, Kelly C, Lim KB, Gao JF, et al. Structural basis of death domain signaling in the p75 neurotrophin receptor. eLife. 2015 Dec 8;4:e11692.

108. Yuan W, Ibáñez CF, Lin Z. Death domain of p75 neurotrophin receptor: a structural perspective on an intracellular signalling hub. Biol Rev Camb Philos Soc. 2019;94(4):1282–93.

109. Mineev KS, Goncharuk SA, Kuzmichev PK, Vilar M, Arseniev AS. NMR Dynamics of Transmembrane and Intracellular Domains of p75NTR in Lipid-Protein Nanodiscs. Biophys J. 2015 Aug 18;109(4):772–82.

110. Vilar M, Sung TC, Chen Z, García-Carpio I, Fernandez EM, Xu J, et al. Heterodimerization of p45-p75 modulates p75 signaling: structural basis and mechanism of action. PLoS Biol. 2014 Aug;12(8):e1001918.

111. Davies AM. The neurotrophic hypothesis: where does it stand? Philos Trans R Soc Lond B Biol Sci. 1996 Mar 29;351(1338):389–94.

112. Loeb DM, Stephens RM, Copeland T, Kaplan DR, Greene LA. A Trk nerve growth factor (NGF) receptor point mutation affecting interaction with phospholipase C-gamma 1 abolishes NGF-promoted peripherin induction but not neurite outgrowth. J Biol Chem. 1994 Mar 25;269(12):8901–10.

113. Obermeier A, Bradshaw RA, Seedorf K, Choidas A, Schlessinger J, Ullrich A. Neuronal differentiation signals are controlled by nerve growth factor receptor/Trk binding sites for SHC and PLC gamma. EMBO J. 1994 Apr 1;13(7):1585–90.

114. Stephens RM, Loeb DM, Copeland TD, Pawson T, Greene LA, Kaplan DR. Trk receptors use redundant signal transduction pathways involving SHC and PLC-gamma 1 to mediate NGF responses. Neuron. 1994 Mar;12(3):691–705.

115. Grewal SS, York RD, Stork PJ. Extracellular-signal-regulated kinase signalling in neurons. Curr Opin Neurobiol. 1999 Oct;9(5):544–53.

116. Ballif BA, Blenis J. Molecular mechanisms mediating mammalian mitogen-activated protein kinase (MAPK) kinase (MEK)-MAPK cell survival signals. Cell Growth Differ Mol Biol J Am Assoc Cancer Res. 2001 Aug;12(8):397–408.

117. Vetter ML, Martin-Zanca D, Parada LF, Bishop JM, Kaplan DR. Nerve growth factor rapidly stimulates tyrosine phosphorylation of phospholipase C-gamma 1 by a kinase

activity associated with the product of the trk protooncogene. Proc Natl Acad Sci U S A. 1991 Jul 1;88(13):5650–4.

118. Corbit KC, Foster DA, Rosner MR. Protein kinase Cdelta mediates neurogenic but not mitogenic activation of mitogen-activated protein kinase in neuronal cells. Mol Cell Biol. 1999 Jun;19(6):4209–18.

119. Hempstead BL, Martin-Zanca D, Kaplan DR, Parada LF, Chao MV. High-affinity NGF binding requires coexpression of the trk proto-oncogene and the low-affinity NGF receptor. Nature. 1991 Apr 25;350(6320):678–83.

120. Mahadeo D, Kaplan L, Chao MV, Hempstead BL. High affinity nerve growth factor binding displays a faster rate of association than p140trk binding. Implications for multi-subunit polypeptide receptors. J Biol Chem. 1994 Mar 4;269(9):6884–91.

121. Barker PA, Shooter EM. Disruption of NGF binding to the low affinity neurotrophin receptor p75LNTR reduces NGF binding to TrkA on PC12 cells. Neuron. 1994 Jul;13(1):203–15.

122. Verdi JM, Birren SJ, Ibáñez CF, Persson H, Kaplan DR, Benedetti M, et al. p75LNGFR regulates Trk signal transduction and NGF-induced neuronal differentiation in MAH cells. Neuron. 1994 Apr;12(4):733–45.

123. Ceni C, Kommaddi RP, Thomas R, Vereker E, Liu X, McPherson PS, et al. The p75NTR intracellular domain generated by neurotrophin-induced receptor cleavage potentiates Trk signaling. J Cell Sci. 2010 Jul 1;123(Pt 13):2299–307.

124. Kommaddi RP, Thomas R, Ceni C, Daigneault K, Barker PA. Trk-dependent ADAM17 activation facilitates neurotrophin survival signaling. FASEB J Off Publ Fed Am Soc Exp Biol. 2011 Jun;25(6):2061–70.

125. O'Neill LA, Kaltschmidt C. NF-kappa B: a crucial transcription factor for glial and neuronal cell function. Trends Neurosci. 1997 Jun;20(6):252–8.

126. Maggirwar SB, Sarmiere PD, Dewhurst S, Freeman RS. Nerve growth factor-dependent activation of NF-kappaB contributes to survival of sympathetic neurons. J Neurosci Off J Soc Neurosci. 1998 Dec 15;18(24):10356–65.

127. Yoon SO, Casaccia-Bonnefil P, Carter B, Chao MV. Competitive signaling between TrkA and p75 nerve growth factor receptors determines cell survival. J Neurosci Off J Soc Neurosci. 1998 May 1;18(9):3273–81.

128. Hamanoue M, Middleton G, Wyatt S, Jaffray E, Hay RT, Davies AM. p75-mediated NF-kappaB activation enhances the survival response of developing sensory neurons to nerve growth factor. Mol Cell Neurosci. 1999 Jul;14(1):28–40.

129. Gentry JJ, Casaccia-Bonnefil P, Carter BD. Nerve growth factor activation of nuclear factor kappaB through its p75 receptor is an anti-apoptotic signal in RN22 schwannoma cells. J Biol Chem. 2000 Mar 17;275(11):7558–65.

130. Foehr ED, Lin X, O'Mahony A, Geleziunas R, Bradshaw RA, Greene WC. NF-kappa B signaling promotes both cell survival and neurite process formation in nerve growth factor-stimulated PC12 cells. J Neurosci Off J Soc Neurosci. 2000 Oct 15;20(20):7556–63.

131. Descamps S, Toillon RA, Adriaenssens E, Pawlowski V, Cool SM, Nurcombe V, et al. Nerve growth factor stimulates proliferation and survival of human breast cancer cells through two distinct signaling pathways. J Biol Chem. 2001 May 25;276(21):17864–70.

132. Khursigara G, Bertin J, Yano H, Moffett H, DiStefano PS, Chao MV. A prosurvival function for the p75 receptor death domain mediated via the caspase recruitment domain receptor-interacting protein 2. J Neurosci Off J Soc Neurosci. 2001 Aug 15;21(16):5854–63.

133. Hughes AL, Messineo-Jones D, Lad SP, Neet KE. Distinction between differentiation, cell cycle, and apoptosis signals in PC12 cells by the nerve growth factor mutant delta9/13, which is selective for the p75 neurotrophin receptor. J Neurosci Res. 2001 Jan 1;63(1):10–9.

134. Khursigara G, Orlinick JR, Chao MV. Association of the p75 neurotrophin receptor with TRAF6. J Biol Chem. 1999 Jan 29;274(5):2597–600.

135. Wooten MW, Seibenhener ML, Mamidipudi V, Diaz-Meco MT, Barker PA, Moscat J. The atypical protein kinase C-interacting protein p62 is a scaffold for NF-kappaB activation by nerve growth factor. J Biol Chem. 2001 Mar 16;276(11):7709–12.

136. Irie S, Hachiya T, Rabizadeh S, Maruyama W, Mukai J, Li Y, et al. Functional interaction of Fas-associated phosphatase-1 (FAP-1) with p75(NTR) and their effect on NF-kappaB activation. FEBS Lett. 1999 Oct 29;460(2):191–8.

137. Salehi AH, Roux PP, Kubu CJ, Zeindler C, Bhakar A, Tannis LL, et al. NRAGE, a novel MAGE protein, interacts with the p75 neurotrophin receptor and facilitates nerve growth factor-dependent apoptosis. Neuron. 2000 Aug;27(2):279–88.

138. Salehi AH, Xanthoudakis S, Barker PA. NRAGE, a p75 neurotrophin receptor-interacting protein, induces caspase activation and cell death through a JNK-dependent mitochondrial pathway. J Biol Chem. 2002 Dec 13;277(50):48043–50.

139. Bertrand MJM, Kenchappa RS, Andrieu D, Leclercq-Smekens M, Nguyen HNT, Carter BD, et al. NRAGE, a p75NTR adaptor protein, is required for developmental apoptosis in vivo. Cell Death Differ. 2008 Dec;15(12):1921–9.

140. Yi JS, Lee SK, Sato TA, Koh JY. Co-induction of p75(NTR) and the associated death executor NADE in degenerating hippocampal neurons after kainate-induced seizures in the rat. Neurosci Lett. 2003 Aug 21;347(2):126–30.

141. Casademunt E, Carter BD, Benzel I, Frade JM, Dechant G, Barde YA. The zinc finger protein NRIF interacts with the neurotrophin receptor p75(NTR) and participates in programmed cell death. EMBO J. 1999 Nov 1;18(21):6050–61.

142. Zeinieh M, Salehi A, Rajkumar V, Barker PA. p75NTR-dependent Rac1 activation requires receptor cleavage and activation of an NRAGE and NEDD9 signaling cascade. J Cell Sci. 2015 Feb 1;128(3):447–59.

143. Linggi MS, Burke TL, Williams BB, Harrington A, Kraemer R, Hempstead BL, et al. Neurotrophin receptor interacting factor (NRIF) is an essential mediator of apoptotic signaling by the p75 neurotrophin receptor. J Biol Chem. 2005 Apr 8;280(14):13801–8.

144. Kenchappa RS, Zampieri N, Chao MV, Barker PA, Teng HK, Hempstead BL, et al. Ligand-dependent cleavage of the P75 neurotrophin receptor is necessary for NRIF nuclear translocation and apoptosis in sympathetic neurons. Neuron. 2006 Apr 20;50(2):219–32.

145. Zupan AA, Osborne PA, Smith CE, Siegel NR, Leimgruber RM, Johnson EM. Identification, purification, and characterization of truncated forms of the human nerve growth factor receptor. J Biol Chem. 1989 Jul 15;264(20):11714–20.

146. Barker PA, Miller FD, Large TH, Murphy RA. Generation of the truncated form of the nerve growth factor receptor by rat Schwann cells. Evidence for post-translational processing. J Biol Chem. 1991 Oct 5;266(28):19113–9.

147. DiStefano PS, Chelsea DM, Schick CM, McKelvy JF. Involvement of a metalloprotease in low-affinity nerve growth factor receptor truncation: inhibition of truncation in vitro and in vivo. J Neurosci Off J Soc Neurosci. 1993 Jun;13(6):2405–14.

148. Majdan M, Lachance C, Gloster A, Aloyz R, Zeindler C, Bamji S, et al. Transgenic mice expressing the intracellular domain of the p75 neurotrophin receptor undergo neuronal apoptosis. J Neurosci Off J Soc Neurosci. 1997 Sep 15;17(18):6988–98.

149. Kanning KC, Hudson M, Amieux PS, Wiley JC, Bothwell M, Schecterson LC. Proteolytic processing of the p75 neurotrophin receptor and two homologs generates C-terminal fragments with signaling capability. J Neurosci Off J Soc Neurosci. 2003 Jul 2;23(13):5425–36.

150. Weskamp G, Schlöndorff J, Lum L, Becherer JD, Kim TW, Saftig P, et al. Evidence for a critical role of the tumor necrosis factor alpha convertase (TACE) in ectodomain shedding of the p75 neurotrophin receptor (p75NTR). J Biol Chem. 2004 Feb 6;279(6):4241–9.

151. Zampieri N, Xu CF, Neubert TA, Chao MV. Cleavage of p75 neurotrophin receptor by alpha-secretase and gamma-secretase requires specific receptor domains. J Biol Chem. 2005 Apr 15;280(15):14563–71.

152. Jung KM, Tan S, Landman N, Petrova K, Murray S, Lewis R, et al. Regulated intramembrane proteolysis of the p75 neurotrophin receptor modulates its association with the TrkA receptor. J Biol Chem. 2003 Oct 24;278(43):42161–9.

153. Matusica D, Skeldal S, Sykes AM, Palstra N, Sharma A, Coulson EJ. An intracellular domain fragment of the p75 neurotrophin receptor (p75(NTR)) enhances tropomyosin receptor kinase A (TrkA) receptor function. J Biol Chem. 2013 Apr 19;288(16):11144–54.

154. Bao X, Shi J, Xie F, Liu Z, Yu J, Chen W, et al. Proteolytic Release of the p75NTR Intracellular Domain by ADAM10 Promotes Metastasis and Resistance to Anoikis. Cancer Res. 2018 01;78(9):2262–76.

155. Skeldal S, Matusica D, Nykjaer A, Coulson EJ. Proteolytic processing of the p75 neurotrophin receptor: A prerequisite for signalling?: Neuronal life, growth and death signalling are crucially regulated by intra-membrane proteolysis and trafficking of p75(NTR). BioEssays News Rev Mol Cell Dev Biol. 2011 Aug;33(8):614–25.

156. Pathak A, Stanley EM, Hickman FE, Wallace N, Brewer B, Li D, et al. Retrograde Degenerative Signaling Mediated by the p75 Neurotrophin Receptor Requires p150Glued Deacetylation by Axonal HDAC1. Dev Cell. 2018 06;46(3):376-387.e7.

157. Waterman-Storer CM, Karki S, Holzbaur EL. The p150Glued component of the dynactin complex binds to both microtubules and the actin-related protein centractin (Arp-1). Proc Natl Acad Sci U S A. 1995 Feb 28;92(5):1634–8.

158. Vaughan KT, Vallee RB. Cytoplasmic dynein binds dynactin through a direct interaction between the intermediate chains and p150Glued. J Cell Biol. 1995 Dec;131(6 Pt 1):1507–16.

159. Simon DJ, Pitts J, Hertz NT, Yang J, Yamagishi Y, Olsen O, et al. Axon Degeneration Gated by Retrograde Activation of Somatic Pro-apoptotic Signaling. Cell. 2016 Feb 25;164(5):1031–45.

160. Frade JM. Nuclear translocation of the p75 neurotrophin receptor cytoplasmic domain in response to neurotrophin binding. J Neurosci Off J Soc Neurosci. 2005 Feb 9;25(6):1407–11.

161. Provenzano MJ, Minner SA, Zander K, Clark JJ, Kane CJ, Green SH, et al. p75(NTR) expression and nuclear localization of p75(NTR) intracellular domain in spiral ganglion Schwann cells following deafness correlate with cell proliferation. Mol Cell Neurosci. 2011 Aug;47(4):306–15.

162. Parkhurst CN, Zampieri N, Chao MV. Nuclear localization of the p75 neurotrophin receptor intracellular domain. J Biol Chem. 2010 Feb 19;285(8):5361–8.

163. Wang L, Rahn JJ, Lun X, Sun B, Kelly JJP, Weiss S, et al. Gamma-secretase represents a therapeutic target for the treatment of invasive glioma mediated by the p75 neurotrophin receptor. PLoS Biol. 2008 Nov 25;6(11):e289.

164. Wang X, Cui M, Wang L, Chen X, Xin P. Inhibition of neurotrophin receptor p75 intramembran proteolysis by gamma-secretase inhibitor reduces medulloblastoma spinal metastasis. Biochem Biophys Res Commun. 2010 Dec 17;403(3–4):264–9.

165. Forsyth PA, Krishna N, Lawn S, Valadez JG, Qu X, Fenstermacher DA, et al. p75 neurotrophin receptor cleavage by α- and γ-secretases is required for neurotrophin-mediated proliferation of brain tumor-initiating cells. J Biol Chem. 2014 Mar 21;289(12):8067–85.

166. Berghoff J, Jaisimha AV, Duggan S, MacSharry J, McCarthy JV. Gamma-secretase-independent role for cadherin-11 in neurotrophin receptor p75 (p75(NTR)) mediated glioblastoma cell migration. Mol Cell Neurosci. 2015 Nov;69:41–53.

167. Urra S, Escudero CA, Ramos P, Lisbona F, Allende E, Covarrubias P, et al. TrkA receptor activation by nerve growth factor induces shedding of the p75 neurotrophin receptor followed by endosomal gamma-secretase-mediated release of the p75 intracellular domain. J Biol Chem. 2007 Mar 9;282(10):7606–15.

168. Kenchappa RS, Tep C, Korade Z, Urra S, Bronfman FC, Yoon SO, et al. p75 neurotrophin receptor-mediated apoptosis in sympathetic neurons involves a biphasic activation of JNK and up-regulation of tumor necrosis factor-alpha-converting enzyme/ADAM17. J Biol Chem. 2010 Jun 25;285(26):20358–68.

169. Oakley FD, Abbott D, Li Q, Engelhardt JF. Signaling components of redox active endosomes: the redoxosomes. Antioxid Redox Signal. 2009 Jun;11(6):1313–33.

170. Barrett GL, Bartlett PF. The p75 nerve growth factor receptor mediates survival or death depending on the stage of sensory neuron development. Proc Natl Acad Sci U S A. 1994 Jul 5;91(14):6501–5.

171. Rydén M, Hempstead B, Ibáñez CF. Differential modulation of neuron survival during development by nerve growth factor binding to the p75 neurotrophin receptor. J Biol Chem. 1997 Jun 27;272(26):16322–8.

172. Walsh GS, Krol KM, Kawaja MD. Absence of the p75 neurotrophin receptor alters the pattern of sympathosensory sprouting in the trigeminal ganglia of mice overexpressing nerve growth factor. J Neurosci Off J Soc Neurosci. 1999 Jan 1;19(1):258–73.

173. Wiese S, Metzger F, Holtmann B, Sendtner M. The role of p75NTR in modulating neurotrophin survival effects in developing motoneurons. Eur J Neurosci. 1999 May;11(5):1668–76.

174. Poser R, Dokter M, von Bohlen Und Halbach V, Berger SM, Busch R, Baldus M, et al. Impact of a deletion of the full-length and short isoform of p75NTR on cholinergic innervation and the population of postmitotic doublecortin positive cells in the dentate gyrus. Front Neuroanat. 2015;9:63.

175. Puschban Z, Sah A, Grutsch I, Singewald N, Dechant G. Reduced Anxiety-Like Behavior and Altered Hippocampal Morphology in Female p75NTR(exon IV-/-) Mice. Front Behav Neurosci. 2016;10:103.

176. Hickman FE, Stanley EM, Carter BD. Neurotrophin Responsiveness of Sympathetic Neurons Is Regulated by Rapid Mobilization of the p75 Receptor to the Cell Surface through TrkA Activation of Arf6. J Neurosci Off J Soc Neurosci. 2018 13;38(24):5606–19.

177. Cheng I, Jin L, Rose LC, Deppmann CD. Temporally restricted death and the role of p75NTR as a survival receptor in the developing sensory nervous system. Dev Neurobiol. 2018 Jul;78(7):701–17.

178. Meier S, Alfonsi F, Kurniawan ND, Milne MR, Kasherman MA, Delogu A, et al. The p75 neurotrophin receptor is required for the survival of neuronal progenitors and normal formation of the basal forebrain, striatum, thalamus and neocortex. Dev Camb Engl. 2019 Sep 18;146(18).

179. Kozma R, Sarner S, Ahmed S, Lim L. Rho family GTPases and neuronal growth cone remodelling: relationship between increased complexity induced by Cdc42Hs, Rac1, and acetylcholine and collapse induced by RhoA and lysophosphatidic acid. Mol Cell Biol. 1997 Mar;17(3):1201–11.

180. Walsh GS, Krol KM, Crutcher KA, Kawaja MD. Enhanced neurotrophin-induced axon growth in myelinated portions of the CNS in mice lacking the p75 neurotrophin receptor. J Neurosci Off J Soc Neurosci. 1999 May 15;19(10):4155–68.

181. Yamashita T, Tucker KL, Barde YA. Neurotrophin binding to the p75 receptor modulates Rho activity and axonal outgrowth. Neuron. 1999 Nov;24(3):585–93.

182. Bentley CA, Lee KF. p75 is important for axon growth and schwann cell migration during development. J Neurosci Off J Soc Neurosci. 2000 Oct 15;20(20):7706–15.

183. Yasui H, Katoh H, Yamaguchi Y, Aoki J, Fujita H, Mori K, et al. Differential responses to nerve growth factor and epidermal growth factor in neurite outgrowth of PC12 cells are determined by Rac1 activation systems. J Biol Chem. 2001 May 4;276(18):15298–305.

184. Estrach S, Schmidt S, Diriong S, Penna A, Blangy A, Fort P, et al. The Human Rho-GEF trio and its target GTPase RhoG are involved in the NGF pathway, leading to neurite outgrowth. Curr Biol CB. 2002 Feb 19;12(4):307–12.

185. Gehler S, Gallo G, Veien E, Letourneau PC. p75 neurotrophin receptor signaling regulates growth cone filopodial dynamics through modulating RhoA activity. J Neurosci Off J Soc Neurosci. 2004 May 5;24(18):4363–72.

186. Gehler S, Shaw AE, Sarmiere PD, Bamburg JR, Letourneau PC. Brain-derived neurotrophic factor regulation of retinal growth cone filopodial dynamics is mediated through actin depolymerizing factor/cofilin. J Neurosci Off J Soc Neurosci. 2004 Nov 24;24(47):10741–9.

187. Neubrand VE, Thomas C, Schmidt S, Debant A, Schiavo G. Kidins220/ARMS regulates Rac1-dependent neurite outgrowth by direct interaction with the RhoGEF Trio. J Cell Sci. 2010 Jun 15;123(Pt 12):2111–23.

188. Deinhardt K, Kim T, Spellman DS, Mains RE, Eipper BA, Neubert TA, et al. Neuronal growth cone retraction relies on proneurotrophin receptor signaling through Rac. Sci Signal. 2011 Dec 6;4(202):ra82.

189. Spillane M, Ketschek A, Donnelly CJ, Pacheco A, Twiss JL, Gallo G. Nerve growth factor-induced formation of axonal filopodia and collateral branches involves the intra-axonal synthesis of regulators of the actin-nucleating Arp2/3 complex. J Neurosci Off J Soc Neurosci. 2012 Dec 5;32(49):17671–89.

190. Howard L, Wyatt S, Nagappan G, Davies AM. ProNGF promotes neurite growth from a subset of NGF-dependent neurons by a p75NTR-dependent mechanism. Dev Camb Engl. 2013 May;140(10):2108–17.

191. Negrini S, D'Alessandro R, Meldolesi J. NGF signaling in PC12 cells: the cooperation of p75(NTR) with TrkA is needed for the activation of both mTORC2 and the PI3K signalling cascade. Biol Open. 2013 Aug 15;2(8):855–66.

192. Ito H, Morishita R, Iwamoto I, Mizuno M, Nagata K ichi. MAGI-1 acts as a scaffolding molecule for NGF receptor-mediated signaling pathway. Biochim Biophys Acta. 2013 Oct;1833(10):2302–10.

193. Lotta LT, Conrad K, Cory-Slechta D, Schor NF. Cerebellar Purkinje cell p75 neurotrophin receptor and autistic behavior. Transl Psychiatry. 2014 Jul 29;4:e416.

194. Ben-Zvi A, Ben-Gigi L, Klein H, Behar O. Modulation of semaphorin3A activity by p75 neurotrophin receptor influences peripheral axon patterning. J Neurosci Off J Soc Neurosci. 2007 Nov 21;27(47):13000–11.

195. Lim YS, McLaughlin T, Sung TC, Santiago A, Lee KF, O'Leary DDM. p75(NTR) mediates ephrin-A reverse signaling required for axon repulsion and mapping. Neuron. 2008 Sep 11;59(5):746–58.

196. Anton ES, Weskamp G, Reichardt LF, Matthew WD. Nerve growth factor and its low-affinity receptor promote Schwann cell migration. Proc Natl Acad Sci U S A. 1994 Mar 29;91(7):2795–9.

197. Yamauchi J, Chan JR, Shooter EM. Neurotrophins regulate Schwann cell migration by activating divergent signaling pathways dependent on Rho GTPases. Proc Natl Acad Sci U S A. 2004 Jun 8;101(23):8774–9.

198. Chan JR, Jolicoeur C, Yamauchi J, Elliott J, Fawcett JP, Ng BK, et al. The polarity protein Par-3 directly interacts with p75NTR to regulate myelination. Science. 2006 Nov 3;314(5800):832–6.

199. Tep C, Kim ML, Opincariu LI, Limpert AS, Chan JR, Appel B, et al. Brain-derived neurotrophic factor (BDNF) induces polarized signaling of small GTPase (Rac1) protein at the onset of Schwann cell myelination through partitioning-defective 3 (Par3) protein. J Biol Chem. 2012 Jan 6;287(2):1600–8.

200. Guo J, Wang J, Liang C, Yan J, Wang Y, Liu G, et al. proNGF inhibits proliferation and oligodendrogenesis of postnatal hippocampal neural stem/progenitor cells through p75NTR in vitro. Stem Cell Res. 2013 Sep;11(2):874–87.

201. Xu ZQ, Sun Y, Li HY, Lim Y, Zhong JH, Zhou XF. Endogenous proBDNF is a negative regulator of migration of cerebellar granule cells in neonatal mice. Eur J Neurosci. 2011 Apr;33(8):1376–84.

202. Zanin JP, Verpeut JL, Li Y, Shiflett MW, Wang SSH, Santhakumar V, et al. The p75NTR Influences Cerebellar Circuit Development and Adult Behavior via Regulation of Cell Cycle Duration of Granule Cell Progenitors. J Neurosci Off J Soc Neurosci. 2019 Nov 13;39(46):9119–29.

203. Baho E, Chattopadhyaya B, Lavertu-Jolin M, Mazziotti R, Awad PN, Chehrazi P, et al. p75 Neurotrophin Receptor Activation Regulates the Timing of the Maturation of Cortical Parvalbumin Interneuron Connectivity and Promotes Juvenile-like Plasticity in Adult Visual Cortex. J Neurosci Off J Soc Neurosci. 2019 Jun 5;39(23):4489–510.

204. Pérez V, Bermedo-Garcia F, Zelada D, Court FA, Pérez MÁ, Fuenzalida M, et al. The p75NTR neurotrophin receptor is required to organize the mature neuromuscular synapse by regulating synaptic vesicle availability. Acta Neuropathol Commun. 2019 12;7(1):147.

205. Catts VS, Al-Menhali N, Burne THJ, Colditz MJ, Coulson EJ. The p75 neurotrophin receptor regulates hippocampal neurogenesis and related behaviours. Eur J Neurosci. 2008 Sep;28(5):883–92.

206. Zuccaro E, Bergami M, Vignoli B, Bony G, Pierchala BA, Santi S, et al. Polarized expression of p75(NTR) specifies axons during development and adult neurogenesis. Cell Rep. 2014 Apr 10;7(1):138–52.

207. Yeo TT, Chua-Couzens J, Butcher LL, Bredesen DE, Cooper JD, Valletta JS, et al. Absence of p75NTR causes increased basal forebrain cholinergic neuron size, choline acetyltransferase activity, and target innervation. J Neurosci Off J Soc Neurosci. 1997 Oct 15;17(20):7594–605.

208. Bamji SX, Majdan M, Pozniak CD, Belliveau DJ, Aloyz R, Kohn J, et al. The p75 neurotrophin receptor mediates neuronal apoptosis and is essential for naturally occurring sympathetic neuron death. J Cell Biol. 1998 Feb 23;140(4):911–23.

209. Frade JM, Barde YA. Genetic evidence for cell death mediated by nerve growth factor and the neurotrophin receptor p75 in the developing mouse retina and spinal cord. Dev Camb Engl. 1999 Feb;126(4):683–90.

210. Friedman WJ. Neurotrophins induce death of hippocampal neurons via the p75 receptor. J Neurosci Off J Soc Neurosci. 2000 Sep 1;20(17):6340–6.

211. Harrington AW, Kim JY, Yoon SO. Activation of Rac GTPase by p75 is necessary for c-jun N-terminal kinase-mediated apoptosis. J Neurosci Off J Soc Neurosci. 2002 Jan 1;22(1):156–66.

212. Florez-McClure ML, Linseman DA, Chu CT, Barker PA, Bouchard RJ, Le SS, et al. The p75 neurotrophin receptor can induce autophagy and death of cerebellar Purkinje neurons. J Neurosci Off J Soc Neurosci. 2004 May 12;24(19):4498–509.

213. Teng HK, Teng KK, Lee R, Wright S, Tevar S, Almeida RD, et al. ProBDNF induces neuronal apoptosis via activation of a receptor complex of p75NTR and sortilin. J Neurosci Off J Soc Neurosci. 2005 Jun 1;25(22):5455–63.

214. Volosin M, Song W, Almeida RD, Kaplan DR, Hempstead BL, Friedman WJ. Interaction of survival and death signaling in basal forebrain neurons: roles of neurotrophins and proneurotrophins. J Neurosci Off J Soc Neurosci. 2006 Jul 19;26(29):7756–66.

215. Volosin M, Trotter C, Cragnolini A, Kenchappa RS, Light M, Hempstead BL, et al. Induction of proneurotrophins and activation of p75NTR-mediated apoptosis via neurotrophin receptor-interacting factor in hippocampal neurons after seizures. J Neurosci Off J Soc Neurosci. 2008 Sep 24;28(39):9870–9.

216. Park KJ, Grosso CA, Aubert I, Kaplan DR, Miller FD. p75NTR-dependent, myelin-mediated axonal degeneration regulates neural connectivity in the adult brain. Nat Neurosci. 2010 May;13(5):559–66.

217. Sharma N, Deppmann CD, Harrington AW, St Hillaire C, Chen ZY, Lee FS, et al. Long-distance control of synapse assembly by target-derived NGF. Neuron. 2010 Aug 12;67(3):422–34.

218. Song W, Volosin M, Cragnolini AB, Hempstead BL, Friedman WJ. ProNGF induces PTEN via p75NTR to suppress Trk-mediated survival signaling in brain neurons. J Neurosci Off J Soc Neurosci. 2010 Nov 17;30(46):15608–15.

219. Sun Y, Lim Y, Li F, Liu S, Lu JJ, Haberberger R, et al. ProBDNF collapses neurite outgrowth of primary neurons by activating RhoA. PloS One. 2012;7(4):e35883.

220. Boskovic Z, Alfonsi F, Rumballe BA, Fonseka S, Windels F, Coulson EJ. The role of p75NTR in cholinergic basal forebrain structure and function. J Neurosci Off J Soc Neurosci. 2014 Sep 24;34(39):13033–8.

221. Von Bohlen Und Halbach V, Von Bohlen Und Halbach O. Deletion of p75NTR enhances the cholinergic innervation pattern of the visual cortex. Vis Neurosci. 2016;33:E012.

222. Courter LA, Shaffo FC, Ghogha A, Parrish DJ, Lorentz CU, Habecker BA, et al. BMP7-induced dendritic growth in sympathetic neurons requires p75(NTR) signaling. Dev Neurobiol. 2016;76(9):1003–13.

223. Blanquie O, Liebmann L, Hübner CA, Luhmann HJ, Sinning A. NKCC1-Mediated GABAergic Signaling Promotes Postnatal Cell Death in Neocortical Cajal-Retzius Cells. Cereb Cortex N Y N 1991. 2017 01;27(2):1644–59.

224. Greenwood SG, Montroull L, Volosin M, Scharfman HE, Teng KK, Light M, et al. A Novel Neuroprotective Mechanism for Lithium That Prevents Association of the p75NTR-Sortilin Receptor Complex and Attenuates proNGF-Induced Neuronal Death In Vitro and In Vivo. eNeuro. 2018 Feb;5(1).

225. Kisiswa L, Fernández-Suárez D, Sergaki MC, Ibáñez CF. RIP2 Gates TRAF6 Interaction with Death Receptor p75NTR to Regulate Cerebellar Granule Neuron Survival. Cell Rep. 2018 24;24(4):1013–24.

226. Riffault B, Kourdougli N, Dumon C, Ferrand N, Buhler E, Schaller F, et al. Pro-Brain-Derived Neurotrophic Factor (proBDNF)-Mediated p75NTR Activation Promotes Depolarizing Actions of GABA and Increases Susceptibility to Epileptic Seizures. Cereb Cortex N Y N 1991. 2018 01;28(2):510–27.

227. Reichardt LF. Neurotrophin-regulated signalling pathways. Philos Trans R Soc Lond B Biol Sci. 2006 Sep 29;361(1473):1545–64.

228. Schor NF. The p75 neurotrophin receptor in human development and disease. Prog Neurobiol. 2005 Oct;77(3):201–14.

229. Omotade OF, Pollitt SL, Zheng JQ. Actin-based growth cone motility and guidance. Mol Cell Neurosci. 2017;84:4–10.

230. Schecterson LC, Bothwell M. An all-purpose tool for axon guidance. Sci Signal. 2008 Nov 25;1(47):pe50.

231. Ozdinler PH, Ulupinar E, Erzurumlu RS. Dose and age-dependent axonal responses of embryonic trigeminal neurons to localized NGF via p75NTR receptor. J Neurobiol. 2005 Feb 5;62(2):189–206.

232. Naska S, Lin DC, Miller FD, Kaplan DR. p75NTR is an obligate signaling receptor required for cues that cause sympathetic neuron growth cone collapse. Mol Cell Neurosci. 2010 Oct;45(2):108–20.

233. Marler KJM, Poopalasundaram S, Broom ER, Wentzel C, Drescher U. Pro-neurotrophins secreted from retinal ganglion cell axons are necessary for ephrinA-p75NTR-mediated axon guidance. Neural Develop. 2010 Nov 2;5:30.

234. Uesugi N, Kimura Y, Yamashita T. Suppression of the p75 receptor signal attenuates the effect of ephrin-B3 and promotes axonal regeneration of the injured optic nerve. Cell Death Dis. 2013 Mar 21;4:e557.

235. Kania A, Klein R. Mechanisms of ephrin-Eph signalling in development, physiology and disease. Nat Rev Mol Cell Biol. 2016 Apr;17(4):240–56.

236. Flanagan JG. Neural map specification by gradients. Curr Opin Neurobiol. 2006 Feb;16(1):59–66.

237. Alto LT, Terman JR. Semaphorins and their Signaling Mechanisms. Methods Mol Biol Clifton NJ. 2017;1493:1–25.

238. Pramanik S, Sulistio YA, Heese K. Neurotrophin Signaling and Stem Cells-Implications for Neurodegenerative Diseases and Stem Cell Therapy. Mol Neurobiol. 2017;54(9):7401–59.

239. Borghesani PR, Peyrin JM, Klein R, Rubin J, Carter AR, Schwartz PM, et al. BDNF stimulates migration of cerebellar granule cells. Dev Camb Engl. 2002 Mar;129(6):1435–42.

240. Hu H, Gan J, Jonas P. Interneurons. Fast-spiking, parvalbumin^{+} GABAergic interneurons: from cellular design to microcircuit function. Science. 2014 Aug 1;345(6196):1255263.

241. Xue L, Igaki T, Kuranaga E, Kanda H, Miura M, Xu T. Tumor suppressor CYLD regulates JNK-induced cell death in Drosophila. Dev Cell. 2007 Sep;13(3):446–54.

242. Keller LC, Cheng L, Locke CJ, Müller M, Fetter RD, Davis GW. Glial-derived prodegenerative signaling in the Drosophila neuromuscular system. Neuron. 2011 Dec 8;72(5):760–75.

243. Johnstone AD, de Léon A, Unsain N, Gibon J, Barker PA. Developmental Axon Degeneration Requires TRPV1-Dependent Ca2+ Influx. eNeuro. 2019 Feb;6(1).

244. Unsain N, Barker PA. New Views on the Misconstrued: Executioner Caspases and Their Diverse Non-apoptotic Roles. Neuron. 2015 Nov 4;88(3):461–74.

245. Unsain N, Higgins JM, Parker KN, Johnstone AD, Barker PA. XIAP regulates caspase activity in degenerating axons. Cell Rep. 2013 Aug 29;4(4):751–63.

246. Troy CM, Friedman JE, Friedman WJ. Mechanisms of p75-mediated death of hippocampal neurons. Role of caspases. J Biol Chem. 2002 Sep 13;277(37):34295–302.

247. Anstötz M, Quattrocolo G, Maccaferri G. Cajal-Retzius cells and GABAergic interneurons of the developing hippocampus: Close electrophysiological encounters of the third kind. Brain Res. 2018 15;1697:124–33.

248. Sotthibundhu A, Sykes AM, Fox B, Underwood CK, Thangnipon W, Coulson EJ. Beta-amyloid(1-42) induces neuronal death through the p75 neurotrophin receptor. J Neurosci Off J Soc Neurosci. 2008 Apr 9;28(15):3941–6.

249. Jiao SS, Bu XL, Liu YH, Wang QH, Liu CH, Yao XQ, et al. Differential levels of p75NTR ectodomain in CSF and blood in patients with Alzheimer's disease: a novel diagnostic marker. Transl Psychiatry. 2015 Oct 6;5:e650.

250. Yao XQ, Jiao SS, Saadipour K, Zeng F, Wang QH, Zhu C, et al. p75NTR ectodomain is a physiological neuroprotective molecule against amyloid-beta toxicity in the brain of Alzheimer's disease. Mol Psychiatry. 2015 Nov;20(11):1301–10.

251. Bobkova N, Vorobyov V, Medvinskaya N, Nesterova I, Tatarnikova O, Nekrasov P, et al. Immunization Against Specific Fragments of Neurotrophin p75 Receptor Protects Forebrain Cholinergic Neurons in the Olfactory Bulbectomized Mice. J Alzheimers Dis JAD. 2016 06;53(1):289–301.

252. Wang QH, Wang YR, Zhang T, Jiao SS, Liu YH, Zeng F, et al. Intramuscular delivery of p75NTR ectodomain by an AAV vector attenuates cognitive deficits and Alzheimer's disease-like pathologies in APP/PS1 transgenic mice. J Neurochem. 2016;138(1):163–73.

253. Chen J, Zhang T, Jiao S, Zhou X, Zhong J, Wang Y, et al. proBDNF Accelerates Brain Amyloid-β Deposition and Learning and Memory Impairment in APPswePS1dE9 Transgenic Mice. J Alzheimers Dis JAD. 2017;59(3):941–9.

254. May LM, Anggono V, Gooch HM, Jang SE, Matusica D, Kerbler GM, et al. G-Protein-Coupled Inwardly Rectifying Potassium (GIRK) Channel Activation by the p75 Neurotrophin Receptor Is Required for Amyloid β Toxicity. Front Neurosci. 2017;11:455.

255. Shen LL, Mañucat-Tan NB, Gao SH, Li WW, Zeng F, Zhu C, et al. The ProNGF/p75NTR pathway induces tau pathology and is a therapeutic target for FTLD-tau. Mol Psychiatry. 2018;23(8):1813–24.

256. Wang YR, Wang J, Liu YH, Hu GL, Gao CY, Wang YJ, et al. Cysteine-Rich Repeat Domains 2 and 4 are Amyloid-β Binding Domains of Neurotrophin Receptor p75NTR and Potential Targets to Block Amyloid-β Neurotoxicity. J Alzheimers Dis JAD. 2018;63(1):139–47.

257. Fahnestock M, Shekari A. ProNGF and Neurodegeneration in Alzheimer's Disease. Front Neurosci. 2019;13:129.

258. Sycheva M, Sustarich J, Zhang Y, Selvaraju V, Geetha T, Gearing M, et al. Pro-Nerve Growth Factor Induces Activation of RhoA Kinase and Neuronal Cell Death. Brain Sci. 2019 Aug 19;9(8).

259. Wang Y, Tang H, Yang C, Zhao H, Jian C. Involvement of p75NTR in the effects of Aβ on L-type Ca2+ channel in cultured neuronal networks. Life Sci. 2020 Feb 15;243:117293.

260. Montroull LE, Danelon V, Cragnolini AB, Mascó DH. Loss of TrkB Signaling Due to Status Epilepticus Induces a proBDNF-Dependent Cell Death. Front Cell Neurosci. 2019;13:4.

261. Park JA, Lee JY, Sato TA, Koh JY. Co-induction of p75NTR and p75NTR-associated death executor in neurons after zinc exposure in cortical culture or transient ischemia in the rat. J Neurosci Off J Soc Neurosci. 2000 Dec 15;20(24):9096–103.

262. Harrington AW, Leiner B, Blechschmitt C, Arevalo JC, Lee R, Mörl K, et al. Secreted proNGF is a pathophysiological death-inducing ligand after adult CNS injury. Proc Natl Acad Sci U S A. 2004 Apr 20;101(16):6226–30.

263. Sebastiani A, Gölz C, Werner C, Schäfer MKE, Engelhard K, Thal SC. Proneurotrophin Binding to P75 Neurotrophin Receptor (P75ntr) Is Essential for Brain Lesion Formation and Functional Impairment after Experimental Traumatic Brain Injury. J Neurotrauma. 2015 Oct 15;32(20):1599–607.

264. Lee S, Mattingly A, Lin A, Sacramento J, Mannent L, Castel MN, et al. A novel antagonist of p75NTR reduces peripheral expansion and CNS trafficking of pro-inflammatory monocytes and spares function after traumatic brain injury. J Neuroinflammation. 2016 Apr 22;13(1):88.

265. Delbary-Gossart S, Lee S, Baroni M, Lamarche I, Arnone M, Canolle B, et al. A novel inhibitor of p75-neurotrophin receptor improves functional outcomes in two models of traumatic brain injury. Brain J Neurol. 2016;139(Pt 6):1762–82.

266. Alder J, Fujioka W, Giarratana A, Wissocki J, Thakkar K, Vuong P, et al. Genetic and pharmacological intervention of the p75NTR pathway alters morphological and behavioural recovery following traumatic brain injury in mice. Brain Inj. 2016;30(1):48–65.

267. Ding X, Wu HH, Ji SJ, Cai S, Dai PW, Xu ML, et al. The p75 neurotrophin receptor regulates cranial irradiation-induced hippocampus-dependent cognitive dysfunction. Oncotarget. 2017 Jun 20;8(25):40544–57.

268. Zhou T, Wang H, Shen J, Li W, Cao M, Hong Y, et al. The p35/CDK5 signaling is regulated by p75NTR in neuronal apoptosis after intracerebral hemorrhage. J Cell Physiol. 2019 Feb 15;

269. Choucry AM, Al-Shorbagy MY, Attia AS, El-Abhar HS. Pharmacological Manipulation of Trk, p75NTR, and NGF Balance Restores Memory Deficit in Global Ischemia/Reperfusion Model in Rats. J Mol Neurosci MN. 2019 May;68(1):78–90.

270. Beattie MS, Harrington AW, Lee R, Kim JY, Boyce SL, Longo FM, et al. ProNGF induces p75-mediated death of oligodendrocytes following spinal cord injury. Neuron. 2002 Oct 24;36(3):375–86.

271. Dubreuil CI, Winton MJ, McKerracher L. Rho activation patterns after spinal cord injury and the role of activated Rho in apoptosis in the central nervous system. J Cell Biol. 2003 Jul 21;162(2):233–43.

272. Wang YT, Lu XM, Zhu F, Huang P, Yu Y, Long ZY, et al. Ameliorative Effects of p75NTR-ED-Fc on Axonal Regeneration and Functional Recovery in Spinal Cord-Injured Rats. Mol Neurobiol. 2015 Dec;52(3):1821–34.

273. Lebrun-Julien F, Duplan L, Pernet V, Osswald I, Sapieha P, Bourgeois P, et al. Excitotoxic death of retinal neurons in vivo occurs via a non-cell-autonomous mechanism. J Neurosci Off J Soc Neurosci. 2009 Apr 29;29(17):5536–45.

274. Lebrun-Julien F, Bertrand MJ, De Backer O, Stellwagen D, Morales CR, Di Polo A, et al. ProNGF induces TNFalpha-dependent death of retinal ganglion cells through a p75NTR non-cell-autonomous signaling pathway. Proc Natl Acad Sci U S A. 2010 Feb 23;107(8):3817–22.

275. Barcelona PF, Sitaras N, Galan A, Esquiva G, Jmaeff S, Jian Y, et al. p75NTR and Its Ligand ProNGF Activate Paracrine Mechanisms Etiological to the Vascular, Inflammatory, and Neurodegenerative Pathologies of Diabetic Retinopathy. J Neurosci Off J Soc Neurosci. 2016 24;36(34):8826–41.

276. Platón-Corchado M, Barcelona PF, Jmaeff S, Marchena M, Hernández-Pinto AM, Hernández-Sánchez C, et al. p75NTR antagonists attenuate photoreceptor cell loss in murine models of retinitis pigmentosa. Cell Death Dis. 2017 13;8(7):e2922.

277. Elshaer SL, El-Remessy AB. Deletion of p75NTR prevents vaso-obliteration and retinal neovascularization via activation of Trk- A receptor in ischemic retinopathy model. Sci Rep. 2018 21;8(1):12490.

278. Elshaer SL, Alwhaibi A, Mohamed R, Lemtalsi T, Coucha M, Longo FM, et al. Modulation of the p75 neurotrophin receptor using LM11A-31 prevents diabetes-induced retinal vascular permeability in mice via inhibition of inflammation and the RhoA kinase pathway. Diabetologia. 2019;62(8):1488–500.

279. Miguez A, García-Díaz Barriga G, Brito V, Straccia M, Giralt A, Ginés S, et al. Fingolimod (FTY720) enhances hippocampal synaptic plasticity and memory in Huntington's disease by preventing p75NTR up-regulation and astrocyte-mediated inflammation. Hum Mol Genet. 2015 Sep 1;24(17):4958–70.

280. Brito V, Ginés S. p75NTR in Huntington's disease: beyond the basal ganglia. Oncotarget. 2016 Jan 5;7(1):1–2.

281. Simmons DA, Belichenko NP, Ford EC, Semaan S, Monbureau M, Aiyaswamy S, et al. A small molecule p75NTR ligand normalizes signalling and reduces Huntington's disease phenotypes in R6/2 and BACHD mice. Hum Mol Genet. 2016 15;25(22):4920–38.

282. Suelves N, Miguez A, López-Benito S, Barriga GGD, Giralt A, Alvarez-Periel E, et al. Early Downregulation of p75NTR by Genetic and Pharmacological Approaches Delays the Onset of Motor Deficits and Striatal Dysfunction in Huntington's Disease Mice. Mol Neurobiol. 2019 Feb;56(2):935–53.

283. Gonsalvez DG, Tran G, Fletcher JL, Hughes RA, Hodgkinson S, Wood RJ, et al. A Brain-Derived Neurotrophic Factor-Based p75NTR Peptide Mimetic Ameliorates Experimental Autoimmune Neuritis Induced Axonal Pathology and Demyelination. eNeuro. 2017 Jun;4(3).

284. Theotokis P, Grigoriadis N. p75NTR and TROY: Uncharted Roles of Nogo Receptor Complex in Experimental Autoimmune Encephalomyelitis. Mol Neurobiol. 2018 Aug;55(8):6329–36.

285. Delivanoglou N, Boziki M, Theotokis P, Kesidou E, Touloumi O, Dafi N, et al. Spatio-temporal expression profile of NGF and the two-receptor system, TrkA and p75NTR, in experimental autoimmune encephalomyelitis. J Neuroinflammation. 2020 Jan 29;17(1):41.

286. Bachis A, Wenzel E, Boelk A, Becker J, Mocchetti I. The neurotrophin receptor p75 mediates gp120-induced loss of synaptic spines in aging mice. Neurobiol Aging. 2016;46:160–8.

287. Düsedau HP, Kleveman J, Figueiredo CA, Biswas A, Steffen J, Kliche S, et al. p75NTR regulates brain mononuclear cell function and neuronal structure in Toxoplasma infection-induced neuroinflammation. Glia. 2019;67(1):193–211.

288. Speidell A, Asuni GP, Avdoshina V, Scognamiglio S, Forcelli P, Mocchetti I. Reversal of Cognitive Impairment in gp120 Transgenic Mice by the Removal of the p75 Neurotrophin Receptor. Front Cell Neurosci. 2019;13:398.

289. Selkoe DJ, Hardy J. The amyloid hypothesis of Alzheimer's disease at 25 years. EMBO Mol Med. 2016;8(6):595–608.

290. Riek R, Eisenberg DS. The activities of amyloids from a structural perspective. Nature. 2016 10;539(7628):227–35.

291. Iadanza MG, Jackson MP, Hewitt EW, Ranson NA, Radford SE. A new era for understanding amyloid structures and disease. Nat Rev Mol Cell Biol. 2018;19(12):755–73.

292. Reiss AB, Arain HA, Stecker MM, Siegart NM, Kasselman LJ. Amyloid toxicity in Alzheimer's disease. Rev Neurosci. 2018 28;29(6):613–27.

293. Jaroudi W, Garami J, Garrido S, Hornberger M, Keri S, Moustafa AA. Factors underlying cognitive decline in old age and Alzheimer's disease: the role of the hippocampus. Rev Neurosci. 2017 26;28(7):705–14.

294. Yaar M, Zhai S, Pilch PF, Doyle SM, Eisenhauer PB, Fine RE, et al. Binding of beta-amyloid to the p75 neurotrophin receptor induces apoptosis. A possible mechanism for Alzheimer's disease. J Clin Invest. 1997 Nov 1;100(9):2333–40.

295. Rossner S, Ueberham U, Schliebs R, Perez-Polo JR, Bigl V. The regulation of amyloid precursor protein metabolism by cholinergic mechanisms and neurotrophin receptor signaling. Prog Neurobiol. 1998 Dec;56(5):541–69.

296. Jaffar S, Counts SE, Ma SY, Dadko E, Gordon MN, Morgan D, et al. Neuropathology of mice carrying mutant APP(swe) and/or PS1(M146L) transgenes: alterations in the p75(NTR) cholinergic basal forebrain septohippocampal pathway. Exp Neurol. 2001 Aug;170(2):227–43.

297. Yaar M, Zhai S, Fine RE, Eisenhauer PB, Arble BL, Stewart KB, et al. Amyloid beta binds trimers as well as monomers of the 75-kDa neurotrophin receptor and activates receptor signaling. J Biol Chem. 2002 Mar 8;277(10):7720–5.

298. Perini G, Della-Bianca V, Politi V, Della Valle G, Dal-Pra I, Rossi F, et al. Role of p75 neurotrophin receptor in the neurotoxicity by beta-amyloid peptides and synergistic effect of inflammatory cytokines. J Exp Med. 2002 Apr 1;195(7):907–18.

299. Yi C, Goh KY, Wong LW, Ramanujan A, Tanaka K, Sajikumar S, et al. Inactive variants of death receptor p75NTR reduce Alzheimer's neuropathology by interfering with APP internalization. EMBO J. 2021 Jan 15;40(2):e104450.

300. Bartolomei F, Khalil M, Wendling F, Sontheimer A, Régis J, Ranjeva JP, et al. Entorhinal cortex involvement in human mesial temporal lobe epilepsy: an electrophysiologic and volumetric study. Epilepsia. 2005 May;46(5):677–87.

301. Mathern GW, Kuhlman PA, Mendoza D, Pretorius JK. Human fascia dentata anatomy and hippocampal neuron densities differ depending on the epileptic syndrome and age at first seizure. J Neuropathol Exp Neurol. 1997 Feb;56(2):199–212.

302. Curia G, Longo D, Biagini G, Jones RSG, Avoli M. The pilocarpine model of temporal lobe epilepsy. J Neurosci Methods. 2008 Jul 30;172(2):143–57.

303. VonDran MW, LaFrancois J, Padow VA, Friedman WJ, Scharfman HE, Milner TA, et al. p75NTR, but not proNGF, is upregulated following status epilepticus in mice. ASN Neuro. 2014;6(5).

304. Unsain N, Nuñez N, Anastasía A, Mascó DH. Status epilepticus induces a TrkB to p75 neurotrophin receptor switch and increases brain-derived neurotrophic factor interaction with p75 neurotrophin receptor: an initial event in neuronal injury induction. Neuroscience. 2008 Jun 26;154(3):978–93.

305. Sofroniew MV. Dissecting spinal cord regeneration. Nature. 2018;557(7705):343–50.

306. Lechner J, O'Leary OE, Stitt AW. The pathology associated with diabetic retinopathy. Vision Res. 2017;139:7–14.

307. McColgan P, Tabrizi SJ. Huntington's disease: a clinical review. Eur J Neurol. 2018;25(1):24–34.

308. Brito V, Puigdellívol M, Giralt A, del Toro D, Alberch J, Ginés S. Imbalance of p75(NTR)/TrkB protein expression in Huntington's disease: implication for neuroprotective therapies. Cell Death Dis. 2013 Apr 18;4:e595.

309. Brito V, Giralt A, Enriquez-Barreto L, Puigdellívol M, Suelves N, Zamora-Moratalla A, et al. Neurotrophin receptor p75(NTR) mediates Huntington's disease-associated synaptic and memory dysfunction. J Clin Invest. 2014 Oct;124(10):4411–28.

310. Plotkin JL, Day M, Peterson JD, Xie Z, Kress GJ, Rafalovich I, et al. Impaired TrkB receptor signaling underlies corticostriatal dysfunction in Huntington's disease. Neuron. 2014 Jul 2;83(1):178–88.

311. Dobson R, Giovannoni G. Multiple sclerosis - a review. Eur J Neurol. 2019;26(1):27–40.

312. Dowling P, Ming X, Raval S, Husar W, Casaccia-Bonnefil P, Chao M, et al. Up-regulated p75NTR neurotrophin receptor on glial cells in MS plaques. Neurology. 1999 Nov 10;53(8):1676–82.

313. Domeniconi M, Zampieri N, Spencer T, Hilaire M, Mellado W, Chao MV, et al. MAG induces regulated intramembrane proteolysis of the p75 neurotrophin receptor to inhibit neurite outgrowth. Neuron. 2005 Jun 16;46(6):849–55.

314. Yamashita T, Tohyama M. The p75 receptor acts as a displacement factor that releases Rho from Rho-GDI. Nat Neurosci. 2003 May;6(5):461–7.

315. Green MV, Raybuck JD, Zhang X, Wu MM, Thayer SA. Scaling Synapses in the Presence of HIV. Neurochem Res. 2019 Jan;44(1):234–46.

316. Rösch H, Schweigreiter R, Bonhoeffer T, Barde YA, Korte M. The neurotrophin receptor p75NTR modulates long-term depression and regulates the expression of AMPA receptor subunits in the hippocampus. Proc Natl Acad Sci U S A. 2005 May 17;102(20):7362–7.

317. Woo NH, Teng HK, Siao CJ, Chiaruttini C, Pang PT, Milner TA, et al. Activation of p75NTR by proBDNF facilitates hippocampal long-term depression. Nat Neurosci. 2005 Aug;8(8):1069–77.

318. Harward SC, Hedrick NG, Hall CE, Parra-Bueno P, Milner TA, Pan E, et al. Autocrine BDNF-TrkB signalling within a single dendritic spine. Nature. 2016 Oct 6;538(7623):99–103.

319. Hedrick NG, Harward SC, Hall CE, Murakoshi H, McNamara JO, Yasuda R. Rho GTPase complementation underlies BDNF-dependent homo- and heterosynaptic plasticity. Nature. 2016 Oct 6;538(7623):104–8.

320. Buhusi M, Etheredge C, Granholm AC, Buhusi CV. Increased Hippocampal ProBDNF Contributes to Memory Impairments in Aged Mice. Front Aging Neurosci. 2017;9:284.

321. Kaila K, Ruusuvuori E, Seja P, Voipio J, Puskarjov M. GABA actions and ionic plasticity in epilepsy. Curr Opin Neurobiol. 2014 Jun;26:34–41.

322. Porcher C, Medina I, Gaiarsa JL. Mechanism of BDNF Modulation in GABAergic Synaptic Transmission in Healthy and Disease Brains. Front Cell Neurosci. 2018;12:273.

323. Wong LW, Tann JY, Ibanez CF, Sajikumar S. The p75 Neurotrophin Receptor Is an Essential Mediator of Impairments in Hippocampal-Dependent Associative Plasticity and

Memory Induced by Sleep Deprivation. J Neurosci Off J Soc Neurosci. 2019 Jul 10;39(28):5452–65.

324. Gibon J, Buckley SM, Unsain N, Kaartinen V, Séguéla P, Barker PA. proBDNF and p75NTR Control Excitability and Persistent Firing of Cortical Pyramidal Neurons. J Neurosci Off J Soc Neurosci. 2015 Jul 1;35(26):9741–53.

325. Gibon J, Barker PA, Séguéla P. Opposing presynaptic roles of BDNF and ProBDNF in the regulation of persistent activity in the entorhinal cortex. Mol Brain. 2016 Mar 1;9:23.

326. Darcq E, Morisot N, Phamluong K, Warnault V, Jeanblanc J, Longo FM, et al. The Neurotrophic Factor Receptor p75 in the Rat Dorsolateral Striatum Drives Excessive Alcohol Drinking. J Neurosci Off J Soc Neurosci. 2016 28;36(39):10116–27.

327. Podyma B, Johnson DA, Sipe L, Remcho TP, Battin K, Liu Y, et al. The p75 neurotrophin receptor in AgRP neurons is necessary for homeostatic feeding and food anticipation. eLife. 2020 Jan 29;9.

328. Sabariego M, Schönwald A, Boublil BL, Zimmerman DT, Ahmadi S, Gonzalez N, et al. Time Cells in the Hippocampus Are Neither Dependent on Medial Entorhinal Cortex Inputs nor Necessary for Spatial Working Memory. Neuron. 2019 19;102(6):1235-1248.e5.

329. Jacquet M, Lecourtier L, Cassel R, Loureiro M, Cosquer B, Escoffier G, et al. Dorsolateral striatum and dorsal hippocampus: a serial contribution to acquisition of cue-reward associations in rats. Behav Brain Res. 2013 Feb 15;239:94–103.

330. Giuliano C, Belin D, Everitt BJ. Compulsive Alcohol Seeking Results from a Failure to Disengage Dorsolateral Striatal Control over Behavior. J Neurosci Off J Soc Neurosci. 2019 27;39(9):1744–54.

331. Aponte Y, Atasoy D, Sternson SM. AGRP neurons are sufficient to orchestrate feeding behavior rapidly and without training. Nat Neurosci. 2011 Mar;14(3):351–5.

332. Pham DD, Do HT, Bruelle C, Kukkonen JP, Eriksson O, Mogollón I, et al. p75 Neurotrophin Receptor Signaling Activates Sterol Regulatory Element-binding Protein-2 in Hepatocyte Cells via p38 Mitogen-activated Protein Kinase and Caspase-3. J Biol Chem. 2016 May 13;291(20):10747–58.

333. Pham DD, Bruelle C, Thi Do H, Pajanoja C, Jin C, Srinivasan V, et al. Caspase-2 and p75 neurotrophin receptor (p75NTR) are involved in the regulation of SREBP and lipid genes in hepatocyte cells. Cell Death Dis. 2019 11;10(7):537.

334. Zhou X, Hao Q, Liao P, Luo S, Zhang M, Hu G, et al. Nerve growth factor receptor negates the tumor suppressor p53 as a feedback regulator. eLife. 2016 10;5.

335. Nguyen D, Yang K, Chao L, Deng Y, Zhou X, Zhang Z, et al. Inhibition of tumor suppressor p73 by nerve growth factor receptor via chaperone-mediated autophagy. J Mol Cell Biol. 2020 Apr 13;

336. Herrmann JL, Menter DG, Hamada J, Marchetti D, Nakajima M, Nicolson GL. Mediation of NGF-stimulated extracellular matrix invasion by the human melanoma low-affinity p75 neurotrophin receptor: melanoma p75 functions independently of trkA. Mol Biol Cell. 1993 Nov;4(11):1205–16.

337. Papandreou C, Bogenrieder T, Loganzo F, Chao MV, Nanus DM, Albino AP. Mutation and expression of the low affinity neurotrophin receptor in human malignant melanoma. Melanoma Res. 1996 Oct;6(5):373–8.

338. Iwamoto S, Odland PB, Piepkorn M, Bothwell M. Evidence that the p75 neurotrophin receptor mediates perineural spread of desmoplastic melanoma. J Am Acad Dermatol. 1996 Nov;35(5 Pt 1):725–31.

339. Iwamoto S, Burrows RC, Agoff SN, Piepkorn M, Bothwell M, Schmidt R. The p75 neurotrophin receptor, relative to other Schwann cell and melanoma markers, is abundantly Expressed in spindled melanomas. Am J Dermatopathol. 2001 Aug;23(4):288–94.

340. Shonukan O, Bagayogo I, McCrea P, Chao M, Hempstead B. Neurotrophin-induced melanoma cell migration is mediated through the actin-bundling protein fascin. Oncogene. 2003 Jun 5;22(23):3616–23.

341. Marchetti D, Aucoin R, Blust J, Murry B, Greiter-Wilke A. p75 neurotrophin receptor functions as a survival receptor in brain-metastatic melanoma cells. J Cell Biochem. 2004 Jan 1;91(1):206–15.

342. Chu C shun, Xue B, Tu C, Feng Z hua, Shi Y huan, Miao Y, et al. NRAGE suppresses metastasis of melanoma and pancreatic cancer in vitro and in vivo. Cancer Lett. 2007 Jun 8;250(2):268–75.

343. Truzzi F, Marconi A, Lotti R, Dallaglio K, French LE, Hempstead BL, et al. Neurotrophins and their receptors stimulate melanoma cell proliferation and migration. J Invest Dermatol. 2008 Aug;128(8):2031–40.

344. Chan MM, Tahan SR. Low-affinity nerve growth factor receptor (P75 NGFR) as a marker of perineural invasion in malignant melanomas. J Cutan Pathol. 2010 Mar;37(3):336–43.

345. Boiko AD, Razorenova OV, van de Rijn M, Swetter SM, Johnson DL, Ly DP, et al. Human melanoma-initiating cells express neural crest nerve growth factor receptor CD271. Nature. 2010 Jul 1;466(7302):133–7.

346. Lazova R, Tantcheva-Poor I, Sigal AC. P75 nerve growth factor receptor staining is superior to S100 in identifying spindle cell and desmoplastic melanoma. J Am Acad Dermatol. 2010 Nov;63(5):852–8.

347. Civenni G, Walter A, Kobert N, Mihic-Probst D, Zipser M, Belloni B, et al. Human CD271-positive melanoma stem cells associated with metastasis establish tumor heterogeneity and long-term growth. Cancer Res. 2011 Apr 15;71(8):3098–109.

348. Sigal AC, Keenan M, Lazova R. P75 nerve growth factor receptor as a useful marker to distinguish spindle cell melanoma from other spindle cell neoplasms of sun-damaged skin. Am J Dermatopathol. 2012 Apr;34(2):145–50.

349. Goh ETH, Lin Z, Ahn BY, Lopes-Rodrigues V, Dang NH, Salim S, et al. A Small Molecule Targeting the Transmembrane Domain of Death Receptor p75NTR Induces Melanoma Cell Death and Reduces Tumor Growth. Cell Chem Biol. 2018 20;25(12):1485-1494.e5.

350. Filipp FV, Li C, Boiko AD. CD271 is a molecular switch with divergent roles in melanoma and melanocyte development. Sci Rep. 2019 22;9(1):7696.

351. Weis C, Wiesenhofer B, Humpel C. Nerve growth factor plays a divergent role in mediating growth of rat C6 glioma cells via binding to the p75 neurotrophin receptor. J Neurooncol. 2002 Jan;56(1):59–67.

352. Johnston ALM, Lun X, Rahn JJ, Liacini A, Wang L, Hamilton MG, et al. The p75 neurotrophin receptor is a central regulator of glioma invasion. PLoS Biol. 2007 Aug;5(8):e212.

353. Morrison LC, McClelland R, Aiken C, Bridges M, Liang L, Wang X, et al. Deconstruction of medulloblastoma cellular heterogeneity reveals differences between the most highly invasive and self-renewing phenotypes. Neoplasia N Y N. 2013 Apr;15(4):384–98.

354. Liang L, Aiken C, McClelland R, Morrison LC, Tatari N, Remke M, et al. Characterization of novel biomarkers in selecting for subtype specific medulloblastoma phenotypes. Oncotarget. 2015 Nov 17;6(36):38881–900.

355. Alshehri MM, Robbins SM, Senger DL. The Role of Neurotrophin Signaling in Gliomagenesis: A Focus on the p75 Neurotrophin Receptor (p75NTR/CD271). Vitam Horm. 2017;104:367–404.

356. Liang L, Coudière-Morrison L, Tatari N, Stromecki M, Fresnoza A, Porter CJ, et al. CD271+ Cells Are Diagnostic and Prognostic and Exhibit Elevated MAPK Activity in SHH Medulloblastoma. Cancer Res. 2018 15;78(16):4745–59.

357. Verbeke S, Meignan S, Lagadec C, Germain E, Hondermarck H, Adriaenssens E, et al. Overexpression of p75(NTR) increases survival of breast cancer cells through p21(waf1). Cell Signal. 2010 Dec;22(12):1864–73.

358. Wilmet JP, Tastet C, Desruelles E, Ziental-Gelus N, Blanckaert V, Hondermarck H, et al. Proteome changes induced by overexpression of the p75 neurotrophin receptor (p75NTR) in breast cancer cells. Int J Dev Biol. 2011;55(7–9):801–9.

359. Vanhecke E, Adriaenssens E, Verbeke S, Meignan S, Germain E, Berteaux N, et al. Brain-derived neurotrophic factor and neurotrophin-4/5 are expressed in breast cancer and can be targeted to inhibit tumor cell survival. Clin Cancer Res Off J Am Assoc Cancer Res. 2011 Apr 1;17(7):1741–52.

360. Deng X, Xu G, He L, Xu M. p75NTR promotes survival of breast cancer resistant cells by regulating Bcl-2/Bax and MAPK pathway. Int J Clin Exp Pathol. 2017;10(12):11685–94.

361. Jin H, Pan Y, He L, Zhai H, Li X, Zhao L, et al. p75 neurotrophin receptor inhibits invasion and metastasis of gastric cancer. Mol Cancer Res MCR. 2007 May;5(5):423–33.

362. Jin H, Pan Y, Zhao L, Zhai H, Li X, Sun L, et al. p75 neurotrophin receptor suppresses the proliferation of human gastric cancer cells. Neoplasia N Y N. 2007 Jun;9(6):471–8.

363. Jin H, Wang Z, Liu L, Gao L, Sun L, Li X, et al. R-flurbiprofen reverses multidrug resistance, proliferation and metastasis in gastric cancer cells by p75(NTR) induction. Mol Pharm. 2010 Feb 1;7(1):156–68.

364. Blondy S, Christou N, David V, Verdier M, Jauberteau MO, Mathonnet M, et al. Neurotrophins and their involvement in digestive cancers. Cell Death Dis. 2019 11;10(2):123.

365. Nalbandian A, Djakiew D. The p75(NTR) metastasis suppressor inhibits urokinase plasminogen activator, matrix metalloproteinase-2 and matrix metalloproteinase-9 in PC-3 prostate cancer cells. Clin Exp Metastasis. 2006;23(2):107–16.

366. Wynne S, Djakiew D. NSAID inhibition of prostate cancer cell migration is mediated by Nag-1 Induction via the p38 MAPK-p75(NTR) pathway. Mol Cancer Res MCR. 2010 Dec;8(12):1656–64.

367. De la Cruz-Morcillo MA, Berger J, Sánchez-Prieto R, Saada S, Naves T, Guillaudeau A, et al. p75 neurotrophin receptor and pro-BDNF promote cell survival and migration in clear cell renal cell carcinoma. Oncotarget. 2016 Jun 7;7(23):34480–97.

368. Tabassum A, Khwaja F, Djakiew D. The p75(NTR) tumor suppressor induces caspase-mediated apoptosis in bladder tumor cells. Int J Cancer. 2003 May 20;105(1):47–52.

369. Wang W, Zhao H, Zhang S, Kang E, Chen Y, Ni C, et al. Patterns of expression and function of the p75(NGFR) protein in pancreatic cancer cells and tumours. Eur J Surg Oncol J Eur Soc Surg Oncol Br Assoc Surg Oncol. 2009 Aug;35(8):826–32.

370. Maldonado MDM, Dharmawardhane S. Targeting Rac and Cdc42 GTPases in Cancer. Cancer Res. 2018 15;78(12):3101–11.

371. Hirata E, Yukinaga H, Kamioka Y, Arakawa Y, Miyamoto S, Okada T, et al. In vivo fluorescence resonance energy transfer imaging reveals differential activation of Rho-family GTPases in glioblastoma cell invasion. J Cell Sci. 2012 Feb 15;125(Pt 4):858–68.

372. Yukinaga H, Shionyu C, Hirata E, Ui-Tei K, Nagashima T, Kondo S, et al. Fluctuation of Rac1 activity is associated with the phenotypic and transcriptional heterogeneity of glioma cells. J Cell Sci. 2014 Apr 15;127(Pt 8):1805–15.

373. Kallop DY, Meilandt WJ, Gogineni A, Easley-Neal C, Wu T, Jubb AM, et al. A death receptor 6-amyloid precursor protein pathway regulates synapse density in the mature CNS but does not contribute to Alzheimer's disease-related pathophysiology in murine models. J Neurosci Off J Soc Neurosci. 2014 May 7;34(19):6425–37.

374. Hu Y, Lee X, Shao Z, Apicco D, Huang G, Gong BJ, et al. A DR6/p75(NTR) complex is responsible for β-amyloid-induced cortical neuron death. Cell Death Dis. 2013 Apr 4;4:e579.

375. Iyer A, van Scheppingen J, Anink J, Milenkovic I, Kovács GG, Aronica E. Developmental patterns of DR6 in normal human hippocampus and in Down syndrome. J Neurodev Disord. 2013 Apr 24;5(1):10.

376. Huang G, Lee X, Bian Y, Shao Z, Sheng G, Pepinsky RB, et al. Death receptor 6 (DR6) antagonist antibody is neuroprotective in the mouse SOD1G93A model of amyotrophic lateral sclerosis. Cell Death Dis. 2013 Oct 10;4:e841.

377. Xu Y, Wang D, Luo Y, Li W, Shan Y, Tan X, et al. Beta amyloid-induced upregulation of death receptor 6 accelerates the toxic effect of N-terminal fragment of amyloid precursor protein. Neurobiol Aging. 2015 Jan;36(1):157–68.

378. Wang Y, Zhao D, Pan B, Song Z, Shah SZA, Yin X, et al. Death Receptor 6 and Caspase-6 Regulate Prion Peptide-Induced Axonal Degeneration in Rat Spinal Neurons. J Mol Neurosci MN. 2015 Aug;56(4):966–76.

379. Chen X, Jiang XM, Zhao LJ, Sun LL, Yan ML, Tian Y, et al. MicroRNA-195 prevents dendritic degeneration and neuron death in rats following chronic brain hypoperfusion. Cell Death Dis. 2017 01;8(6):e2850.

380. Fernandes KA, Mitchell KL, Patel A, Marola OJ, Shrager P, Zack DJ, et al. Role of SARM1 and DR6 in retinal ganglion cell axonal and somal degeneration following axonal injury. Exp Eye Res. 2018;171:54–61.

381. Kuester M, Kemmerzehl S, Dahms SO, Roeser D, Than ME. The crystal structure of death receptor 6 (DR6): a potential receptor of the amyloid precursor protein (APP). J Mol Biol. 2011 Jun 3;409(2):189–201.

382. Xu K, Olsen O, Tzvetkova-Robev D, Tessier-Lavigne M, Nikolov DB. The crystal structure of DR6 in complex with the amyloid precursor protein provides insight into death receptor activation. Genes Dev. 2015 Apr 15;29(8):785–90.

383. Pan G, Bauer JH, Haridas V, Wang S, Liu D, Yu G, et al. Identification and functional characterization of DR6, a novel death domain-containing TNF receptor. FEBS Lett. 1998 Jul 24;431(3):351–6.

384. Bridgham JT, Bobe J, Goetz FW, Johnson AL. Conservation of death receptor-6 in avian and piscine vertebrates. Biochem Biophys Res Commun. 2001 Jun 29;284(5):1109–15.

385. Klíma M, Zájedová J, Doubravská L, Andera L. Functional analysis of the posttranslational modifications of the death receptor 6. Biochim Biophys Acta. 2009 Oct;1793(10):1579–87.

386. Zeng L, Li T, Xu DC, Liu J, Mao G, Cui MZ, et al. Death receptor 6 induces apoptosis not through type I or type II pathways, but via a unique mitochondria-dependent pathway by interacting with Bax protein. J Biol Chem. 2012 Aug 17;287(34):29125–33.

387. Hu R, Du Q, Yin X, Li J, Wang T, Zhang L. Agonist antibody activates death receptor 6 downstream signaling involving TRADD recruitment. FEBS Lett. 2014 Jan 31;588(3):401–7.

388. Yuan J, Amin P, Ofengeim D. Necroptosis and RIPK1-mediated neuroinflammation in CNS diseases. Nat Rev Neurosci. 2019;20(1):19–33.

389. Cabon L, Galán-Malo P, Bouharrour A, Delavallée L, Brunelle-Navas MN, Lorenzo HK, et al. BID regulates AIF-mediated caspase-independent necroptosis by promoting BAX activation. Cell Death Differ. 2012 Feb;19(2):245–56.

390. Zhang J, Zhao ZJ, Fu X, Niu H, Hu C, Dong Y, et al. Proapoptotic Mitochondrial Carrier Homolog Protein PSAP Mediates Death Receptor 6 Induced Apoptosis. J Alzheimers Dis JAD. 2020;74(4):1097–106.

391. Wang Z, Fan C, Zhou HF, Lu JS, Sun MJ, Song JW, et al. S5a binds to death receptor-6 to induce THP-1 monocytes to differentiate through the activation of the NF-κB pathway. J Cell Sci. 2014 Aug 1;127(Pt 15):3257–68.

392. Yang X, Shi B, Li L, Xu Z, Ge Y, Shi J, et al. Death receptor 6 (DR6) is required for mouse B16 tumor angiogenesis via the NF-κB, P38 MAPK and STAT3 pathways. Oncogenesis. 2016 Mar 7;5:e206.

393. Tam SJ, Richmond DL, Kaminker JS, Modrusan Z, Martin-McNulty B, Cao TC, et al. Death receptors DR6 and TROY regulate brain vascular development. Dev Cell. 2012 Feb 14;22(2):403–17.

394. Zhang D, Cao X, Li J, Zhao G. MiR-210 inhibits NF-κB signaling pathway by targeting DR6 in osteoarthritis. Sci Rep. 2015 Aug 5;5:12775.

395. Fujikura D, Ikesue M, Endo T, Chiba S, Higashi H, Uede T. Death receptor 6 contributes to autoimmunity in lupus-prone mice. Nat Commun. 2017 03;8:13957.

396. Shi B, Bao J, Liu Y, Shi J. Death receptor 6 promotes ovarian cancer cell migration through KIF11. FEBS Open Bio. 2018 Sep;8(9):1497–507.

397. Marik SA, Olsen O, Tessier-Lavigne M, Gilbert CD. Death receptor 6 regulates adult experience-dependent cortical plasticity. J Neurosci Off J Soc Neurosci. 2013 Sep 18;33(38):14998–5003.

398. Mi S, Lee X, Hu Y, Ji B, Shao Z, Yang W, et al. Death receptor 6 negatively regulates oligodendrocyte survival, maturation and myelination. Nat Med. 2011 Jul 3;17(7):816–21.

399. Colombo A, Hsia HE, Wang M, Kuhn PH, Brill MS, Canevazzi P, et al. Non-cell-autonomous function of DR6 in Schwann cell proliferation. EMBO J. 2018 03;37(7).

400. Schmidt CS, Zhao J, Chain J, Hepburn D, Gitter B, Sandusky G, et al. Resistance to myelin oligodendrocyte glycoprotein-induced experimental autoimmune encephalomyelitis by death receptor 6-deficient mice. J Immunol Baltim Md 1950. 2005 Aug 15;175(4):2286–92.

401. Park JB, Yiu G, Kaneko S, Wang J, Chang J, He XL, et al. A TNF receptor family member, TROY, is a coreceptor with Nogo receptor in mediating the inhibitory activity of myelin inhibitors. Neuron. 2005 Feb 3;45(3):345–51.

402. Schwab JM, Tuli SK, Failli V. The Nogo receptor complex: confining molecules to molecular mechanisms. Trends Mol Med. 2006 Jul;12(7):293–7.

403. Satoh J, Tabunoki H, Yamamura T, Arima K, Konno H. TROY and LINGO-1 expression in astrocytes and macrophages/microglia in multiple sclerosis lesions. Neuropathol Appl Neurobiol. 2007 Feb;33(1):99–107.

404. Venkatesh K, Chivatakarn O, Sheu SS, Giger RJ. Molecular dissection of the myelin-associated glycoprotein receptor complex reveals cell type-specific mechanisms for neurite outgrowth inhibition. J Cell Biol. 2007 May 7;177(3):393–9.

405. Mi S. Troy/Taj and its role in CNS axon regeneration. Cytokine Growth Factor Rev. 2008 Aug;19(3–4):245–51.

406. Karlén A, Karlsson TE, Mattsson A, Lundströmer K, Codeluppi S, Pham TM, et al. Nogo receptor 1 regulates formation of lasting memories. Proc Natl Acad Sci U S A. 2009 Dec 1;106(48):20476–81.

407. Wills ZP, Mandel-Brehm C, Mardinly AR, McCord AE, Giger RJ, Greenberg ME. The nogo receptor family restricts synapse number in the developing hippocampus. Neuron. 2012 Feb 9;73(3):466–81.

408. Sun L, Liu S, Sun Q, Li Z, Xu F, Hou C, et al. Inhibition of TROY promotes OPC differentiation and increases therapeutic efficacy of OPC graft for spinal cord injury. Stem Cells Dev. 2014 Sep 1;23(17):2104–18.

409. Saha N, Kolev M, Nikolov DB. Structural features of the Nogo receptor signaling complexes at the neuron/myelin interface. Neurosci Res. 2014 Oct;87:1–7.

410. Theotokis P, Touloumi O, Lagoudaki R, Nousiopoulou E, Kesidou E, Siafis S, et al. Nogo receptor complex expression dynamics in the inflammatory foci of central nervous system experimental autoimmune demyelination. J Neuroinflammation. 2016 11;13(1):265.

411. Thomas RA, Gibon J, Chen CXQ, Chierzi S, Soubannier VG, Baulac S, et al. The Nogo Receptor Ligand LGI1 Regulates Synapse Number and Synaptic Activity in Hippocampal and Cortical Neurons. eNeuro. 2018 Aug;5(4).

412. Paulino VM, Yang Z, Kloss J, Ennis MJ, Armstrong BA, Loftus JC, et al. TROY (TNFRSF19) is overexpressed in advanced glial tumors and promotes glioblastoma cell invasion via Pyk2-Rac1 signaling. Mol Cancer Res MCR. 2010 Nov;8(11):1558–67.

413. Jacobs VL, Liu Y, De Leo JA. Propentofylline targets TROY, a novel microglial signaling pathway. PloS One. 2012;7(5):e37955.

414. Loftus JC, Dhruv H, Tuncali S, Kloss J, Yang Z, Schumacher CA, et al. TROY (TNFRSF19) promotes glioblastoma survival signaling and therapeutic resistance. Mol Cancer Res MCR. 2013 Aug;11(8):865–74.

415. Dhruv HD, Roos A, Tomboc PJ, Tuncali S, Chavez A, Mathews I, et al. Propentofylline inhibits glioblastoma cell invasion and survival by targeting the TROY signaling pathway. J Neurooncol. 2016 Feb;126(3):397–404.

416. Ding Z, Dhruv H, Kwiatkowska-Piwowarczyk A, Ruggieri R, Kloss J, Symons M, et al. PDZ-RhoGEF Is a Signaling Effector for TROY-Induced Glioblastoma Cell Invasion and Survival. Neoplasia N Y N. 2018;20(10):1045–58.

417. Ding Z, Roos A, Kloss J, Dhruv H, Peng S, Pirrotte P, et al. A Novel Signaling Complex between TROY and EGFR Mediates Glioblastoma Cell Invasion. Mol Cancer Res MCR. 2018;16(2):322–32.

418. Liu X, Bao Y, Meng W, Yang P, An Y, Ma J, et al. TROY interacts with RKIP to promote glioma development. Oncogene. 2019;38(9):1544–59.

419. Lu Y, Liu X, Zhou J, Huang A, Zhou J, He C. TROY interacts with Rho guanine nucleotide dissociation inhibitor α (RhoGDIα) to mediate Nogo-induced inhibition of neurite outgrowth. J Biol Chem. 2013 Nov 22;288(47):34276–86.

420. Kong M, Kim Y, Lee C. A strong synergistic epistasis between FAM134B and TNFRSF19 on the susceptibility to vascular dementia. Psychiatr Genet. 2011 Feb;21(1):37–41.

421. van Niel G, D'Angelo G, Raposo G. Shedding light on the cell biology of extracellular vesicles. Nat Rev Mol Cell Biol. 2018 Apr;19(4):213–28.

422. Kalluri R, LeBleu VS. The biology, function, and biomedical applications of exosomes. Science. 2020 Feb 7;367(6478):eaau6977.

423. Mulcahy LA, Pink RC, Carter DRF. Routes and mechanisms of extracellular vesicle uptake. J Extracell Vesicles. 2014;3.

424. Krämer-Albers EM. Extracellular Vesicles at CNS barriers: Mode of action. Curr Opin Neurobiol. 2022 Jun 3;75:102569.

425. Schubert A, Boutros M. Extracellular vesicles and oncogenic signaling. Mol Oncol. 2021 Jan;15(1):3–26.

426. Bahram Sangani N, Gomes AR, Curfs LMG, Reutelingsperger CP. The role of Extracellular Vesicles during CNS development. Prog Neurobiol. 2021 Oct;205:102124.

427. Lizarraga-Valderrama LR, Sheridan GK. Extracellular vesicles and intercellular communication in the central nervous system. FEBS Lett. 2021 May;595(10):1391–410.

428. Fan Y, Chen Z, Zhang M. Role of exosomes in the pathogenesis, diagnosis, and treatment of central nervous system diseases. J Transl Med. 2022 Jun 27;20(1):291.

429. Teng F, Fussenegger M. Shedding Light on Extracellular Vesicle Biogenesis and Bioengineering. Adv Sci Weinh Baden-Wurtt Ger. 2020 Jan;8(1):2003505.

430. Williams RL, Urbé S. The emerging shape of the ESCRT machinery. Nat Rev Mol Cell Biol. 2007 May;8(5):355–68.

431. Vietri M, Radulovic M, Stenmark H. The many functions of ESCRTs. Nat Rev Mol Cell Biol. 2020 Jan;21(1):25–42.

432. Hurley JH, Hanson PI. Membrane budding and scission by the ESCRT machinery: it's all in the neck. Nat Rev Mol Cell Biol. 2010 Aug;11(8):556–66.

433. Hanson PI, Cashikar A. Multivesicular body morphogenesis. Annu Rev Cell Dev Biol. 2012;28:337–62.

434. Henne WM, Stenmark H, Emr SD. Molecular mechanisms of the membrane sculpting ESCRT pathway. Cold Spring Harb Perspect Biol. 2013 Sep 1;5(9):a016766.

435. Wurmser AE, Emr SD. Phosphoinositide signaling and turnover: PtdIns(3)P, a regulator of membrane traffic, is transported to the vacuole and degraded by a process that requires lumenal vacuolar hydrolase activities. EMBO J. 1998 Sep 1;17(17):4930–42.

436. Odorizzi G, Babst M, Emr SD. Fab1p PtdIns(3)P 5-kinase function essential for protein sorting in the multivesicular body. Cell. 1998 Dec 11;95(6):847–58.

437. Raiborg C, Bremnes B, Mehlum A, Gillooly DJ, D'Arrigo A, Stang E, et al. FYVE and coiled-coil domains determine the specific localisation of Hrs to early endosomes. J Cell Sci. 2001 Jun;114(Pt 12):2255–63.

438. Raiborg C, Bache KG, Mehlum A, Stang E, Stenmark H. Hrs recruits clathrin to early endosomes. EMBO J. 2001 Sep 3;20(17):5008–21.

439. Lu Q, Hope LW, Brasch M, Reinhard C, Cohen SN. TSG101 interaction with HRS mediates endosomal trafficking and receptor down-regulation. Proc Natl Acad Sci U S A. 2003 Jun 24;100(13):7626–31.

440. Bache KG, Brech A, Mehlum A, Stenmark H. Hrs regulates multivesicular body formation via ESCRT recruitment to endosomes. J Cell Biol. 2003 Aug 4;162(3):435–42.

441. Katzmann DJ, Stefan CJ, Babst M, Emr SD. Vps27 recruits ESCRT machinery to endosomes during MVB sorting. J Cell Biol. 2003 Aug 4;162(3):413–23.

442. Gill DJ, Teo H, Sun J, Perisic O, Veprintsev DB, Emr SD, et al. Structural insight into the ESCRT-I/-II link and its role in MVB trafficking. EMBO J. 2007 Jan 24;26(2):600–12.

443. Teo H, Gill DJ, Sun J, Perisic O, Veprintsev DB, Vallis Y, et al. ESCRT-I core and ESCRT-II GLUE domain structures reveal role for GLUE in linking to ESCRT-I and membranes. Cell. 2006 Apr 7;125(1):99–111.

444. Babst M, Katzmann DJ, Estepa-Sabal EJ, Meerloo T, Emr SD. Escrt-III: an endosome-associated heterooligomeric protein complex required for mvb sorting. Dev Cell. 2002 Aug;3(2):271–82.

445. Babst M, Katzmann DJ, Snyder WB, Wendland B, Emr SD. Endosome-associated complex, ESCRT-II, recruits transport machinery for protein sorting at the multivesicular body. Dev Cell. 2002 Aug;3(2):283–9.

446. Teo H, Perisic O, González B, Williams RL. ESCRT-II, an endosome-associated complex required for protein sorting: crystal structure and interactions with ESCRT-III and membranes. Dev Cell. 2004 Oct;7(4):559–69.

447. Wollert T, Hurley JH. Molecular mechanism of multivesicular body biogenesis by ESCRT complexes. Nature. 2010 Apr 8;464(7290):864–9.

448. Teis D, Saksena S, Emr SD. Ordered assembly of the ESCRT-III complex on endosomes is required to sequester cargo during MVB formation. Dev Cell. 2008 Oct;15(4):578–89.

449. Wollert T, Wunder C, Lippincott-Schwartz J, Hurley JH. Membrane scission by the ESCRT-III complex. Nature. 2009 Mar 12;458(7235):172–7.

450. Saksena S, Wahlman J, Teis D, Johnson AE, Emr SD. Functional reconstitution of ESCRT-III assembly and disassembly. Cell. 2009 Jan 9;136(1):97–109.

451. Trajkovic K, Hsu C, Chiantia S, Rajendran L, Wenzel D, Wieland F, et al. Ceramide triggers budding of exosome vesicles into multivesicular endosomes. Science. 2008 Feb 29;319(5867):1244–7.

452. Mittelbrunn M, Gutiérrez-Vázquez C, Villarroya-Beltri C, González S, Sánchez-Cabo F, González MÁ, et al. Unidirectional transfer of microRNA-loaded exosomes from T cells to antigen-presenting cells. Nat Commun. 2011;2:282.

453. Martín-Cófreces NB, Baixauli F, Sánchez-Madrid F. Immune synapse: conductor of orchestrated organelle movement. Trends Cell Biol. 2014 Jan;24(1):61–72.

454. Hoshino D, Kirkbride KC, Costello K, Clark ES, Sinha S, Grega-Larson N, et al. Exosome secretion is enhanced by invadopodia and drives invasive behavior. Cell Rep. 2013 Dec 12;5(5):1159–68.

455. Sinha S, Hoshino D, Hong NH, Kirkbride KC, Grega-Larson NE, Seiki M, et al. Cortactin promotes exosome secretion by controlling branched actin dynamics. J Cell Biol. 2016 Jul 18;214(2):197–213.

456. Koles K, Nunnari J, Korkut C, Barria R, Brewer C, Li Y, et al. Mechanism of evenness interrupted (Evi)-exosome release at synaptic boutons. J Biol Chem. 2012 May 11;287(20):16820–34.

457. Jahn R, Scheller RH. SNAREs--engines for membrane fusion. Nat Rev Mol Cell Biol. 2006 Sep;7(9):631–43.

458. Martens S, McMahon HT. Mechanisms of membrane fusion: disparate players and common principles. Nat Rev Mol Cell Biol. 2008 Jul;9(7):543–56.

459. Südhof TC, Rothman JE. Membrane fusion: grappling with SNARE and SM proteins. Science. 2009 Jan 23;323(5913):474–7.

460. Rao SK, Huynh C, Proux-Gillardeaux V, Galli T, Andrews NW. Identification of SNAREs involved in synaptotagmin VII-regulated lysosomal exocytosis. J Biol Chem. 2004 May 7;279(19):20471–9.

461. Fader CM, Sánchez DG, Mestre MB, Colombo MI. TI-VAMP/VAMP7 and VAMP3/cellubrevin: two v-SNARE proteins involved in specific steps of the autophagy/multivesicular body pathways. Biochim Biophys Acta. 2009 Dec;1793(12):1901–16.

462. Proux-Gillardeaux V, Raposo G, Irinopoulou T, Galli T. Expression of the Longin domain of TI-VAMP impairs lysosomal secretion and epithelial cell migration. Biol Cell. 2007 May;99(5):261–71.

463. Gross JC, Chaudhary V, Bartscherer K, Boutros M. Active Wnt proteins are secreted on exosomes. Nat Cell Biol. 2012 Oct;14(10):1036–45.

464. Ruiz-Martinez M, Navarro A, Marrades RM, Viñolas N, Santasusagna S, Muñoz C, et al. YKT6 expression, exosome release, and survival in non-small cell lung cancer. Oncotarget. 2016 Aug 9;7(32):51515–24.

465. Wei Y, Wang D, Jin F, Bian Z, Li L, Liang H, et al. Pyruvate kinase type M2 promotes tumour cell exosome release via phosphorylating synaptosome-associated protein 23. Nat Commun. 2017 Jan 9;8:14041.

466. Matusek T, Wendler F, Polès S, Pizette S, D'Angelo G, Fürthauer M, et al. The ESCRT machinery regulates the secretion and long-range activity of Hedgehog. Nature. 2014 Dec 4;516(7529):99–103.

467. Nabhan JF, Hu R, Oh RS, Cohen SN, Lu Q. Formation and release of arrestin domain-containing protein 1-mediated microvesicles (ARMMs) at plasma membrane by recruitment of TSG101 protein. Proc Natl Acad Sci U S A. 2012 Mar 13;109(11):4146–51.

468. Bianco F, Perrotta C, Novellino L, Francolini M, Riganti L, Menna E, et al. Acid sphingomyelinase activity triggers microparticle release from glial cells. EMBO J. 2009 Apr 22;28(8):1043–54.

469. Awojoodu AO, Keegan PM, Lane AR, Zhang Y, Lynch KR, Platt MO, et al. Acid sphingomyelinase is activated in sickle cell erythrocytes and contributes to inflammatory microparticle generation in SCD. Blood. 2014 Sep 18;124(12):1941–50.

470. Schlienger S, Campbell S, Claing A. ARF1 regulates the Rho/MLC pathway to control EGF-dependent breast cancer cell invasion. Mol Biol Cell. 2014 Jan;25(1):17–29.

471. Muralidharan-Chari V, Clancy J, Plou C, Romao M, Chavrier P, Raposo G, et al. ARF6-regulated shedding of tumor cell-derived plasma membrane microvesicles. Curr Biol CB. 2009 Dec 1;19(22):1875–85.

472. Li B, Antonyak MA, Zhang J, Cerione RA. RhoA triggers a specific signaling pathway that generates transforming microvesicles in cancer cells. Oncogene. 2012 Nov 8;31(45):4740–9.

473. Escudero CA, Lazo OM, Galleguillos C, Parraguez JI, Lopez-Verrilli MA, Cabeza C, et al. The p75 neurotrophin receptor evades the endolysosomal route in neuronal cells, favouring multivesicular bodies specialised for exosomal release. J Cell Sci. 2014 May 1;127(Pt 9):1966–79.

474. Gonçalves NP, Yan Y, Ulrichsen M, Venø MT, Poulsen ET, Enghild JJ, et al. Modulation of Small RNA Signatures in Schwann-Cell-Derived Extracellular Vesicles by the p75 Neurotrophin Receptor and Sortilin. Biomedicines. 2020 Oct 24;8(11):E450.

475. García-Silva S, Benito-Martín A, Nogués L, Hernández-Barranco A, Mazariegos MS, Santos V, et al. Melanoma-derived small extracellular vesicles induce lymphangiogenesis and metastasis through an NGFR-dependent mechanism. Nat Cancer. 2021 Dec;2(12):1387–405.

476. Sica GL, Zhu G, Tamada K, Liu D, Ni J, Chen L. RELT, a new member of the tumor necrosis factor receptor superfamily, is selectively expressed in hematopoietic tissues and activates transcription factor NF-kappaB. Blood. 2001 May 1;97(9):2702–7.

477. Bossen C, Ingold K, Tardivel A, Bodmer JL, Gaide O, Hertig S, et al. Interactions of tumor necrosis factor (TNF) and TNF receptor family members in the mouse and human. J Biol Chem. 2006 May 19;281(20):13964–71.

478. Polek TC, Talpaz M, Spivak-Kroizman T. The TNF receptor, RELT, binds SPAK and uses it to mediate p38 and JNK activation. Biochem Biophys Res Commun. 2006 Apr 28;343(1):125–34.

479. Cusick JK, Mustian A, Goldberg K, Reyland ME. RELT induces cellular death in HEK 293 epithelial cells. Cell Immunol. 2010;261(1):1–8.

480. Choi BK, Kim SH, Kim YH, Lee DG, Oh HS, Han C, et al. RELT negatively regulates the early phase of the T-cell response in mice. Eur J Immunol. 2018 Oct;48(10):1739–49.

481. Kim JW, Zhang H, Seymen F, Koruyucu M, Hu Y, Kang J, et al. Mutations in RELT cause autosomal recessive amelogenesis imperfecta. Clin Genet. 2019 Mar;95(3):375–83.

482. Ikeda A, Shahid S, Blumberg BR, Suzuki M, Bartlett JD. ADAM10 is Expressed by Ameloblasts, Cleaves the RELT TNF Receptor Extracellular Domain and Facilitates Enamel Development. Sci Rep. 2019 Oct 1;9(1):14086.

483. Nikolopoulos G, Smith CEL, Brookes SJ, El-Asrag ME, Brown CJ, Patel A, et al. New missense variants in RELT causing hypomineralised amelogenesis imperfecta. Clin Genet. 2020 May;97(5):688–95.

484. Yao W, Chen Q, Li S, Jia X, Xu L, Wei L. RELT promotes the growth of esophageal squamous cell carcinoma by activating the NF-κB pathway. Cell Cycle Georget Tex. 2021 Jul;20(13):1231–41.

485. Jung H, Park S, Gunassekaran GR, Jeon M, Cho YE, Baek MC, et al. A Peptide Probe Enables Photoacoustic-Guided Imaging and Drug Delivery to Lung Tumors in K-rasLA2 Mutant Mice. Cancer Res. 2019 Aug 15;79(16):4271–82.

486. Wu D, Zhang P, Ma J, Xu J, Yang L, Xu W, et al. Serum biomarker panels for the diagnosis of gastric cancer. Cancer Med. 2019 Apr;8(4):1576–83.

487. Cusick JK, Alhomsy Y, Wong S, Talbott G, Uversky VN, Hart C, et al. RELT stains prominently in B-cell lymphomas and binds the hematopoietic transcription factor MDFIC. Biochem Biophys Rep. 2020 Dec;24:100868.

488. Cusick JK, Xu LG, Bin LH, Han KJ, Shu HB. Identification of RELT homologues that associate with RELT and are phosphorylated by OSR1. Biochem Biophys Res Commun. 2006 Feb 10;340(2):535–43.

489. Moua P, Checketts M, Xu LG, Shu HB, Reyland ME, Cusick JK. RELT family members activate p38 and induce apoptosis by a mechanism distinct from TNFR1. Biochem Biophys Res Commun. 2017 Sep 9;491(1):25–32.

490. Rosenberg AB, Roco CM, Muscat RA, Kuchina A, Sample P, Yao Z, et al. Single-cell profiling of the developing mouse brain and spinal cord with split-pool barcoding. Science. 2018 Apr 13;360(6385):176–82.

491. Lein ES, Hawrylycz MJ, Ao N, Ayres M, Bensinger A, Bernard A, et al. Genome-wide atlas of gene expression in the adult mouse brain. Nature. 2007 Jan 11;445(7124):168–76.

492. Mancarci BO, Toker L, Tripathy SJ, Li B, Rocco B, Sibille E, et al. Cross-Laboratory Analysis of Brain Cell Type Transcriptomes with Applications to Interpretation of Bulk Tissue Data. eNeuro. 2017 Dec;4(6):ENEURO.0212-17.2017.

493. Huang HS, Huang XY, Yu HZ, Xue Y, Zhu PL. Circular RNA circ-RELL1 regulates inflammatory response by miR-6873-3p/MyD88/NF-κB axis in endothelial cells. Biochem Biophys Res Commun. 2020 Apr 30;525(2):512–9.

494. Li Y, Shang W, Xiao G, Zhang LK, Zheng C. A Comparative Quantitative Proteomic Analysis of HCMV-Infected Cells Highlights pUL138 as a Multifunctional Protein. Mol Basel Switz. 2020 May 28;25(11):E2520.

495. Feng L, Hu J, Zhang W, Dong Y, Xiong S, Dong C. RELL1 inhibits autophagy pathway and regulates Mycobacterium tuberculosis survival in macrophages. Tuberc Edinb Scotl. 2020 Jan;120:101900.

496. Jin X, Xie H, Liu X, Shen Q, Wang Z, Hao H, et al. RELL1, a novel oncogene, accelerates tumor progression and regulates immune infiltrates in glioma. Int Immunopharmacol. 2020 Oct;87:106707.

497. Rose M, Cardon T, Aboulouard S, Hajjaji N, Kobeissy F, Duhamel M, et al. Surfaceome Proteomic of Glioblastoma Revealed Potential Targets for Immunotherapy. Front Immunol. 2021;12:746168.

498. Sang H, Zhang W, Peng L, Wei S, Zhu X, Huang K, et al. Exosomal circRELL1 serves as a miR-637 sponge to modulate gastric cancer progression via regulating autophagy activation. Cell Death Dis. 2022 Jan 13;13(1):56.

499. Dickinson ME, Flenniken AM, Ji X, Teboul L, Wong MD, White JK, et al. High-throughput discovery of novel developmental phenotypes. Nature. 2016 Sep 22;537(7621):508–14.

500. Roux KJ, Kim DI, Raida M, Burke B. A promiscuous biotin ligase fusion protein identifies proximal and interacting proteins in mammalian cells. J Cell Biol. 2012 Mar 19;196(6):801–10.

501. Gingras AC, Raught B. Beyond hairballs: The use of quantitative mass spectrometry data to understand protein-protein interactions. FEBS Lett. 2012 Aug 14;586(17):2723–31.

502. Mehta V, Trinkle-Mulcahy L. Recent advances in large-scale protein interactome mapping. F1000Research. 2016;5.

503. Mousson F, Kolkman A, Pijnappel WWMP, Timmers HTM, Heck AJR. Quantitative proteomics reveals regulation of dynamic components within TATA-binding protein (TBP) transcription complexes. Mol Cell Proteomics MCP. 2008 May;7(5):845–52.

504. Wang X, Huang L. Identifying dynamic interactors of protein complexes by quantitative mass spectrometry. Mol Cell Proteomics MCP. 2008 Jan;7(1):46–57.

505. Subbotin RI, Chait BT. A pipeline for determining protein-protein interactions and proximities in the cellular milieu. Mol Cell Proteomics MCP. 2014 Nov;13(11):2824–35.

506. Yu C, Yang Y, Wang X, Guan S, Fang L, Liu F, et al. Characterization of Dynamic UbR-Proteasome Subcomplexes by In vivo Cross-linking (X) Assisted Bimolecular Tandem Affinity Purification (XBAP) and Label-free Quantitation. Mol Cell Proteomics MCP. 2016;15(7):2279–92.

507. Samavarchi-Tehrani P, Samson R, Gingras AC. Proximity dependent biotinylation: key enzymes and adaptation to proteomics approaches. Mol Cell Proteomics MCP. 2020 Mar 3;

508. Choi H, Larsen B, Lin ZY, Breitkreutz A, Mellacheruvu D, Fermin D, et al. SAINT: probabilistic scoring of affinity purification-mass spectrometry data. Nat Methods. 2011 Jan;8(1):70–3.

509. Mellacheruvu D, Wright Z, Couzens AL, Lambert JP, St-Denis NA, Li T, et al. The CRAPome: a contaminant repository for affinity purification-mass spectrometry data. Nat Methods. 2013 Aug;10(8):730–6.

510. Trinkle-Mulcahy L. Recent advances in proximity-based labeling methods for interactome mapping. F1000Research. 2019;8.

511. Gingras AC, Abe KT, Raught B. Getting to know the neighborhood: using proximity-dependent biotinylation to characterize protein complexes and map organelles. Curr Opin Chem Biol. 2019;48:44–54.

512. Rees JS, Li XW, Perrett S, Lilley KS, Jackson AP. Protein Neighbors and Proximity Proteomics. Mol Cell Proteomics MCP. 2015 Nov;14(11):2848–56.

513. Kim DI, Roux KJ. Filling the Void: Proximity-Based Labeling of Proteins in Living Cells. Trends Cell Biol. 2016;26(11):804–17.

514. Kim DI, Birendra KC, Zhu W, Motamedchaboki K, Doye V, Roux KJ. Probing nuclear pore complex architecture with proximity-dependent biotinylation. Proc Natl Acad Sci U S A. 2014 Jun 17;111(24):E2453-2461.

515. Guo Z, Neilson LJ, Zhong H, Murray PS, Zanivan S, Zaidel-Bar R. E-cadherin interactome complexity and robustness resolved by quantitative proteomics. Sci Signal. 2014 Dec 2;7(354):rs7.

516. Manshouri R, Coyaud E, Kundu ST, Peng DH, Stratton SA, Alton K, et al. ZEB1/NuRD complex suppresses TBC1D2b to stimulate E-cadherin internalization and promote metastasis in lung cancer. Nat Commun. 2019 Nov 12;10(1):1–15.

517. Coyaud E, Mis M, Laurent EMN, Dunham WH, Couzens AL, Robitaille M, et al. BioID-based Identification of Skp Cullin F-box (SCF)β-TrCP1/2 E3 Ligase Substrates. Mol Cell Proteomics MCP. 2015 Jul;14(7):1781–95.

518. Couzens AL, Knight JDR, Kean MJ, Teo G, Weiss A, Dunham WH, et al. Protein interaction network of the mammalian Hippo pathway reveals mechanisms of kinase-phosphatase interactions. Sci Signal. 2013 Nov 19;6(302):rs15.

519. Dong JM, Tay FPL, Swa HLF, Gunaratne J, Leung T, Burke B, et al. Proximity biotinylation provides insight into the molecular composition of focal adhesions at the nanometer scale. Sci Signal. 2016 14;9(432):rs4.

520. Van Itallie CM, Tietgens AJ, Aponte A, Fredriksson K, Fanning AS, Gucek M, et al. Biotin ligase tagging identifies proteins proximal to E-cadherin, including lipoma preferred partner, a regulator of epithelial cell-cell and cell-substrate adhesion. J Cell Sci. 2014 Feb 15;127(Pt 4):885–95.

521. Hennigan RF, Fletcher JS, Guard S, Ratner N. Proximity biotinylation identifies a set of conformation-specific interactions between Merlin and cell junction proteins. Sci Signal. 2019 23;12(578).

522. Li Y, Merkel CD, Zeng X, Heier JA, Cantrell PS, Sun M, et al. The N-cadherin interactome in primary cardiomyocytes as defined using quantitative proximity proteomics. J Cell Sci. 2019 11;132(3).

523. Firat-Karalar EN, Rauniyar N, Yates JR, Stearns T. Proximity interactions among centrosome components identify regulators of centriole duplication. Curr Biol CB. 2014 Mar 17;24(6):664–70.

524. Sternicki LM, Wegener KL, Bruning JB, Booker GW, Polyak SW. Mechanisms Governing Precise Protein Biotinylation. Trends Biochem Sci. 2017;42(5):383–94.

525. Feng J, Paparella AS, Booker GW, Polyak SW, Abell AD. Biotin Protein Ligase Is a Target for New Antibacterials. Antibiot Basel Switz. 2016 Jul 25;5(3).

526. Tong L. Structure and function of biotin-dependent carboxylases. Cell Mol Life Sci CMLS. 2013 Mar;70(5):863–91.

527. Azhar A, Booker GW, Polyak SW. Mechanisms of Biotin Transport. Biochem Anal Biochem [Internet]. 2015 [cited 2020 Apr 25];04(04). Available from: https://www.omicsonline.org/open-access/mechanisms-of-biotin-transport-2161-1009-1000210.php?aid=62501

528. Chapman-Smith A, Mulhern TD, Whelan F, Cronan JE, Wallace JC. The C-terminal domain of biotin protein ligase from E. coli is required for catalytic activity. Protein Sci Publ Protein Soc. 2001 Dec;10(12):2608–17.

529. Xu Y, Beckett D. Evidence for interdomain interaction in the Escherichia coli repressor of biotin biosynthesis from studies of an N-terminal domain deletion mutant. Biochemistry. 1996 Feb 13;35(6):1783–92.

530. Weaver LH, Kwon K, Beckett D, Matthews BW. Corepressor-induced organization and assembly of the biotin repressor: a model for allosteric activation of a transcriptional regulator. Proc Natl Acad Sci U S A. 2001 May 22;98(11):6045–50.

531. Xu Y, Beckett D. Kinetics of biotinyl-5'-adenylate synthesis catalyzed by the Escherichia coli repressor of biotin biosynthesis and the stability of the enzyme-product complex. Biochemistry. 1994 Jun 14;33(23):7354–60.

532. Chapman-Smith A, Cronan JE. Molecular biology of biotin attachment to proteins. J Nutr. 1999;129(2S Suppl):477S-484S.

533. Yao X, Wei D, Soden C, Summers MF, Beckett D. Structure of the carboxy-terminal fragment of the apo-biotin carboxyl carrier subunit of Escherichia coli acetyl-CoA carboxylase. Biochemistry. 1997 Dec 9;36(49):15089–100.

534. Streaker ED, Beckett D. Nonenzymatic biotinylation of a biotin carboxyl carrier protein: unusual reactivity of the physiological target lysine. Protein Sci Publ Protein Soc. 2006 Aug;15(8):1928–35.

535. Barker DF, Campbell AM. Use of bio-lac fusion strains to study regulation of biotin biosynthesis in Escherichia coli. J Bacteriol. 1980 Aug;143(2):789–800.

536. Buoncristiani MR, Howard PK, Otsuka AJ. DNA-binding and enzymatic domains of the bifunctional biotin operon repressor (BirA) of Escherichia coli. Gene. 1986;44(2–3):255–61.

537. Kwon K, Beckett D. Function of a conserved sequence motif in biotin holoenzyme synthetases. Protein Sci Publ Protein Soc. 2000 Aug;9(8):1530–9.

538. Kwon K, Streaker ED, Ruparelia S, Beckett D. Multiple disordered loops function in corepressor-induced dimerization of the biotin repressor. J Mol Biol. 2000 Dec 15;304(5):821–33.

539. Cronan JE. Targeted and proximity-dependent promiscuous protein biotinylation by a mutant Escherichia coli biotin protein ligase. J Nutr Biochem. 2005 Jul;16(7):416–8.

540. Branon TC, Bosch JA, Sanchez AD, Udeshi ND, Svinkina T, Carr SA, et al. Efficient proximity labeling in living cells and organisms with TurboID. Nat Biotechnol. 2018;36(9):880–7.

541. Lam SS, Martell JD, Kamer KJ, Deerinck TJ, Ellisman MH, Mootha VK, et al. Directed evolution of APEX2 for electron microscopy and proximity labeling. Nat Methods. 2015 Jan;12(1):51–4.

542. Kim DI, Jensen SC, Noble KA, Kc B, Roux KH, Motamedchaboki K, et al. An improved smaller biotin ligase for BioID proximity labeling. Mol Biol Cell. 2016 Apr 15;27(8):1188–96.

543. Groft CM, Uljon SN, Wang R, Werner MH. Structural homology between the Rap30 DNA-binding domain and linker histone H5: implications for preinitiation complex assembly. Proc Natl Acad Sci U S A. 1998 Aug 4;95(16):9117–22.

544. Gao XD, Tu LC, Mir A, Rodriguez T, Ding Y, Leszyk J, et al. C-BERST: defining subnuclear proteomic landscapes at genomic elements with dCas9-APEX2. Nat Methods. 2018;15(6):433–6.

545. Myers SA, Wright J, Peckner R, Kalish BT, Zhang F, Carr SA. Discovery of proteins associated with a predefined genomic locus via dCas9-APEX-mediated proximity labeling. Nat Methods. 2018;15(6):437–9.

546. Liu X, Zhang Y, Chen Y, Li M, Shao Z, Zhang MQ, et al. CAPTURE: In Situ Analysis of Chromatin Composition of Endogenous Genomic Loci by Biotinylated dCas9. Curr Protoc Mol Biol. 2018;123(1):e64.

547. De Munter S, Görnemann J, Derua R, Lesage B, Qian J, Heroes E, et al. Split-BioID: a proximity biotinylation assay for dimerization-dependent protein interactions. FEBS Lett. 2017;591(2):415–24.

548. Schopp IM, Amaya Ramirez CC, Debeljak J, Kreibich E, Skribbe M, Wild K, et al. Split-BioID a conditional proteomics approach to monitor the composition of spatiotemporally defined protein complexes. Nat Commun. 2017 06;8:15690.

549. Chojnowski A, Sobota RM, Ong PF, Xie W, Wong X, Dreesen O, et al. 2C-BioID: An Advanced Two Component BioID System for Precision Mapping of Protein Interactomes. iScience. 2018 Dec 21;10:40–52.

550. Liberles SD, Diver ST, Austin DJ, Schreiber SL. Inducible gene expression and protein translocation using nontoxic ligands identified by a mammalian three-hybrid screen. Proc Natl Acad Sci U S A. 1997 Jul 22;94(15):7825–30.

551. Bobrow MN, Litt GJ, Shaughnessy KJ, Mayer PC, Conlon J. The use of catalyzed reporter deposition as a means of signal amplification in a variety of formats. J Immunol Methods. 1992 Jun 24;150(1–2):145–9.

552. Kotani N, Gu J, Isaji T, Udaka K, Taniguchi N, Honke K. Biochemical visualization of cell surface molecular clustering in living cells. Proc Natl Acad Sci U S A. 2008 May 27;105(21):7405–9.

553. Honke K, Miyagawa-Yamaguchi A, Kotani N. The EMARS Reaction for Proximity Labeling. Methods Mol Biol Clifton NJ. 2019;2008:1–12.

554. Li XW, Rees JS, Xue P, Zhang H, Hamaia SW, Sanderson B, et al. New insights into the DT40 B cell receptor cluster using a proteomic proximity labeling assay. J Biol Chem. 2014 May 23;289(21):14434–47.

555. Connolly CN, Futter CE, Gibson A, Hopkins CR, Cutler DF. Transport into and out of the Golgi complex studied by transfecting cells with cDNAs encoding horseradish peroxidase. J Cell Biol. 1994 Nov;127(3):641–52.

556. Miyagawa-Yamaguchi A, Kotani N, Honke K. Expressed glycosylphosphatidylinositol-anchored horseradish peroxidase identifies co-clustering molecules in individual lipid raft domains. PloS One. 2014;9(3):e93054.

557. Loh KH, Stawski PS, Draycott AS, Udeshi ND, Lehrman EK, Wilton DK, et al. Proteomic Analysis of Unbounded Cellular Compartments: Synaptic Clefts. Cell. 2016 Aug 25;166(5):1295-1307.e21.

558. Martell JD, Deerinck TJ, Sancak Y, Poulos TL, Mootha VK, Sosinsky GE, et al. Engineered ascorbate peroxidase as a genetically encoded reporter for electron microscopy. Nat Biotechnol. 2012 Nov;30(11):1143–8.

559. Patterson WR, Poulos TL. Crystal structure of recombinant pea cytosolic ascorbate peroxidase. Biochemistry. 1995 Apr 4;34(13):4331–41.

560. Rhee HW, Zou P, Udeshi ND, Martell JD, Mootha VK, Carr SA, et al. Proteomic mapping of mitochondria in living cells via spatially restricted enzymatic tagging. Science. 2013 Mar 15;339(6125):1328–31.

561. Hung V, Zou P, Rhee HW, Udeshi ND, Cracan V, Svinkina T, et al. Proteomic mapping of the human mitochondrial intermembrane space in live cells via ratiometric APEX tagging. Mol Cell. 2014 Jul 17;55(2):332–41.

562. Chen CL, Hu Y, Udeshi ND, Lau TY, Wirtz-Peitz F, He L, et al. Proteomic mapping in live Drosophila tissues using an engineered ascorbate peroxidase. Proc Natl Acad Sci U S A. 2015 Sep 29;112(39):12093–8.

563. Markmiller S, Soltanieh S, Server KL, Mak R, Jin W, Fang MY, et al. Context-Dependent and Disease-Specific Diversity in Protein Interactions within Stress Granules. Cell. 2018 25;172(3):590-604.e13.

564. Bersuker K, Peterson CWH, To M, Sahl SJ, Savikhin V, Grossman EA, et al. A Proximity Labeling Strategy Provides Insights into the Composition and Dynamics of Lipid Droplet Proteomes. Dev Cell. 2018 08;44(1):97-112.e7.

565. Paek J, Kalocsay M, Staus DP, Wingler L, Pascolutti R, Paulo JA, et al. Multidimensional Tracking of GPCR Signaling via Peroxidase-Catalyzed Proximity Labeling. Cell. 2017 06;169(2):338-349.e11.

566. Lobingier BT, Hüttenhain R, Eichel K, Miller KB, Ting AY, von Zastrow M, et al. An Approach to Spatiotemporally Resolve Protein Interaction Networks in Living Cells. Cell. 2017 06;169(2):350-360.e12.

567. Zámocký M, Hofbauer S, Schaffner I, Gasselhuber B, Nicolussi A, Soudi M, et al. Independent evolution of four heme peroxidase superfamilies. Arch Biochem Biophys. 2015 May 15;574:108–19.

568. Hopkins C, Gibson A, Stinchcombe J, Futter C. Chimeric molecules employing horseradish peroxidase as reporter enzyme for protein localization in the electron microscope. Methods Enzymol. 2000;327:35–45.

569. Zámocký M, Furtmüller PG, Obinger C. Evolution of structure and function of Class I peroxidases. Arch Biochem Biophys. 2010 Aug 1;500(1):45–57.

570. Maruta T, Sawa Y, Shigeoka S, Ishikawa T. Diversity and Evolution of Ascorbate Peroxidase Functions in Chloroplasts: More Than Just a Classical Antioxidant Enzyme? Plant Cell Physiol. 2016 Jul;57(7):1377–86.

571. Turner DD, Lad L, Kwon H, Basran J, Carr KH, Moody PCE, et al. The role of Ala134 in controlling substrate binding and reactivity in ascorbate peroxidase. J Inorg Biochem. 2018;180:230–4.

572. Martell JD, Yamagata M, Deerinck TJ, Phan S, Kwa CG, Ellisman MH, et al. A split horseradish peroxidase for the detection of intercellular protein-protein interactions and sensitive visualization of synapses. Nat Biotechnol. 2016;34(7):774–80.

573. Xue M, Hou J, Wang L, Cheng D, Lu J, Zheng L, et al. Optimizing the fragment complementation of APEX2 for detection of specific protein-protein interactions in live cells. Sci Rep. 2017 27;7(1):12039.

574. Han Y, Branon TC, Martell JD, Boassa D, Shechner D, Ellisman MH, et al. Directed Evolution of Split APEX2 Peroxidase. ACS Chem Biol. 2019 19;14(4):619–35.

575. Zuzow N, Ghosh A, Leonard M, Liao J, Yang B, Bennett EJ. Mapping the mammalian ribosome quality control complex interactome using proximity labeling approaches. Mol Biol Cell. 2018 15;29(10):1258–69.

576. Veitch NC. Horseradish peroxidase: a modern view of a classic enzyme. Phytochemistry. 2004 Feb;65(3):249–59.

577. Gross AJ, Sizer IW. The oxidation of tyramine, tyrosine, and related compounds by peroxidase. J Biol Chem. 1959 Jun;234(6):1611–4.

578. Minamihata K, Goto M, Kamiya N. Site-specific protein cross-linking by peroxidase-catalyzed activation of a tyrosine-containing peptide tag. Bioconjug Chem. 2011 Jan 19;22(1):74–81.

579. Roux PP, Barker PA. Neurotrophin signaling through the p75 neurotrophin receptor. Prog Neurobiol. 2002 Jun;67(3):203–33.

580. Lebrun-Julien F, Bertrand MJ, De Backer O, Stellwagen D, Morales CR, Di Polo A, et al. ProNGF induces TNFalpha-dependent death of retinal ganglion cells through a p75NTR non-cell-autonomous signaling pathway. Proc Natl Acad Sci U S A. 2010 Feb 23;107(8):3817–22.

581. Gibon J, Buckley SM, Unsain N, Kaartinen V, Séguéla P, Barker PA. proBDNF and p75NTR Control Excitability and Persistent Firing of Cortical Pyramidal Neurons. J Neurosci Off J Soc Neurosci. 2015 Jul 1;35(26):9741–53.

582. Wang KC, Kim JA, Sivasankaran R, Segal R, He Z. P75 interacts with the Nogo receptor as a co-receptor for Nogo, MAG and OMgp. Nature. 2002 Nov 7;420(6911):74–8.

583. Hu Y, Lee X, Shao Z, Apicco D, Huang G, Gong BJ, et al. A DR6/p75(NTR) complex is responsible for β-amyloid-induced cortical neuron death. Cell Death Dis. 2013 Apr 4;4:e579.

584. Ahmed Z, Mazibrada G, Seabright RJ, Dent RG, Berry M, Logan A. TACE-induced cleavage of NgR and p75NTR in dorsal root ganglion cultures disinhibits outgrowth and promotes branching of neurites in the presence of inhibitory CNS myelin. FASEB J Off Publ Fed Am Soc Exp Biol. 2006 Sep;20(11):1939–41.

585. Ceni C, Kommaddi RP, Thomas R, Vereker E, Liu X, McPherson PS, et al. The p75NTR intracellular domain generated by neurotrophin-induced receptor cleavage potentiates Trk signaling. J Cell Sci. 2010 Jul 1;123(Pt 13):2299–307.

586. Kommaddi RP, Thomas R, Ceni C, Daigneault K, Barker PA. Trk-dependent ADAM17 activation facilitates neurotrophin survival signaling. FASEB J Off Publ Fed Am Soc Exp Biol. 2011 Jun;25(6):2061–70.

587. Zeinieh M, Salehi A, Rajkumar V, Barker PA. p75NTR-dependent Rac1 activation requires receptor cleavage and activation of an NRAGE and NEDD9 signaling cascade. J Cell Sci. 2015 Feb 1;128(3):447–59.

588. Raposo G, Stahl PD. Extracellular vesicles: a new communication paradigm? Nat Rev Mol Cell Biol. 2019 Sep;20(9):509–10.

589. Lopez-Verrilli MA, Picou F, Court FA. Schwann cell-derived exosomes enhance axonal regeneration in the peripheral nervous system. Glia. 2013 Nov;61(11):1795–806.

590. Unsain N, Heard KN, Higgins JM, Barker PA. Production and isolation of axons from sensory neurons for biochemical analysis using porous filters. J Vis Exp JoVE. 2014 Jul 8;(89).

591. Berg S, Kutra D, Kroeger T, Straehle CN, Kausler BX, Haubold C, et al. ilastik: interactive machine learning for (bio)image analysis. Nat Methods. 2019 Dec;16(12):1226–32.

592. Lebrun-Julien F, Duplan L, Pernet V, Osswald I, Sapieha P, Bourgeois P, et al. Excitotoxic death of retinal neurons in vivo occurs via a non-cell-autonomous mechanism. J Neurosci Off J Soc Neurosci. 2009 Apr 29;29(17):5536–45.

593. McQuillen PS, DeFreitas MF, Zada G, Shatz CJ. A novel role for p75NTR in subplate growth cone complexity and visual thalamocortical innervation. J Neurosci Off J Soc Neurosci. 2002 May 1;22(9):3580–93.

594. Gehler S, Gallo G, Veien E, Letourneau PC. p75 neurotrophin receptor signaling regulates growth cone filopodial dynamics through modulating RhoA activity. J Neurosci Off J Soc Neurosci. 2004 May 5;24(18):4363–72.

595. Naska S, Lin DC, Miller FD, Kaplan DR. p75NTR is an obligate signaling receptor required for cues that cause sympathetic neuron growth cone collapse. Mol Cell Neurosci. 2010 Oct;45(2):108–20.

596. Deinhardt K, Kim T, Spellman DS, Mains RE, Eipper BA, Neubert TA, et al. Neuronal growth cone retraction relies on proneurotrophin receptor signaling through Rac. Sci Signal. 2011 Dec 6;4(202):ra82.

597. Marchetti L, Bonsignore F, Gobbo F, Amodeo R, Calvello M, Jacob A, et al. Fast-diffusing p75NTR monomers support apoptosis and growth cone collapse by neurotrophin ligands. Proc Natl Acad Sci U S A. 2019 22;116(43):21563–72.

598. Brann AB, Scott R, Neuberger Y, Abulafia D, Boldin S, Fainzilber M, et al. Ceramide signaling downstream of the p75 neurotrophin receptor mediates the effects of nerve growth factor on outgrowth of cultured hippocampal neurons. J Neurosci Off J Soc Neurosci. 1999 Oct 1;19(19):8199–206.

599. DeFreitas MF, McQuillen PS, Shatz CJ. A novel p75NTR signaling pathway promotes survival, not death, of immunopurified neocortical subplate neurons. J Neurosci Off J Soc Neurosci. 2001 Jul 15;21(14):5121–9.

600. Ahmed Z, Douglas MR, John G, Berry M, Logan A. AMIGO3 is an NgR1/p75 co-receptor signalling axon growth inhibition in the acute phase of adult central nervous system injury. PloS One. 2013;8(4):e61878.

601. Vicario A, Kisiswa L, Tann JY, Kelly CE, Ibáñez CF. Neuron-type-specific signaling by the p75NTR death receptor is regulated by differential proteolytic cleavage. J Cell Sci. 2015 Apr 15;128(8):1507–17.

602. Faulkner S, Jobling P, Rowe CW, Rodrigues Oliveira SM, Roselli S, Thorne RF, et al. Neurotrophin Receptors TrkA, p75NTR, and Sortilin Are Increased and Targetable in Thyroid Cancer. Am J Pathol. 2018;188(1):229–41.

603. Yang WH, Cheng CY, Chen MF, Wang TC. Cell Subpopulations Overexpressing p75NTR Have Tumor-initiating Properties in the C6 Glioma Cell Line. Anticancer Res. 2018 Sep;38(9):5183–92.

604. Kuner P, Hertel C. NGF induces apoptosis in a human neuroblastoma cell line expressing the neurotrophin receptor p75NTR. J Neurosci Res. 1998 Nov 15;54(4):465–74.

605. Majdan M, Walsh GS, Aloyz R, Miller FD. TrkA mediates developmental sympathetic neuron survival in vivo by silencing an ongoing p75NTR-mediated death signal. J Cell Biol. 2001 Dec 24;155(7):1275–85.

606. Iobbi C, Korte M, Zagrebelsky M. Nogo-66 Restricts Synaptic Strengthening via Lingo1 and the ROCK2-Cofilin Pathway to Control Actin Dynamics. Cereb Cortex N Y N 1991. 2017 01;27(5):2779–92.

607. Bossen C, Ingold K, Tardivel A, Bodmer JL, Gaide O, Hertig S, et al. Interactions of tumor necrosis factor (TNF) and TNF receptor family members in the mouse and human. J Biol Chem. 2006 May 19;281(20):13964–71.

608. Gao C, Zhang L, Sun D, Li J, Yao X, Zhou H, et al. Roles of p75NTR in Maintaining Brain Hemostasis and the Implications for p75NTR-targeted Therapies. Curr Alzheimer Res. 2017;14(5):554–61.

609. Shen LL, Li WW, Xu YL, Gao SH, Xu MY, Bu XL, et al. Neurotrophin receptor p75 mediates amyloid β-induced tau pathology. Neurobiol Dis. 2019;132:104567.

610. Wang YJ, Wang X, Lu JJ, Li QX, Gao CY, Liu XH, et al. p75NTR regulates Abeta deposition by increasing Abeta production but inhibiting Abeta aggregation with its extracellular domain. J Neurosci Off J Soc Neurosci. 2011 Feb 9;31(6):2292–304.

611. Mellacheruvu D, Wright Z, Couzens AL, Lambert JP, St-Denis NA, Li T, et al. The CRAPome: a contaminant repository for affinity purification-mass spectrometry data. Nat Methods. 2013 Aug;10(8):730–6.

612. Choi H, Larsen B, Lin ZY, Breitkreutz A, Mellacheruvu D, Fermin D, et al. SAINT: probabilistic scoring of affinity purification-mass spectrometry data. Nat Methods. 2011 Jan;8(1):70–3.

613. Huang DW, Sherman BT, Lempicki RA. Bioinformatics enrichment tools: paths toward the comprehensive functional analysis of large gene lists. Nucleic Acids Res. 2009 Jan;37(1):1–13.

614. Huang DW, Sherman BT, Lempicki RA. Systematic and integrative analysis of large gene lists using DAVID bioinformatics resources. Nat Protoc. 2009;4(1):44–57.

615. Fabregat A, Jupe S, Matthews L, Sidiropoulos K, Gillespie M, Garapati P, et al. The Reactome Pathway Knowledgebase. Nucleic Acids Res. 2018 04;46(D1):D649–55.

616. Benjamini Y, Drai D, Elmer G, Kafkafi N, Golani I. Controlling the false discovery rate in behavior genetics research. Behav Brain Res. 2001 Nov 1;125(1–2):279–84.

617. Poopalasundaram S, Marler KJM, Drescher U. EphrinA6 on chick retinal axons is a key component for p75(NTR)-dependent axon repulsion and TrkB-dependent axon branching. Mol Cell Neurosci. 2011 Jun;47(2):131–6.

618. Strasser A, Jost PJ, Nagata S. The many roles of FAS receptor signaling in the immune system. Immunity. 2009 Feb 20;30(2):180–92.

619. Vanamee ÉS, Faustman DL. Structural principles of tumor necrosis factor superfamily signaling. Sci Signal. 2018 02;11(511).

620. Barker PA, Barbee G, Misko TP, Shooter EM. The low affinity neurotrophin receptor, p75LNTR, is palmitoylated by thioester formation through cysteine 279. J Biol Chem. 1994 Dec 2;269(48):30645–50.

621. Zhou F, Xue Y, Yao X, Xu Y. CSS-Palm: palmitoylation site prediction with a clustering and scoring strategy (CSS). Bioinforma Oxf Engl. 2006 Apr 1;22(7):894–6.

622. Morris ME, Rodriguez-Cruz V, Felmlee MA. SLC and ABC Transporters: Expression, Localization, and Species Differences at the Blood-Brain and the Blood-Cerebrospinal Fluid Barriers. AAPS J. 2017;19(5):1317–31.

623. Bröer S. The SLC6 orphans are forming a family of amino acid transporters. Neurochem Int. 2006 Jun;48(6–7):559–67.

624. Braissant O, Henry H. AGAT, GAMT and SLC6A8 distribution in the central nervous system, in relation to creatine deficiency syndromes: a review. J Inherit Metab Dis. 2008 Apr;31(2):230–9.

625. Garcia N, Santafe MM, Tomas M, Lanuza MA, Besalduch N, Tomas J. Neurotrophin-4 couples to locally modulated ACh release at the end of neuromuscular synapse maturation. Neurosci Lett. 2010 Jan 1;468(1):72–4.

626. Cusick JK, Mustian A, Jacobs AT, Reyland ME. Identification of PLSCR1 as a protein that interacts with RELT family members. Mol Cell Biochem. 2012 Mar;362(1–2):55–63.

627. Ashkenazy H, Erez E, Martz E, Pupko T, Ben-Tal N. ConSurf 2010: calculating evolutionary conservation in sequence and structure of proteins and nucleic acids. Nucleic Acids Res. 2010 Jul;38(Web Server issue):W529-533.

628. Vilar M, Sung TC, Chen Z, García-Carpio I, Fernandez EM, Xu J, et al. Heterodimerization of p45-p75 modulates p75 signaling: structural basis and mechanism of action. PLoS Biol. 2014 Aug;12(8):e1001918.

629. Kanning KC, Hudson M, Amieux PS, Wiley JC, Bothwell M, Schecterson LC. Proteolytic processing of the p75 neurotrophin receptor and two homologs generates C-terminal fragments with signaling capability. J Neurosci Off J Soc Neurosci. 2003 Jul 2;23(13):5425–36.

630. Murray SS, Perez P, Lee R, Hempstead BL, Chao MV. A novel p75 neurotrophin receptor-related protein, NRH2, regulates nerve growth factor binding to the TrkA receptor. J Neurosci Off J Soc Neurosci. 2004 Mar 17;24(11):2742–9.

631. Wong AW, Willingham M, Xiao J, Kilpatrick TJ, Murray SS. Neurotrophin receptor homolog-2 regulates nerve growth factor signaling. J Neurochem. 2008 Aug;106(4):1964–76.

632. Kim T, Hempstead BL. NRH2 is a trafficking switch to regulate sortilin localization and permit proneurotrophin-induced cell death. EMBO J. 2009 Jun 3;28(11):1612–23.

633. Unsain N, Dorval G, Sheen JH, Barker PA. Generation and characterization of mice bearing null alleles of nradd/Nrh2. Genes N Y N 2000. 2016 Dec;54(12):605–12.

634. Zhao Z, Fagerlund R, Baur AS, Saksela K. HIV-1 Nef-Induced Secretion of the Proinflammatory Protease TACE into Extracellular Vesicles Is Mediated by Raf-1 and Can Be Suppressed by Clinical Protein Kinase Inhibitors. J Virol. 2021 Apr 12;95(9):e00180-21.

635. Srinivasan B, Wang Z, Brun-Zinkernagel AM, Collier RJ, Black RA, Frank SJ, et al. Photic injury promotes cleavage of p75NTR by TACE and nuclear trafficking of the p75 intracellular domain. Mol Cell Neurosci. 2007 Dec;36(4):449–61.

636. Gravestein LA, Blom B, Nolten LA, de Vries E, van der Horst G, Ossendorp F, et al. Cloning and expression of murine CD27: comparison with 4-1BB, another lymphocyte-specific member of the nerve growth factor receptor family. Eur J Immunol. 1993 Apr;23(4):943–50.

637. Gravestein LA, Amsen D, Boes M, Calvo CR, Kruisbeek AM, Borst J. The TNF receptor family member CD27 signals to Jun N-terminal kinase via Traf-2. Eur J Immunol. 1998 Jul;28(7):2208–16.

638. Meeker ND, Stafford AN, Lunceford JK, Avner P, Ma RZ, Teuscher C. Physical mapping of the autoimmune disease susceptibility locus, Bphs: co-localization with a cluster of genes from the TNF receptor superfamily on mouse chromosome 6. Mamm Genome Off J Int Mamm Genome Soc. 1999 Sep;10(9):858–63.

639. Vazquez SE, Inlay MA, Serwold T. CD201 and CD27 identify hematopoietic stem and progenitor cells across multiple murine strains independently of Kit and Sca-1. Exp Hematol. 2015 Jul;43(7):578–85.

640. Teoh JJ, Gamache AE, Gillespie AL, Stadnisky MD, Yagita H, Bullock TNJ, et al. Acute Virus Control Mediated by Licensed NK Cells Sets Primary CD8+ T Cell Dependence on CD27 Costimulation. J Immunol Baltim Md 1950. 2016 Dec 1;197(11):4360–70.

641. Al Sayed MF, Ruckstuhl CA, Hilmenyuk T, Claus C, Bourquin JP, Bornhauser BC, et al. CD70 reverse signaling enhances NK cell function and immunosurveillance in CD27-expressing B-cell malignancies. Blood. 2017 Jul 20;130(3):297–309.

642. Li Y, Gao L, Hadland B, Tan K, Speck NA. CD27 marks murine embryonic hematopoietic stem cells and type II prehematopoietic stem cells. Blood. 2017 Jul 20;130(3):372–6.

643. Simonart T, Noel JC, Andrei G, Parent D, Van Vooren JP, Hermans P, et al. Iron as a potential co-factor in the pathogenesis of Kaposi's sarcoma? Int J Cancer. 1998 Dec 9;78(6):720–6.

644. McIndoe RA, Bohlman B, Chi E, Schuster E, Lindhardt M, Hood L. Localization of non-Mhc collagen-induced arthritis susceptibility loci in DBA/1j mice. Proc Natl Acad Sci U S A. 1999 Mar 2;96(5):2210–4.

645. Mathieu C, Beltra JC, Charpentier T, Bourbonnais S, Di Santo JP, Lamarre A, et al. IL-2 and IL-15 regulate CD8+ memory T-cell differentiation but are dispensable for protective recall responses. Eur J Immunol. 2015 Dec;45(12):3324–38.

646. Meighan-Mantha RL, Hsu DK, Guo Y, Brown SA, Feng SL, Peifley KA, et al. The mitogen-inducible Fn14 gene encodes a type I transmembrane protein that modulates fibroblast adhesion and migration. J Biol Chem. 1999 Nov 12;274(46):33166–76.

647. Feng SL, Guo Y, Factor VM, Thorgeirsson SS, Bell DW, Testa JR, et al. The Fn14 immediate-early response gene is induced during liver regeneration and highly expressed in both human and murine hepatocellular carcinomas. Am J Pathol. 2000 Apr;156(4):1253–61.

648. Wiley SR, Cassiano L, Lofton T, Davis-Smith T, Winkles JA, Lindner V, et al. A novel TNF receptor family member binds TWEAK and is implicated in angiogenesis. Immunity. 2001 Nov;15(5):837–46.

649. Brown SAN, Richards CM, Hanscom HN, Feng SLY, Winkles JA. The Fn14 cytoplasmic tail binds tumour-necrosis-factor-receptor-associated factors 1, 2, 3 and 5 and mediates nuclear factor-kappaB activation. Biochem J. 2003 Apr 15;371(Pt 2):395–403.

650. Polek TC, Talpaz M, Darnay BG, Spivak-Kroizman T. TWEAK mediates signal transduction and differentiation of RAW264.7 cells in the absence of Fn14/TweakR. Evidence for a second TWEAK receptor. J Biol Chem. 2003 Aug 22;278(34):32317–23.

651. Mustafa S, Martin HL, Burkly L, Costa A, Martins ML, Schwaninger M, et al. The role of TWEAK/Fn14 signaling in the MPTP-model of Parkinson's disease. Neuroscience. 2016 Apr 5;319:116–22.

652. Di Martino L, Dave M, Menghini P, Xin W, Arseneau KO, Pizarro TT, et al. Protective Role for TWEAK/Fn14 in Regulating Acute Intestinal Inflammation and Colitis-Associated Tumorigenesis. Cancer Res. 2016 Nov 15;76(22):6533–42.

653. Doerner J, Chalmers SA, Friedman A, Putterman C. Fn14 deficiency protects lupus-prone mice from histological lupus erythematosus-like skin inflammation induced by ultraviolet light. Exp Dermatol. 2016 Dec;25(12):969–76.

654. Sezaki T, Hirata Y, Hagiwara T, Kawamura YI, Okamura T, Takanashi R, et al. Disruption of the TWEAK/Fn14 pathway prevents 5-fluorouracil-induced diarrhea in mice. World J Gastroenterol. 2017 Apr 7;23(13):2294–307.

655. Martin-Sanchez D, Fontecha-Barriuso M, Carrasco S, Sanchez-Niño MD, Mässenhausen A von, Linkermann A, et al. TWEAK and RIPK1 mediate a second wave of cell death during AKI. Proc Natl Acad Sci U S A. 2018 Apr 17;115(16):4182–7.

656. Lin L, Yee SW, Kim RB, Giacomini KM. SLC transporters as therapeutic targets: emerging opportunities. Nat Rev Drug Discov. 2015 Aug;14(8):543–60.

657. Pérez V, Bermedo-Garcia F, Zelada D, Court FA, Pérez MÁ, Fuenzalida M, et al. The p75NTR neurotrophin receptor is required to organize the mature neuromuscular synapse by regulating synaptic vesicle availability. Acta Neuropathol Commun. 2019 12;7(1):147.

658. Kaila K, Ruusuvuori E, Seja P, Voipio J, Puskarjov M. GABA actions and ionic plasticity in epilepsy. Curr Opin Neurobiol. 2014 Jun;26:34–41.

659. Schomberg SL, Bauer J, Kintner DB, Su G, Flemmer A, Forbush B, et al. Cross talk between the GABA(A) receptor and the Na-K-Cl cotransporter is mediated by intracellular Cl-. J Neurophysiol. 2003 Jan;89(1):159–67.

660. Rivera C, Voipio J, Payne JA, Ruusuvuori E, Lahtinen H, Lamsa K, et al. The K+/Cl- co-transporter KCC2 renders GABA hyperpolarizing during neuronal maturation. Nature. 1999 Jan 21;397(6716):251–5.

661. Riffault B, Kourdougli N, Dumon C, Ferrand N, Buhler E, Schaller F, et al. Pro-Brain-Derived Neurotrophic Factor (proBDNF)-Mediated p75NTR Activation Promotes Depolarizing Actions of GABA and Increases Susceptibility to Epileptic Seizures. Cereb Cortex N Y N 1991. 2018 01;28(2):510–27.

662. Kania A, Klein R. Mechanisms of ephrin-Eph signalling in development, physiology and disease. Nat Rev Mol Cell Biol. 2016 Apr;17(4):240–56.

663. Lim YS, McLaughlin T, Sung TC, Santiago A, Lee KF, O'Leary DDM. p75(NTR) mediates ephrin-A reverse signaling required for axon repulsion and mapping. Neuron. 2008 Sep 11;59(5):746–58.

664. Marler KJM, Poopalasundaram S, Broom ER, Wentzel C, Drescher U. Pro-neurotrophins secreted from retinal ganglion cell axons are necessary for ephrinA-p75NTR-mediated axon guidance. Neural Develop. 2010 Nov 2;5:30.

665. Poopalasundaram S, Marler KJM, Drescher U. EphrinA6 on chick retinal axons is a key component for p75(NTR)-dependent axon repulsion and TrkB-dependent axon branching. Mol Cell Neurosci. 2011 Jun;47(2):131–6.

666. Uesugi N, Kimura Y, Yamashita T. Suppression of the p75 receptor signal attenuates the effect of ephrin-B3 and promotes axonal regeneration of the injured optic nerve. Cell Death Dis. 2013 Mar 21;4:e557.

667. Gibon J, Barker PA, Séguéla P. Opposing presynaptic roles of BDNF and ProBDNF in the regulation of persistent activity in the entorhinal cortex. Mol Brain. 2016 Mar 1;9:23.

668. Frank LM, Brown EN. Persistent activity and memory in the entorhinal cortex. Trends Neurosci. 2003 Aug;26(8):400–1.

669. Wu X, Chi RJ, Baskin JM, Lucast L, Burd CG, De Camilli P, et al. Structural insights into assembly and regulation of the plasma membrane phosphatidylinositol 4-kinase complex. Dev Cell. 2014 Jan 13;28(1):19–29.

670. Brigidi GS, Sun Y, Beccano-Kelly D, Pitman K, Mobasser M, Borgland SL, et al. Palmitoylation of δ-catenin by DHHC5 mediates activity-induced synapse plasticity. Nat Neurosci. 2014 Apr;17(4):522–32.

671. Brigidi GS, Santyr B, Shimell J, Jovellar B, Bamji SX. Activity-regulated trafficking of the palmitoyl-acyl transferase DHHC5. Nat Commun. 2015 Sep 3;6:8200.

672. Barker PA, Barbee G, Misko TP, Shooter EM. The low affinity neurotrophin receptor, p75LNTR, is palmitoylated by thioester formation through cysteine 279. J Biol Chem. 1994 Dec 2;269(48):30645–50.

673. Pradhan AJ, Lu D, Parisi LR, Shen S, Berhane IA, Galster SL, et al. Protein acylation by saturated very long chain fatty acids and endocytosis are involved in necroptosis. Cell Chem Biol. 2021 Sep 16;28(9):1298-1309.e7.

674. Mariscal J, Vagner T, Kim M, Zhou B, Chin A, Zandian M, et al. Comprehensive palmitoyl-proteomic analysis identifies distinct protein signatures for large and small cancer-derived extracellular vesicles. J Extracell Vesicles. 2020 Jun 10;9(1):1764192.